African Journal of Biotechnology

Volume 16 Number 18, 3 May 2017

ISSN 1684-5315

Academic Journals

ABOUT AJB

The African Journal of Biotechnology (AJB) (ISSN 1684-5315) is published weekly (one volume per year) by Academic Journals.

African Journal of Biotechnology (AJB), a new broad-based journal, is an open access journal that was founded on two key tenets: To publish the most exciting research in all areas of applied biochemistry, industrial microbiology, molecular biology, genomics and proteomics, food and agricultural technologies, and metabolic engineering. Secondly, to provide the most rapid turn-around time possible for reviewing and publishing, and to disseminate the articles freely for teaching and reference purposes. All articles published in AJB are peer-reviewed.

Contact Us

Editorial Office: ajb@academicjournals.org

Help Desk: helpdesk@academicjournals.org

Website: http://www.academicjournals.org/journal/AJB

Submit manuscript online http://ms.academicjournals.me/

Editor-in-Chief

George Nkem Ude, Ph.D
Plant Breeder & Molecular Biologist
Department of Natural Sciences
Crawford Building, Rm 003A
Bowie State University
14000 Jericho Park Road
Bowie, MD 20715, USA

Editor

N. John Tonukari, Ph.D
Department of Biochemistry
Delta State University
PMB 1
Abraka, Nigeria

Associate Editors

Prof. Dr. AE Aboulata
Plant Path. Res. Inst., ARC, POBox 12619, Giza, Egypt
30 D, El-Karama St., Alf Maskan, P.O. Box 1567,
Ain Shams, Cairo,
Egypt

Dr. S.K Das
Department of Applied Chemistry
and Biotechnology, University of Fukui,
Japan

Prof. Okoh, A. I.
Applied and Environmental Microbiology Research Group (AEMREG),
Department of Biochemistry and Microbiology,
University of Fort Hare.
P/Bag X1314 Alice 5700,
South Africa

Dr. Ismail TURKOGLU
Department of Biology Education,
Education Faculty, Fırat University,
Elazığ, Turkey

Prof T.K.Raja, PhD FRSC (UK)
Department of Biotechnology
PSG COLLEGE OF TECHNOLOGY (Autonomous)
(Affiliated to Anna University)
Coimbatore-641004, Tamilnadu,
INDIA.

Dr. George Edward Mamati
Horticulture Department,
Jomo Kenyatta University of Agriculture
and Technology,
P. O. Box 62000-00200,
Nairobi, Kenya.

Dr. Gitonga
Kenya Agricultural Research Institute,
National Horticultural Research Center,
P.O Box 220,
Thika, Kenya.

Editorial Board

Prof. Sagadevan G. Mundree

Department of Molecular and Cell Biology
University of Cape Town
Private Bag Rondebosch 7701
South Africa

Dr. Martin Fregene

Centro Internacional de Agricultura Tropical (CIAT)
Km 17 Cali-Palmira Recta
AA6713, Cali, Colombia

Prof. O. A. Ogunseitan

Laboratory for Molecular Ecology
Department of Environmental Analysis and Design
University of California,
Irvine, CA 92697-7070. USA

Dr. Ibrahima Ndoye

UCAD, Faculte des Sciences et Techniques
Departement de Biologie Vegetale
BP 5005, Dakar, Senegal.
Laboratoire Commun de Microbiologie
IRD/ISRA/UCAD
BP 1386, Dakar

Dr. Bamidele A. Iwalokun

Biochemistry Department
Lagos State University
P.M.B. 1087. Apapa – Lagos, Nigeria

Dr. Jacob Hodeba Mignouna

Associate Professor, Biotechnology
Virginia State University
Agricultural Research Station Box 9061
Petersburg, VA 23806, USA

Dr. Bright Ogheneovo Agindotan

Plant, Soil and Entomological Sciences Dept
University of Idaho, Moscow
ID 83843, USA

Dr. A.P. Njukeng

Département de Biologie Végétale
Faculté des Sciences
B.P. 67 Dschang
Université de Dschang
Rep. du CAMEROUN

Dr. E. Olatunde Farombi

Drug Metabolism and Toxicology Unit
Department of Biochemistry
University of Ibadan, Ibadan, Nigeria

Dr. Stephen Bakiamoh

Michigan Biotechnology Institute International
3900 Collins Road
Lansing, MI 48909, USA

Dr. N. A. Amusa

Institute of Agricultural Research and Training
Obafemi Awolowo University
Moor Plantation, P.M.B 5029, Ibadan, Nigeria

Dr. Desouky Abd-El-Haleem

Environmental Biotechnology Department &
Bioprocess Development Department,
Genetic Engineering and Biotechnology Research Institute (GEBRI),
Mubarak City for Scientific Research and Technology Applications,
New Burg-Elarab City, Alexandria, Egypt.

Dr. Simeon Oloni Kotchoni

Department of Plant Molecular Biology
Institute of Botany, Kirschallee 1,
University of Bonn, D-53115 Germany.

Dr. Eriola Betiku

German Research Centre for Biotechnology,
Biochemical Engineering Division,
Mascheroder Weg 1, D-38124,
Braunschweig, Germany

Dr. Daniel Masiga

International Centre of Insect Physiology and Ecology,
Nairobi,
Kenya

Dr. Essam A. Zaki

Genetic Engineering and Biotechnology Research Institute, GEBRI,
Research Area,
Borg El Arab, Post Code 21934, Alexandria
Egypt

Dr. Alfred Dixon
International Institute of Tropical Agriculture (IITA)
PMB 5320, Ibadan
Oyo State, Nigeria

Dr. Sankale Shompole
Dept. of Microbiology, Molecular Biology and Biochemisty,
University of Idaho, Moscow,
ID 83844, USA.

Dr. Mathew M. Abang
Germplasm Program
International Center for Agricultural Research in the Dry Areas
(ICARDA)
P.O. Box 5466, Aleppo, SYRIA.

Dr. Solomon Olawale Odemuyiwa
Pulmonary Research Group
Department of Medicine
550 Heritage Medical Research Centre
University of Alberta
Edmonton
Canada T6G 2S2

Prof. Anna-Maria Botha-Oberholster
Plant Molecular Genetics
Department of Genetics
Forestry and Agricultural Biotechnology Institute
Faculty of Agricultural and Natural Sciences
University of Pretoria
ZA-0002 Pretoria, South Africa

Dr. O. U. Ezeronye
Department of Biological Science
Michael Okpara University of Agriculture
Umudike, Abia State, Nigeria.

Dr. Joseph Hounhouigan
Maître de Conférence
Sciences et technologies des aliments
Faculté des Sciences Agronomiques
Université d'Abomey-Calavi
01 BP 526 Cotonou
République du Bénin

Prof. Christine Rey
Dept. of Molecular and Cell Biology,
University of the Witwatersand,
Private Bag 3, WITS 2050, Johannesburg, South Africa

Dr. Kamel Ahmed Abd-Elsalam
Molecular Markers Lab. (MML)
Plant Pathology Research Institute (PPathRI)
Agricultural Research Center, 9-Gamma St., Orman, 12619,
Giza, Egypt

Dr. Jones Lemchi
International Institute of Tropical Agriculture (IITA)
Onne, Nigeria

Prof. Greg Blatch
Head of Biochemistry & Senior Wellcome Trust Fellow
Department of Biochemistry, Microbiology & Biotechnology
Rhodes University
Grahamstown 6140
South Africa

Dr. Beatrice Kilel
P.O Box 1413
Manassas, VA 20108
USA

Dr. Jackie Hughes
Research-for-Development
International Institute of Tropical Agriculture (IITA)
Ibadan, Nigeria

Dr. Robert L. Brown
Southern Regional Research Center,
U.S. Department of Agriculture,
Agricultural Research Service,
New Orleans, LA 70179.

Dr. Deborah Rayfield
Physiology and Anatomy
Bowie State University
Department of Natural Sciences
Crawford Building, Room 003C
Bowie MD 20715,USA

Dr. Marlene Shehata
University of Ottawa Heart Institute
Genetics of Cardiovascular Diseases
40 Ruskin Street
K1Y-4W7, Ottawa, ON, CANADA

Dr. Hany Sayed Hafez
The American University in Cairo,
Egypt

Dr. Clement O. Adebooye
Department of Plant Science
Obafemi Awolowo University, Ile-Ife
Nigeria

Dr. Ali Demir Sezer
Marmara Üniversitesi Eczacilik Fakültesi,
Tibbiye cad. No: 49, 34668, Haydarpasa, Istanbul,
Turkey

Dr. Ali Gazanchain
P.O. Box: 91735-1148, Mashhad,
Iran.

Dr. Anant B. Patel
Centre for Cellular and Molecular Biology
Uppal Road, Hyderabad 500007
India

Prof. Arne Elofsson
Department of Biophysics and Biochemistry
Bioinformatics at Stockholm University,
Sweden

Prof. Bahram Goliaei
Departments of Biophysics and Bioinformatics
Laboratory of Biophysics and Molecular Biology
University of Tehran, Institute of Biochemistry and Biophysics
Iran

Dr. Nora Babudri
Dipartimento di Biologia cellulare e ambientale
Università di Perugia
Via Pascoli
Italy

Dr. S. Adesola Ajayi
Seed Science Laboratory
Department of Plant Science
Faculty of Agriculture
Obafemi Awolowo University
Ile-Ife 220005, Nigeria

Dr. Yee-Joo TAN
Department of Microbiology
Yong Loo Lin School of Medicine,
National University Health System (NUHS),
National University of Singapore
MD4, 5 Science Drive 2,
Singapore 117597
Singapore

Prof. Hidetaka Hori
Laboratories of Food and Life Science,
Graduate School of Science and Technology,
Niigata University.
Niigata 950-2181,
Japan

Prof. Thomas R. DeGregori
University of Houston,
Texas 77204 5019,
USA

Dr. Wolfgang Ernst Bernhard Jelkmann
Medical Faculty, University of Lübeck,
Germany

Dr. Moktar Hamdi
Department of Biochemical Engineering,
Laboratory of Ecology and Microbial Technology
National Institute of Applied Sciences and Technology.
BP: 676. 1080,
Tunisia

Dr. Salvador Ventura
Department de Bioquímica i Biologia Molecular
Institut de Biotecnologia i de Biomedicina
Universitat Autònoma de Barcelona
Bellaterra-08193
Spain

Dr. Claudio A. Hetz
Faculty of Medicine, University of Chile
Independencia 1027
Santiago, Chile

Prof. Felix Dapare Dakora
Research Development and Technology Promotion
Cape Peninsula University of Technology,
Room 2.8 Admin. Bldg. Keizersgracht, P.O. 652, Cape Town 8000,
South Africa

Dr. Geremew Bultosa
Department of Food Science and Post harvest Technology
Haramaya University
Personal Box 22, Haramaya University Campus
Dire Dawa,
Ethiopia

Dr. José Eduardo Garcia
Londrina State University
Brazil

Prof. Nirbhay Kumar
Malaria Research Institute
Department of Molecular Microbiology and Immunology
Johns Hopkins Bloomberg School of Public Health
E5144, 615 N. Wolfe Street
Baltimore, MD 21205

Prof. M. A. Awal
Department of Anatomy and Histplogy,
Bangladesh Agricultural University,
Mymensingh-2202,
Bangladesh

Prof. Christian Zwieb
Department of Molecular Biology
University of Texas Health Science Center at Tyler
11937 US Highway 271
Tyler, Texas 75708-3154
USA

Prof. Danilo López-Hernández
Instituto de Zoología Tropical, Facultad de Ciencias,
Universidad Central de Venezuela.
Institute of Research for the Development (IRD),
Montpellier,
France

Prof. Donald Arthur Cowan
Department of Biotechnology,
University of the Western Cape Bellville 7535 Cape Town, South Africa

Dr. Ekhaise Osaro Frederick
University Of Benin, Faculty of Life Science
Department of Microbiology
P. M. B. 1154, Benin City, Edo State,
Nigeria.

Dr. Luísa Maria de Sousa Mesquita Pereira
IPATIMUP R. Dr. Roberto Frias, s/n 4200-465 Porto
Portugal

Dr. Min Lin
Animal Diseases Research Institute
Canadian Food Inspection Agency
Ottawa, Ontario,
Canada K2H 8P9

Prof. Nobuyoshi Shimizu
Department of Molecular Biology,
Center for Genomic Medicine
Keio University School of Medicine,
35 Shinanomachi, Shinjuku-ku
Tokyo 160-8582,
Japan

Dr. Adewunmi Babatunde Idowu
Department of Biological Sciences
University of Agriculture Abia
Abia State,
Nigeria

Dr. Yifan Dai
Associate Director of Research
Revivicor Inc.
100 Technology Drive, Suite 414
Pittsburgh, PA 15219
USA

Dr. Zhongming Zhao
Department of Psychiatry, PO Box 980126,
Virginia Commonwealth University School of Medicine,
Richmond, VA 23298-0126,
USA

Prof. Giuseppe Novelli
Human Genetics,
Department of Biopathology,
Tor Vergata University, Rome,
Italy

Dr. Moji Mohammadi
402-28 Upper Canada Drive
Toronto, ON, M2P 1R9 (416) 512-7795
Canada

Prof. Jean-Marc Sabatier
Directeur de Recherche Laboratoire ERT-62
Ingénierie des Peptides à Visée Thérapeutique,
Université de la Méditerranée-Ambrilia Biopharma inc.,
Faculté de Médecine Nord, Bd Pierre Dramard, 13916,
Marseille cédex 20.
France

Dr. Fabian Hoti
PneumoCarr Project
Department of Vaccines
National Public Health Institute
Finland

Prof. Irina-Draga Caruntu
Department of Histology
Gr. T. Popa University of Medicine and Pharmacy
16, Universitatii Street, Iasi,
Romania

Dr. Dieudonné Nwaga
Soil Microbiology Laboratory,
Biotechnology Center. PO Box 812,
Plant Biology Department,
University of Yaoundé I, Yaoundé,
Cameroon

Dr. Gerardo Armando Aguado-Santacruz
Biotechnology CINVESTAV-Unidad Irapuato
Departamento Biotecnología
Km 9.6 Libramiento norte Carretera Irapuato-León
Irapuato,
Guanajuato 36500
Mexico

Dr. Abdolkaim H. Chehregani
Department of Biology
Faculty of Science
Bu-Ali Sina University
Hamedan,
Iran

Dr. Abir Adel Saad
Molecular oncology
Department of Biotechnology
Institute of graduate Studies and Research
Alexandria University,
Egypt

Dr. Azizul Baten
Department of Statistics
Shah Jalal University of Science and Technology
Sylhet-3114,
Bangladesh

Dr. Bayden R. Wood
Australian Synchrotron Program
Research Fellow and Monash Synchrotron
Research Fellow Centre for Biospectroscopy
School of Chemistry Monash University Wellington Rd.
Clayton,
3800 Victoria,
Australia

Dr. G. Reza Balali
Molecular Mycology and Plant Pthology
Department of Biology
University of Isfahan
Isfahan
Iran

Dr. Beatrice Kilel
P.O Box 1413
Manassas, VA 20108
USA

Prof. H. Sunny Sun
Institute of Molecular Medicine
National Cheng Kung University Medical College
1 University road Tainan 70101,
Taiwan

Prof. Ima Nirwana Soelaiman
Department of Pharmacology
Faculty of Medicine
Universiti Kebangsaan Malaysia
Jalan Raja Muda Abdul Aziz
50300 Kuala Lumpur,
Malaysia

Prof. Tunde Ogunsanwo
Faculty of Science,
Olabisi Onabanjo University,
Ago-Iwoye.
Nigeria

Dr. Evans C. Egwim
Federal Polytechnic,
Bida Science Laboratory Technology Department,
PMB 55, Bida, Niger State,
Nigeria

Prof. George N. Goulielmos
Medical School,
University of Crete
Voutes, 715 00 Heraklion, Crete,
Greece

Dr. Uttam Krishna
Cadila Pharmaceuticals limited ,
India 1389, Tarsad Road,
Dholka, Dist: Ahmedabad, Gujarat,
India

Prof. Mohamed Attia El-Tayeb Ibrahim
Botany Department, Faculty of Science at Qena,
South Valley University, Qena 83523,
Egypt

Dr. Nelson K. Ojijo Olang'o
Department of Food Science & Technology,
JKUAT P. O. Box 62000, 00200, Nairobi,
Kenya

Dr. Pablo Marco Veras Peixoto
University of New York NYU College of Dentistry
345 E. 24th Street, New York, NY 10010
USA

Prof. T E Cloete
University of Pretoria Department of Microbiology and Plant Pathology,
University of Pretoria,
Pretoria,
South Africa

Prof. Djamel Saidi
Laboratoire de Physiologie de la Nutrition et de Sécurité
Alimentaire Département de Biologie,
Faculté des Sciences,
Université d'Oran, 31000 - Algérie
Algeria

Dr. Tomohide Uno
Department of Biofunctional chemistry,
Faculty of Agriculture Nada-ku,
Kobe., Hyogo, 657-8501,
Japan

Dr. Ulises Urzúa
Faculty of Medicine,
University of Chile Independencia 1027, Santiago,
Chile

Dr. Aritua Valentine
National Agricultural Biotechnology Center, Kawanda Agricultural Research Institute (KARI)
P.O. Box, 7065, Kampala,
Uganda

Prof. Yee-Joo Tan
Institute of Molecular and Cell Biology 61 Biopolis Drive,
Proteos, Singapore 138673
Singapore

Prof. Viroj Wiwanitkit
Department of Laboratory Medicine,
Faculty of Medicine, Chulalongkorn University,
Bangkok
Thailand

Dr. Thomas Silou
Universit of Brazzaville BP 389
Congo

Prof. Burtram Clinton Fielding
University of the Western Cape
Western Cape,
South Africa

Dr. Brnčić (Brncic) Mladen
Faculty of Food Technology and Biotechnology,
Pierottijeva 6,
10000 Zagreb,
Croatia.

Dr. Meltem Sesli
College of Tobacco Expertise,
Turkish Republic, Celal Bayar University 45210,
Akhisar, Manisa,
Turkey.

Dr. Idress Hamad Attitalla
Omar El-Mukhtar University,
Faculty of Science,
Botany Department,
El-Beida, Libya.

Dr. Linga R. Gutha
Washington State University at Prosser,
24106 N Bunn Road,
Prosser WA 99350-8694

Dr Helal Ragab Moussa
Bahnay, Al-bagour, Menoufia,
Egypt.

Dr VIPUL GOHEL
DuPont Industrial Biosciences
Danisco (India) Pvt Ltd
5th Floor, Block 4B,
DLF Corporate Park
DLF Phase III
Gurgaon 122 002
Haryana (INDIA)

Dr. Sang-Han Lee
Department of Food Science & Biotechnology,
Kyungpook National University
Daegu 702-701,
Korea.

Dr. Bhaskar Dutta
DoD Biotechnology High Performance Computing
Software Applications
Institute (BHSAI)
U.S. Army Medical Research and Materiel Command
2405 Whittier Drive
Frederick, MD 21702

Dr. Muhammad Akram
Faculty of Eastern Medicine and Surgery,
Hamdard Al-Majeed College of Eastern Medicine,
Hamdard University,
Karachi.

Dr. M. Muruganandam
Departtment of Biotechnology
St. Michael College of Engineering & Technology,
Kalayarkoil,
India.

Dr. Gökhan Aydin
Suleyman Demirel University,
Atabey Vocational School,
Isparta-Türkiye,

Dr. Rajib Roychowdhury
Centre for Biotechnology (CBT),
Visva Bharati,
West-Bengal,
India.

Dr Takuji Ohyama
Faculty of Agriculture, Niigata University

Dr Mehdi Vasfi Marandi
University of Tehran

Dr FÜgen DURLU-ÖZKAYA
Gazi Üniversity, Tourism Faculty, Dept. of Gastronomy and Culinary Art

Dr. Reza Yari
Islamic Azad University, Boroujerd Branch

Dr Zahra Tahmasebi Fard
Roudehen branche, Islamic Azad University

Dr Albert Magrí
Giro Technological Centre

Dr Ping ZHENG
Zhejiang University, Hangzhou, China

Dr. Kgomotso P. Sibeko
University of Pretoria

Dr Greg Spear
Rush University Medical Center

Prof. Pilar Morata
University of Malaga

Dr Jian Wu
Harbin medical university , China

Dr Hsiu-Chi Cheng
National Cheng Kung University and Hospital.

Prof. Pavel Kalac
University of South Bohemia, Czech Republic

Dr Kürsat Korkmaz
Ordu University, Faculty of Agriculture, Department of Soil Science and Plant Nutrition

Dr. Shuyang Yu
Department of Microbiology, University of Iowa
Address: 51 newton road, 3-730B BSB bldg. Iowa City, IA, 52246, USA

Dr. Mousavi Khaneghah
College of Applied Science and Technology-Applied Food Science, Tehran, Iran.

Dr. Qing Zhou
Department of Biochemistry and Molecular Biology, Oregon Health and Sciences University Portland.

Dr Legesse Adane Bahiru
Department of Chemistry,
Jimma University,
Ethiopia.

Dr James John
School Of Life Sciences,
Pondicherry University,
Kalapet, Pondicherry

African Journal of Biotechnology

Table of Contents: Volume 16 Number 18, 3 May, 2017

ARTICLES

African Journal of Biotechnology

Table of Contents: Volume 16 Number 18, 3 May, 2017

academicJournals

Vol. 16(18), pp. 1007-1015, 3 May, 2017
DOI: 10.5897/AJB2015. 14937
Article Number: 9C6BD0064047
ISSN 1684-5315
Copyright © 2017
Author(s) retain the copyright of this article
http://www.academicjournals.org/AJB

African Journal of Biotechnology

Full Length Research Paper

Genetics and environmental trends in growth performance of Horro (Zebu) and crosses of Holstein Friesian and Jersey cattle breeds

Habtamu Abera

Oromia Agricultural Research Institute, Bako Agricultural Research Center P. O. Box 03, Bako, Ethiopia.

Received 21 August, 2015; Accepted 12 November, 2015

Phenotypic, genetics and environmental trends of birth (BW), weaning (WW) and one year weight (YW), and average daily gain were considered on data collected from Horro cattle and their crosses during the year 1980-2008. Estimated breeding value (EBV) of all animals were generated from a univariate model analysis by the general linear mixed model by residual maximum likelihood (ASREML) while least square means for annual breeding values was calculated by the General Linear Model procedure of the statistical analysis systems (SAS). Direct heritability estimates from bivariate analyses in the present study were 0.61, 0.34 and 0.42 for BW, WW, and YW, respectively. The overall mean predicted breeding value for birth, weaning and one year weight were 0.11±0.06 kg, 0.13± 0.09 kg and1.2 ±1.4 kg, respectively. The results shown that breeding value trends have been improving and there was about 0.016 kg, 0.031 kg, 0.14 kg genetic gain in BW, WW and YW per year. The negative phenotypic and environmental trends were more pronounced for weaning weight and pre-weaning average daily gains in this study. Therefore, selection of in Horro and their crosses at one year weight would be suggested from present result due to high breeding annual value, high genetic correlation and positive environmental regression value.

Key words: Breeds genetics, environment, trends.

INTRODUCTION

Genetic and environmental trends are measures of changes that take place in herds (Falconer and Mackay, 1996). They are indicators of genetic and management progresses made and thus are important in evaluation of the efficiency of breeding and determining the success of a selection programme (Musani and Mayer, 1997; Hofgren and Schinckel, 1998; Ebangi et al., 2000). Genetic and environmental trends provide information about herd improvement over time and are a reflection of the herd's progress compared to the breed as a whole (Hofgren and Schinckel, 1998). Positive genetic and environmental trends are indicators of favorable selection methods and good management, respectively. Therefore, to determine the effectiveness of genetic selection, genetic trends in the population can be considered (Van Wyk et al., 1993). Wilson and Willham (1986) reported

E-mail: HMaassee@gmail.com.

Author(s) agree that this article remains permanently open access under the terms of the Creative Commons Attribution License 4.0 International License

that trend lines are alternative methods of selection and strengthen the selection and management. Genetic and environmental trends are measures of changes that take place in herds (Wasike et al., 2006). Genetics and environment trends were important for selection within the indigenous breeds due to selection depends on correctly identifying animals with the highest true breeding value. Phenotypic, genetic and environmental trend are a quick assessment of a breeder's selection success in previous generations (Wilson and Willham, 1986).

There is scarcity of information on genetic and environmental trends in cattle breed in developing countries, which clearly indicate lack of evaluation of breeding programmes of these herds (Plasse et al., 2002). This study was, therefore, conducted with the objective of segregating the phenotypic value into environmental and genetic values and look into trends during the studies years. Therefore, examination of trends in Horro (Zebu) and crosses of Holstein Friesian and Jersey cattle breeds will provide information for re-evaluation of management practices and earlier selection programmes for efficient growth performance of these cattle.

MATERIALS AND METHODS

Study site

The data used in this study was generated from Horro cattle and their crosses kept at Bako Agricultural Research Centre during the year 1980-2008. The centre is located at about 250 km West of Addis Ababa at an altitude of 1650 m above sea level. The centre lies at about 09°6'N and 37°09'E. The area has a hot and sub humid climate and receives a mean annual rainfall of about 1220 mm, of which more than 80% falls in the months of May to September. Mean monthly minimum and maximum temperatures are about 14 and 28°C, respectively, with an average monthly temperature of 21°C. The daily mean minimum and maximum temperatures are 9.4 and 31.3°C, respectively. The vegetation cover of the area is woodland and open wood grassland type. The dominant pasture species include Hyperhenia (*Hyperhenia anamasa*) and Sporobolus (*Sporobolus prraminmidalis*) grasses and the legume Neonotonia (*Ninotonia wighti*) (Lemma et al., 1993 as cited by Temesgen, 2010).

Breeding system

Heifers are bred when they are at least two years of age and when they attain a body weight of 200 kg. Heat detection was done visually every day from 06:00 to 08:00 h in the morning and from 17:00-18:00 h in the afternoon by trained inseminator and during the grazing time by the herdsmen. Cows and heifers observed in heat were bred either naturally (local or crossbred bull) or inseminated with frozen semen of Holstein Friesian and Jersey which purchased from the National Artificial Insemination Center, within 24 h after heat.

Animals and managements

Calves were separated from their dams at birth, weighed and fed colostrum from a bucket for the first five days of life. A total of 227 L of milk was fed to each calf and a concentrate mix (49.5% ground maize, 49.5% noug seed cake and 1% salt) were offered until three months of age (weaning). After three months of age, weaned calves were maintained on natural pastures for approximately eight hours a day and supplemented with silage or hay *adlibitum* during the night and were kept as a group (male and female separately),where concentrate were supplemented to heifer calves only on availability.

Data collection

A total of 2359 calves' records were used in which produced from 184 sires and 710 dams, born from 1980 to 2008 years. Data were recorded from birth weight, weaning weight (age ranges from 61-111 days) and one year weight (age ranges 336-388 day) of Horro and its crossbred animals.

Statistical analysis

Estimation of genetic parameters

Five variables were analyzed for genetic parameters using a univariate of Animal model of procedure: birth weight (BW), weaning weight (WW), pre-weaning average daily gain (DG), post-weaning average daily gain (PDG) and one year weight (YW). Correlations among the different components of the different traits were estimated from bivariate analyses using the direct animal model. The direct animal model was chosen because of limitation of data and inability of the analysis to converge to a global maximum solution when models other than the direct animal were used.

Genetic and environmental parameters were calculated using the (co) variances estimated at convergence. Direct (h^2_a) and the direct additive covariance were calculated as (where σ^2_p is total phenotypic variance) σ^2_a/σ^2_p, and $\sigma^2_{am}/\sigma^2_{p,}$ respectively. Total heritability were calculated as $(\sigma^2_a + 0.5\sigma^2_m + 1.5\sigma_{am})/ \sigma^2_{p,}$ while direct and maternal additive correlation was expressed as a ratio of the covariance to the square root of the product of direct variance ($r_{am} = \sigma_{am} / (\sigma^2 a)$.

The models are numbered, according to Meyer (1994) as follows:

$$Y = X\beta + Z_1 a + e$$

Where: Y is the vector of observations; ß is the vector of fixed effects; X is the incidence matrix that associates ß with Y; a is the vector of breeding values for direct genetic effects; Z_1, is the incidence matrices that associate a, with Y; and e is the vector of residual effects.

Furthermore, with A, the numerator relationship matrix between animals, In, an identity matrix with order n, the number of dams, and I, an identity matrix with order of the number of records the (co) variance structure of random effects can be described as: $V(a) = \delta^2_a A$, $V(e) = \delta^2_e I$, where δ^2_a is the direct genetic variance; δ^2_e is the residual variance and δ_{am} is the genetic covariance between direct and maternal effects. All calculations were done using the options available in ASREML (Gilmour et al., 1999) for parameter and sampling error estimation.

Estimation of breeding value

Estimated breeding value (EBV) of all animals was generated from a univariate model analysis by the ASREML (Gilmour et al., 1999). Animal model where the additive effect of the animal was considered was used. Least square means for annual breeding

Table 1. (Co) variance components and genetic parameters for growth of Horro and their crosses by using Animal model.

Items	Birth weight	Weaning weight	Pre-weaning weight	One year weight	Post-weaning weight
δ^2_a	8.8±11.2	31.6±6.79	2131.0±4.1	243.9±6.6	1024±5.2
δ^2_e	5.4±10.3	47.9±12.7	8427.4±16.6	298.1±10.1	2033.9±11.9
δ^2_p	14.26±0.48	79.6±2.9	10558±360	542±22.2	3058±122
h^2_a	0.62±0.042	0.40±0.052	0.20±0.05	0.45±0.06	0.33±0.06
h^2_t	0.62±0.042	0.397±0.052	0.202±0.05	0.46±0.06	0.34±0.06

$\delta^2_{a-=}$direct additive genetic variance; δ^2p=Phenotypic variance; $h^2_{a=}$direct additive heritability; $h^2_{t=}$total heritability; and $\delta^2_{e\ =}$ error variance.

Table 2. Estimates of phenotypic (r_{p12}), direct genetic (r_{a12}) and residual (r_{e12}) correlations and heritability (h^2_a) birth (BW), weaning weight (WW), pre-weaning average daily gain (DG), one year weight (YW) and post-weaning average daily gain (PDG)

Trait1 Trait2	BW WW	BW DG	BW YW	BW PDG	WW DG	WW YW	WW PDG	DG YW	DG PDG	YW PDG
r_{p12}	0.37±0.02	-0.05±0.02	0.29±0.03	0.16±0.03	0.91±0.04	0.58±0.02	0.23±0.03	0.49±0.02	0.19±0.1	0.92±0.01
r_{a12}	0.75±0.06	0.25±0.11	0.66±0.07	0.54±0.09	0.84±0.03	0.79±0.07	0.58±0.11	0.63±0.11	0.44±0.2	0.95±0.01
r_{e12}	0.067±0.06	-0.24±0.05	-0.11±0.07	-0.15±0.07	0.95±0.06	0.45±0.05	0.048±0.0	0.47±0.04	0.12±0.1	0.92±0.01
h^2_{a1}	0.61±0.04									
h^2_{a2}	0.34±0.05	0.19±0.05	0.42±0.06	0.32±0.06						

BW=Birth weight; WW= weaning weight; DG=pre-weaning average daily gain; YW=one year weight; PDG=post-weaning average daily gain

values was calculated by the General Linear Model procedure of the statistical analysis systems (SAS, 2004) and deviations from the mean of the base year (1980) were considered as estimates of annual breeding value. Deviation from least squares means of growth performance from the base year (1980) were assumed to be estimates of annual phenotypic values. Annual environmental values were calculated as the difference between phenotypic and breeding values. Phenotypic, breeding and environmental trends were evaluated by regression of annual values (deviations from the base year) on year.

RESULTS

The overall mean predicted breeding value for birth, weaning, one year weight; pre-weaning and post-weaning average daily gains were 0.11±0.060 kg, 0.13± 0.089 kg, 1.2 ±1.4 kg, 0.93±0.57 gm and 4.6±1.1gm, respectively. The regression coefficients of breeding value for BW, WW, YW, DG and PDG with year of birth were 0.0157±0.012 kg, 0.031±0.02 kg, 0.14±0.06 kg and 0.16±0.1 g and 0.21±0.11 g, respectively. All coefficients were highly significantly different from zero (P<0.001) (Table 1). It was shown that breeding value trends have been improving and there was about 0.0157 kg, 0.031 kg, 0.14 kg and 0.16, and 0.21 g genetic gain in BW, WW, YW, DG and PDG per year. Mean of predicated breeding value for animal born in the different years ranged between, - 0.96 to 1.8 kg, -1.4 to 2.5 kg, -3.4 to 11.3 kg, -6.7 to 10.8 g and -6.2 to 22 g, respectively, for BW, WW, YW, DG and PDG. Individual breeding values for the total year ranged from -6.6 to 15 kg, -11 to 14.5 kg, -23.9 to 55 kg, -76 to 87.5 g and -50 to 96 g, respectively, for BW, WW, YW, DG and PDG, respectively. Phenotypic, genetic (breeding values) and environmental trends on year of birth for birth weight (BW), weaning weight (WW), one year weight (YW), pre-weaning average daily gain (DG) and post-weaning average daily gain (PDG) are presented in Figures 1, 2, 3, 4 and 5, respectively (Tables 3 and 4).

DISCUSSIONS

Direct heritability estimates in all models were higher than the usually accepted range of heritability of 0.4 to 0.45 for birth weight in cattle (Woldehawariate et al., 1977). Using animal model and sire model, Mohamed (2004) reported heritability estimates for birth weight for Holstein Friesian calf in Ethiopia at 0.22±0.064 and 0.27±0.11, while Demeke et al. (2003) reported direct heritability estimates of 0.14±0.03 for birth weight of purebred and crossbred cattle in Ethiopia. Values lower than those found in the current study were reported for Bos *taurus* and *Bos taurus* x *Bos indicus* crosses by Meyer (1992). The higher heritability obtained in this study is in agreement with the findings of Schoeman and Jordaan (1999) and Skrypzeck et al. (2000) who found a higher direct heritability estimates of 0.62 and 0.72 for birth weight, respectively. Both authors mentioned that fairly high

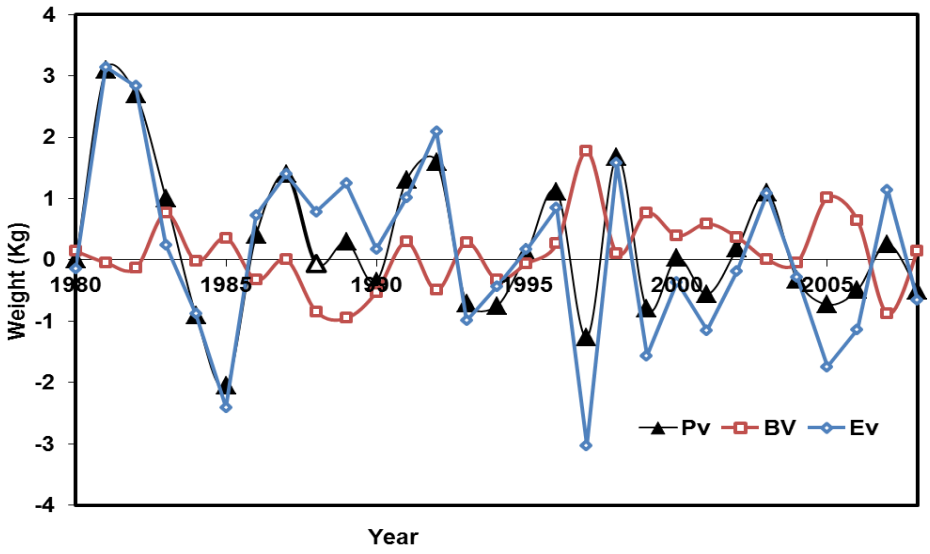

Figure 1. Annual phenotypic (PV), breeding value (BV) and environmental (EV) value trends of birth weight of Horro cattle and their crosses between 1980 and 2008.

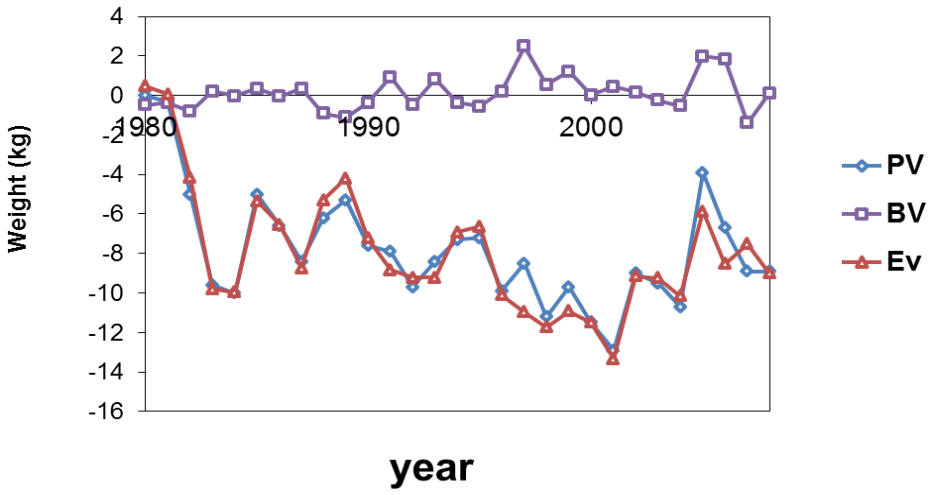

Figure 2. Annual phenotypic (PV), breeding value (BV) and environmental (EV) value trends of weaning weight of Horro cattle and their crosses between 1980 and 2008.

heritability, arising from large genetic variances due to the multibreed composition of the herd could have been expected, since the population consists of 15 breeds and this effect was not accounted for by the model. Similarly, in the current study large numbers of genetic groups were categorized into only three groups to have reasonable number of observations in each category. This would create a high level of genetic variability within a group and inflating the estimate of heritability. Direct heritability of weaning weight was lower than birth weight (Table 1). Banjaw and Haile-Mariam, (1994), Demeke et al. (2003) and Aynalem (2006) have reported lower direct heritability estimates for weaning weight of cattle in Ethiopia. Direct heritability of weaning weight was 0.40±0.052. Direct heritability estimates for one-year weight were 0.45. The result is disagreement with a value of 0.73± 0.06 reported by Aynalem (2006) for Boran cattle breeds while it is comparable than the values of 0.48, 0.32 and 0.13 reported by Banjaw and Haile-Mariam (1994) on Boran, Aynalem, (2006) for Boran crosses and Demeke et al. (2003) for purebred and crossbreds in Ethiopia. Direct heritability estimates from bivariate analyses in the present study were 0.61±0.04, 0.34±0.05, 0.19±0.05, 0.42±0.06 and 0.32±0.06 for BW,

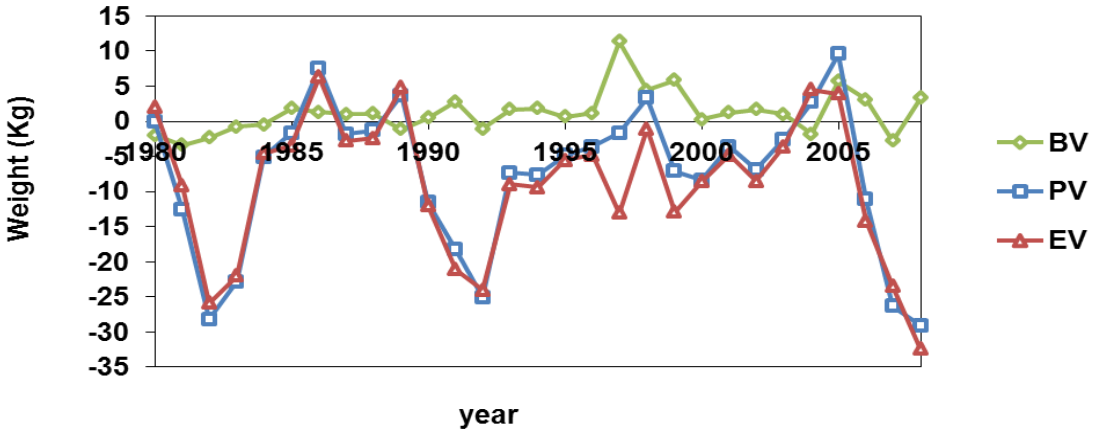

Figure 3. Annual phenotypic (PV), breeding value (BV) and environmental (EV) value trends of one year weight of Horro cattle and their crosses between 1980 and 2008.

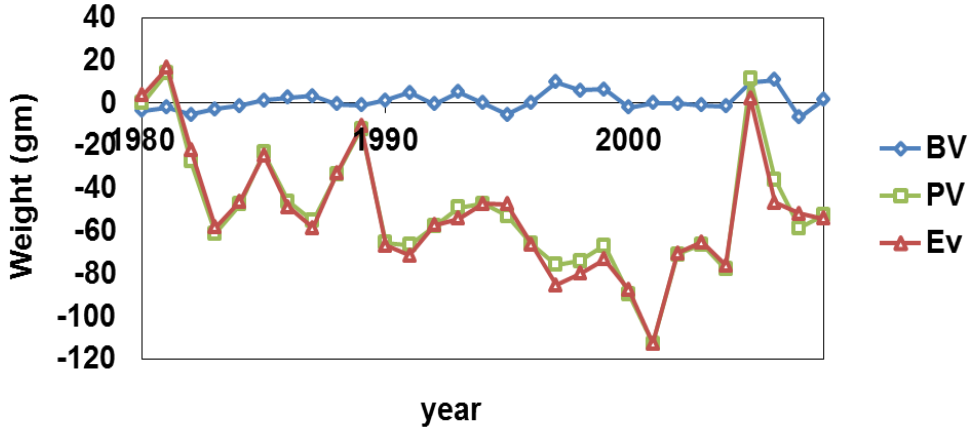

Figure 4. Annual phenotypic (PV), breeding value (BV) and environmental (EV) value trends of pre-weaning average daily gains of Horro cattle and their crosses.

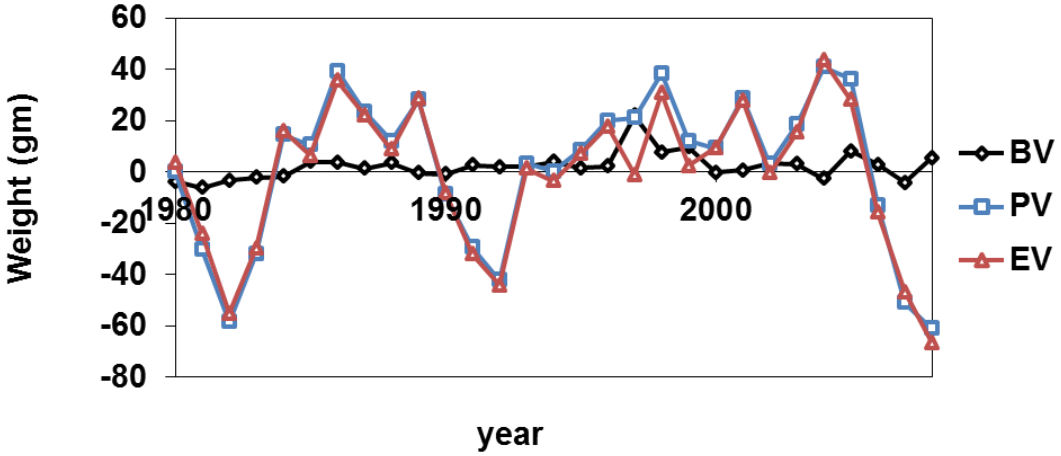

Figure 5. Annual phenotypic (PV), breeding value (BV) and environmental (EV) value trends of post-weaning average daily gains of Horro cattle and their crosses between 1980 and 2008

Table 3. Regression coefficients of phenotypic, breeding and environmental trends in birth, weaning and one year weight, pre-weaning and post-weaning average daily gains (1980-2008).

Component	Traits				
	BW	WW	DG	YW	PDG
Phenotypic	-0.043±0.03	-0.18±0.06	-1.5±0.6	-0.012±0.24	0.31±0.7
Breeding	0.0157±0.012	0.031±0.02	0.16±0.1	0.14±0.06	0.21±0.11
Environmental	-0.059±0.03	-0.21±0.06	-1.6±0.6	-0.15±0.22	0.094±0.64

BW=Birth weight; WW= weaning weight; DG=pre-weaning average daily gain; YW=one year weight; PDG=post-weaning average daily gain.

Table 4. Range of breeding values of individual Animals born in the different years (1980-2008).

Year of birth	N	Range of breeding values				
		BW (kg)	WW (kg)	YW (kg)	DG (g)	PDG (g)
1980	62	-4.5 to7.5	-8 to 11.3	-16.4 to 21.9	-52.4 to 77	-32.3 to 35.2
1981	50	5.6 to 7.2	-5.9 to 6.7	-14.4 to 17.7	-36.2 to 67	-28.3 to30
1982	85	-6.1 to 8.3	-7.7 to9.9	-20.4 to 20.4	-54 to 38	-30 to 34.1
1983	32	-2.6 to 10.6	-5.9 to4.8	-17.1 to 27	-41.9 to 26	-24 to 43
1984	40	-4.2 to5.9	-6.3 to7.3	-13.4 to 22.3	-37.6 to 37.3	-29 to 38
1985	24	-2.9 to 3.2	-5.3 to 6.2	-10.6 to 14.6	-30.4 to 28.1	-18 to 25
1986	37	-6.6 to 5.4	-6.6 to 5.9	-14.3 to 28.2	-37.6 to53.7	-40 to 51.7
1987	65	-4.9 to 7.7	-4.4 to 9.6	-18.7 to 33	-30.8 to 49.9	-34 to 63.3
1988	55	-5.8 to 5.9	-6.2 to 5.6	-11.5 to 20.3	-34.2 to 30.3	-17 to 50
1989	33	-6.2 to 7.2	-8.2 to 7.9	-15.3 to 18	-48.9 to 30	-36 to 32
1990	58	-6.3 to 5.4	-7.9 to 9.7	-15 to 14	-37 to 56.0	-21 to 21
1991	40	-3.4 to 4.6	-8.6 to 8.8	-11.9 to 25	-45.1 to 62.7	-19 to 47
1992	52	-5.4 to 3.6	-5.8 to 4.0	-12.6 to 12.4	-25 to 28	-23 to 33
1993	39	-6.5 to 5.9	-8 to 9.4	-17.6 to 18.5	-45 to 52.3	-28 to33
1994	57	-4.4 to 5.6	-8.5 to 5	-10.3 to 16.5	-68 to 32.2	-20 to 34
1995	60	-5 to 6.9	-6.6 to 8.5	-18.7 to 18.6	-54.8 to 37.3	-24 to 31
1996	80	-5.9 to 4.8	-7.2 to 6.6	-17.5 to 17.8	-54 to 39	-28 to 31
1997	95	-4.9 to 11.2	-7.2 to 11	-13.2 to 14	-52.8 to 62.7	24 to 77
1998	97	-5.8 to 6.5	-6.1 to 10.5	-14.8 to 55.1	-56.7 to 67	-37 to 96
1999	108	-5.7 to 7.9	-9.6 to 14.5	-14.1 to 28.3	-61 to 69	-32 to 60
2000	128	-5.5 to 6.9	-9.8 to 12.5	-19.9 to 39.8	-76 to 78	-37 to 65
2001	104	-5.3 to 15	-7.1 to 11.7	-23.5 to 51.4	-59 to 99	-50 to 91
2002	122	-5 to 10.6	-8.7 to 13.9	-23.9 to 43.7	-57 to 86	-45 to 78.1
2003	134	-6.7 to 12.9	-8.5 to 10.3	-21.4 to 54.4	-55 to 68.6	-46 to 91
2004	177	-4.6 to 5.9	-11 to 9.8	-21.2 to36.5	-57.8 to 65.6	-45 to 60
2005	131	-4.9 to 13	-7.8 to 13.9	-17.9 to 35.2	-47.1 to 87.5	-37 to 65
2006	171	-4.2 to 5.9	-9.5 to 13.6	-22.2 to 37.4	-63.2 to 91	-35 to 58
2007	135	-6.4 to 7.9	-10.3 to 8.1	-19.8 to 36.7	-63.5 to 60.3	-39 to 63
2008	88	-5.4 to 7.7	-8.1 to 10.9	-15.3 to 21.9	-52.1 to 75.6	-25 to 42

BW=Birth weight; WW= weaning weight; DG=pre-weaning average daily gain; YW=one year weight; PDG=post-weaning average daily gain.

WW, DG, YW and PDG, respectively. These findings were consistent with those of Meyer (1993) and Wasike (2006) on birth weight of Australian Polled Hereford cattle and Boran cattle, respectively. Other studies have reported increase in magnitude of the estimates of genetic variances and heritability from multivariate analyses as compared to parameters in univariate analyses, since univariate analyses used to compare or selected the best model from different model. This was attributed to elimination of selection bias (Mrode, 2000).

Wasike (2006) reported higher heritability estimates for weaning weight and one year weight when multivariate models were used. The direct genetic correlations between birth weight and weaning weight, pre-weaning average daily gain, one year weight and post-weaning average daily gain were: 0.75±0.06, 0.25±0.11, 0.66±0.07 and 0.54±0.09, respectively, whereas, genetic correlation between weaning weight and pre-weaning average daily gain, one year weight and post-weaning average daily gain were: 0.84±0.03, 0.79±0.07 and 0.58±0.11, respectively, in Horro cattle and its crosses. The results are in agreement with the findings of Demeke et al. (2003). There was high genetic correlation between one year weight and post-weaning average daily gain (0.95±0.01). Low and weak genetic correlations between birth weight and other growth performance traits have been reported in other studies (Haile-Mariam and Kassa-Mersha, 1994; Aynalem, 2006). The genetic correlation between birth weight with weaning weight and one year weights were positive and high, which is in agreement with the results obtained by Wasike (2006) but in disagreement with the results obtained by Aynalem (2006). The strong positive correlation may not be desirable since selection, for instance on the basis of weaning weight, could result in calving difficulties due to increased birth weight (Solomon and Gemeda, 2002; Aynalem, 2006). The phenotypic correlation between BW and other growth traits (WW, YW and PDG) were low and range from 0.16±0.03 to 0.37±0.02 but negative and low between WW and DG (-0.05±0.02). This is implies managemental problems at weaning and pre-weaning average daily gain. Phenotypic correlation between WW and YW was 0.58±0.02. Phenotypic correlation between YW and PDG were high (0.92±0.01). The high phenotypic correlation values between weaning and one year weight and between one year weight and post-weaning average daily gain. With the exception of correlation between WW and DG, genetic correlations between the traits were higher than the corresponding phenotypic correlations.

The annual breeding value trends have been improving and there was about 0.016 kg, 0.031 kg, 0.14 kg and 0.16 g and 0.21 g genetic gain in BW, WW, YW, DG and PDG per year. The possible reason for inconsistent genetic improvement in the present study could be because in the herds from which the current data was used there was no careful selection exercised. However, selection of Horro and crossbreds males calves based on total volume, total count and motility and testicular measurement for natural services at one year weight had been reported (Habtamu et al., 2007). Furthermore, selections of breeding bulls were based on visual observation (body size) and culling of inferior animals was possible reason. Relatively higher genetic gain in one year weight was presented in present results. Similarly, the largest genetic trend which could be because of the heritability of the traits since the genetic trend depends on heritability of a trait (Gray et al., 1999; Shaat et al., 2004; Temesgen, 2010). Thus it was only YW that was subjected to any kind of selection in Horro and crossbred cattle at Bako Agricultural Research Center of livestock farms.

The regression value of environmental effect on year of birth was -0.059±0.03, -0.21±0.06, -0.15±0.22, and -1.6±0.6 and 0.094±0.64 for BW, WW, YW, DG and PDG, respectively. These values were very large in magnitude when compared to genetic value and could not be counteracted by the improvement in genetic value. Thus the phenotypic trend in all traits was shown to follow the pattern of the environmental trend. The results are in agreement with findings of Solomon and Gemeda (2002) on Horro sheep at same location. Environmental and phenotypic trends showed a large decline and fluctuating patterns crosses the years (Figures 1-5).

The genetic trends for growth traits indicated a slow but positive rate of progress in growth performance in the Horro and crossbred cattle in the area studied (Figures 1-5). Improved breeding values were observed in this study, particularly between the years 1997 and 2005 for all growth traits due to crossbreeding (AI used). Herds selected on the basis of estimated breeding values have higher genetic trends than those selected based on physical appraisal. This was also the scenario in herds where proven bulls are used against herds where untested bulls are used (Plasse et al., 2002). As shown in Figures 1 and 2, the insignificant change in trends of BW and fluctuations in WW imply, calf BW was independent of environmental influence while WW fluctuated due to the fluctuation in availability feed, health and the availability of supplemented feed. The negative trends in post weaning growth traits up to 1984 were due to a lapse in management on the farms, which improved, in the later years. This shows that management of cattle has a great impact on their growth performance of the calves. The environment provided determines the ultimate growth achieved in Horro and crossbred cattle Bako Agricultural Research Center of livestock farms.

Despite some amount of genetic gain in all the traits, the phenotypic trend has shown significant decline. Wilson and Willham (1986) revealed that there is not necessary to remove environmental trends from phenotypic trends to obtain unbiased estimates of genetic trends. The same authors confirmed that environmental trends could be instructive to a commercial breeder to monitor actual management effects and/or climatic changes. However, negative phenotypic and environmental trends were more pronounced for pre-weaning average daily gains in this study. This indicates that attention needs to be given to environmental factors such as nutrition, health and management. Breeding values were almost positive, but the magnitudes varied considerably among the traits. Positive genetic and environmental trends are indicators of favorable selection methods and good management (Plasse et al., 2002).

Similar decline in the phenotypic trend in the presence of genetic gain have been reported for weaning and one year weight in Boran cattle (Haile-Mariam and Philipson, 1996), for milk yield in Sahiwal cattle in Kenya (Rege and Wakhungu, 1992) and for Horro sheep (Solomon and Gemeda, 2002). Solomon and Gemeda (2002) reported that increase in stocking rate, increasing crop land, deterioration of grazing area, fluctuations in climatic conditions, morbidity, the turnover of people who worked in the management of the Horro sheep flock and more use of portion of the flock to stressful experiments might have contributed to the decline and erratic nature of the environmental and phenotypic trend. This explanation is probably true for the present results since the animals reared under the same management and environmental situations. Plasse et al. (2002) observed fluctuating phenotypic trends for 548- day weight, which was attributed to the deterioration in pastures during the study period. From this result it can be suggested that genetic improvement work should be supported by improved environment.

CONCLUSIONS AND RECOMMENDATIONS

This study has also shown higher estimates genetic parameters when animal models used for growth performance of Horro and their crosses. The genetic correlation estimates between various growth traits are strong. The genetic correlation between birth weight with weaning and one year weights were positive and high. This may not be desirable since selection for instance on the basis of weaning weight could result in calving difficulties due to increased birth weight. Similarly, the negative phenotypic and environmental trends were more pronounced for weaning weight and pre-weaning average daily gains in this study. This indicates that attention needs to be given to environmental factors such as nutrition and management. However, breeding values were almost positive, but the magnitudes varied considerably among the traits. The result also suggests that improvement in genetic gain should be accompanied by either improvement of the management. This ensures whatever is gained through genetic means may not be lost due to decline in level of management. Selection of Horro and their crosses at one year weight would be suggested from present result due to high breeding annual value, high genetic correlation and positive environmental regression value.

CONFLICT OF INTERESTS

The author has not declared any conflict of interests.

REFERENCES

Aynalem H (2006). Genetic and Economic Analysis of Ethiopian Boran Cattle and their Crosses with Holstein Friesian in Central Ethiopia. A Ph.D. Thesis division of dairy cattle breeding National dairy research institute, Karnal-132001 (Haryana), India. Pp.65-146.

Banjaw K, Haile-Mariam M (1994). Productivity of Boran cattle and their Friesian crosses at Abernossa ranch, rift valley of Ethiopia. II. Growth performance. Trop. Anim. Health Prod. 26:49-57.

Demeke S, Neser FWC, Schoeman SJ (2003). Variance components and genetic parameters for early growth traits in a mixed population of purebred Bos indicus and crossbred cattle. Livest. Prod. Sci. 84:1-11.

Ebangi AL, Erasmus GJ, Neser FWC, Tawah CL (2000). Genetic trends for growth in the Gudali and Wakwa cattle breeds of Cameroon. S. Afr. J. Anim. Sci. 30:36-37.

Falconer DS, Mackay TFC (1996). Introduction to Quantitative Genetics. 4th Ed. Longman Group, LTD., Harlow, Essex, UK.

Gilmour AR, Cullis BR, Welham SJ, Thompson R (1999). ASREML reference manual. NSW Agriculture Biometric Bulletin No 3.NSW Agriculture, Orange, NSW, Australia, 210p.

Gray HQ, Neser FWC, Erasmus GJ, Van WYK (1999). Genetic trends in South African Mutton Merino nucleus breeding scheme. S. Afr. J. Anim. Sci. 29(1):48-53.

Habtamu A, Ulfina G, Chala M, Yosef K, Mulugeta K, Jiregna D (2007). Seminal attributes and testicular measurements of Horro-Friesian dairy bulls at different age and season under Bako condition, Western Oromia. Institutional arrangement and challenges in market-oriented livestock agriculture in Ethiopia. Proceeding of the 14th Annual Conference of the Ethiopia Society of Animal Production (ESAP) held in Addis Ababa, Ethiopia, September 5-7, 2006. P.171.

Haile-Mariam M, Kassa-Mersha H (1994). Estimates of direct and maternal (co)variance components of growth traits in Boran cattle. In: Genetic analysis of Boran, Friesian and crossbred cattle in Ethiopia. PhD Thesis, Swedish University of Agricultural Sciences, Uppsala, Sweden. P.85.

Haile-Mariam M, Philipson J (1996). Estimates of genetic and environmental trends of growth traits in Boran cattle. J. Anim. Breed. Genet. 113:43-55.

Hofgren DL, Schinckel AP (1998). Within-herd genetic trends provide important information for breeders. In Proceedings of the Swine day Symposium, University of Purdue. pp. 185-187.

Meyer K (1992). Variance components due to direct and maternal effects for growth traits of Australian beef cattle. Livest. Prod. Sci. 31:179-204.

Meyer K (1993). Covariance matrices for growth traits of Australian Polled Hereford cattle. Animal Production. 57:37.

Meyer K (1994). Estimates of direct and maternal correlations among growth traits in Australian beef cattle. Livest Prod. Sci. 38: 91-105.

Mohamed A (2004). Estimates of genetic parameters of birth weight, age at first calving and milk production traits in Holstein Friesian dairy herds kept in three state farms. An MSc Thesis presented to School of Graduate studies of Alemaya University. 89p.

Mrode RA (2000). Linear Models for Animal Breeding Values.CABI International, UK. London. Pp. 20-150.

Musani SK, Mayer M (1997). Genetic and environmental trends in a large scale commercial Jersey herd in the central Rift Valley, Kenya. Trop. Anim. Health Prod. 29:108-116.

Plasse DO, Verd H, Fossi R, Romero R, Hoogesteijn P, Bastardo J (2002). (Co)variance components, genetic parameters and annual trends for calf weights in a pedigree Brahman herd under selection for three decades. J. Anim.Breed. Genet. 119: 141-153.

Rege JEO, Wakhungu JW (1992). An evaluation of long-term breeding programme in a closed Sahiwal herd in Kenya II. Genetic and Phenotypic trends and levels of inbreeding. J. Anim. Breed. Genet. 109:374-384.

SAS (Stasitical Analyses System) (2004). SAS User's Guide. Cary, North Carolina, USA, SAS Institute Inc., NY, Cary.

Schoeman SJ, Jordaan GF (1999). Multitrait estimation of direct and maternal (co)variances for growth and efficiency traits in a multibreed beef cattle herd. S. Afr. J. Anim. Sci. 29:124.

Shaat IS, Galal H, Mansour (2004). Genetic trends for lamb weights in flocks of Egyptian Rahmani and Ossimi sheep. Small Rumin. Res. 51(1):23-28.

Skrypzeck H, Schoeman SJG, Jordaan F, Neser FWC (2000). Pre-

weaning growth traits of the Hereford breed in a multibreed composite beef cattle population. S. Afr. J. Anim. Sci. 30(3):220-229.
Solomon A, Gemeda D (2002). Genetic and Environmental Trends in Growth Performance in a Flock of Horro Sheep. Ethiop. J. Anim. Prod. 2(1):49-58.
Temesgen J (2010). Estimation of Genetic Parameters, Breeding Values and Trends in Cumulative Monthly Weights and Daily Gains of Ethiopian Horro Sheep. MSc thesis, Haramaya University, Haramaya, Ethiopia.
Van Wyk JB, Erasmus GJ, Konstantinov KV (1993). Genetic and environmental trends of early growth traits in the Elsenburg Dormer sheep stud. S. Afr. J. Anim. Sci. 23(3):85-87.
Wasike CB (2006). Genetic evaluation of growth and reproductive performance of Kenya Boran Cattle. A MSc. Thesis, Egerton University, Njoro, Kenya. pp. 65-77.
Wasike CB, Ilatsia ED, Ojango JMK, Kahi AK (2006). Genetic parameters for weaning weight of Kenyan Boran cattle accounting for direct-maternal genetic covariance. S. Afr. J. Anim. Sci. 36(4):275-281.
Wilson DE, Willham RL (1986). Within-herd phenotypic, genetic and environmental trend lines for beef cattle breeders. J. Anim. Sci. 63:1087-1094.
Woldehawariate GMA, Talamantes RR, Petty JR, Cartwright TC (1977). A summary of Genetic and environmental statistics for growth and conformation characterters in young beef cattle. (II ed) Texas Agric. Exp. Stat. Dep. Teh. Rep. No. 103.

academicJournals

Vol. 16(18), pp. 1016-1031, 3 May, 2017
DOI: 10.5897/AJB2017.15910
Article Number: 982454764051
ISSN 1684-5315
Copyright © 2017
Author(s) retain the copyright of this article
http://www.academicjournals.org/AJB

African Journal of Biotechnology

Full Length Research Paper

Silencing of the rift valley fever virus s-genome segment transcripts using RNA interference in *Sf*21 insect cells

Juliette Rose Ongus*, Evans Kiplangat Rono and Fred Alexander Wafula Wamunyokoli

Jomo Kenyatta University of Agriculture and Technology, P. O. Box 62000-00200 Nairobi, Kenya.

Received 23 January, 2017; Accepted 10 April, 2017

Rift Valley fever (RVF) is a mosquito-borne disease that affects humans and livestock. It results in economically disastrous livestock deaths in Africa. The causative agent is RVF virus (RVFV), which possesses a tripartite negative-sense, single-stranded RNA genome, with large (L), medium (M) and small (S) segments. The lack of effective vaccines and anti-RVFV therapies motivates concerted efforts in search for safe and effective remedies. Recent advances in the RNA interference (RNAi) may provide promising tools to control RVFV. This study aimed to use the Baculovirus Expression Vector System to demonstrate that the RVFV S-genome segment is susceptible to RNAi. A multiplex short hairpin RNA (shRNA) transcription cassette was constructed for generating small interfering RNA (siRNA) that target both the RVFV genomic RNA transcripts and the Green Fluorescent Protein (GFP) which was used as a reporter gene. Two expression vectors were constructed; one for expressing the RVFV S-genome alone and the other one for simultaneous expression of both the RVFV S-genome and the shRNA cassette. A separate transiently expressed GFP only vector was included as an internal positive control to be expressed simultaneously when co-transfected into *Sf*21 insect cells with each RVFV-S construct to monitor the effectiveness of the shRNA to trigger RNAi. By design, the RNAi effect on both the RVFV-S and the GFP transcripts was driven from the same shRNA. A statistically significant reduction in the relative GFP fluorescence ($P < 0.05$) was demonstrated and a drop in GFP and the RVFV S transcript levels observed. Collectively, these results suggest the potential application of RNAi as an antiviral strategy against RVFV.

Key words: Baculovirus Expression, rift valley fever, RNA interference, green fluorescent protein.

INTRODUCTION

Rift Valley fever virus (RVFV) (genus: *Phlebovirus*, family: Bunyaviridae) is an enveloped virus (Muller et al., 1994; Giorgi, 1996; Ellis et al., 1988; Nichol et al., 2005; Sindato et al., 2015). The primary vectors of the virus are transovarially-infected floodwater mosquitoes of the *Aedes* species (Linthicum et al., 1999; Nichol et al., 2005;

*Corresponding author. E-mail: julietteongus@jkuat.ac.ke. Tel: +254 722 339682.

Author(s) agree that this article remains permanently open access under the terms of the Creative Commons Attribution License 4.0 International License

Sang et al., 2017). The virus causes an arthropod-borne RVF disease, which is a major public health threat due to its serious epizootics and epidemics in sub-Saharan Africa (WHO, 2007; Breiman et al., 2008; Boshra et al., 2011). The epizootics result in devastating abortions in pregnant animals (Swanepoel and Coetzer, 2004) and up to 100% mortality rates in domestic animals (Easterday et al., 1962; Meegan et al., 1979; Meegan et al., 1981).

In Kenya, the virus was first isolated in 1930 along Lake Naivasha in the greater Rift Valley, during which sweeping deaths and abortion storms among sheep were reported (Daubney et al., 1931). The 2006/2007 RVFV outbreak in eastern Africa (Sindato et al., 2015) caused 45% human case fatality, and 100 and 60% mortality rates in young and adult livestock respectively (WHO, 2007; CDC, 2007). Effective vaccines for animals and prevention methods for humans are lacking. The currently ineffective or short-acting vaccines for animals against the RVFV and lack of prevention and treatment methods for humans mean that the affected populations remain susceptible (Ikegami and Makino, 2009; Pepin et al., 2010; Boshra et al., 2011). Thus, concerted efforts in search for safe antiviral therapies that will offer effective treatment and prevention strategies are needed. Research on recombinant subunit vaccine development based on the RVFV surface glycoproteins is currently underway (Faburay et al., 2016).

The RVFV possesses a tripartite genome, which is composed of three negative-sense, and single-stranded RNA segments designated as large (L), medium (M) and small (S) where the L and M are of negative polarity while S is of ambisense polarity (Elliott, 1990; Muller et al., 1994; Giorgi, 1996). The L segment (6,404 nucleotides, nt) codes for a 237-kDa L protein, which is the viral RNA-dependent RNA polymerase in a single ORF (Muller et al., 1994). The M segment (3885 nt) codes for a polyprotein precursor to the glycoproteins encoded in a single ORF (Collett et al., 1985). The S segment (1690 nt) codes for two proteins, the 27 kDa nucleoprotein N and a 31-kDa non-structural protein called NSs by utilizing an ambisense strategy (Giorgi et al., 1991).

RNA interference (RNAi) is a highly sequence specific RNA-dependent gene regulatory mechanism by which double-stranded RNA (dsRNA) targets complementary mRNA for degradation (Hannon, 2002; Agrawal et al., 2003; Kang et al., 2008). RNA interference is one of the most promising platform for the development of therapeutics against viral pathogens (Faburay et al., 2016). RNAi can be triggered experimentally by exogenous introduction of dsRNA or using DNA-based vectors, which express short hairpin RNA (shRNA) in the cytoplasm that are processed by Dicer into siRNAs (Swamy et al., 2016; McGinnis, 2010). Expression of short hairpin RNA (shRNA) from plasmids triggers the RNAi pathway, and this gives the promise of developing new RNAi -based gene therapies for controlling of some pathogens (McCaffrey et al., 2002). This gene-specific therapeutic tool may escape some of the limitations of conventional medicinal chemistry (Hannon and Rossi, 2004). RNAi has been widely demonstrated *in vitro* against many viruses (Ge et al., 2004; Nishitsuji et al., 2006; Carmona et al., 2006; Shi et al., 2010). The RVFV genome sequence in highly conserved at 95% (Liu et al., 2003; Nderitu et al., 2011) making it a good candidate silencing using the RNA approach.

The Baculovirus Expression Vector System (BEVS) (Invitrogen, Carlsbad, CA, USA) uses a recombinant *Autographa californica* Multiple Nuclear Polyhedrosis Virus (*Ac*MNPV) to express high levels of heterologous gene products in lepidopterans *Spodoptera frugiperda* and *Trichoplusia ni* as host insects. The *Ac*MNPV can accommodate foreign genes of interest that are transferred from the expression cassette to the baculovirus genome by site-specific homologous recombination *in vivo* (Vlak and Keus, 1990). It allows expression in a variety of lepidopteran cells including those derived from *S. frugiperda* such as *Sf*21 cells (Theilmann and Stewart, 1992). The pFastBac™ Dual vector is an example of the expression vectors that are used in the BEVS, which has two strong baculovirus promoters, P_{PH} and P_{P10} to allow simultaneous high-level expression in insect cells (Harris and Polayes, 1997; O'Reilly et al., 1992) and two large multiple cloning sites to facilitate cloning. Another example is the *OpIE2* immediate-early promoter from the baculovirus *Orgyia pseudotsugata* Multicapsid Nuclear Polyhedrosis Virus (*Op*MNPV) in the pIZ/V5-His vector, is employed to express genes of interest (Invitrogen). The *OpIE2* promoter synthesizes high levels of constitutive expression at levels equivalent to those obtained from the P_{PH} and P_{P10} promoters (Theilmann and Stewart, 1992).

The goal of this study was to demonstrate the susceptibility of the RVFV S-genome segment to RNAi in a BEVS model system. The P_{p10} and P_{PH} dual promoter feature of the pFastBac™ Dual vector was used to show the activity of short hairpin RNA (shRNA) transcription cassette against the RVFV S-genome transcript in a dual gene knock-down approach in insect cells.

MATERIALS AND METHODS

The RVFV isolate

A collaborative effort of the Centers for Disease Control and Prevention (CDC) in Kenya and the Kenya Medical Research Institute (KEMRI) isolated the RVFV isolate that was used in this study from infected human serum that was obtained in a separate outbreak investigation from Garissa County in the North Eastern part of Kenya during the 2006/2007 epidemics (Nderitu et al., 2011). This isolate was named the Garissa 004. The isolate was already classified, sequenced, cultured and archived at -80°C as KEN/ Gar-004/06 (GenBank accession no. HM586975 for S segment, HM586964 for M segment, HM586953 for L segment) (Nderitu et al., 2011). For this study, the archived RVFV isolate was amplified by passaging in Vero cells in the Biosafety level-3 (BSL-3) laboratory facility at CDC/KEMRI in Nairobi, Kenya.

Table 1. Primers to amplify full-length RVFV S-genome segment cDNA and GFP.

Name	5´-3´ sequence	Restriction site
RVFV-S-F	***CTCGAG***TACACAAAGCTCCCTAGAGATAC	*Xho*I
RVFV-S-R	***GGTACC***TACACAAAGACCCCCTAGTGC	*Kpn*I
GFP-F	***GAATTC***ATGGCTAGCAAAGGAGAAGAAC	*Eco*RI
GFP-R	***GAATTCATGCAT***TTATTTGTAGAGCTCATCCATGCC	*Eco*RI-*Nsi*I

Total RVFV genomic RNA isolation

The positive cell culture supernatant was used to isolate RVFV genomic RNA using QIAamp® Viral RNA Kit (Qiagen) as per the manufacturer's instructions. The quality of the isolated RVFV genomic RNA assessed by quantification in BioSpec-Mini Spectrophotometer (Shimadzu Corporation) at 120 ng/µl and observed by gel electrophoresis. The RNA was finally aliquoted and stored at -80°C to await the RT-PCR application.

Promoters and recombinant transcription vectors

Very-late strong baculovirus promoters P_{PH} and P_{P10} in the pFastBac™ Dual vector (Invitrogen, Carlsbad, CA, USA) were utilized to express both the RVFV S-genome and the shRNA cassette. These allow simultaneous high-level expression in insect cells and two large multiple cloning sites to facilitate cloning were used (Harris and Polayes, 1997; O'Reilly et al., 1992). A second expression vector the pIZ/V5-His vector plasmid (Invitrogen, Carlsbad, CA, USA) was used to expresses the GFP reporter gene using the *OpIE2* immediate-early promoter. The *OpIE2*, promoter utilizes the host cell transcription machinery and does not require viral factors for activation but is activated upon arrival in the cytoplasm of the host cell (Friesen and Muller, 2001). It allows expression in a variety of lepidopteran cells including those derived from *S. frugiperda* (such as *Sf*21 cells) (Theilmann and Stewart, 1992).

Construction of recombinant pFastBacDual-S (pFBD-S) transcription vector

To amplify the entire length of the RVFV S-genome segment for cloning into the pFastBac Dual™ expression vector vector, 2 µg of the RVFV total genomic RNA sample was used in the RT-PCR in complementary DNA (cDNA) synthesis with SuperScript III/ Platinum *Taq* DNA polymerase high fidelity enzyme mix as per the manufacturer's instructions (Invitrogen, Carlsbad, CA, USA).

Primers RVFV-S-F and RVFV-S-R were used for the amplification and to introduce *Kpn*I and *Xho*I restriction enzymes restriction sites respectively for cloning (Table 1). The other two RVFV full-length genome segments (L and M) were unsuccessfully cloned, and therefore are not analysed in this study. The RT-PCR cycling parameters were 1 cycle of 51°C for 60 min and 94°C for 2 min, followed by 40 cycles of 94°C for 15 s, 56°C for 30 s, and 68°C for 2 min, followed by a final extension at 68°C for 5 min. The PCR products were detected by electrophoresis in a 1% agarose gel stained with ethidium bromide and running at 10 volts/cm for 45 min. The amplicons were purified from the agarose gel using the S.N.A.P™ gel purification kit (Invitrogen, Carlsbad, CA, USA) according to the manufacturer's instructions.

The purified PCR products of the RVFV S-genome segment were ligated into the pGEM®-T Easy Vector (Promega) for TA cloning as per the manufacturer's instructions to generate pGEM®-T Easy-S construct (Abbreviated as pGEMT-S). Following the blue-white screening, white colonies carrying the cloned inserts were selected from the LB agar plates (containing 100 µg/ml ampicillin and 20 µg/ml X-gal) for colony PCR screening and sequencing to further confirm the positive clones.

Recombinant plasmids were purified using the GenScript kit (GenScript Corporation, Piscataway, NJ) from the overnight LB broth culture containing 100 µg/ml ampicillin. The RVFV S-segment cDNA insert was directionally subcloned from the pGEMT-S plasmid into the pFastBac Dual™ vector under the control of the P_{P10} promoter in order to generate a recombinant plasmid pFastBac Dual™ -*S* (abbreviated as pFBD-S) construct.

To do this, the plasmid pGEMT-S was digested with *Kpn*I and *Xho*I restriction enzymes and subcloned into the pFastBac Dual™ vector digested with the same enzymes (Table 1) according to the manufacturer's instructions. The recombinant pFBD–S clones were selected on LB agar plates (containing 100 µg/ml ampicillin and 7 µg/ml gentamycine) and confirmed by the *Kpn*I-*Xho*I restriction enzyme double digestions.

Construction of recombinant pFBD-shRNA transcription vector

In order to generate fragments for the short hairpin RNA (shRNA) transcription cassette, a 1253 bp multiplex shRNA template containing 150 bp fragments each from the RVFV L, M and S genome segments and 150 bp of GFP (Figure 1, Figure S3) was designed and amplified by PCR (Table 2). These fragments were selected from the regions with 30 to 50% GC content (for optimal activity), which were identified using the Ambion siRNA Target Finder (www.ambion.com/techlib/misc/siRNA_finder.html). The RVFV L (genome location 6056-6205), M (genome location 3437-3586) and S (genome location 1127-1276) segment portions were amplified by the RT-PCR from the RVFV RNA templates (Nderitu et al., 2011). The GFP fragment was amplified by PCR using the pcDNA-DEST47 Gateway® Vector as DNA template (Invitrogen, Carlsbad, CA, USA) (plasmid location 2628-3347) (GFP ORF location 193-342) was amplified by PCR. The optimized shRNA PCR primer annealing temperatures were as follows: For shGFP-F/shGFP-R, RVFV-shL-F/RVFV-shL-R, RVFV-shM-F/RVFV-shM-R and RVFV-shS-F/RVFV-shS-F were 58, 52, 56 and 60°C respectively. The extension and final extension times in all their PCR cycling parameters were 45 s and 3 min respectively. All the PCR products were detected and purified as described earlier.

The four fragments were first sequentially cloned into the pGEMT vector to generate the recombinant plasmid pGEM®-T -*shRNA* (abbreviated as pGEMT-shRNA). In brief, the shRNA chimeric gene construct (Figure 1) was cloned in the following sequential order: First the 640 bp forward-facing, that is, genomic sense (GS) construct was cloned starting with the 150 bp L segment which was cloned using the restriction enzymes *Bam*HI and *Spe*I; 150 bp M using *Spe*I and *Not*I; 150 bp S using *Not*I and *Pst*I; and 150 bp GFP using *Pst*I and *Hind*III. A 13-nucleotide loop spacer containing an *Eco*RI restriction site was introduced using the shGFP-R primer to create a separator between the GS and reverse complement (RC) regions to allow for the shRNA transcript to fold on itself to create a dsRNA that would trigger RNAi in the cells (Figure 1). Next, the 632

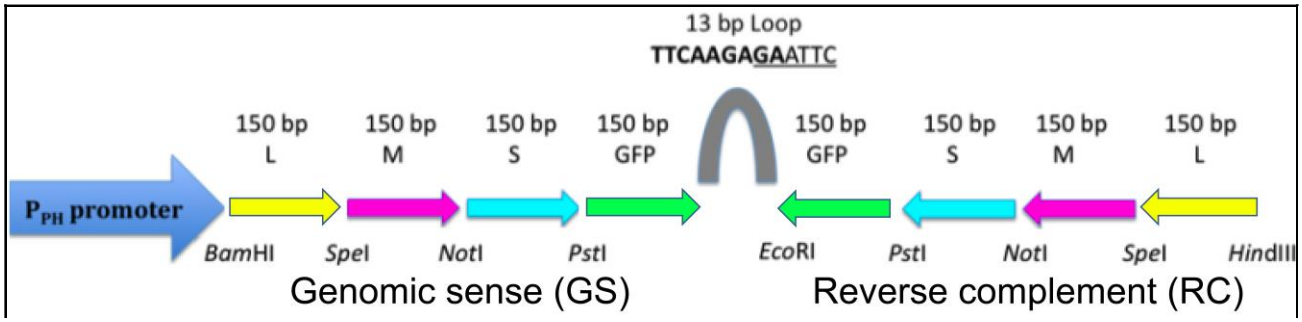

Figure 1. Schematic representation of the complete 1253 bp multiplex shRNA transcription constructs. The colour codes correspond to the same fragments and the arrow points to the direction of the ORF of the cloned insert/fragment in the schematic illustration. The restriction sites that are indicated were used for sequential cloning of the fragments. The 150 bp L, M and S fragments respectively were cloned from the cDNA from the RVFV KEN/ Gar-004/06 isolate (GenBank accession no. HM586953 for L segment, HM586964 for M segment and HM586975 for S segment) using the primers indicated in Table 2. The 150 bp DNA fragments of the GFP was amplified from the GFP ORF in the pcDNA-DEST47 Gateway® Vector. The whole piece of the GS region was used as a DNA template in PCR to amplify and directionally cloned the RC region separated by a 13 bp loop as showed. Upon transcription in the insect cells, the RNA transcript that is transcribed forms a shRNA cassette with an hairpin structure, because the GS portion is complementary to the RC portion. When the *RNAi* is induced, the shRNA cassette is processed by dicing to produce a mixed population of *siRNAs* for different fragments (L, M, S and GFP). In this study, the ability of the S and the GFP *siRNAs* to degrade the transcripts of the RVFV S-genome segment and the GFP respectively were assessed.

Table 2. Primers for construction of 150 bp fragments of multiplex shRNA transcription cassette.

Name	5´-3´ sequence	Restriction site
RVFV-shL-F	CGC***GGATCC***AGAGAACCTTTGATAAATCATAGTC	*Bam*HI
RVFV-shL-R	CGC***ACTAGT***AGGACATCAGTTCATTATCTATGATTGC	*Spe*I
RVFV-shM-F	CGC***ACTAGT***CACATTTTAGAGAGGCCTGTTCTTCC	*Spe*I
RVFV-shM-R	CGC***GCGGCCGC***TTGGAATTTCTTTGACTGGTTTTCTGG	*Not*I
RVFV-shS-F	CGC***GCGGCCGC***CTTCCTGTCACTGGGACAACCATGG	*Not*I
RVFV-shS-R	CGC***CTGCAG***CAGATACAGAGAGTGAGC	*Pst*I
shGFP-F	CGC***CTGCAG***TTCTCTTATGGTGTTCAATGCTTTTCC	*Pst*I
shGFP-R	CGC***AAGCTTCGGAATTC***TCTTGAACTTGACTTCAGCACGCGTCTTGTAG	*Hin*dIII-*Eco*RI
shRC-F	GCG***GAATTC***TCTTGAACTTTGATTCC	*Eco*RI
shRC-R	CGC***AAGCTT***AGAGAACCTTTGATAAATCATAGTC	*Hin*dIII

bp reverse-facing, that is, RC construct (complementary to the GS construct) was amplified by PCR from the entire GS portion using the RC primer pair shRC-F and shRC-R (Table 2) and Platinum *Taq* DNA polymerase (Invitrogen, Carlsbad, CA, USA). The following optimized PCR cycling parameters were used; 1 cycle of 94°C for 2 min, followed by 40 cycles of 94°C for 30 s, 60°C for 30 s and 72°C for 1 min, and a cycle of final extension at 72°C for 5 min. The PCR products were analyzed as mentioned before, and directionally cloned into the pGEMT-GS recombinant plasmid construct using *Hind*III and *Eco*RI restriction enzymes in order to form a complete shRNA transcription construct that constitutes the GS and the RC parts.

Using the same restriction enzymes, the shRNA insert was then directionally subcloned from the pGEMT-shRNA construct into the pFastBac Dual™ vector under the control of the P_H promoter to generate the recombinant plasmid pFastBac Dual™ *-shRNA* (abbreviated as pFBD-shRNA). Colonies carrying the recombinant pFBD-shRNA clones were selected on LB agar plates as described previously.

Construction of recombinant pFBD-S/shRNA transcription vector

To generate the recombinant plasmid with the ability to transcribe both the RVFV-S genome transcript and the shRNA, *pFastBacDual-S/shRNA* (abbreviated as pFBD-S/shRNA), the RVFV S-segment was then directionally subcloned from pGEMT-S recombinant construct into pFBD-shRNA under the control of the P_{p10} promoter using the *Kpn*I and *Xho*I restriction enzymes. Colonies carrying the recombinant pFBD-S/shRNA plasmid clones were screened, propagated and purified as mentioned previously.

Construction of recombinant pIZ/V5–GFP transcription vector

The GFP expression vector for transcribing the GFP as an internal positive control in insect cells, was constructed. To do this, an Open Reading Frame of 720 bp GFP was amplified from the pcDNA-DEST47 Gateway® Vector (Invitrogen, Carlsbad, CA, USA) using

Table 3. Duplicate *in vitro* transcription experimental setup on 6-well cell culture plates.

Well no. 1	**Well no. 2**	**Well no. 3**
Well no. 4	**Well no. 5**	**Well no. 6**
Well 1 and 4: Mock-transfected control cells.		
Well 2 and 5: siRNA-negative control cells (Co-transfection of *Ac*MNPV Bacmid-S and pIZ/V5–GFP).		
Well 3 and 6: siRNA-positive test cells (Co-transfection of *Ac*MNPV Bacmid-S/shRNA and pIZ/V5–GFP)		

the Platinum *Taq* DNA polymerase enzyme (Invitrogen, Carlsbad, CA, USA).

The pcDNA-DEST47 Gateway® Vector (1 µg) was used as the GFP template in 50 µl PCR reaction volume. The cycling parameters were 1 cycle of 94°C for 2 min, followed by 40 cycles of 94°C for 30 s, 60°C for 30 s, and 72°C for 1 min, followed by a final extension at 72°C for 7 min utilizing the GFP PCR primers GFP-F and GFP-R (Table 1).

The PCR products were analyzed and purified as described earlier, then cloned into the pGEM®-T Easy Vector in order to construct a pGEMT-GFP recombinant plasmid. The PCR primers introduced into the PCR product 18 bp additional *Eco*RI and *Eco*RI-*Nsi*I restriction sites for cloning. Using the *Eco*RI restriction enzyme, the GFP insert was then sub-cloned from the pGEMT-GFP construct into the pIZ/V5-His vector (Invitrogen, Carlsbad, CA, USA) under the *OpIE2* promoter in order to construct GFP expression vector (pIZ/V5-GFP) for transfecting into insect cells. Colonies carrying the recombinant pIZ/V5-GFP clones were selected on 50 µg/ml Zeocine selective LB agar plates.

Sequencing the recombinant plasmid constructs

All the purified plasmid constructs were sequenced by Sanger sequencing at Macrogen, Inc. (South Korea). The sequences were edited using Bioedit software version 5.0.6 (Ibis Biosciences) and a similarity nucleotide search was obtained by BLAST in the National Center for Biotechnology Information (NCBI) website (http://blast.ncbi.nlm.nih.gov/Blast.cgi. ClustalX and Mega 4 (Tamura et al., 2007) software were also used to align the sequences. These analyses confirmed that there were no PCR-generated mutations, which would interfere with the sequence specificity of the RNAi mechanism.

Propagation of recombinant pFBD-S and the pFBD-S/shRNA bacmids in DH10Bac™ *E. coli* cells

To generate recombinant *Ac*MNPV Bacmid DNA for transfecting into insect cells, 2 ng of each of the pFBD-S and the pFBD-S/shRNA expression vectors were propagated and isolated independently from chemo-competent DH10Bac™ cells following manufacturer's instructions (http://tools.invitrogen.com/content/sfs/manuals/bactobac_man.pdf) (Invitrogen, Carlsbad, CA, USA). In summary, the pFBD-S was used to generate large molecular weight *Ac*MNPV recombinant baculovirus genome containing the S-genome segment (*Ac*MNPV Bacmid-S DNA). While the pFBD-S/shRNA was used to generate large molecular weight *Ac*MNPV recombinant baculovirus genome containing the S segment and the multiplex chimeric shRNA transcription cassette (*Ac*MNPV Bacmid-S/shRNA DNA).

Transfection of recombinant pFBD-S and the pFBD-S/shRNA Bacmid DNAs into *Sf*21 cells for *in vitro* transcription

To transcribe in insect cells the S-genome, the shRNA transcription cassette, and the GFP, the recombinant AcMNPV Bacmid-S and Bacmid-S/shRNA were standardized and transfected into *Sf*21 cells according to the supplier's Bac-to-Bac® guidelines (Invitrogen, Carlsbad, CA, USA). The *Sf*21 cells (2.0×10^6) of greater than 95% viability for use in the transfections were seeded in a 6-well plate (Invitrogen, Carlsbad, CA, USA). A master mix was separately prepared by diluting gently 10 µl of 16.9 µg/ml recombinant pFBD-S Bacmid DNA and 10 µl of 12.6 µg/ml pIZ/V5–GFP plasmid construct in 100 µl of 0.2 µm filter sterilized Grace's Unsupplemented Medium, without antibiotics or serum per well. The same procedure was repeated for co-transfection of the *Sf*21 cells with 24.5 µl of 6.9 µg/ml recombinant pFBD-S/shRNA Bacmid DNA and 10 µl of 12.6 µg/ml pIZ/V5–GFP plasmid construct. The quantitation of the Bacmid DNA and the pIZ/V5-GFP plasmid constructs was done to ensure that the concentrations across all the wells were standardized.

The Cellfectin® reagent (Invitrogen) (liposome for mediating the transfection) and DNA mixtures were gently combined and incubated for 20 min at room temperature. The DNA-lipid transfection mixtures were added drop wise onto the cells in the wells and incubated at 27°C for 5 h.

The transfection mixtures were removed and replaced with 2 ml of 0.2 µm filter sterilized complete Grace's Insect Medium (Supplemented medium with 10% FBS and penicillin/Streptomycin antibiotics to final concentration of 100 Unit/ml and 100 µg/ml respectively. The cells were incubated at 27°C as per the time-course set up in duplicate using five 6-well plates incubated at 27°C for 0, 24, 48, 72 and 96 h respectively.

Duplicate sets of wells were set up as follows: The cells in the first pair of wells were not transfected (mock transfected negative control with no constructs). The cells in the second pair of wells were co-transfected with the pFBD-S and pIZ/V5–GFP plasmid constructs (RNAi-negative). The cells in the third pair of wells were co-transfected with pFBD-S/shRNA and pIZ/V5–GFP plasmid constructs (RNAi-positive). Table 3 summarizes the outline of the 6-well plate transfection set up. A time-course experiment at 0, 24, 48, 72 and` 96 h incubations respectively was set up by preparing five (5) identical plates as per the setup in Table 3. Each time point was analysed in duplicate. For the 0 h duplicated sets, all the cells from the mock-transfected wells as well as from the recombinant vector wells were harvested immediately upon transfecting, while the other sets were harvested after the stated time of incubations. After each incubation time, the medium was harvested by sloughing off the cells to the medium and clarifying them at 500 X g for 5 min. The cells were resuspended immediately in 1 ml freezing medium constituting 20% glycerol, 50% sterile-filtered Grace's medium, unsupplemented (without antibiotics and serum) and 30% FBS. The cells were divided for further analyses into three aliquots; one with 500 µl stocks for -80°C storage, another one with 460 µl for RNA isolation and finally the third one with 40 µl for fluorescence microscopy.

Monitoring of RNAi by GFP fluorescence microscopy

The *Sf*21 cells were harvested at 24 h intervals (0, 24, 48, 72 and 96 h) post-transfection. An aliquot of 10 µl of *Sf*21 from each of

Table 4. Relative GFP fluorescence unit from the experimental set-ups.

Set-up	Time of incubation (h) and other parameters	*siRNA-negative*	*siRNA-positive*	Change	Absolute deviation from median
Set 1	24	796381.84	656335.83	140046.02	148732.25
	48	1042817.80	834261.32	208556.50	208556.50
	72	1280084.70	911084.66	369000.04	228954.02
	96	1807415.60	1095757.00	711658.57	503102.07
	Total	4926699.94	3497438.81	1429261.12	1089344.84
	Mean	1231675.00	874359.70	357315.28	272336.21
	Variance	1.86E+11	3.32E+10	6.50E+10	2.48E+10
	SD	431651.06	182124.29	254970.85	157565.53
	Median			288778.27	
	n	4	4	4	4
Set 2	24	740429.58	689822.41	50607.17	235743.90
	48	1031367.30	793270.40	238096.90	238097.00
	72	1327613.10	993007.90	334605.20	283998.00
	96	1799000.00	1079644.90	719355.10	481258.00
	Total	4898410.00	3555745.61	1342664.37	1239096.90
	Mean	1224603.00	888936.40	335666.09	309774.23
	Variance	2.04E+11	3.20E+10	7.90E+10	1.36E+10
	SD	451776.84	178884.48	281659.79	116460.60
	Median			286351.07	1239096.90
	n	4	4	4	4

time-course experiment was put on a microscope slide. The cells were allowed to attach for 45 min and then fixed for 15 min by adding an equal volume of 4% paraformaldehyde in PBS pH 7.4. The cover slips were laid on the slides and excess flow-over medium was wiped out carefully. The attached *Sf*21cells were analyzed by fluorescence microscopy using iMIC microscope (TILL photonics) with Pike F-145b camera (Allied Vision Technologies, GmbH, Germany). The GFP filter was chosen at excitation wavelength of 500 nm. The exposure time was also finally adjusted to 50 milli-seconds. Following image acquisition, the raw data were exported to ImageJ 1.45 software (National Insitutites of Health) (Collins, 2007). Using the software, images were edited and time-course average GFP fluorescence per cell was measured. These readings were used to compute the relative GFP fluorescence according to the formular by the ImageJ 1.45 software (Table 4). Strengths of correlation were measured between the effects of RNAi treatment and the time to describe the variations due to the effects of *RNAi* treatment in time. The *t*-test statistical analysis was used to measure the average relative GFP fluorescence per cell at 95% confidence level with $P<0.05$ level of significance. Duplex RT-PCR assays were done on total RNAs that were isolated from the cell samples. RVFV-S specific primers (RVFV-S-F and RVFV-shS-R) and GFP-specific primers GFP-F (Table 1) and shGFP-R (Table 2) were used.

Monitoring of RNAi by GFP and RVFV S semi-quantitative duplex RT-PCR

Total RNA was isolated from the harvested *Sf*21 cells using Trizol™ reagent method (Invitrogen, Carlsbad, CA, USA). Duplex semi-quantitative RT-PCR assays for analyzing GFP and RVFV S-genome RNA transcript levels were done on equal volumes (1 µl) of the total RNA from the time-course experiments merging different time points post-transfection. The RT-PCR was carried out using SuperScript III/ Platinum *Taq* DNA polymerase high fidelity enzyme mix (Invitrogen, Carlsbad, CA, USA). The GFP-specific (GFP-F and shGFP-R) and RVFV-S specific (RVFV-S-F (Table 1) and RVFV-shS-R (Table 2) primer combinations were utilized. The RVFV S primer combinations detected the S RNA transcript by amplifying a 572 bp cDNA fragment while that of the GFP primers detected the GFP RNA transcript by amplifying a 370 bp cDNA fragment. The optimized RT-PCR cycling parameters were 1 cycle of 51°C for 60 min and 94°C for 2 min, followed by 20 cycles of 94°C for 15 s, 56°C for 30 s, and 68°C for 1 min, followed by a final extension at 68°C for 3 min. The expected band sizes of the RT-PCR products were checked by running on a 1% agarose gel at 10 volts/cm for 1 h. Semi-quantitative RT-PCR was used in place of qPCR since at the time of this experimentation the study could not access qPCR infrastructure. However, it is recommended that future studies should improve similar investigatins with qPCR.

Statistical analyses on the time-course experiment

To statistically support the molecular data, the pairwise statistical testing on relative GFP fluorescence per cell was analysed using Pearson's correlation strength and *t*-distribution at a level of significance of $P=0.05$ with a 95% confidence interval.

RESULTS

Expression of the RVFV S genome, shRNA and GFP cassettes in the BEVS

This study aimed to show the susceptibility of the RVFV

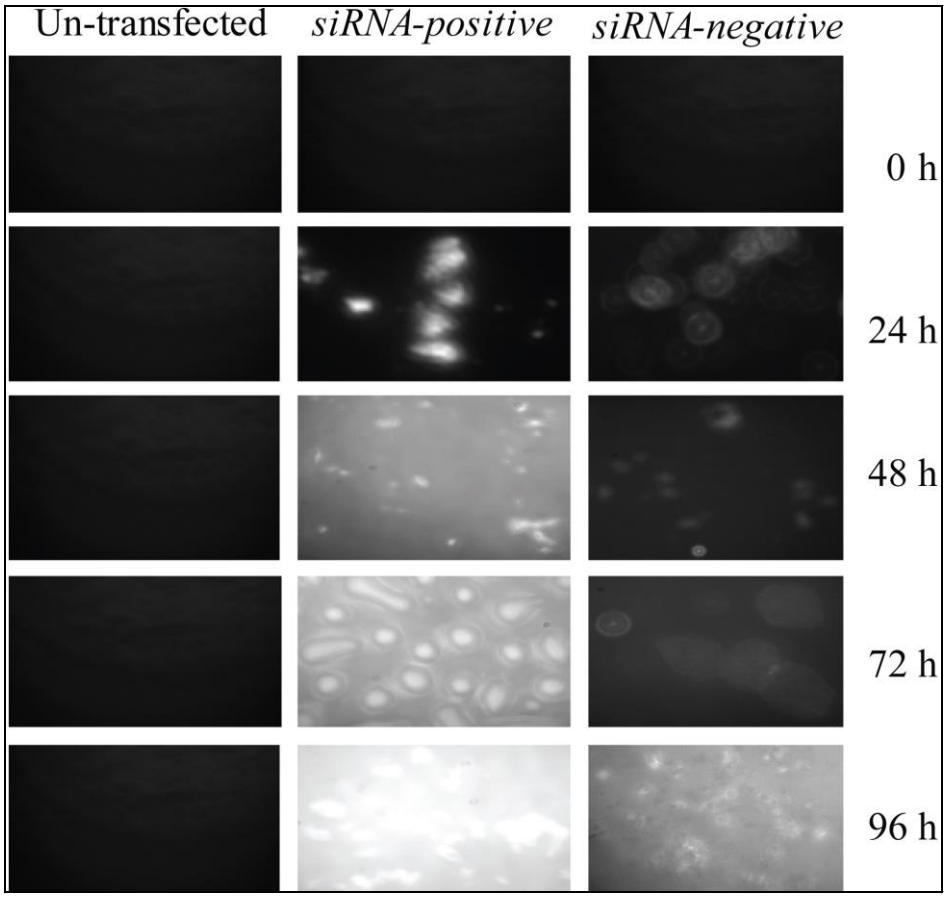

Figure 2. Time-course assessment of the effects of the *RNAi* on the relative GFP fluorescence per cell. First column: Un-transfected *Sf*21 control cells, where no recombinant construct was transfected. . Second column: GFP fluorescence in the *Sf*21 test cells that were co-transfected with pIZ/V5-GFP and recombinant *Ac*MNPV Bacmid-S (*siRNA-negative*). Third column: Declined GFP fluorescent intensities detected from the *Sf*21 test cells that were co-transfected with pIZ/V5-GFP plasmid construct and recombinant *Ac*MNPV Bacmid-S/shRNA (*siRNA-positive*). The apparently higher amounts of the GFP fluorescence intensities in the *siRNA-negative* than those for the *siRNA-positive* were observed per time point. Moreover, the increase in the GFP fluorescence intensities positively correlated with the increase in the time of incubation. This amount of change was quantified and presented in Figure 4 and Tables 4 and 5.

S-genome segment to RNAi using the Baculovirus Expression Vector System as a model (Ciccarone et al., 1997) guided by the GFP reporter gene as an internal control.

Monitoring RNAi by GFP fluorescence microscopy in *Sf*21 cells

GFP fluorescence microscopy in *Sf*21 cells was monitored from the samples harvested at 0, 24, 48, 72 and 96 h post-transfection respectively. At each time point, the duplicated wells of each of the mock-transfected (control group), the siRNA-negative control cells (Co-transfection of AcMNPV Bacmid-S and pIZ/V5-GFP) and the siRNA-positive test cells (Co-transfection of AcMNPV Bacmid-S/shRNA and pIZ/V5-GFP) were included (Table 3). GFP fluorescent signals were not detected from the mock-transfected controls and at time 0 h (Figures 2 and S1). Progressive decline in the GFP expression was however observed by a decreasing GFP fluorescence intensity (iMIC, Till Photonics GmbH) in the course of time. The difference of means between duplicate experiments for the average relative GFP fluorescence per cell in the siRNA-positive and the siRNA-negative wells upon correction by GFP background subtraction was computed (Figures 2 and S1, and Tables 4, 5 and S2). The average (Figures 2 and S1). Percentage reduction in GFP intensity due to RNAi increased with time (Figure 3). Average percentage

Table 5. Average relative GFP fluorescence unit of *Sf*21 cells from the two sets.

Time after transfection (h)	Average GFP relative fluorescence		Reduction in GFP intensity (%)
	siRNA-negative	***siRNA-positive***	
0	0.00	0.00	0.0
24	768405.71	673079.12	12.4
48	1037092.56	813765.86	21.5
72	1303848.91	952046.28	27.0
96	1803207.78	1087700.97	39.7
Total	4912554.96	3526592.23	28.2
Average	9825110.00	705318.45	28.2

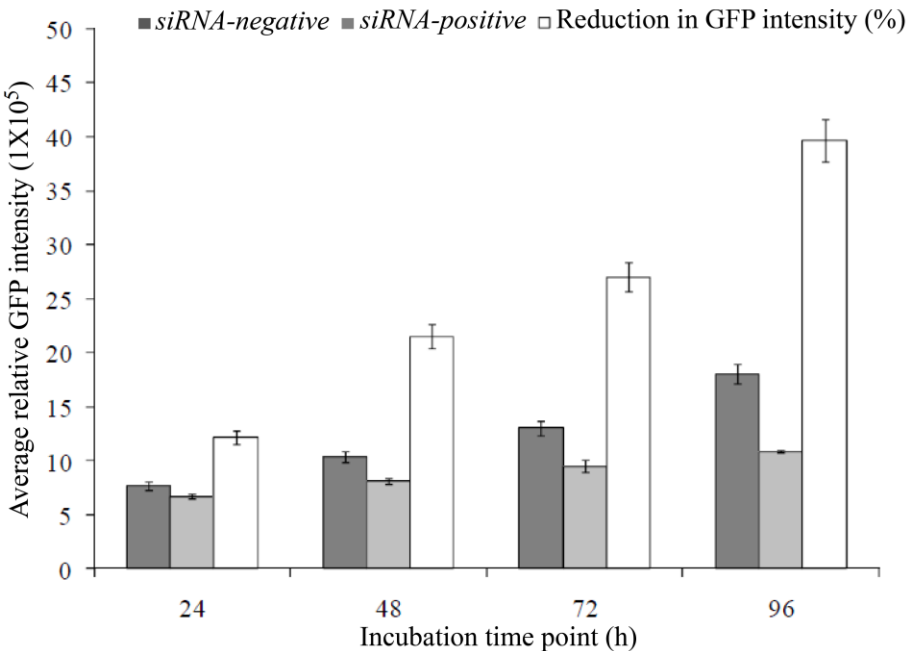

Figure 3. Average relative GFP expression over time in siRNA-positive and SiRNA-negative *Sf*21 cells. Percentage amount of reduction (the difference between the GFP fluorescence of the *siRNA-negative* and the *siRNA-positive*) in the GFP fluorescence intensity due to RNA silencing was observed to increase with the time of incubation. In average, the percentage reduction in the relative GFP fluorescence of up to 39.7% was observed by the 96th h (Table 5).

reduction of the relative GFP fluorescence of up to 39.7% was achieved by the 96th hour. A graph of percentage reduction in the amount of the GFP fluorescence against incubation time showed that the reduction in the GFP intensity increased with time.

All the promoters (P_{PH}, P_{10} and *OpIE2*) are very strong and remained active throughout the course of the experiment; therefore, it was not possible to achieved absolute transcript knockdowns. The experimental setup was designed in such a way that siRNAs which are both anti-RVFV S-genome segment and anti-GFP transcripts would be generated from the same multiplexed shRNA transcription cassette. As such, the expression of these siRNAs for targeting the RVFV S-genome segment was positively correlated with the expression anti-GFP siRNAs (Figure S2 and Tables S3 and S4). The transcription of RVFV S-genome and shRNA cassette respectively occurred simultaneously in one pFBD-S/shRNA vector. The two baculovirus promoters being equally powerful and are turned on at the same time enabled the *RNAi* pathway to occur as their respective *siRNA* were processed.

To statistically evaluate the null hypothesis that the siRNA-positive treatment had “no effect” on the RVFV S-genome segment transcript, the Pearson product-moment correlation coefficient (Tables S3 and Table S4)

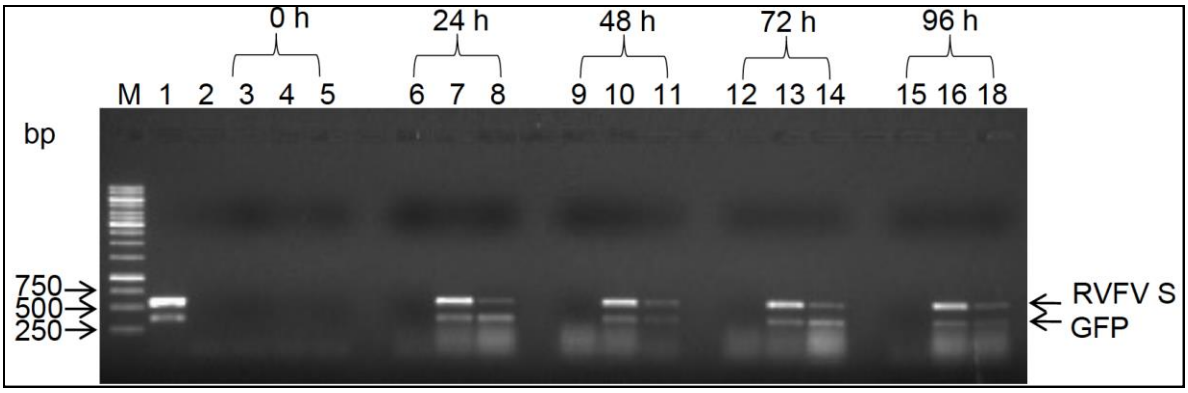

Figure 4. Duplex semi-quantitative RT-PCR to measure the *in vitro* RNAi effects on RVFV S-genome segment RNA transcript. M: 1 Kb DNA ladder (Fermentas). Lanes 1 and 2: Positive and no-template negative controls respectively. Lane 3 through lane 18: Duplex semi-quantitative RT-PCR results from the time-course experiment at 0, 24, 48, 72 and 96 h arranged in groups of threes indicating the 370 bp GFP and the 572 bp RVFV S. In each of these groups; first well shows the results of RNA from the un-transfected *Sf*21 negative control cells, second well shows the RT-PCR results of total RNA from *Sf*21 cells that were co-transfected with pIZ/V5-GFP construct and recombinant *Ac*MNPV Bacmid-S (*siRNA-negative*), and third well displays the RT-PCR results of RNA from *Sf*21 cells co-transfected with pIZ/V5-GFP construct and recombinant *Ac*MNPV Bacmid-S/shRNA (*siRNA-positive*). There is apparent reduction in the cDNA band densities in the *siRNA-positive* groups compared to the *siRNA-negative* groups that were amplified from both the GFP and the RVFV S transcripts.

and *t*-test analyses were done on the data sets (Supplementary information). The Pearson product-moment correlation coefficient, *r* (Pearson's *r*) was used to measure the strength of the linear relationship between incubation times and amount of change in the relative GFP fluorescence intensities (Figure S2). The Pearson's r between X = Incubation time and Y = change in relative GFP fluorescence, r = 0.9584 and 0.9511 in sets 1 and 2 respectively showed strong positive relationship (Tables S3 and S4). The mean Pearson product-moment correlation coefficient (r = 0.95475) between the siRNA-negative and siRNA-positive groups of cells in the two independent experiments showed a strong positive correlation. Strengths of correlation were measured between the RNAi treatments and the time variables. The percentage reduction in GFP intensity increased with time.

The relative GFP fluorescence per cell from the duplicate experiments were also used to test the null hypothesis at $P<0.05$ confidence level of significance using the *t*-test statistics (Supplementary material) (Chap, 2003; Fisher and Belle, 2004; Kaps and Lamberson, 2004). The corresponding *t*-test analysis for these correlation strengths showed significant variation between the siRNA-negative and siRNA-positive groups ($t_{1-0.05/1,\ 4-2} = 2.92$; $P<0.05$). A second *t*-test analysis done on each independent time-course experiment also showed significant effect of *RNAi* treatment between the two groups ($t_{1\text{-}0.05/1,3} = 2.80$, $P<0.05$). There was no significant difference in the amount of change achieved by the two separate independent experiments ($t_{1\text{-}0.05/1,6} = 0.0806$, $P>0.05$) suggesting that the two independent experiments were similar. The pattern of GFP transcription post-RNAi was thus assumed to mirror that of the RVFV S-genome segment because the source of siRNA originated from the same shRNA chimeric construct. As there was a statistically significant effect due to the RNAi in the RNAi-positive test group on the transcript levels of the RVFV S-genome transcript, the null hypothesis of "no-effect", that is, H_0: $\mu_1 = \mu_2$ was therefore rejected.

Verification of the effects of the *RNAi* on the transcripts of GFP and RVFV S by semi-quantitative RT-PCR

In the RNAi-positive groups, transcription of shRNA transcription cassette generated siRNAs that triggered gene-specific degradation of the RVFV S and GFP transcripts via the RNAi pathway. The monitoring of the RNAi was achieved by using duplex semi-quantitative RT-PCR to detect both GFP (as the experimental control) and RVFV S-genome RNA transcript levels (Figure 4 and Table S1). The duplex RT-PCR detections yielded expected fragments of RVFV-S and GFP of 572 and 370 bp, respectively from the transfected cells only at 24, 48, 72 and 96 h time points. The results further indicated that the RVFV-S-genome segment transcript levels in the siRNA-negative *Sf*21 cells were apparently higher relative to that of the siRNA-positive *Sf*21 cells.

DISCUSSION

RNAi is a naturally occurring pathway thought to have

evolved in plants and animals over millions of years as a form of innate immunity defence against viruses, suggesting an important role in pathogen resistance (Meng et al., 2013). RNAi can be triggered experimentally by exogenous introduction of dsRNA or using DNA-based vectors, which express short hairpin RNA (shRNA) in the cytoplasm that are processed by Dicer into siRNAs (Swamy et al., 2016; McGinnis, 2010). RNAi can also be induced directly by transfecting cells with siRNAs with dinucleotide 3' overhangs (Fitzgerald et al., 2017).

This study described a BEVS-based strategy of demonstrating simultaneous RNA silencing of multiple sequences, in a multiplex RNAi experiment using a single transgenic construct of defined size. The dual promoter capacity of pFBD vector to clone and simultaneously express the two recombinant genes under the P_{10} and the P_{PH} promoter from a single vector offered a major advantage over the use of two separate vectors. It suggests a possible way to enhance multiple gene knockdowns in a single organism, and could also be applied in mammalian cells. RNAi is a specific, potent, and highly successful approach for loss-of-function studies in virtually all eukaryotic organisms (McGinnis, 2010; Pompey et al., 2014; Koch et al., 2016). RNAi technology takes advantage of the cell's natural machinery, facilitated by short interfering RNA molecules, to effectively knock down expression of a gene of interest (Swamy et al., 2016). Simultaneous RNA silencing using a multiplex *RNAi* construct has been demonstrated by Bucher et al. (2006). The Bucher et al. (2006) demonstrated a simple procedure to obtain broad virus resistance at a high frequency by RNA silencing, using a single transgene construct of limited size. This shown that efficient simultaneous targeting of four different tospoviruses can be achieved by using a single small transgene based on the production of minimal sized chimeric cassettes. The shRNA is processed into specific *siRNA*, which are directed against a viral genome resulting in down regulation of the genome products (Li and Patel, 2016). In this study, a four-fragment shRNA chimeric construct was made using the BEVS technology for use to target all the three RVFV genome segments (L, M and S) and the GFP as a requirement of the larger study. The multiplex shRNA consisted of successive fragments of 150 bp each of RVFV L, M and S genome fragments and 150 bp GFP (excluding the restriction sites). The 13 bp loop structure separated the genomic sense (GS) constructs and reverse-complement (RC) constructs. Upon transcription in insect cells, the RNA forms a shRNA structure because the RC is complementary sequence to GS. The primers, the multiplex shRNA construct and the respective methods used here are original to this study. However, the idea of the 150 bp shRNA segments was obtained from Bucher et al. (2006) whose cloning method was different from the one used here. The Bucher et al. (2006) PCR merging strategy did not work in this study, therefore the restriction cloning option was developed. It has been shown that shRNA production increases efficiency of silencing better than dsRNA (Brummelkamp et al., 2002).

The constitutive expression of GFP by the independent pIZ/V5-GFP construct allowed the visualization of the RNAi effects over time since the *siRNA* targeting both the RVFV S-genome and GFP were generated from the same shRNA transcript. The co-delivery of this pIZ/V5-GFP construct with either Bacmid-S or Bacmid-S/shRNA into the insect cells allowed monitoring of the RNAi using the duplex semi-quantitative RT-PCR and the GFP fluorescence detection methods. GFP is often used as a reporter gene in a range of qualitative and quantitative studies, real time and an indicator for protein production due to its ability to emit luminescence under UV transillumination (Chalfie et al., 1994; Chalfie and Kain, 1998). The P_{PH} and P_{10} promoters are activated during late stages post-infection (transfection) between 18 to 76 h (Braunagel and Summers, 2007; Yang and Miller, 1999). The immediate early *OpIE2* promoter becomes active between 30 min and 4 h post-infection with the aid of host RNA polymerase II (Theilmann and Stewart, 1992; Amer, 2011). In the present study, GFP expression preceded that of the RVFV S segment and the shRNA transcripts due to the very late baculovirus P_{PH}, and P_{10} promoter activities. Transcripts of RVFV S-genome and GFP RNA were detected at as early as 24 h post-transfection, indicating that these very late P_{10} and immediate early *OpIE2* promoters respectively were already activated. These observations were in agreement with the documented data about properties of the baculovirus promoters. Once activated, the P_{PH}, P_{10} and *OpIE2* promoters remained activated throughout the course of this experiment and thus RNAi did not decrease the transcript levels to undetectable levels.

In conclusion, the BEVS experimental model shows that the high level RNA silencing against RVFV S-genome segment and GFP transcripts simultaneously is achievable using a single transgenic construct, and may provide new ideas and strategies of targeting the RVFV in the infected cells. Importantly, the model has demonstrated that the RVFV S-genome segment transcript is susceptible to RNA silencing. The findings suggest that by employing the use the multiple gene knockdowns in a single organism, the *RNAi* strategy could be applied to arrest or abrogate the *in vitro* and *in vivo* RVFV replications. By extension, the other two RVFV genome segments (L and M) can be silenced by the same multiplexed shRNA cassette designed in this study. Recent advances in RNAi applications make it possible to specifically suppress one or more genes simultaneously (Jung et al., 2017). Future studies should consider the next challenge of carrying out similar study using this or similar shRNA transcription cassette to target the wild type RVFV *in vitro* replication. Where, accordingly, in the design and the analyses, more appropriate internal controls, and more sensitive and

accurate transcript detection methods such as qPCR and western blots are incorporated in the analyses to confirm the effect and the degree of the *RNAi*. Broadly, the BEVS-based model is a suitable model for studying *RNAi* particularly for demonstrating simultaneous RNA silencing of multiple sequences, in a multiplex *RNAi* using a single transgenic construct of defined size. Moreover, the model may be used in *RNAi* trials and testing the power of shRNA constructs by selecting and optimizing shRNA clones because the differential transcript levels and *siRNA* concentrations are quantifiable.

CONFLICT OF INTERESTS

The authors have not declared any conflict of interests.

ACKNOWLEDGEMENTS

This work was done as part of a larger on-going study in search for safe antiviral therapies that will offer effective treatment and prevention remedies to combat any future RVFV outbreaks. It was sponsored by Jomo Kenyatta University of Agriculture and Technology (JKUAT) research grant No. JKU/RPE/RPPC/RP/65 for the study entitled “Controlling Rift Valley Fever virus using RNA Silencing”. The authors acknowledge the Center for Disease Control and Prevention (CDC), Nairobi, Kenya for supporting the virus isolation phase. Dr. M. Kariuki Njenga of CDC Kenya donated the RVFV isolate that was used in this work. They appreciate the technical support contributed by Leonard Nderitu and Solomon Gikundi in the CDC cell culture laboratory. They also acknowledge the support offered by the International Center of Insect Physiology and Ecology (*icipe*) Molecular Biology and Bioinformatics Unit (MBBU), Nairobi, Kenya for the molecular analyses phase. Particularly, they recognise Dr. Daniel Masiga for allowing this work to be done in his lab. They also appreciate Dr. Joel L. Bargul for offering technical assistance for the molecular and GFP fluorescence analyses.

REFERENCES

Agrawal N, Dasaradhi PVN, Mohmmed A, Malhotra P, Bhatnagar RK, Sunil KM (2003). RNA Interference: Biology, Mechanism, and Applications. Microbiol. Mol. Biol. Rev. 67:657-685.

Amer HM (2011). Baculovirus expression vector system: An efficient tool for the production of heterologous recombinant proteins. Afr. J. Biotechnol. 10(32):5927-5933.

Boshra H, Lorenzo G, Busquets N, Brun A (2011). Rift Valley Fever: Recent Insights into Pathogenesis and Prevention. J. Virol. 85(13):6098-6105.

Braunagel SC, Summers MD (2007). Molecular biology of the baculovirus occlusion-derived virus envelope. Curr. Drug Targets 8(10):1084-1095.

Breiman RF, Njenga MK, Cleaveland S, Sharif SK, Mbabu M, King L (2008). Lessons from the 2006–2007 Rift Valley fever outbreak in East Africa: Implications for prevention of emerging infectious diseases. Future Virol. 3:411-417.

Brummelkamp TR, Bernards R, Agami R (2002). A system for stable expression of short interfering RNAs in mammalian cells. Science 296(5567):550-553.

Bucher E, Lohuis D, van Poppel PMJA, Geerts-Dimitriadou C, Goldbach R, Prins M (2006). Multiple virus resistance at a high frequency using a single transgene construct. J. Gen. Virol. 87:3697-3701.

Carmona S, Ely A, Crowther C, Moolla N, Salazar FH, Marion PL (2006). Effective inhibition of HBV replication in vivo by anti-HBx short hairpin RNAs. Mol. Ther. 13(2):411-421.

CDC-Centers for Disease Control and Prevention (2007). Rift Valley fever outbreak Kenya, November 2006-January 2007. MMWR. Morbidity and mortality weekly report 56:73-76.

Chalfie M, Kain S (1998). Green fluorescent protein: properties, applications, and protocols. New York: Wiley-Liss.

Chalfie M, Tu Y, Euskirchen G, Prasher DC (1994). Green fluorescent protein as a marker for gene expression. Science 263(5148):802-805.

Chap TL (2003). Introductory to Bioinformatics. John Wiley and Sons Publishing Inc., Hoboken, New Jersey, pp. 209-313.

Ciccarone VC, Polayes D, Luckow VA (1997). Generation of Recombinant Baculovirus DNA in *E. coli* Using Baculovirus Shuttle Vector. In Methods Molec. Med. Edited by U. Reischt. Humana Press Inc., Totowa, NJ. P 13.

Collett MS, Purchio AF, Keegan K, Frazier S, Hays W, Anderson DK (1985). Complete nucleotide sequence of the M RNA segment of Rift Valley fever virus. J. Virol. 144:228-245.

Collins TJ (2007). ImageJ for microscopy. BioTechniques 43(1):25-30.

Daubney R, Hudson JR, Garnham PC (1931). Enzootic hepatitis or Rift Valley fever. An undescribed virus disease of sheep, cattle and man from East Africa. J. Pathol. Bacteriol. 34:545-579.

Easterday BC, McGavran MH, Rooney JR, Murphy LC (1962). The pathogenesis of Rift Valley fever in lambs. Am. J. Vet. Res. 23:470-479.

Elliott RM (1990). Molecular biology of the Bunyaviridae. J. Gen. Virol. 71:501-522.

Ellis DS, Shirodaria PV, Fleming E, Simpson DI (1988). Morphology and development of Rift Valley fever virus in Vero cell cultures. J. Med. Virol. 24(2):161-174.

Faburay B, Wilson WC, Gaudreault NN, Davis AS, Shivanna V, Bawa B, Sunwoo SY, Ma W, Drolet BS, Morozov I, McVey DS (2016). A Recombinant Rift Valley Fever Virus Glycoprotein Subunit Vaccine Confers Full Protection against Rift Valley Fever Challenge in Sheep. Sci. Rep. 6:27719.

Fisher LD, Belle GV (2004). Biostatistics: A methodology for the health sciences. Heagerty P. J and Lumley T. 2nd edition. John Wiley and Sons Inc., Hoboken, New Jersey, pp. 123-133.

Fitzgerald K, White S, Borodovsky A, Bettencourt BR, Strahs A, Clausen V, Wijngaard P, Horton JD, Taubel J, Brooks A, Fernando C (2017). A Highly Durable RNAi Therapeutic Inhibitor of PCSK9. New Engl. J. Med. 376:41-51.

Ge Q, Eisen HN, Chen J (2004). Use of siRNAs to prevent and treat influenza virus infection. J. Virus Res. 102(1):37-42.

Giorgi C, Accardi L, Nicoletti L, Gro MC, Takehara K, Hilditch C, Morikawa S, Bishop DH (1991). Sequences and coding strategies of the S RNAs of Toscana and Rift Valley fever viruses compared to those of Punta Toro, Sicilian Sandfly fever, and Uukuniemi viruses. J. Virol. 180:738-753.

Giorgi C (1996). Molecular biology of phlebovirus. In. The Bunyaviridae, Edited by R. M. Elliott. New York: Plenum Press. Pp. 105-128.

Hannon GJ (2002). RNA interference. Nature 418:244-251.

Hannon GJ, Rossi JJ (2004). Insightful review articles: Unlocking the potential of the human genome with RNA interference. Nature 431:371-378.

Harris R, Polayes D (1997). A New Baculovirus Expression Vector for the Simultaneous Expression of Two Heterologous Proteins in the Same Insect Cell. Focus 19:6-8.

Ikegami T, Makino S (2009). Rift Valley fever vaccines. Vaccine 27(S4):D69-D72.

Jung J, Nayak A, Schaeffer V, Starzetz T, Kirsch AK, Müller S, Dikic I, Mittelbronn M, Behrends C (2017). Multiplex image-based autophagy RNAi screening identifies SMCR8 as ULK1 kinase activity and gene expression regulator. eLife 6:e23063.

Kang S, Hong YS (2008). RNA Interference in Infectious Tropical Diseases. Korean J. Parasitol. 46(1):1-15.
Kaps M, Lamberson WR (2004). Biostatistics for Animal Science. CAB international publishing, UK, pp. 53-153.
Koch A, Biedenkopf D, Furch A, Weber L, Rossbach O, Abdellatef E, Linicus L, Johannsmeier J, Jelonek L, Goesmann A, Cardoza V (2016). An RNAi- Based Control of Fusarium graminearum Infections Through Spraying of Long dsRNAs Involves a Plant Passage and Is Controlled by the Fungal Silencing Machinery. PLoS Pathog. 12(10):e1005901.
Li S, Patel DJ (2016). Drosha and Dicer: Slicers cut from the same cloth. Cell Res. 26:511-512.
Linthicum KJ, Anyamba A, Tucker CJ, Kelley PW, Myers MF, Peters CJ (1999). Climate and satellite indicators to forecast Rift Valley fever epidemics in Kenya. Science 285:397-400.
Liu DY, Tesh RB, Travassos D, Rosa AP, Peters CJ, Yang Z, Guzman H, Xiao SY (2003). Phylogenetic relationships among members of the genus Phlebovirus (Bunyaviridae) based on partial M segment sequence analyses. J. Gen. Virol. 84:465-473.
McCaffrey AP, Meuse L, Pham TT, Conklin DS, Hannon GJ, Kay MA (2002). Gene expression: RNA interference in adult mice. Nature 418:338-339.
McGinnis KM (2010). RNAi for functional genomics in plants. Brief. Funct. Genomics 9(2):111-117.
Meegan JM, Hoogstraal H, Moussa MI (1979). An epizootic of Rift Valley fever in Egypt in 1977. J. Vet. Res. 105:124-125.
Meegan JM, Watten RH, Laughlin LW (1981). Clinical experience with Rift Valley fever in humans during the 1977 Egyptian epizootic. Contribution on Epi Biostat 3:114-123.
Meng Z, Zhang X, Wu J, Pei R, Xu Y, Yang D, Roggendorf M, Lu M (2013). RNAi Induces Innate Immunity through Multiple Cellular Signaling Pathways. PLoS One 8(5):e64708.
Muller R, Poch O, Delarue M, Bishop DHL, Bouloy M (1994). Rift Valley fever virus L segment: correction of the sequence and possible functional role of newly identified regions conserved in RNA-dependent polymerases. J. Gen. Virol. 75(6):1345-1352.
Nderitu L, Lee JS, Omolo J, Omulo S, O'Guinn ML, Hightower A, Mosha F, Mohamed M, Munyua P, Nganga Z, Hiett K, Seal B, Feikin DR, Breiman RF, Kariuki MN (2011). Sequential Rift Valley Fever Outbreaks in Eastern Africa Caused by Multiple Lineages of the Virus. J. Infect. Dis. 203(5):655-665.
Nichol ST, Beaty BJ, Elliott RM, Goldbach RW, Plyusnin A, Tesh RB (2005). Classification and nomenclature of viruses. VIIIth report of the International Committee on Taxonomy of Viruses. In. The Bunyaviridae, Virus taxonomy. Edited by C. Fauquet, M.A. Mayo, L.S.M. Maniloff, U. Desselberger & L.A. Ball. Elsevier Academic Press, London. pp. 695-716.
Nishitsuji H, Kohara M, Kannagi M, Masuda T (2006). Effective suppression of human immunodeficiency virus type 1 through a combination of short- or long-hairpin RNAs targeting essential sequences for retroviral integration. J. Virol. 80(15):7658-7666.
O'Reilly DR, Miller LK, Luckow VA (1992). Baculovirus Expression Vectors: A Laboratory Manual, W. H. Freeman and Company, New York.
Pepin M, Bouloy M, Bird BH, Kemp A, Paweska J (2010). Rift Valley fever virus (*Bunyaviridae*: *Phlebovirus*): an update on pathogenesis, molecular epidemiology, vectors, diagnostics and prevention. J. Vet. Res. 41(6):61.
Pompey JM, Morf L, Singh U (2014). RNAi Pathway Genes Are Resistant to Small RNA Mediated Gene Silencing in the Protozoan Parasite Entamoeba histolytica. PLoS One 9(9):e106477.
Sang R, Arum S, Chepkorir E, Mosomtai G, Tigoi C, Sigei F, Lwande OW, Landmann T, Affognon H, Ahlm C, Evander M (2017). Distribution and abundance of key vectors of Rift Valley fever and other arboviruses in two ecologically distinct counties in Kenya. PLoS Negl. Trop. Dis. 11(2):e0005341.
Shi JY, Liu B, Wang M, Luo EJ (2010). Short hairpin RNA-mediated inhibition of measles virus replication *in vitro*. Can. J. Microbiol. 56:77-80.
Sindato C, Pfeiffer DU, Karimuribo ED, Mboera LEG, Rweyemamu MM, Paweska JT (2015). A Spatial Analysis of Rift Valley Fever Virus Seropositivity in Domestic Ruminants in Tanzania. PLoS One 10(7):e0131873.
Swamy MN, Wu H, Shankar P (2016). Recent advances in RNAi-based strategies for therapy and prevention of HIV-1/AIDS. Adv. Drug Deliv. Rev. 103:174-86.
Swanepoel R, Coetzer JAW (2004). Rift Valley fever, In. Infectious diseases of livestock, Edited by J. A. W. Coetzer & R. C. Tustin. Oxford University Press, Cape Town, South Africa. Pp. 1037-1070.
Tamura K, Dudley J, Nei M, Kumar S (2007). MEGA4: Molecular Evolutionary Genetics Analysis (MEGA) software version 4.0. Mol. Biol. Evol. 24:1596-1599.
Theilmann DA, Stewart S (1992). Molecular Analysis of the trans-Activating IE-2 Gene of Orgyia pseudotsugata Multicapsid Nuclear Polyhedrosis Virus. J. Virol. 187:84-96.
Vlak JM, Keus RJA (1990). Baculovirus Expression Vector System for Production of Viral Vaccines. In. Viral Vaccines, Wiley-Liss Inc. pp. 91-128.
WHO-World Health Organization (2007). Rift Valley Fever outbreak-Kenya, November 2006-January 2007. MMWR. Morbidity and Mortality Weekly Report 56:73-76.
Yang S, Miller LK (1999). Activation of Baculovirus Very Late Promoters by Interaction with Very Late Factor 1. J. Virol. 73(4):3404-3409.

SUPPLEMENTARY INFORMATION

Table S1. Average concentrations of the total RNA of duplicate *in vitro* transcription time-course experiments.

Time (h)	Total RNA (µg/mL)		
	Un-transfected control cells	***siRNA-negative***	***siRNA-positive***
0	863.10	325.45	700.40
24	429.64	661.88	611.06
48	515.76	652.86	644.94
72	406.18	489.84	556.08
96	578.26	1312.14	707.54

Table S2. Computation of relative GFP fluorescence using the Image J 1.45 software.

Big boxes (Within the cells)	**Area**	**Mean**	**Raw integrated density**
1	22528	27.89	628295
Small boxes (Background outside the cells)	**Area**	**Mean**	**Raw integrated density**
2	420	6	2520
3	210	6	1260
4	196	5.98	1172
5	208	6.096	1268
		Mean of means	Corrected integrated density
Mean of Means		6.019	
Corrected integrated density			492698.968

The ImageJ software was used to automatically measure the parameters highlighted in red in the excel image example below. The regions within the images of *Sf*21 cells emitting the GFP fluorescence were selected. The same readings were scored for the background smaller selections outside the fluorescing cells. All the readings were exported to spread sheet where the averages were computed. The cells incubated at different time points (0, 24, 48, 72 and 96 h) from the time-course experiments were analyzed separately. The averages from the two independent experiments were summarized in Table 4. To compute the corrected integrated density (Relative GFP fluorescence) the following formular was used; Corrected Integrated Density (relative GFP fluorescence) = *(The difference between the Average raw intensity readings within the Sf21 cells and the means of means of the background readings outside the cells) multiplied by the average area selected within the Sf21 cells.*

Table S3. Time-course correlation of relative GFP fluorescence, set 1.

x_i	y_i	x_i-xbar	(x_i-xbar)^2	y_i-ybar	(y_i-ybar)^2	DxDy
0	0	-48	2304	-2.86	8.17	137.21
24	1.40046018	-24	576	-1.46	2.13	34.99
48	2.08556495	0	0	-0.77	0.60	0.0
72	3.69000036	24	576	0.83	0.69	19.96
96	7.11857	48	2304	4.26	18.13	204.39
Sum			5760		29.72	396.55

r= 0.9584; r^2= 0.9186

Table S4. Time-course correlation of relative GFP fluorescence, set 2.

x_i	y_{ii}	x_i-xbar	(x_i-xbar)^2	y_{ii}-ybar	(y_{ii}-ybar)^2	DxDy
0	0	-48	2304	2.69	7.21	128.90
24	0.50607173	-24	576	-2.18	4.75	52.30
48	2.3809691	0	0	-0.30	0.09	0
72	3.3460522	24	576	0.66	0.44	15.86
96	7.1935507	48	2304	4.51	20.32	216.39
Sum			5760		32.81	413.45

r =0.9511; r^2=0.9045.

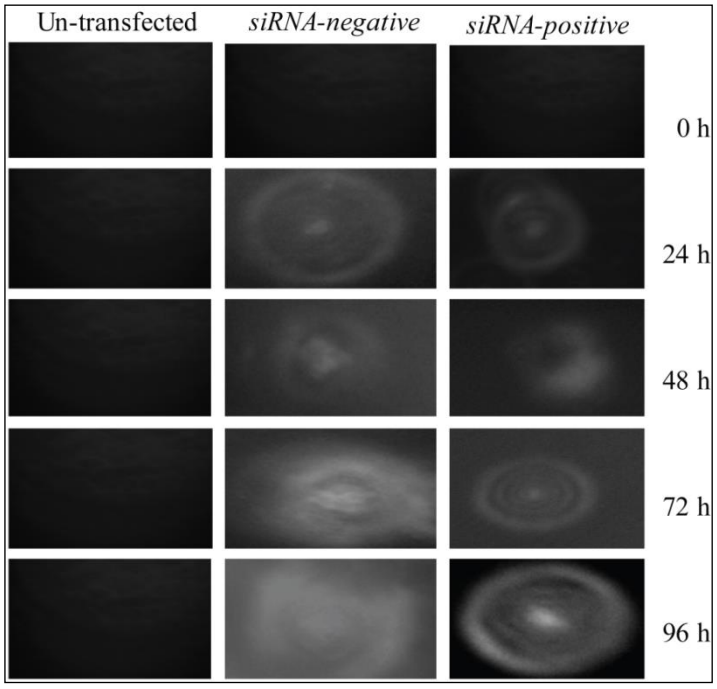

Figure S1. The relative GFP fluorescence per cell. Column 1: Un-transfected *Sf*21 cell (Control group). Column 2: GFP fluorescence in the *Sf*21 test cell (*RNAi-negative* group). Column 3: Declined GFP fluorescent intensity in *Sf*21 cell (*RNAi-positive* group).

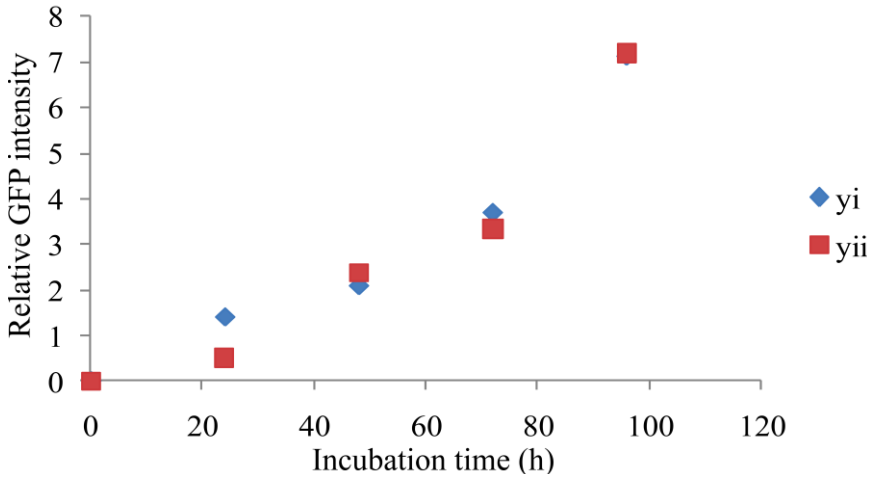

Figure S2. Apparent positive correlation between *x* and *y*.

Here below, *t* statistic analyses are provided in detail.
To answer the question whether there was linear association between the incubation time and amount of change in the relative GFP fluorescence, the sums of squares and sum of products were computed as follows: *SSxx* = 5760, *SSyy* = 29.72 and *SSxy* = 396.55 in set 1 and *SSxx* = 5760, *SSyy* = 32.81 and *SSxy* = 413.45 in set 2. The average sums of squares and sum of products from both sets were *SSxx* = 5760, *SSyy* = 31.05 and *SSxy* = 404.5.
Using the average sums of squares and sum of products, the sample coefficient of correlation was:

$$r = \frac{SS_{xy}}{\sqrt{SS_{xx} \quad SS_{yy}}} = \frac{404.5}{\sqrt{(5760) \quad (31.05)}} = 0.96$$

The calculated value of the *t* statistic was:

$$t = \frac{r\sqrt{n\text{-}2}}{\sqrt{1\text{-}r^2}} = \frac{0.96\sqrt{5\text{-}2}}{\sqrt{1\text{-}0.96^2}} = 17.3$$

The critical value with 5% significance level and 3 degrees of freedom (*df*) was:

$$t_{\alpha/2,3} = t_{0.25/3} = 3.18$$

The calculated *t* = 17.3 was more extreme than 3.18, so *H*0 is rejected. There is linear association between incubation time and amount of change in relative GFP fluorescence due to *RNAi*.
Hypothesis of no difference (H_0: $\mu = 0$) that the RNAi-positive had no effect based on the relative GFP fluorescence between *RNAi*-negative and RNAi-positive groups in the two sets was tested. Considering the values from 24 h incubation, *df* was 4-1 = 3.
The *t*-statistic for the set 1 was:

$$t = \frac{\overline{x_d} - c}{S_d/\sqrt{n}} = \frac{357315.28 - 0}{254970.85/\sqrt{4}} = 2.80$$

The *t*-statistic in set 2 was:

$$t = \frac{\overline{x_d} - c}{S_d/\sqrt{n}} = \frac{335666.09 - 0}{281659.79/\sqrt{4}} = 2.38$$

The critical *t*-statistic value for 3 *df* at 95% ($\alpha = 0.05$) confidence level $t_{1\text{-}0.05/1,3} = 2.3534$ hence *P* value for these statistics was <0.05. This indicated that the observed values clearly fell into the rejection regions, hence the null hypothesis were rejected.
Differences in the amount of change were also tested by comparing their means between the two sets. The null hypothesis was that the mean change between set 1 and set 2 groups was equal (H_0: $\mu_1 = \mu_2$). Both sample standard deviations were used to compute the "pooled"standard deviation which has n_1+n_2-2 *df*. Brown-Forsythe (BF) test, which is a 2-sample *t*-test that looks at the spread of the data in absolute terms, was used. The BF test is usually used with comparison of multiple groups in analyses of variance but may be used with 2 groups. To compute the BF statistic, first the median of each group was calculated, *mdi*, and then computed the absolute value of the difference between each sample and its group median.

$$S_p = \sqrt{\frac{(n_1 - 1)S_1^2 + (n_2 - 1)S_2^2}{n_1 + n_2 - 2}} = \sqrt{\frac{(4 - 1)281659.79^2 + (4 - 1)281659.79^2}{4 + 4 - 2}} = 268646.95$$

The *t*-statistic for these data with 6 *df* considering values from 24 h incubation was:

$$t = \sqrt{\frac{357315.28 - 335666.09}{(268646.95)\sqrt{\frac{1}{4}+\frac{1}{4}}}} = 0.0806$$

The critical *t* value for 6 (n_1+n_2-2) *df* at 95% (α = 0.05) confidence level, $t_{1\text{-}0.05/1,6}$ = 1.9432 hence *P* value for this statistic is >0.05. This observed values clearly fell into the acceptance region in favour of null hypothesis. Hence the null hypothesis was accepted and concluded that the average in relative GFP fluorescence observed in set 1 was not significantly different from that observed in set 2 in terms of the amount of change.

>GGATCCAGAGAACCTTTGATAAATCATAGTCTTTGCTGGAGCACCGACCTGTTTC
TAGAACTTTCCTAACTGAGGCTCTCCCCATCTTAGAAATAGCATAATCAACAAACTT
ATCCATCAAGGGATGAGCAATCATAGATAATGAACTGATGTCCT***ACTAGT***CACATTT
TAGAGAGGCCTGTTCTTCCAAGATATATAAGGAGGAAGAAGAGCCCAATTGATAAT
GCAACATACAGGCAAATGAGGAGTATAGTTTTAAGCGGCCCTCCAAACCAACTCAT
GAGTCCAGAAAACCAGTCAAAGAAATTCCAA***GCGGCCGC***CTTCCTGTCACTGGGA
CAACCATGGACGGTCTATCCCCTGCGTACCCGAGGCATATGATGCATCCCAGCTTT
GCTGGCATGGTGGACCCTTCTCTACCAGAAGACTATCTAAGGGCAATATTAGATGC
TCACTCTCTGTA*TCTG****CTGCAG***TTCTCTTATGGTGTTCAATGCTTTTCCCGTTATCC
GGATCATATGAAACGGCATGACTTTTTCAAGAGTGCCATGCCCGAAGGTTATGTAC
AGGAACGCACTATATCTTTCAAAGATGACGGGAACTACAAGACGCGTGCTGAAGTC
AAG***TTCAAGAGAATTC***CTTGACTTCAGCACGCGTCTTGTAGTTCCCGTCATCTTTG
AAAGATATAGTGCGTTCCTGTACATAACCTTCGGGCATGGCACTCTTGAAAAAGTC
ATGCCGTTTCATATGATCCGGATAACGGGAAAAGCATTGAACACCATAAGAGAA***CT***
GCAGCAGATACAGAGAGTGAGCATCTAATATTGCCCTTAGATAGTCTTCTGGTAGA
GAAGGGTCCACCATGCCAGCAAAGCTGGGATGCATCATATGCCTCGGGTACGCAG
GGGATAGACCGTCCATGGTTGTCCCAGTGACAGGAAG***GCGGCCGC***TTGGAATTTC
TTTGACTGGTTTTCTGGACTCATGAGTTGGTTTGGAGGGCCGCTTAAAACTATACT
CCTCATTTGCCTGTATGTTGCATTATCAATTGGGCTCTTCTTCCTCCTTATATATCTT
GGAAGAACAGGCCTCTCTAAAATGTG***ACTAGT***AGGACATCAGTTCATTATCTATGA
TTGCTCATCCCTTGATGGATAAGTTTGTTGATTATGCTATTTCTAAGATGGGGAGAG
CCTCAGTTAGGAAAGTTCTAGAAACAGGTCGGTGCTCCAGCAAAGACTATGATTTA
TCAAAGGTTCTCT***AAGCTT***

Figure S3. Complete 1253 bp shRNA transcripion cassette as was confirmed by Sanger sequencing. Total RNA was isolated from each of the *Sf*21cells that were un-transfected or co-transfected with pIZ/V5-GFP and either the recombinant *Ac*MNPV Bacmid-S or *Ac*MNPV Bacmid-S/shRNA was harvested at 0, 24, 48, 72 and 96 h post-transfection. The total RNA samples isolated from control cells was also quantified (Materials and Methods) and recorded. The average concentrations of the total RNA isolated from the duplicate *in vitro* transcription time-course experiments were determined (Table S1). ***The bases highlighted in colour were gene specific sequences used to construct the multiplex shRNA transcription cassette. The colour code representation is as follows:

1. Yellow: shRNA sequences from RVFV L genome segment.
2. Pink: shRNA sequences from RVFV M genome segment.
3. Turguoise: shRNA sequences from RVFV S-genome segment.
4. Bright green: shRNA sequences from GFP.
5. Grey: A 13 bp loop (Spacer) separating the genomic sense and reverse complement shRNA constructs.
6. *Italicized bases:* Restriction enzyme sites used in the costruction of the shRNA transcription cassette.

academicJournals

Vol. 16(18), pp. 1032-1041, 3 May, 2017
DOI: 10.5897/AJB2017.15939
Article Number: 16A399A64053
ISSN 1684-5315
Copyright © 2017
Author(s) retain the copyright of this article
http://www.academicjournals.org/AJB

African Journal of Biotechnology

Full Length Research Paper

Cyclical changes in the histology of the gonads (ovary and testes) of African pike, *Hepsetus odoe*

Idowu, E. O.

Department of Zoology and Environmental Biology, Faculty of Science, Ekiti State University, Ado Ekiti, Ekiti State, Nigeria.

Received 13 February, 2017; Accepted 20 April, 2017

Morphology, stages of maturation and histology of gonads of African pike, *Hepsetus odoe* from Ado Ekiti Reservoir were studied from August 2014 to July 2015 in order to establish its reproductive biology. Out of 685 specimens examined 354 were males and 331 were females giving a sex ratio of 1:1.1 (female:male). There was no significant difference (P>0.05) in the sex ratio. The gonads were in pairs. All the gonad maturity stages were encountered in both male and female gonads. These stages were; immature, developing, mature (ripening), ripe and running, and spent. Histology of female ovary showed that six stages were encountered in the oogenesis, namely, oogonium, primary oocyte, primary vitellogenic oocyte, secondary vitellogenic oocyte, tertiary vitellogenic oocyte and hyaline oocyte while in male spermatogenesis five stages were present which are; spermatogonia, primary spermatocytes, secondary spermatocytes, spermatids and spermatozoa The oocyte diameter of *H. odoe* is higher when compared to freshwater fishes (the range was from 0.25 to 2.07 mean 1.74 ± 0.16 mm). All the five maturation stages occurred every month throughout the study period except the spent stage (stage V) which occurred only in October and ripe and running stage (Stage IV) which was absent only in December. This indicates that *H. odoe* is a multiple spawner in the reservoir.

Key words: African pike, gonads, maturity stages, histology, oogenesis, spermatogenesis.

INTRODUCTION

Hepsetus odoe was thought and believed to be the only species of the family Hepsetidae until recently when other species were discovered. The work of Decru et al. 2011, 2013 on the revision of the Lower Guinea *Hepsetus* species revealed that three different species occur in Lower Guinea instead of one. *Hepsetus akawo*, recently described from West Africa, is present in the northern part of Lower Guinea; *Hepsetus lineata*, the most widespread species within Lower Guinea, is known from the Sanaga (Cameroon) in the north to the Shiloango (Democratic Republic of Congo) in the south and *Hepsetus kingsleyae* is endemic to the Ogowe Basin.

The reproductive cycle of many fishes is reflected by perceptible changes in the size of the gonads throughout the year (Delahunty and Vlaming, 1980). Studies on the gonadal development of tropical fishes include

E-mail: eunice.idowu@eksu.edu.ng, idowunice@yahoo.com. Tel: +2348039422005.

Author(s) agree that this article remains permanently open access under the terms of the Creative Commons Attribution License 4.0 International License

Chrysichthys nigrodigitatus (Fagade and Adebisi, 1979) and *Clarias gariepinus* (Hogendoorn, 1979; Teugel, 1984; Oladosu et al., 1993), Mormyrid, *Hyperopsus bebe* (Oben et al., 2000), *H. odoe* (Idowu, 2007) and *Auchenoglanis occidentalis* (Shinkafi et al., 2011). The principal external factors which are associated with synchronous reproductive activity in temperate fish have been shown to be day length and temperature (Hyder, 1970). The author also revealed that sunlight and temperature are the most important external factors affecting reproductive pattern in *Tilapia leucostica*, and this subsequently influenced the gonadal development and breeding of the fish. However, Lowe (1959) reported that rainfall is the major external factor stimulating breeding activity in tilapias.

Egg diameter of fish varies from one species to another. It may depend on factors like fecundity which in turn is influenced by environmental factors such as temperature, food availability and mode of spawning. Ekpo (1982) reported that egg diameter of *H. odoe* was 1.36 mm in Lekki Lagoon, Idowu (2007) recorded egg diameter value of 1.74±0.2 mm in Ado Ekiti Reservoir. The egg diameter values of species that are closely related to *H. odoe* have also been reported; *Alestes longipinnis* was 0.99 mm and *A. chaperi* was 0.98 mm (Ekpo, 1982)

Studies on gonad histology according to Oben et al. (2000) and Ayoade (2004) reveal not just more developmental stages of the gonads but throws more light on spawning activities and spawning periods in individual fish species. Classification of gonadal stages of fish is based on morphological and histological examination of the gonads. Through this means many workers have been able to elucidate the maturity stages of various species of fish. Ogueri (2004) recognised seven stages; Ayoade (2004) recognized six stages of gonadal development in fishes. Ugwumba (1984) recognized six stages in the ten pounder *Elops lacerta*. These were immature, immature and developing, ripening, ripe, ripe running and spent. Similar observations on stages of gonadal development were reported for *Hyperopisus bebe* by Oben et al. (2000).

Vitellogenic stage of oocyte as well as increased gonad weight; gonadal-somatic index (GSI) value and gonadal histology indicates the maturity of fresh water fishes. The study of gonad stages of maturation as become increasingly important in fish production, notably in induced spawning and hybridization studies (Omotosho, 1993). Knowledge of the gonad maturation of the fishes is also required for many purposes and this include determination of stocks that are mature and the size or age at first maturity (Bagenal, 1978), determination of reproductive potential of fish populations and monitoring of changes in biological characteristics of exploited fish stocks (Williams, 2007), establishing the reproduction period and length of gonadal maturation to allow for accurate implementation of fishery legislation (Goncalves et al., 2006).

Moreover, one of the most important factors necessary in the successful culturing of a fish species is obtaining a basic understanding of its key biological processes. The most important of these biological processes is the reproductive cycle and formation of gametes. However in the course of this research no reference was crossed on the cytology of *H. ode* gonads; most of the previous works on this species were mainly on food and feeding habits, length weight relationship and other aspects of its biology. The objective of this study therefore was the examination of cyclical changes in the histology of the gonads (ovary and testes) of African pike *H. odoe* in Ado Ekiti reservoir which will serve as a biological basis necessary for proper management and sustainability of the species in the reservoir.

MATERIALS AND METHODS

Sex ratio

Sex of each specimen collected was determined by examination of the gonads after dissection and the ratio of male to female calculated.

Egg diameter

The egg diameter was measured using an ocular micrometer in a binocular microscope. A stage micrometer was used to calibrate the microscope. For each ovary, the egg diameter of about 50 randomly selected eggs were measured and the mean taken as the average egg diameter. Egg diameter was measured in millimetre (mm).

Stages of gonad maturation and gonad histology

Gonad maturity stages were assessed and classified according to a modified classification of Hilge (1977) as follow: Stage I, Immature; II, developing; III, mature; IV, ripe and running; V, spent. The fish were dissected and the gonads at each stage of development were removed. Small pieces from the fore part of the gonads at each stage were cut out and fixed in Bouins fluid before embedding in parafin wax of melting point 56°C. Sections were cut at 10 µm and stained with Erlish Haematoxylin and Mallorys triple stain. Details of the procedures for gonad histology were according to Belelander and Ramaley (1979). Conclusive staging of the gonads were made on microscopic examination of the stained sections and photomicrographs taken.

Statistical analysis

Deviations of sex ratio from the expected 1:1 were determined using the Chi-square test.

RESULTS

Sex ratio

Out of 685 specimens examined, 354 were males and

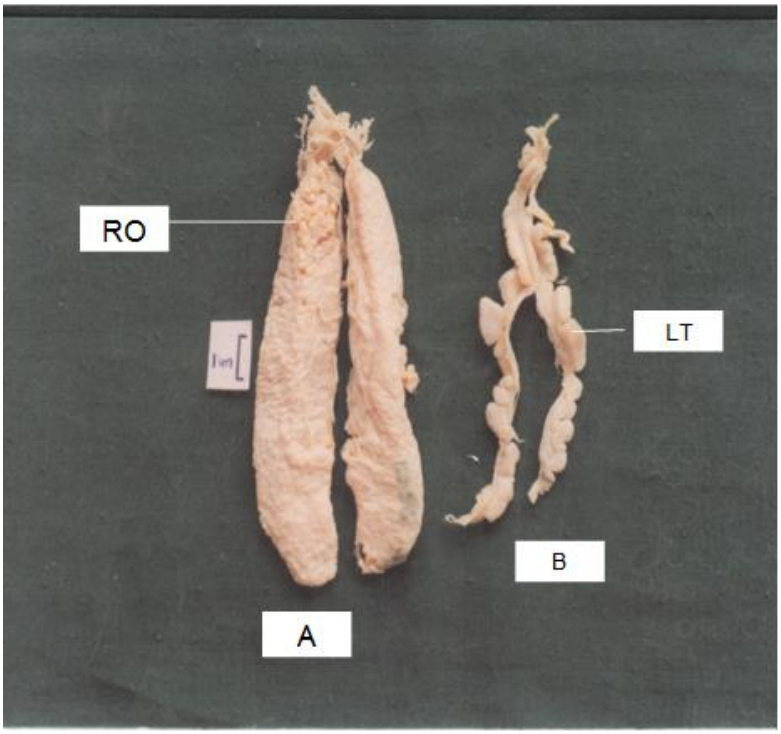

Plate 1. Gonads of *Hepsetus odoe.* A = Ripe ovary of *H. odoe*; B = ripe testes of *H. odoe;* RO = ruptured ovary; LT = lobe of testes.

331 were females giving a sex ratio of 1:1.1 (female: male); there was no significant difference (P>0.05) in the sex ratio.

Egg diameter

Egg diameter ranged between 1.40 to 2.07 mm with mean of 1.74 ± 0.2 mm from ripe/matured stage.

Stages of gonad maturation

Morphology of gonad

The gonads were in pairs. All the gonad maturity stages were encountered. These stages were immature, developing, mature (ripening), ripe and running, and spent.

Female gonad

The description of female gonadal stages was as follows:

Stage 1 (**immature):** Ovaries appeared like pairs of translucent pale white strips and weighed less than 0.5% of fish weight. Eggs were not visible, thus microscopic observations were needed to ascertain sex.

Stage II (immature and developing)**:** Eggs in this stage though minute were visible to naked eye. Ovaries here tended creamy in colour and weighed more than 0.5% fish weight.

S**tage III** (**Ripening):** Ovaries were usually swollen and the lobes were lost. The colour tended yellow and gonad weighed 1-5% of fish weight.

Stage IV (Ripe running stage): ovaries in this maturation stage were fully swollen with anterior bulges and central depression giving a pear like appearance (Plate 1) The ovary wall ruptured and eggs tended reddish due to vascularisation. Ovaries were no longer in strips but occupied more than three quarters (75 to 80%) of the abdominal cavity and rendered alimentary canal and gut almost inconspicuous. Eggs were mostly translucent yellowish and scattered easily on contact. Eggs easily extruded from vent when pressure was applied to the flanks.

Stage V (**Spent**): Ovaries in this stage were brownish towards the vent region. They appeared flaccids.

Males gonads

Stage I (**immature**)**:** The testes in this stage appeared as a pair of white filaments.

Table 1a. Monthly occurrence (by number) of the gonad maturity stages of female *H. odoe* in Ado-Ekiti Reservoir.

Month/year	Gonad maturity stages					
	I	II	III	IV	V	Total number
August, 2014	3	15	-	9	-	27
September	3	12	-	13	-	28
October	12	45	6	9	3	75
November	-	15	3	3	-	21
December	-	3	3	-	-	6
January,2015	-	24	12	15	-	51
February	-	6	9	6	-	21
March	-	6	9	9	-	21
April	6	6	3	9	-	24
May	-	-	3	3	-	6
June	3	6	15	6	-	30
July	6	-	9	9	-	24

Total number (N) = 331.

Table 1b. Monthly occurrence (by number) of the gonad maturity stages of male *H. odoe* in Ado-Ekiti Reservoir.

Month/year	Gonad maturity stages					
	I	II	III	IV	V	Total number
August, 2014	3	12	9	-	-	24
September	15	6	3	-	-	24
October	24	21	15	6	-	66
November	9	3	9	3	-	24
December	6	-	3	-	-	9
January,2015	-	3	3	6	-	12
February	3	3	6	6	-	18
March	15	27	21	9	-	72
April	6	9	6	3	-	24
May	3	-	6	3	-	12
June	3	6	18	12	-	39
July	9	-	6	12	-	27

Total number (N) = 354.

Stage II (immature and developing)**:** The gonads in this stage were still white but increased in size with lobes.

Stage III (ripening): The testes appeared like those in stage II but were larger and softer. The lobes became more prominent.

Stage IV (ripe running): The ripe testes were swollen and multilobed (Plate 1). The colour was creamy white. Blood vessels gave pinkish shades in some areas. When pressure was applied on the flanks, milty drops extruded from the genital pore.

Stage V (spent): Testes in this stage were flabby and pinkish tending brown. Milt still extruded on forced pressure at the flanks.

Table 1a and b show the monthly variations in gonad maturity stages observed in *H. odoe* during the period of investigation. The females had highest ripe eggs (stage IV) in September and January. Stage V (spent stage) was recorded only in October 2014.

Gonad histology

Histology of ovaries

Six stages were encountered in the oogenesis, namely, oogonium, primary oocyte, primary vitellogenic oocyte, secondary vitellogenic oocyte, tertiary vitellogenic oocyte and hyaline oocyte. The development of an oogoniun is shown diagrammatically in Figure 1.

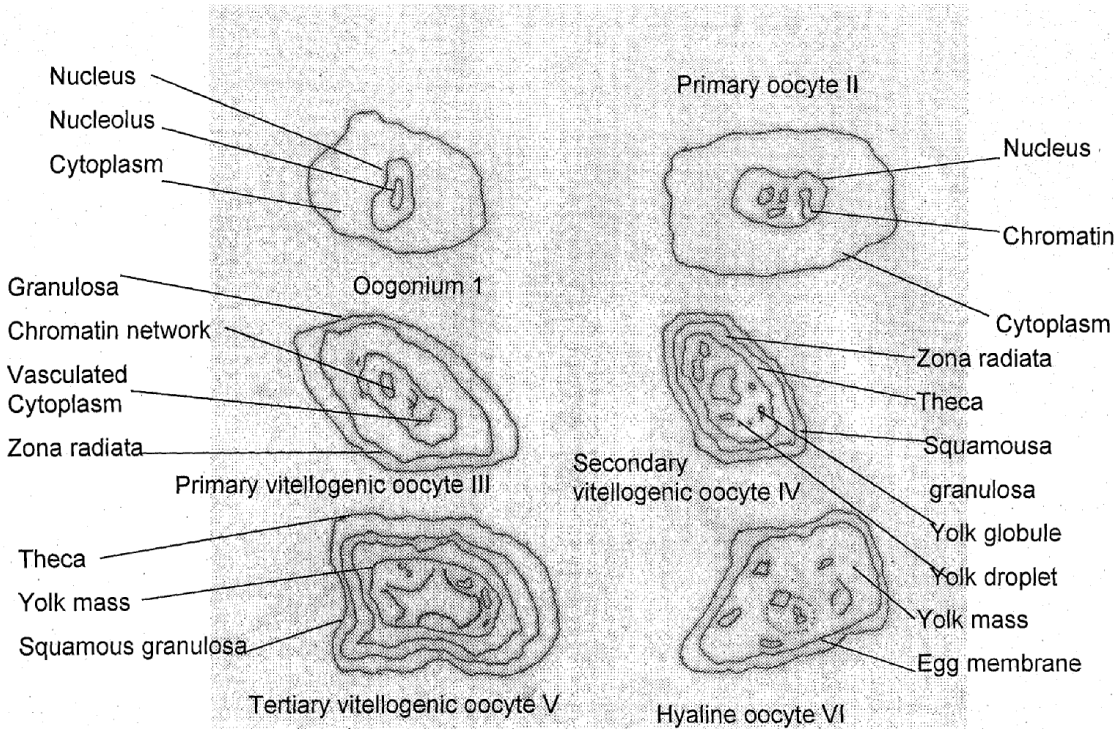

Figure 1. Schematic view of the developmental stages of the egg of *H. odoe* sampled from Ado-Ekiti Reservoir.

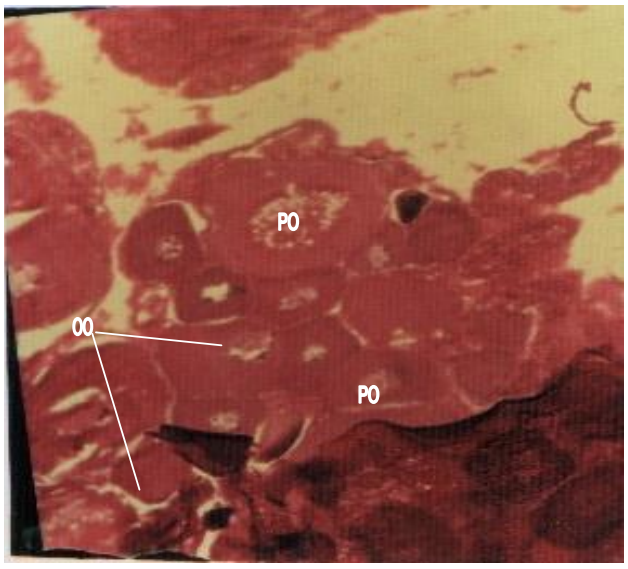

Plate 2. T.S. of stage I (immature) ovary of *H. odoe* showing oogonia (OO) and primary oocytes (PO) H& E (x 100).

Stage 1 (immature): Histological section of stage 1 ovary showed dominance of oogonia and primary oocytes as shown in Plate 2. Oogonia were seen as small spherical cells single or in groups. They were observed in all maturity stages. They were easily identified by the presence of a single large nucleolus in the nucleus.

Ovarian wall thickness had mean value of 0.08±0.01 mm. The mean oocyte diameter was 0.25 ± 0.21 mm and the range was 0.01 to 0.56 mm.

Stage II (developing): Primary vitellogenic oocyte and primary oocytes were found in the histological sections. The primary oocyte is bigger than the oogonium and is characterized by a large nucleus with many nucleoli around its periphery. They were present in all maturation stages. The follicular cells organize themselves around the developing oocytes which develop a larger cytoplasm. Some are ovoid in shape while some are polygonal. Primary vitellogenic oocytes formed 24 to 30% of cells. Mean oocytes diameter was 0.52 ± 0.15 mm. It ranged between 0.3 and 0.7 mm.

Stage III (matured): There were appearances of secondary vitellogenic oocytes forming 10 to 15% of entire cells. Primary vitellogenic oocytes and primary oocytes were also present. Primary vitellogenic oocytes were comprised of irregular shaped cells with vasculated double layered cytoplasm. This stage marks the beginning of yolk development. There is formation of yolk globules in the cytoplasm of secondary vitellogenic oocytes. Yolk globules were present throughout the cytoplasm at the end of this stage. Cells were enveloped by two layers, sqamous granulosa and cellular theca. The

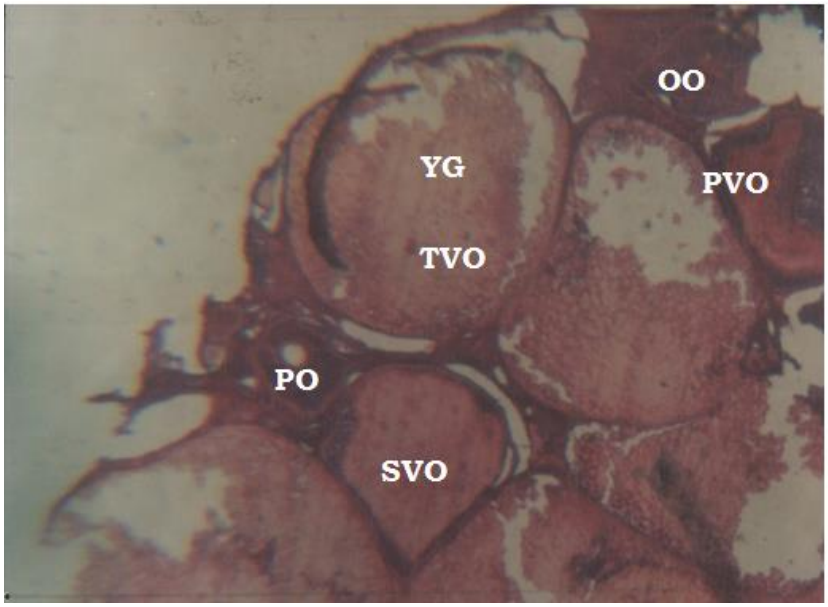

Plate 3. T.S. of stage IV ovary of *H. odoe* showing tertiary vitellogenic oocyte (TVO) with yolk granules (YG), secondary vitellogenic oocyte (SVO), primary oocyte (PO) and oogonium cell (OO) H & E (x 125).

oocyte dimater ranged from 1.26 to 1.76 mm with mean value of 1.53 ± 0.2 mm.

Stage IV (ripe and running): Most of the oocytes were tertiary/mature oocytes and constituted 70 to 75% of entire cells (Plate 3). The interiors were filled with prominent yolk globules and droplets. The two layers enveloping the cells were less defined. The oocyte diameter ranged from 1.40 to 2.07 mm with mean of 1.74 ± 0.16 mm. Mean ovarian wall thickness was 0.01 mm. Yolk globules were prominent in mature oocytes.

Stage V (Spent): There were some ruptured follicles, which appeared empty as if they have released the egg (Plate 4). Hyaline oocytes were also seen and they were filled with yolk and lacked nuclei.

Histology of the testes

Immature (stage I): Sections showed irregular shaped spermatogonia, which aggregated in groups (Plate 5). The spermatogonia were characterized by lightly stained cytoplasm and a large nucleus.

Developing (stage II): Spherical primary spermatocytes predominated. The cell membranes were more defined. The secondary spermatocytes became cusp shaped and were attached to the lobular wall (Plate 6).

Mature (stage III): Sections showed sickle shaped spermatids, which were detached from the lobular wall. Spermatocytes at different stages of development fill the testis at this stage. The testis was filled with spermatids (Plate 7).

Ripe running (stage IV): Empty spaces appeared in the lumen containing loose spermatocytes and spermatozoa (Plate 8).

Spent (stage V): Testis had unfilled lumen with spermatozoa.

DISCUSSION

The sex ratio observed in this study did not differ significantly from the expected 1:1 ratio. According to Nikolsky (1969) and Idowu (2007) a 1:1 sex ratio represents lack of difference in the longetivity of the sexes. Females were slightly heavier than males. This could be due to additional weight gain in ovaries of females especially during the breeding season.

The eggs of *H. odoe* in this study were relatively large and their sizes were higher than 1.36 mm of the same species in Lekki Lagoon reported by Ekpo (1982). This could be as a result of differences in habitat which may reflect the amount of food available and consumed. The egg size of fish varies from one species to another and are affected by various factors such as the degree of parental care (Fryer and Iles, 1972; Fletcher and Wooton, 1995), mode of spawning (Adebisi, 1987), length of interspawning interval (Townsend and Wooton, 1984), amount of food consumed (Springate et al., 1985;

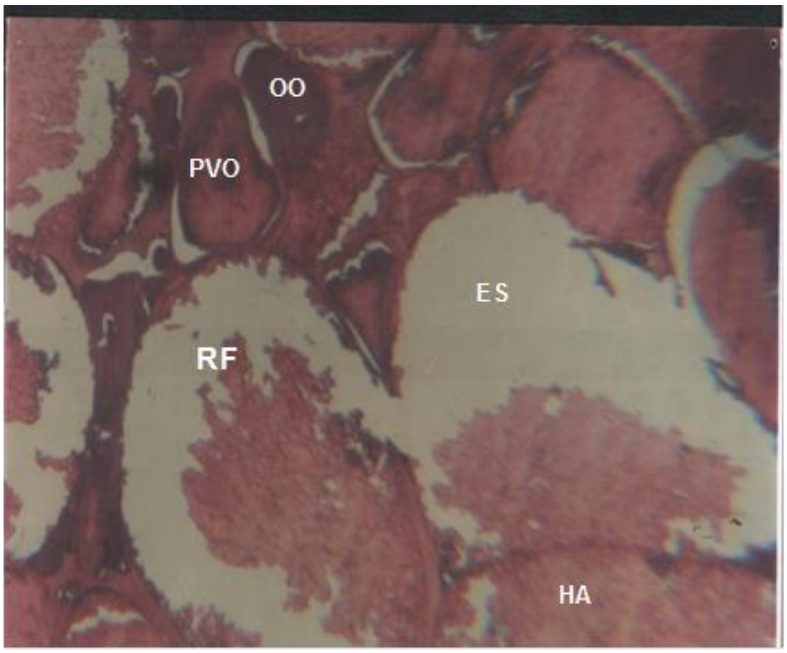

Plate 4. T.S. of stage V (spent) ovary of *H. odoe* showing ruptured follicle (RF), empty space (ES), hyaline oocyte (HA filled with yolk), primary vitellogenic oocyte (PVO) and oogonium cell (OO) H & E (x125), vitellogenic oocyte (PVO) and oogonium cell (OO) H & E (x125).

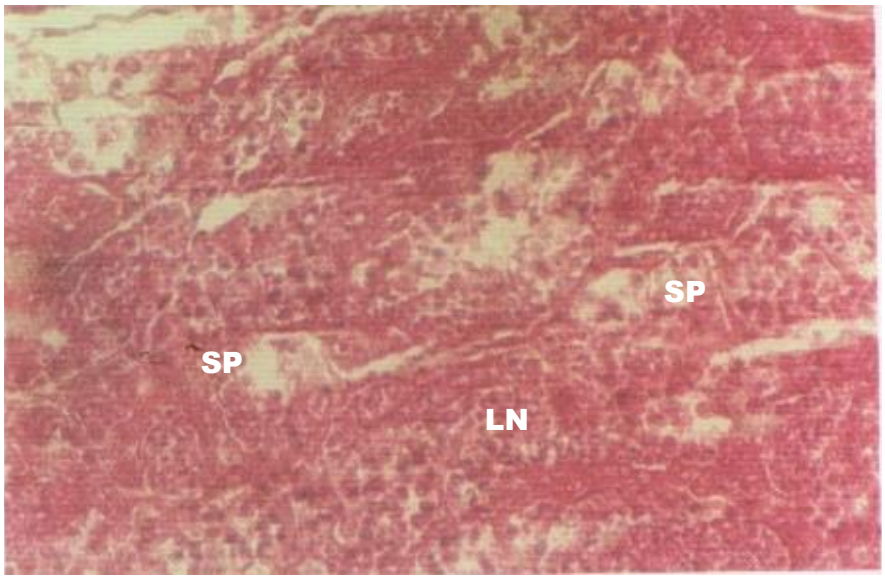

Plate 5. T.S. of stage I (immature) testis of *H. odoe* showing spermatogonia (SP) and large nucleus (LN). H & E (x 400).

Fletcher and Wooton, 1995) and habitat (Elliot, 1986; Ayoade, 2004). Generally, fish species with low egg diameter are usually very fecund while species with large egg diameter are less fecund and may show some degree of parental care (Ekpo, 1982; Adebisi, 1987; Oben et al., 2000).

Fishes with low egg diameters have been reported by some authors. These include; *S. mystus* (Ayoade, 2004), *C. gariepinus* (Abayomi and Arawomo, 1996), *H. bebe* (Adebisi, 1987; Oben et al., 2000), *E. vittata* and *Pellonula afzeliusi* (Ekpo, 1982). Fish species with large egg diameters include, mouth brooding *Tilapia* species

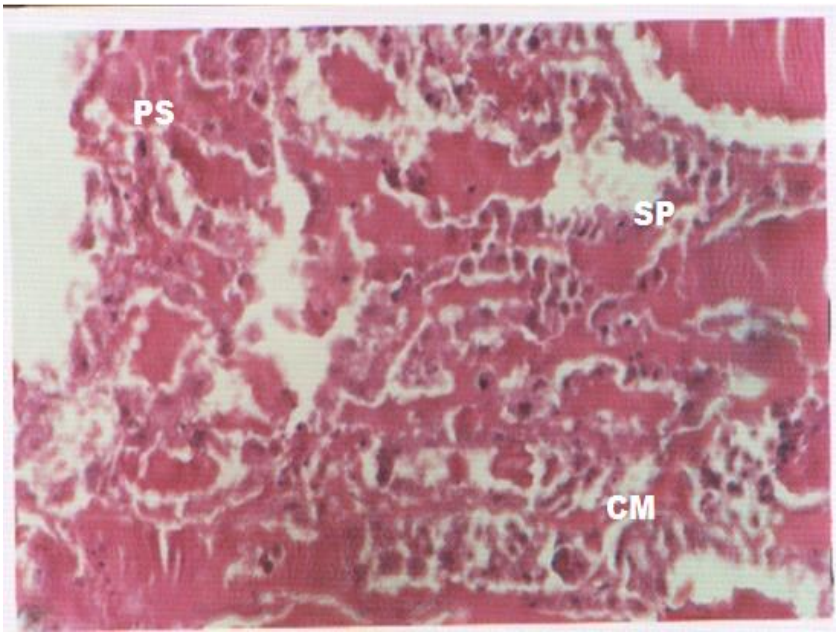

Plate 6. T. S. of stage II (immature and developing) testis of *H. odoe* showing spermatogonia (SP) and primary spermatocyte (PS), cell membrane (CM) H & E (x 400).

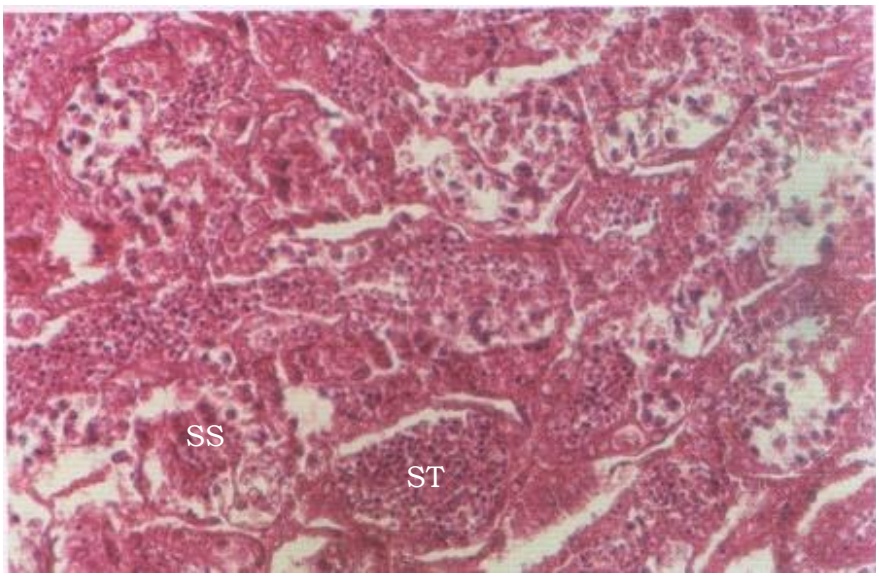

Plate 7. T.S. of stage III (ripening) testis of *H. odoe* showing spermatogonia (SP) and primary spermatocyte (PS), cell membrane (CM) H & E (x 400).

such as *S. galileaus*, *T. aurea,* (Dadzie, 1970). Other fish with large egg diameters include *X. nigri, Pollimyrus adspersus* and *Petrocephalus sanvagii* (Ekpo, 1982). The egg diameters of species that are closely related to *H. odoe* have also been reported to be large. These fish species include *A. longipinnis* and *A. chaperi* (Ekpo, 1982).

The histological analyses permitted precise description of the process of development and maturation. According to Elourduy - Graray and Ramirez - Luna (1994), visual evaluation of maturity of the gonads by microscopic characteristics and the use of gonadal indices are gross indicators of reproductive activity but not accurate enough to establish the stage of gonadal development or

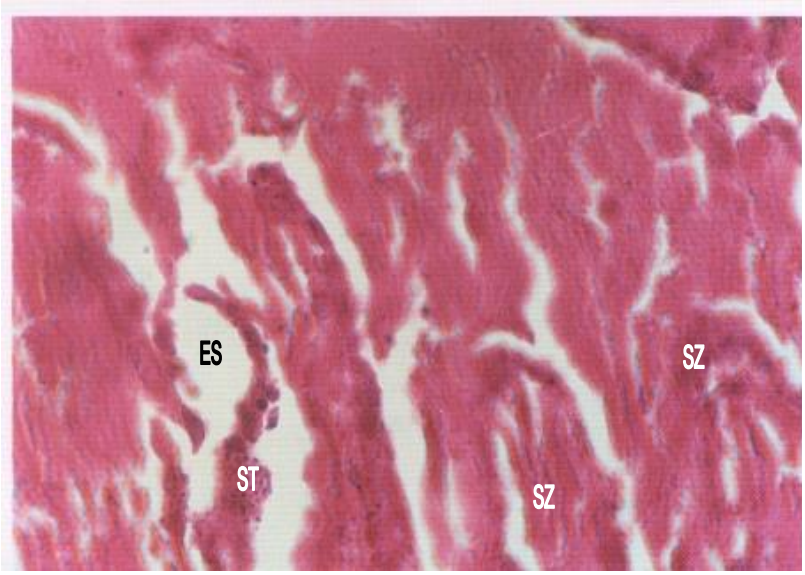

Plate 8. T.S. of stage IV (ripe running) testis of *H. odoe* showing spermatid (ST.) and spermatozoa (SZ) and empty space (ES) H & E (x 400).

to detect subtle differences between gonads. The oocyte diameter of *H. odoe* is higher when compared to freshwater fishes (the range is from 0.25 to 2.07, mean 1.74 ± 0.16 mm). However, Oben (1995) recorded oocyte diameter of 0.17 to 1.23 mm for *Mormyrus rume* while Ayoade (2004) recorded oocyte diameter of 0.06 to 0.66 mm for *Schilbe mystus* in Oyan Lake.

All the five maturation stages occurred every month throughout the study period except the spent stage (Stage V) which occurred only in October and ripe and running stage (Stage IV) which was absent only in December. This indicates that *H. odoe* bred throughout the year (multiple spawner). Abundance of ripe fish was more in October and January, although it was abundant in all other months. This shows that *H. odoe* bred both during the rainy and dry seasons with the peak breeding in these periods of peak abundance of ripe fish.

The peak periods of *H. odoe* abundance were in January, June and September to October. These periods coincided with peak spawning periods. Spawning enhanced new recruits and increased the population during these periods. To avoid the catch of young ones, fishing activities should be reduced or restricted by reduction in number of fishermen and number of fishing periods per day during these peak periods of spawning to allow for steady and adequate recruitment of the species into the population. This will ensure rational exploitation which is the ultimate in sustainable fisheries management.

CONFLICT OF INTERESTS

The authors have not declared any conflict of interests.

REFERENCES

Abayomi OS, Arawomo GAO (1996). Sex ratio and fecundity of *C. gariepinus* in Opa reservoir, Ile-Ife, Nigeria. Proceedings of the Annual Conference of Fisheries Society of Nigeria (FISON). pp. 122-130.

Adebisi AA (1987). The Relationships between the fecundities ,gonadosomatic indices and egg sizes of some fishes of Ogun River Nigeria. Arch. Hydrobiol. 3(I):151-156.

Ayoade AA (2004). The Bionomics of *Schilbe mystus* (Linne, 1766) in Asejire and Oyan Lakes, Southwestern Nigeria. Ph.D. Thesis, University of Ibadan, 275p.

Bagenal TB (1978). Methods for Assessment of fish production in freshwaters. (Ed. Bagenal) Blackwell Scientific Publications. Pp. 219-255

Belelander G, Ramaley JA (1979). Essentials of Histology C.V. Mosboy Comp. St. Loius Toronto, London. Pp. 244-235.

Dadzie S (1970). Laboratory experiment on the fecundity and frequency of spawning in *Tilapia aurea.* Bamidgeh 22:14-18.

Decru E, Vreven E, Snoeks J (2013). A revision of the lower Guinean *Hepsetus* species (Characiformes; Hepsetidae) within the description of *Hepsetus kingsleyae.* J. Fish Biol. 82:1351-1375.

Decru E, Vreven E, Snoeksa J (2011). A revision of the West African *Hepsetus* (Characiformes: Hepsetidae) with a description of *Hepsetus akawo* sp. nov. and a redescription of *Hepsetus odoe* (Bloch, 1794). J. Nat. Hist. 46(1-2):1-23.

Delahunty D, Vlaming VL (1980). Seasonal relationship of ovary weight, liver weight and fat store with body weight in the gold fish *Carassius auratus.* J. Fish Biol. 16:5-13.

Ekpo AEA (1982). Length weight relationship, food habits and fecundity of non – Cichid fishes in Lekki Lagoon, Nigeria. M.Sc. Thesis, University of Lagos.

Elliot OO (1986). Some aspects of the biology of the fishes of Asejire Lake. Ph.D. Thesis, University of Ibadan, Nigeria. 301p.

Elorduy-Garay JF, Ramirez-Luna S (1994). Gonadal development and spawning of female ocean whitefish, *Causioiatilus proinceps* (Pisces: Branchiostegidae) in the Bay of La Paz, BCS, Mexico. J. Fish Biol. 44:553-566.

Fagade SO, Adebisi AA (1979). Observation on the fecundity of *C.nigrodigitatus* (Lacepede of Asejire Dam. Oyo State, Nigeria. Niger. J. Nat. Sci. 1(2):127-131.

Fletcher DA, Wooton RJ (1995). A hierarchical response to differences

in ration size in the reproductive performance of female three-spined stickebacks. J. Fish Biol. 46(4):657-668.
Fryer G, Iles TD (1972). The Cichlid fishes of the great Lake of Africa, Their Biology and Evolution. Edinburgh Oliver and Boyd. 641 p.
Goncalves Tl, Bazzoli N, Brito (2006). Gametogenesis and reproduction of the matrinxa, *Brycon orthotaenia* (Gunther, 1864) (Pisces, Characidae) in the Sao Francisco River, Minas Gerais, Brazil. Braz. J. Biol. 66:513-522.
Hilge V (1977). On the determination of the stages of gonadal ripeness in female bony fishes. Meeresforsch 25:149-155.
Hogendoorn H (1979). Controlled Propagation of the African Catfish, *Clarias lazara* (C. and V.) I – Reproductive biology and field experiments. Aquaculture 17:323-333.
Hyder M (1970). Histological studies on the testes of pond specimens *Tilapia nigra.* (Gunther) Pisces: Cichlidae and the implications of the pituitary – Testis relationship. Gen. Comp. Endocrinol. 14:198-211.
Idowu EO (2007). Aspect of the biology of *Hepsetus odoe* in Ado Reservoir Nigeria. Ph.D. Thesis, University of Ibadan, Pp. 99-120.
Lowe MC (1959). Breeding behaviour patterns and ecological differences between Tilapia species and their significance for evolution within the genus Tilapia (Pisces: Cichlidae). In. Proceedings of the Zoological Society of London. Blackwell Publishing Ltd. 132(1):1-30.
Nikolsky GV (1969). Fish Population Dynamics. Oliver and Boyd, Edinburgh. 323 p.
Oben PM (1995). Age, growth and reproductive biology of some mormyrid species (Pisces: Mormyridae) in the Lekki Lagoon, Nigeria. Ph.D. Thesis, University of Ibadan, Nigeria.
Oben PM Ugwumba OA, Oben BO (2000). Aspects of the reproductive biology of the Mormyrid, *Hyperopisus bebe* (Lacepede) in the Lekki Lagoon, Nigeria. Niger. J. Sci. 34:305-316.
Ogueri C (2004). Physico-chemical parameters, fish fauna and fisheries of River Katsina – Ala, Nigeria. Ph.D. Thesis. University of Ibadan, 351 p.
Oladosu GA, Ayinla, OA Adeyemo AA, Yakubu AF, Ajani AA (1993). A comparative study of the reproductive capacity of the African catfish species *Heterobranchus bidorsalis* (Geoffory), *Clarias gariepinus* (Burchell) and their hybrid "Heteroclarias". Technical paper 92:1-5.
Omotosho JS (1993). Mophological and Histological features of gonadal maturation of *O. Niloticus* (Linn.) Trewavas. J. West Afr. Sci. Assoc. 36:23-26.
Shinkafi BA, Ipinloju JK, Hassan WA (2011). Gonad Maturation Stages of *Auchenoglanis occidentalis* (Valenciennes 1840) in River Rima, North – Western Nigeria. J. Fish. Aquat. Sci. 6:236-246.
Springate JRC, Bromage NR, Cumarantunga PRT (1985). The effects of different ration on fecundity and egg quality in the rainbow trout (*Salmo gairdneri*). In. Nutrition and feeding in fish (Cowey, C.B., Mackie, A.M. and Bell, J.G. Eds) London Academic Press. pp. 371-393.
Teugels GG (1984). The nomenclature of African Clarias species used in aquaculture. Aquaculture 38(4):373-374.
Townsend TJ, Wooton RJ (1984). Effect of food supply on the reproduction of the convict cichlids *Cichlosoma nigrofasciatum.* J. Fish Biol. 29:91-104.
Ugwumba OA (1984). The biology of the Ten-pounder *Elops lacerta* Val. in the freshwater, estuarine and marine environments Ph.D. Thesis, University of Lagos, Lagos.
Williams K (2007). Evaluation of macroscopic staging method for determining maturity of female walleye Pollock, Theragra chalcogramma in Shelikof Strait, Alaska. Alaska Fish Res. Bull. 12:252-263.

academicJournals

Vol. 16(18), pp. 1042-1047, 3 May, 2017
DOI: 10.5897/AJB2015.14975
Article Number: F12241F64055
ISSN 1684-5315
Copyright © 2017
Author(s) retain the copyright of this article
http://www.academicjournals.org/AJB

African Journal of Biotechnology

Full Length Research Paper

The African black soap from *Elaeis guineensis* (Palm kernel oil) and *Theobroma cacao* (Cocoa) and its transition metal complexes

Adebomi A. Ikotun[1*], Oladipupo O. Awosika[1] and Mary A. Oladipo[2]

[1]Department of Chemistry and Industrial Chemistry, Bowen University, Iwo, Nigeria.
[2]Department of Pure and Applied Chemistry, Ladoke Akintola University, Ogbomoso, Nigeria.

Received 17 September, 2015; Accepted 18 November, 2015

African black soap is an indigenous African organic soap formed by esterification. This was prepared by reacting palm kernel oil and the filtrate of cocoa pod ash. Chemical analyses revealed the moisture content was 26% (w/w), total fatty matter (TFM) was 44.75% (w/w), total fatty alkaline (TFA) was 0.22% (w/w), total alkaline (TA) was 11.78% (w/w) and pH was 10. The metal complexes were formed by the reaction of the synthesized black soap with some transition metal salts which included $Cu(CH_3COO)_2.H_2O$, $Pb(CH_3COO)_2.3H_2O$ and $FeCl_3$. The metal:ligand ratio, that is, M:L = 3:1, while the reaction was carried out in an aqueous medium to afford $[Pb(C_{11}H_{23}COO^-K^+)_2(C_{11}H_{23}COO^-)_2].9H_2O$, $[Cu(BL)_4(C_{11}H_{23}COO^-)_2].4H_2O$ and $[Fe(BL)_2(C_{11}H_{23}COO^-)Cl_2]$ with the percentage yield of 56, 48 and 41%, respectively. Characterization of the black soap and complexes was done by spectroscopic analyses and determination of physicochemical properties. The solubility of the metal complexes was determined at room temperature in various solvents. Results showed that solubility increased as polarity decreased and it was most effective with non-polar organic solvents. Potassium ester ($C_{11}H_{23}COO^-K^+$), commonly called African black soap, has acted either as a monodentate or bidentate ligand forming metal complexes by coordinating through one or two of its oxygen donor atoms and also by entirely replacing the potassium ion with the transition metal (displacement reaction). Spectra analyses corroborate an octahedral structure for the Pb(II), a distorted octahedral structure for the Cu(II) and an octahedral Fe(III) complex.

Key words: African black soap, esterification, metal complexes.

INTRODUCTION

Palm kernel oil is an edible plant oil derived from the kernel of the oil palm *Elaeis guineensis* (Poku, 2012). Palm kernel oil is high in lauric acid which has been shown to raise blood cholesterol levels, both as cholesterol contained in low-density lipoprotein (LDL-C) and cholesterol contained in high-density lipoprotein

*Corresponding author. E-mail: lhbcards@yahoo.com or ikotunadebomi@gmail.com.

Author(s) agree that this article remains permanently open access under the terms of the Creative Commons Attribution License 4.0 International License

(HDL-C) (Rakel, 2012). Palm kernel oil does not contain cholesterol or trans fatty acids (Rakel, 2012). Lauric acid is important in soap making: a good soap must contain at least 15% laurate for quick lathering, while soap made for use in sea water is based on virtually 100% laurate (Musa, 2009). *Theobroma cacao* also called cacao tree, is a small (13 to 26 ft tall) evergreen tree in the family Malvaceae, whose parts are very useful to man's daily living (Encyclopedia of Life, 2012). Soaps are mainly used as surfactants for washing, bathing and cleaning, but they are also used in textile spinning and are important components of lubricants. Soaps for cleansing are obtained by treating vegetable oil or animal oils and fats with a strong alkaline solution. Fats and oils are composed of triglycerides; three molecules of fatty acids are attached to a single molecule of glycerol (Beetseh and Anza, 2013). Black soap (BL) widely used by different tribes in Nigeria has different names, such as Ose Dudu in Yoruba and Eko Zhiko in Nupe (Getradeghana, 2000). In the Western part of Africa, black soap is known as Anago soap or Alata simena in Ghana and in Hausa it is known as Sabulun salo. The making of soaps from ash-derived alkali has been an age-old craft in Nigeria and West African countries (Bella, 2008). African black soap or black soap is a natural source of vitamin A and E, and iron (Grieve, 1997). Depending on where it is manufactured, black soap contains leaves and plantain skins, shea tree bark, cocoa pods or palm tree leaves (Bella, 2008). Metal complexes or coordination complexes consist of an atom or ion (usually metallic), and surrounding array of bound molecules or anions, that are in turn known as ligands or complexing agents (IUPAC, 1997). Air stable Ag(I), Co(II) and Cu(II) complexes of pyrimethamine have been synthesized and characterized by Idemudia and Ajibade (2010). The structure of African black soap, a potassium ester, reveals it contains two oxygen donor atoms (Dunn, 2010). These oxygen donor atoms can coordinate to other transition metals. The objectives of this study were to prepare and chemically analyze the African black soap from *E. guineensis* (Palm Kernel Oil) and *T. cacao* (Cocoa) and its transition metal complexes. Therefore, this report serves as the first on the coordination of one or two of the oxygen donor atoms present in the potassium ester, African black soap, to other transition metals, as well as the substitution of the potassium cation with a transition metal.

MATERIALS AND METHODS

Chemical

Palm kernel seeds and cocoa pods were locally sourced from a town called Ifeodan, Osun State, Nigeria. All solvents used (methanol, dimethylsulfoxide (DMSO), dimethylformamide (DMF), acetone, chloroform, ethanol and diethyl ether) were purchased as analytical grades from Sigma-Aldrich and SAARChem.

Instrumentation

Infrared spectra were recorded as KBR plates on a Nicolet Avatar FTIR 330 spectrophotometer. The UV-Visible spectra were recorded on a Schimadzu UV-1800 spectrometer. The percentage metal analyses were determined using Agilent 240FS AA spectrometer.

Preparation of black soap

The palm kernel oil was obtained from palm kernel seeds. These seeds were ground to extract the palm kernel oil locally by squeezing. Thereafter, 20 pieces of cocoa pods were burnt to ashes. 750 g of the ash was mixed with 1 L of water. The mixture was filtered to get the filtrate. A pot was placed on a burner prepared from local firewood, 1 L of the palm kernel oil was poured into the pot and it was allowed to boil. 0.5 L of the potash ash filtrate from cocoa pods was measured in a bowl. 0.3 L of the filtrate was poured gradually with the hand well above the pot into the boiling oil. As the filtrate was poured into the boiling oil, the mixture began to lather. The mixture was left to heat at a regulated temperature. The remaining 0.2 L of the filtrate was poured gradually into the mixture and allowed to boil at a regulated temperature. This process was repeated till the ash filtrate was used up. 10 min later, the mixture was stirred and as the stirring continued, the mixture began to solidify. 50 ml of water was added to the solid mixture and stirred thoroughly to form a dark brown soap. The solid soap was melted to obtain a much softer and feather weight soap, while the stove was maintained at a very low temperature to avoid burning or charring of the soap.

Preparation of the metal complexes of black soap

Various complexes were prepared by reacting metal salt:black soap in the ratio 3:1. 0.00132 mol (0.5 g) of $Pb(CH_3COO)_2.3H_2O$ was reacted with 0.000439 mol (0.105 g) of black soap, 0.0025 mol (0.5 g) of $Cu(CH_3COO)_2$ was reacted with 0.0008348 mol (0.199 g) of black soap and 0.00308 mol (0.5 g) of $FeCl_3$ was also separately reacted with 0.001027 mol (0.24 g) of black soap. Each metal salt was dissolved in 20 ml of distilled water and then added to a stirring solution of the black soap in 10 ml distilled water. The colour of each solution changed in a few minutes. The mixture was refluxed for 1 h and the products precipitated were filtered (after cooling), washed with 5 ml of distilled water, dried and stored in the desiccator.

RESULTS AND DISCUSSION

The reaction for the preparation of African black soap (Dunn, 2010) is presented as Equation 1.

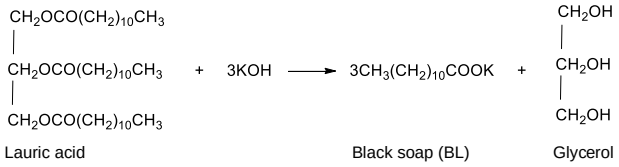

Equation 1: Preparation of African black soap

The general equation for the preparation of the transition metal complexes synthesized from the reaction of black soap and the hydrated acetate salts can be represented

$C_{11}H_{23}COO^-K^+$ (BL) $C_{11}H_{23}COO^-$ (L)

Figure 1. Structures of both ligands, that is, black soap (BL) and its hydrolyzed state (L).

Table 1. Some physical properties of black soap and its metal complexes.

Compound	Colour	Formula weight	Yield (% Yield)	% Metal calculated (Found)
$C_{11}H_{23}COO^-K^+$ (BL)	Dark Brown	238	0.31 g (56)	ND
$[Pb(BL)_2(C_{11}H_{23}COO^-)_2].9H_2O$	White	1243	0.31 g (56)	16.67 (16.70)
$[Cu(BL)_4(C_{11}H_{23}COO^-)_2].4H_2O$	Blue	1489	0.59 g (48)	4.28 (4.30)
$[Fe(BL)_2(C_{11}H_{23}COO^-)Cl_2]$	Red	802	0.42 g (51)	6.97 (7.0)

ND: Not determined.

Table 2. FTIR spectra analyses of the metal complexes and black soap.

Compound	υ (OH) (cm^{-1})	υ (C-H) (cm^{-1})	υ (C=O) (cm^{-1})	υ (C-O) (cm^{-1})	Others
$C_{11}H_{23}COO^-K^+$ (BL)	3250 s 3170 s	2995 s 2877 s	1770 s 1688 s	1305 s	1435 s
Pb(II) complex; $[Pb(BL)_2(C_{11}H_{23}COO^-)_2].9H_2O$	3522 bw	2925 s 2863 s	-	-	1524 s 1411 s
Cu(II) complex; $[Cu(BL)_4(C_{11}H_{23}COO^-)_2].4H_2O$	3472 bm	2932 s 2866 s	-	-	1555 s 1423 s
Fe(III) complex; $[Fe(BL)_2(C_{11}H_{23}COO^-)Cl_2]$	3460 bm	2931 s 2866 s	-	-	1591 s 1448 s

as Equation 2.

$$M(CH_3COO)_2.xH_2O + yBL \xrightarrow{H_2O} [M(BL)_{2m}L_2].nH_2O + 2CH_3COOK$$

where BL is black soap ($C_{11}H_{23}COO^-K^+$) and L is the $C_{11}H_{23}COO^-$ when $M^{2+} = Pb^{2+}$; x = 3, y = 4, m = 1 and n = 9; when $M^{2+} = Cu^{2+}$; x = 1, y = 6, m = 2 and n = 4.

Equation 2: General equation for the reaction of black soap with hydrated acetate salts

But when the salt was changed to anhydrous $FeCl_3$, the equation of the reaction with the prepared black soap is presented as Equation 3.

$$FeCl_3 + yBL \xrightarrow{H_2O} [Fe(BL)_{2m}LCl_2] + KCl$$

where BL is the black soap ($C_{11}H_{23}COO^-K^+$) and L is the $C_{11}H_{23}COO^-$ for y = 2 and m = 1.

Equation 2: The reaction of black soap with anhydrous metal chloride salt

Figure 1 presents the structures of both ligands, that is, black soap and its hydrolyzed state (L).

Some of the physical properties of black soap and its metal complexes are shown in Table 1.

Infrared spectra analysis

The FTIR spectra analyses of the prepared black soap and its metal complexes are shown in Table 2. The characteristic vibrational frequencies have been identified

Table 3. Electronic spectra data for the metal complexes and black soap.

Compound	Band position (nm)	Band position (cm^{-1})	Transition
$C_{11}H_{23}COO^-K^+$ (BL)	350	28,571	n - π*
	277; 299	36,101; 33,445	π - π*
$[Pb(BL)_2(C_{11}H_{23}COO^-)_2].9H_2O$	259	38,610	π - π*
	466; 496	21,459; 20,161	d-d
$[Cu(BL)_4(C_{11}H_{23}COO^-)_2].4H_2O$	262	38,168	π - π*
	688; 721	14,535; 13,870	d-d
$[Fe(BL)_2(C_{11}H_{23}COO^-)Cl_2]$	340	29,411	n- π*
	288	34,722	π - π*
	466; 544	21,459; 18,382	d-d

by comparing the spectra of the complexes with the free ligand. There are two potential donor sites in black soap. These are the keto-oxygen and ester oxygen. The infrared spectrum of the prepared black soap shows two strong bands at 3250 and 3170 cm^{-1} attributed to the stretching vibration of υ (OH) due to hydrogen bonding. This bands appeared as a broad either medium or weak band having undergone a shift to higher frequencies between 3460 and 3522 in the metal complexes due to the presence of the water molecules. The strong bands appearing at 1770 and 1688 cm^{-1} in the spectrum of black soap were attributed to the υ (C=O) frequency of the keto group. These bands have disappeared in all its metal complexes signifying the involvement of the oxygen of the keto group in chelation. The strong band appearing at 1305 cm^{-1} attributable to υ (C-O) frequency has also disappeared in all its metal complexes. This also signifies the involvement of the oxygen of the ester group in chelation (Osowole et al., 2005; Adetoye et al., 2009; Ikotun et al., 2011; Oladipo et al., 2012).

Electronic spectra analyses

The electronic spectra data for black soap and the metal complexes are shown in Table 3. The solid reflectance spectra of these compounds were determined. The ultraviolet spectrum of black soap showed an absorption at 28,571 cm^{-1}, which has been attributed to n - π* transition. This band disappeared in the spectra of its Cu(II) and Pb(II) complexes, but appeared at a higher frequency of 29,411 cm^{-1} in the spectrum of its Fe(III) complex. The bands appearing at 36,101 and 33,445 cm^{-1} have been attributed to π - π* transitions. This π - π* transition appeared as a single band in all its complexes, moving to higher frequencies. It appeared at 38,610 cm^{-1} in complex $[Pb(BL)_2(C_{11}H_{23}COO^-)_2].9H_2O$; 38,168 cm^{-1} in complex $[Cu(BL)_4(C_{11}H_{23}COO^-)_2].4H_2O$ and 34,965 cm^{-1} in complex $[Fe(BL)_2(C_{11}H_{23}COO^-)Cl_2]$. The visible spectrum of the complex $[Pb(BL)_2(C_{11}H_{23}COO^-)_2].9H_2O$ showed d-d transitions at 21,459 and 20,161 cm^{-1} (Lever, 1980). These d-d transitions appeared at 14,535 and 13,870 cm^{-1} in the spectrum of $[Cu(BL)_4(C_{11}H_{23}COO^-)_2].4H_2O$, while also appearing at 21,459 and 18,382 cm^{-1} in the spectrum of $[Fe(BL)_2(C_{11}H_{23}COO^-)Cl_2]$ (Lever, 1980; Oladipo et al., 2012).

Solubility test

The results of the solubility test of black soap and its metal complexes are shown in Table 4. The solubility of the prepared compounds was determined at room temperature (25°C) in water, methanol, ethanol, dimethylsulfoxide (DMSO), dimethylformamide (DMF), acetone, chloroform and diethyl ether, with a decreasing order of polarity. Solubility test results revealed that black soap was soluble in water and diethyl ether, sparingly soluble in the alcohols, while insoluble in all other tested solvents. The Pb(II) complex was only soluble in diethyl ether, sparingly soluble in chloroform and insoluble in all other tested solvents. Cu(II) complex was soluble in DMSO, DMF, chloroform and diethyl ether, but insoluble in water, methanol, ethanol and acetone. Fe(III) complex was soluble in chloroform and diethyl ether. It was sparingly soluble in DMSO and DMF, while it was insoluble in all other tested solvents.

Other physicochemical properties of black soap

Table 5 presents the results for some other determined physicochemical parameters for the prepared black soap. The total fatty matter (TFM) as determined was 44.75% (w/w), total fatty alkaline (TFA) was 0.22% (w/w), the moisture content was 26% (w/w), the pH was 10 and the total alkaline (TA) was 11.78% (w/w). Figure 2 presents the proposed structures for the prepared transition metal complexes of black soap based on spectra analyses.

Table 4. The solubility test of the black soap and its metal complexes.

Compound	Water	Methanol	Ethanol	DMSO	DMF	Acetone	Chloroform	Diethyl ether
$C_{11}H_{23}COO^-K^+$ (BL)	Soluble	Sparingly soluble	Sparingly soluble	Insoluble	Insoluble	Insoluble	Insoluble	Soluble
Pb(II) complex	Insoluble	Insoluble	Insoluble	Insoluble	Insoluble	Insoluble	Sparingly soluble	Soluble
Cu(II) complex	Insoluble	Insoluble	Insoluble	Soluble	Soluble	Insoluble	Soluble	Soluble
Fe(III) complex	Insoluble	Insoluble	Insoluble	Sparingly soluble	Sparingly soluble	Insoluble	Soluble	Soluble

Table 5. Results of the percentage composition of various parameters of black soap).

Parameter	Composition (%)
Total fatty matter	44.75
Total fatty alkaline	0.22
Moisture content	26
pH	10
Total alkaline	11.78

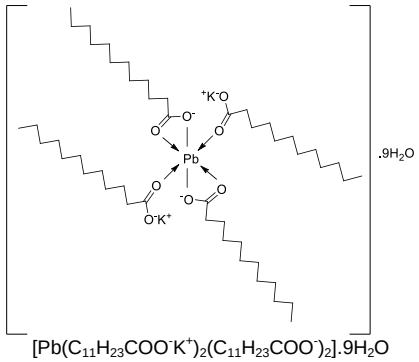

$[Pb(C_{11}H_{23}COO^-K^+)_2(C_{11}H_{23}COO^-)_2].9H_2O$

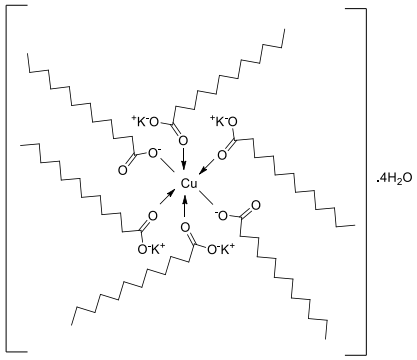

$[Cu(C_{11}H_{23}COO^-K^+)_4(C_{11}H_{23}COO^-)_2].4H_2O$

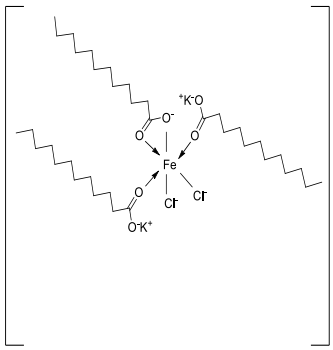

$[Fe(C_{11}H_{23}COO^-K^+)_2(C_{11}H_{23}COO^-)Cl_2]$

Figure 2. Proposed structures for transition metal complexes of black soap.

Conclusion

African black Soap from *E. guineensis* (Palm Kernel Oil) and *T. cacao* (Cocoa) and its transition metal complexes have been successfully prepared. Physicochemical

analyses of this black soap revealed that the moisture content was 26% (w/w), TFM was 44.75% (w/w), TFA was 0.22% (w/w), TA was 11.78% (w/w) and pH was 10. Potassium ester, commonly called African black soap, $C_{11}H_{23}COO^{-}K^{+}$ (BL), has also acted either as a monodentate or a bidentate ligand forming metal complexes by either coordinating through one or two of its oxygen donor atoms or entirely replacing the potassium cation with the transition metal (displacement reaction). Spectra analyses corroborate an octahedral structure for the prepared Pb(II), Cu(II), and Fe(III) complexes, with Pb(II) and Cu(II) complexes possessing some water of hydration. This report presents an arousing interest in the possibility of this ligand to form more complexes with other transition metals, as well as mixed ligand complexes with further studies.

CONFLICT OF INTERESTS

The authors have not declared any conflict of interests.

REFERENCES

Adetoye AA, Egharevba GO, Obafemi CA, Kelly DR (2009). Synthesis and Physicochochemical Properties of Co(II), Cu(II), Fe(III), Mn(II) and Ni(II) Complexes of the Isatin Derivative of Sulfanilamide. Toxicol. Environ. Chem. 91(5):837-846.

Beetseh CI, Anza MK (2013). Chemical characterization of local black soap (chahul mtse) made by using cassava peels ashes (alkali base) and palm oil in North Central Zone of Nigeria. Civ. Environ. Res. 3(4):82-91.

Bella O (2008). African Black Soap, http://www.bellaonline.com/articles/art26846.asp

Dunn KM (2010). Scientific Soap making: The Chemistry of Cold Process. Clavicula Press. Encyclopedia of Life. (2012).

Encyclopedia of Life. (2012). http://eol.org/pages/484592/details

Getradeghana BT (2000). Evaluation of African traditional soap. Glob. J. Pure Appl. Sci. 6:174-179.

Grieve M (1997). Modern Herbal Medicine. 1st ed. Saunders Company Limited. pp. 64-74.

Idemudia OG, Ajibade PA (2010). Antibacterial activity of metal complexes of antifolate drug pyrimethamine. Afr. J. Biotechnol. 9(31):4885-4889.

Ikotun AA, Ojo Y, Obafemi CA, Egharevba GO (2011). Synthesis and antibacterial activity of metal complexes of barbituric acid. Afr. J. Pure Appl. Chem. 5(5):97-103.

IUPAC (1997). Compendium of Chemical Terminology, 2nd ed. (the “Gold book”). Online corrected version (2006): “complex”.

Lever ABP (1980). Inorganic Electronic Spectroscopy, 4th ed. London: Elsevier. pp. 481-579.

Musa JJ (2009). Evaluation of the Lubricating Properties of Palm Kernel Oil. Leonardo Electronic J. Pract. Technol. 14:107-114.

Oladipo MA, Bello OS, Adeagbo AI (2012). Kinetics, mechanism and spectral studies of bis(dibenzoyl-methane) copper (II) complex and its adducts. Afr. J. Pure Appl. Chem. 6(3):35-41.

Osowole AA, Kolawole GA, Fagade OE (2005). Synthesis, physicochemical and Biological properties of Nickel (II), Copper (II) and Zinc (II) complexes of an Unsymmetrical tetradentate Schiff base and their adducts. Synthetic and Reactivity in Inorganic and Metal Organic Chemistry 35:829-836.

Poku K (2002). Origin of oil palm. Small-Scale Palm Oil Processing in Africa. FAO Agricultural Services Bulletin 148, Food and Agriculture Organization; 3. ISBN 92-5-104859-2.

Rakel D (2012). Integrative Medicine. Elsevier Health Sciences. 381p.

academicJournals

Vol. 16(18), pp. 1048-1060, 3 May, 2017
DOI: 10.5897/AJB2017.15911
Article Number: 12183F164057
ISSN 1684-5315
Copyright © 2017
Author(s) retain the copyright of this article
http://www.academicjournals.org/AJB

African Journal of Biotechnology

Full Length Research Paper

Metabolic engineering of *Corynebacterium glutamicum* to enhance L-leucine production

Huang Qingeng, Liang Ling, Wu Weibin, Wu Songgang and Huang Jianzhong*

Engineering Research Center of Industrial Microbiology, Ministry of Education, Fujian Normal University, Qishan Campus, Fuzhou City, Fujian Province, P. R. China.

Received 24 January, 2017; Accepted 20 April, 2017

This work aimed to develop an efficient L-leucine industrial production strain of *Corynebacterium glutamicum* by using metabolic engineering. A recombinant *C. glutamicum* strain was constructed by expressing a feedback-resistant leuA-encoded 2-isopropylmalate synthase (IPMS) that carries three amino acid exchanges (R529H, G532D and L535V) from the mutant strain *C. glutamicum* ML1-9 which was obtained by screening for structural analogues. In order to improve the expression of IPMS, a strong promoter (*tac* promoter) was used to ensure efficient expression of the rate-limiting enzyme. In addition, reasonable metabolic modifications on the central carbon metabolic pathway and competitive metabolic pathways to optimize the L-leucine biosynthesis pathway by redistribution of various types of precursors and repression of negative regulation were used aimed for increased L-leucine production. The modifications involved (1) deletion of the gene encoding the repressor LtbR to increase expression of l*euBCD*, (2) deletion of the gene encoding the AlaT to decrease the concentration of extracellular L-alanine, and increased availability of pyruvate for L-leucine formation, (3) deletion of the gene encoding the threonine dehydratase to abolish L-isoleucine synthesis and to eliminate the intermediate precursor of L-isoleucine biosynthesis competing with L-leucine biosynthesis, (4) inactivation of the pantothenate synthetase to increase α- ketoisovalerate formation, and to enable its further conversion to L-leucine, and (5) inactivation of lactate dehydrogenase to decrease lactate production and its pyruvate consumption, concomitant to decreased glucose consumption rates and prevention of lactic acid to restrict cell growth. The production performance of the engineered strain MDLeu-19/pZ8-1*leuA*^{r} was characterized with cultivations in a bioreactor. Under fed-batch conditions in a 50-L automated fermentor, the best producer strain accumulated 38.1 g L^{-1} of L-leucine; the molar product yield being 0.42 mol L-leucine per mole of glucose (glucose conversion rate attained 26.4%). Moreover, during large-scale fermentation using a 150-m^{3} fermentor, this strain produced more than 37.5 g L^{-1} L-leucine and the glucose conversion rate was 25.8%, making this process potentially viable for industrial production.

Key words: *Corynebacterium glutamicum*, L-leucine, metabolic engineering, fermentation, industrial production.

INTRODUCTION

Corynebacterium glutamicum is a gram-positive, facultatively anaerobic, non-spore-forming, soil bacterium, which was originally discovered as a L-glutamic acid-secreting microorganism in the 1950s (Kinoshita et al.,

2004; Nakayama et al., 1961; Udaka, 1960) and initially known as *Micrococcus glutamicus*; later various isolates were identified (for example *Brevibacterium flavum*, *Brevibacterium lactofermentum*, *Brevibacterium divaricatum*, and *Corynebacterium lilium*) (Liebl et al., 1991). *C. glutamicum* is used in industrial biotechnology to produce several million tons of L-amino acids, such as the flavor enhancer L-glutamate (2,300,000 t/year) and the feed additive L-lysine (1,600,000 t/year) annually (Becker et al., 2011; Chen et al., 2014; Woo and Park, 2014). Thus, *C. glutamicum* has become a platform organism in industrial biotechnology (Becker et al., 2012). Based on the increasing knowledge about this organism, *C. glutamicum*, is a highly efficient host for the expression of heterologous proteins (Scheele et al., 2013), and gradually is being developed into an efficient industrial producer of branched chain amino acids (BCAAs) (Hasegawa et al., 2013; Vogt et al., 2014; Yin et al., 2014).

The BCAAs namely, L-valine, L-leucine, and L-isoleucine, have recently been attracting much attention due to their potential applications in various fields, including animal feed additives, cosmetics, pharmaceuticals, energy drinks and precursors in the chemical synthesis of herbicides (Becker and Wittmann, 2012; Kimball and Jefferson, 2006; Platell et al., 2000). The annual demand of BCAAs is more than 2500 tons, out of which demand of 1000 ton is for L-leucine alone and constantly increasing.

An important member of BCAAs, the role of L-leucine in stimulation of muscle protein synthesis and glucose homeostasis was described (Garlick, 2005; Kimball and Jefferson, 2006; Layman, 2003). L-leucine, in combination with the other BCAAs, has also been reported to be prescribed for patients with hepatic encephalopathy (Freund et al., 1982; Gluud et al., 2013, 2015). In addition, L-leucine is used in the condiment industry and as a lubricant in the pharmaceutical industry (Leuchtenberger, 2008; Mangal et al., 2015; Platell et al., 2000). Moreover, the pentanol isomers, such as 3-methyl-1-butanol, manufactured from the L-leucine precursor 2-ketoisocaproate have a potential application as biofuels (Cann and Liao, 2010; Li et al., 2010).

So far, most L-leucine producers, especially based on *C. glutamicum* production strains have been developed by random mutagenesis and screening of structural analogs and auxotrophic strains. One of the first L-leucine producers was a α-thiazolealanine-resistant, methionine-isoleucine-auxotrophic mutant derived from the glutamate-producing bacterium *B. lactofermentum* 2256, treated with nitrosoguanidine (Tsuchida et al., 1974). This strain was further optimized for higher yields by additional mutagenesis steps (Ambe-Ono et al., 1996; Tsuchida and Momose, 1986). Although this classical approach has been successful in terms of improving the yield of L-leucine by genetic manipulation of *C. glutamicum*; it has some limitations. The genetic alterations caused by random mutagenesis includes the region which is not directly related to amino acid biosynthesis, thereby causing some unwanted changes in cellular physiology such as, growth retardation and by-product formation (Woo and Park, 2014). In particular, the accumulation of large amounts of by-products is a problem in the production of the three BCAAs due to their overlapping biosynthetic pathways, which negatively affects the yield and downstream processing.

The market is growing substantially and requires efficient production processes, strategies for developing microbial strains efficiently producing L-leucine are now in transition from random mutagenesis towards systems metabolic engineering (Becker et al., 2016). The metabolism and regulatory circuits of L-leucine biosynthesis need to be thoroughly understood for designing system-wide metabolic engineering strategies (Park and Lee, 2010; Vogt et al., 2014).

In this study, we report the rational design of a *C. glutamicum* L-leucine producer ML1-9. The source strain used was a methionine prototrophic L-leucine-producing strain resistant to α-thiazolealanine (α-TA), α-amino butyric acid (α-AB) and γ-aminobutyric acid (γ-AB). In order to increase the L-leucine production, we developed genetically defined, highly efficient, and genetic stable producer strains. The main metabolic engineering strategies employed (Figure 1) are beneficial to the construction of engineering strains with the potential of industrial scale fermentation processes.

MATERIALS AND METHODS

Bacterial strains and plasmids

Escherichia coli JM109 was used for cloning. The *C. glutamicum* strains used are listed in Table 1 and plasmids and oligonucleotide primers are listed in Table 2.

Media and growth conditions

E. coli JM109 was cultivated in Luria-Bertani (LB) medium (Bertani, 1951), with kanamycin (25 mg mL^{-1} for *C. glutamicum* strains, 50 mg mL^{-1} for *E. coli* JM109) where appropriate, at 37°C. Bacterial growth was assessed by measuring optical density at 560 nm (OD_{560nm}). Slant cultures of *C. glutamicum* was maintained in LBG (LB plus w/v 0.5% glucose), with kanamycin if necessary at 30°C. In cases where threonine dehydratase (*ilvA*), ketopantoate hydroxymethyl transferase (*panB*), and pantothenate synthetase (*panC*) had to be inactivated, the growth medium was supplemented with L-isoleucine and D-pantothenate or vitamin B_5.

The seed medium for producing L-leucine contained the following

*Corresponding author. E-mail: hjz@fjnu.edu.cn.

Author(s) agree that this article remains permanently open access under the terms of the Creative Commons Attribution License 4.0 International License

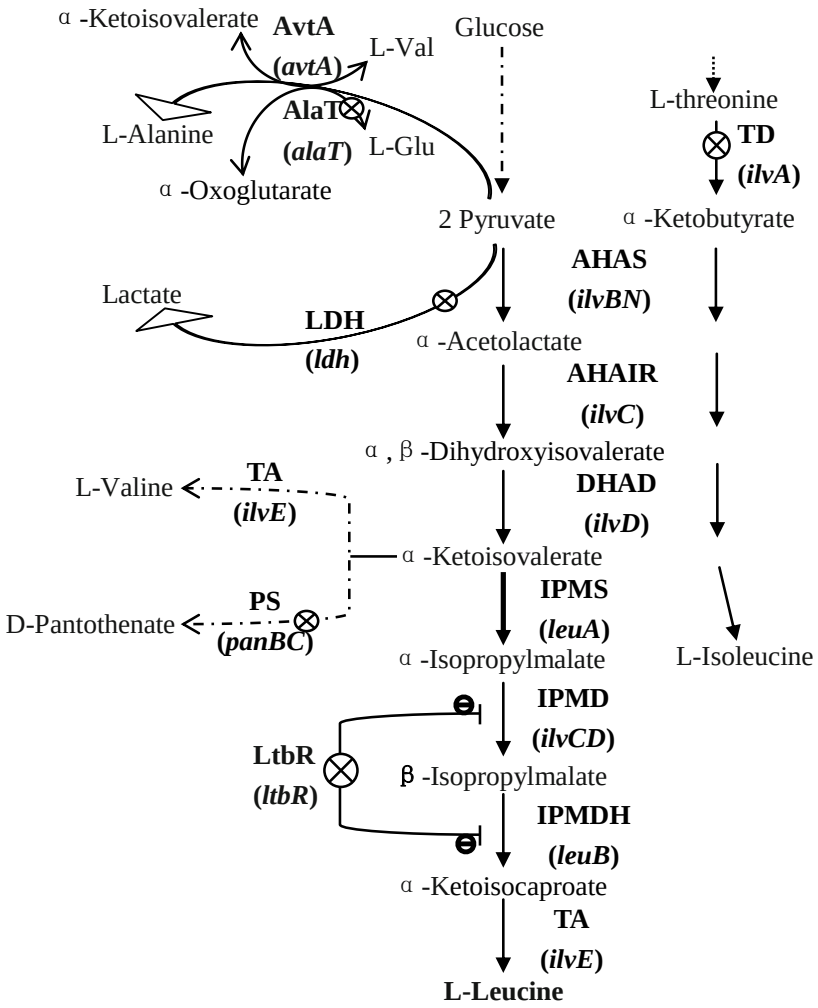

Figure 1. Biosynthetic pathways of L-leucine and their linkage to synthesis of other amino acids and organic acids in *C. glutamicum.* The metabolic engineering strategies for constructing the L-leucine producer (see text). AHAS, acetohydroxyacid synthase; AHAIR, acetohydroxyacid isomeroreductase; DHAD, dihydroxyacid dehydratase; IPMS, 2-isopropylmalate synthase; IPMD, 3-isopropylmalate dehydratase; IPMDH, 3-isopropylmalate dehydrogenase; LtbR, leucine and tryptophan biosynthesis regulator; AT, aminotransferase; TD, threonine dehydratase; AvtA and AlaT, Aminotransferases interacting while AlaT converts pyruvate to L-alanine in a glutamate-dependent reaction, AvtA is able to convert pyruvate to L-alanine in an L-valine dependent manner; LDH, lactate dehydrogenase; PS, pantothenate synthetase. Relevant gene names are given in parentheses. Thick arrows indicate increased gene expression. The "⊖" indicate repression of gene expression. The "⊗ indicate deletion of genes and the respective proteins.

components: 25 g L^{-1} glucose, 2.5 g L^{-1} yeast extract, 25g L^{-1} $(NH_4)_2SO_4$,1.5g L^{-1} Urea, 50 mL L^{-1} Soybean hydrolysate, 0.5 g L^{-1} $MgSO_4 \cdot 7H_2O$, 0.7 g L^{-1} KH_2PO_4, 0.3 g L^{-1} K_2HPO_4 , 0.01 g L^{-1} $FeSO_4 \cdot 7H_2O$, 0.01 g L^{-1} $MnSO_4 \cdot H_2O$, 0.3 mg L^{-1} vitamin B_1, 0.5 mg L^{-1} vitamin B_5 (for Δ*panBC* strains), 0.3 mg L^{-1} vitamin C and 0.15 g L^{-1} L-isoleucine (for Δ*ilvA* strains).

The fermentation medium for producing L-leucine contained the following components: 80 g L^{-1} glucose, 1.5 g L^{-1} yeast extract, 10 g L^{-1} $(NH_4)_2SO_4$, 20 mL L^{-1} Soybean hydrolysate, 0.5 g L^{-1} $MgSO_4 \cdot 7H2O$, 0.7 g L^{-1} KH_2PO_4, 0.3 g L^{-1} K_2HPO_4 , 0.01 g L^{-1} $FeSO_4 \cdot 7H_2O$, 0.01 g L^{-1} $MnSO_4 \cdot H_2O$, 0.3 mg L^{-1} vitamin B_1, 0.5 mg L^{-1} vitamin B_5, 0.3 mg L^{-1} vitamin C and 0.15 g L^{-1} L-isoleucine.

Both seed and fermentation media were adjusted to pH 7.0 with 4 mol L^{-1} NaOH, and 25 μg mL^{-1} kanamycin (Km) was added, as required.

L-leucine batch fermentations were performed in a 50-L automatic fermentor (Zhenjiang East Biotech Equipment and Technology CO., Ltd, Jiangsu, China). 2 mL bacterial suspensions (1×10^8 bacteria per mL) of each test strain was inoculated into a 250-mL flask which contained 30 mL seed medium. The suspension was cultivated at 30°C with shaking at 220 rpm for 16 h.

Two flasks of 60 mL inoculum of this culture were added

Table 1. The main strains and plasmids involved in this study.

Strains	Relevant characteristics	Source or reference
***C. glutamicum* strains**		
ATCC13032	Wild type	ATCC
[a] ML1-9	L-leucine producer *C. glutamicum* strain created by random mutagenesis	Fujian Maidan Biology Group Co., Ltd
ML1-9-*leuA*^{r}	ML1-9 containing shuttle expression vector pZ8-1*leuA*^{r}	This work
MDLeu-19	ML1-9 derivative with inactivated *ilvA*, *alaT*, *ldh*, *panBC* and *ltbR* gene	This work
[b]MDLeu-19/ pZ8-1*leuA*^{r}	Derived from MDLeu-19 which overexpression of *leuA*^{r} by vector pZ8-1	This work
Plasmids		
pZ8-1	Shuttle expression vector (oriV *E. coli*, oriV *C. glutamicum*), containing *tac* promoter, Km^r	(Kassing, et al., 1994)
pZ8-1*leuA*^{r}	pZ8-1 derivative containing *leuA*^{r} gene which increase resistance to feedback inhibition comprise to wide *leuA* gene	This work
pK18*mobsacB*	Shuttle vector for allelic exchange in *C. glutamicum*	(Schäfer, et al., 1994)
pK18*mobsacB*Δ*ilvA*	pK18*mobsacB* containing truncated *ilvA* gene	This work
pK18*mobsacB*Δ*alaT*	pK18*mobsacB* containing truncated *alaT* gene	This work
pK18*mobsacB*Δ*ldh*	pK18*mobsacB* containing truncated *ldh* gene	This work
pK18*mobsacB*Δ*panBC*	pK18*mobsacB* containing truncated *panBC* gene	This work
pK18*mobsacB*Δ*ltbR*	pK18*mobsacB* containing truncated *ltbR* gene	This work

[a]: The ML1-9 strain was stored at Industrial Microbiology, Ministry of Education Engineering Research Center (Fujian Normal University), Fuzhou, China. [b]: The MDLeu-19/ pZ8-1*leuA*^{r} strain was deposited at the China Center for Type Culture Collection under the accession number CCTCC NO: M 2014620.

Table 2. Primers and sequences.

Primers	Sequences
leuA-F	5'-*GAATTC*[b]ATGCCAGTTAACCGCTACATGCCT-3'
leuA-R	5'-*GTCGAC*[c]TTAAACGCCGCCAGCCAGGAC-3'
leuA^r-F	5'-ACGTCACCGTCGATGGCC*G*CGGCAACG*G*CCCAC*T*G-3'
leuA^r-R	5'-GGCCATCGACGGTGACGTCCTTGCCGTTGT-3'
ilvA-P1	5'-*GAATTC*AGGAGAAGATTACACTAGTCAACC-3'
ilvA-P2	5'-AACTACAGACCTAGAACCTATGCAGCCGATGCTTCGTCGAAG-3'
ilvA-P3	5'-TAGGTTCTAGGTCTGTAGTTATGATGAGCGCGACCGAGGGCGC-3'
ilvA-P4	5'-*GTCGAC*TTAGGTCAAGTATTCGTACTCAG-3'
alaT-P1	5'-*GAATTC*GTGACTACAGACAAGCGCAAAACCTC-3'
alaT-P2	5'-AACTACAGACCTAGAACCTATTGAGGAGTGCTTGGGTGGTCATG-3'
alaT-P3	5'-TAGGTTCTAGGTCTGTAGTTACTGGACCAAAGCAATACGCACGTGG-3'
alaT-P4	5'-*GTCGAC*CTACTGCTTGTAAGTGGACAGGAAG-3'
ldh-P1	5'-*GAATTC*CTGCAGGGCATAGATTGGTTTTG -3'
ldh-P2	5'-AACTACAGACCTAGAACCTAATGACATCGCCAACGATGGACTTC-3'
ldh-P3	5'-TAGGTTCTAGGTCTGTAGTT ATCGGCATGGGTCTTGCTCGCATC-3'
ldh-P4	5'-*GTCGAC*TTGGTGCGAAGATGCGCGTAATG-3'
panBC-P1	5'-*GAATTC*CATGTCAGGCATTGATGCAAAG-3'
panBC-P2	5'-AACTACAGACCTAGAACCTAAGCATCAACAATGCGTCGAATC-3'
panBC-P3	5'-TAGGTTCTAGGTCTGTAGTTGCTTATCGACGCCCTCCTCC-3'
panBC-P4	5'-*GTCGAC*CGATCAGGGCGCACCAAATTGAAC-3'
ltbR-P1	5'-*GAATTC*ATGACCTTGAAATACACGGTGAAG-3
ltbR-P2	5'-AACTACAGACCTAGAACCTA ATGCAGGGTCAGCAGCGCGC-3'
ltbR-P3	5'-TAGGTTCTAGGTCTGTAGTTAGCGCCGCGTGCACCCAATG-3'
ltbR-P4	5'-*GTCGAC*ATATCGTTTCATGGGACAGTATAGC-3'

[c]The underlined nucleotides, GAATTC, indicate the restriction enzyme cutting site of *EcoR* I, and the underlined nucleotides, GTCGAC, indicate the restriction enzyme cutting site of *Sal* I.

aseptically to a 30 L automatic fermentor (Zhenjiang East Biotech Equipment and Technology CO., Ltd, Jiangsu, China) containing 12 L seed medium and cultivated at 30°C for 16 h. The seed culture medium was inoculated into (20% inoculum) 30 L of production medium in a 50-L fermentor. The temperature and level of dissolved oxygen were maintained at 30°C and 25-35%, respectively, and the pH was maintained at about 7.0 with ammonium hydroxide (25 % NH_4OH) during the course of the cultivation period. When the initial glucose was consumed at 10 g L^{-1}, sterilization glucose solution (70 %w/v) was fed to the fermentor in order to maintain the glucose concentration in the fermentation broth at 10-15 g L^{-1} according to the batch-feeding strategy of pseudo-exponential growth, and at the end of the fermentation, controlled glucose concentration was 1.0 g L^{-1} or less.

Construction of the modified strains

Conventional techniques of molecular biology like PCR, restriction digestion and ligation were carried out according to the standard protocols (Sambrook, 2001). All enzymes for recombinant DNA work were obtained from TAKARA (Takara, Japan). All primers and DNA extraction and purification kits were obtained from Sangon Biotech (Sangon Biotech, Shanghai, China). Plasmid-based gene expressions were achieved using vector pZ8-1 carrying a *tac* promoter (Frunzke et al., 2008).

All single-and multi-gene in-frame deletions of DNA sequences in *C. glutamicum* strains were done via two-step homologous recombination using the suicide vector pK18mobsacB (Schäfer et al., 1994). The *ilvA* deletion was achieved by constructing pK18*mobsacB*Δ*ilvA* plasmid. The Δ*ilvA* gene fragment (in-frame deletion) was obtained by polymerase chain reaction (PCR) and extension PCR using primers *ilvA*-1, *ilvA*-2 and *ilvA*-3, *ilvA*-4.The fragment was first subcloned into simple pMD18-T (pMD™18-T Vector Cloning Kit, TAKARA) and ligated into pK18*mobsacB,* digested by *EcoRI* and *SalI*. The final plasmid pK18*mobsacB*Δ*ilvA* of 6.56 kb was characterized by restriction analysis. The plasmid was transformed into *C. glutamicum* cells by electroporation. Clones were selected for kanamycin resistance to establish integration of the plasmid in the chromosome through homologous recombination. In a second round of positive selection using sucrose resistance, clones were selected for deletion of the vector and *ilvA*. Disruption of *panBC, alaT* and *ltbR* in the parental strain were performed using the same method as described for disrupting *ilvA* using the primers *panBC*-P1, *panBC*-P2, *panBC*-P3 and *panBC*-P4 for the *panBC gene*; *ldh*-P1, *ldh*-P2, *ldh*-P3 and *ldh*-P4 for the *ldh* gene; primers *alaT*-P1, *alaT*-P2, *alaT*-P3 and *alaT*-P4 for the *alaT* gene; and primers *ltbR*-P1, *ltbR*-P2, *ltbR*-P3 and *ltbR*-P4 for the *ltbR* gene. For strain construction, the techniques specific for *C. glutamicum*, for example transformation of strains via electroporation, were carried out according to the published method (Eggeling and Bott, 2005; van der Rest et al., 1999). All constructed plasmids as well as chromosomal deletions and integrations in the engineered strains were verified by PCR analysis and the nucleotide deletions in the chromosomes were verified by sequencing (Sangon Biotech).

Construction of plasmid pZ8-1*leuA*^{r}

Analysis of *leuA* gene sequences, show that *leuA* sequence of *C. glutamicum* ML1-9 has six sites mutated compared to the wildtype strain. Three of the six mutations were silent and the others involved three amino acid substitutions (R529H, G532D and L535V). Studies have shown that not only these three amino acids are located in binding region of IPMS, but their substitutions in the protein can significantly enhance its activity and relieve the feedback-inhibition by L-leucine (Pátek et al., 1994), consistent with our results. Moreover, L535V substitution is located in the enzyme binding pocket of IPMS, which may increase its affinities towards its substrates (Nayden et al., 2004). Overall, improved resistance to the feedback inhibition effect of IPMS activity by L-leucine and increased expression of *leuA*^{r} are necessary to obtain high L-leucine concentrations.

The *leuA*^{r} was PCR-amplified with the primers *leuA*^{r}-P1and *leuA*^{r}-P2, and ML1-9 chromosomal DNA as the template. The PCR product was purified using a purification kit (Sangon Biotech). Plasmid DNA was also extracted by an isolation kit (Sangon Biotech). The purified leuA^r fragment was first subcloned into simple pMD18-T vector, then digested with *EcoR* I and *Sal* I, and finally inserted into pZ8-1 vector to construct pZ8-1*leuA*^{r}.

Analysis of fermentation products

Bacterial growth was determined by measuring optical density at 560 nm (OD_{560nm}) against distilled water with an UNICO 2802PCS UV/VIS spectrophotometer (Unico Instrument Co., Ltd. Shanghai, China). The cell density was characterized by OD_{560nm}. The concentrations of glucose and lactate were monitored using an SBA-40C biosensor analyzer (Biology Institute of Shandong Academy of Sciences, Jinan, China). Concentrations of amino acids and other organic acids in the culture supernatants were determined by Automatic Amino Acid Analyzer L-8900 (Hitachi, Japan) and Bioprofile 300A biochemical analyzer (Nova Biomedical, USA), respectively.

Enzyme assays

Crude cell extracts were prepared for the determination of IPMS and 3-isopropylmalate dehydratase (IPMD) activity. After 48 h of cultivation, cells were harvested by centrifugation (10 min, 4°C, 10000 rpm), washed twice with 20 mL of the enzyme assay buffer (200 mM Tris-HCl, pH 7.0, 20 mM KCl, 5 mM $MnSO_4$, 0.1 mM ethylenediamine tetraacetic acid, and 2 mM dithiothreitol), subsequently resuspended in 1 mL 200 mM potassium phosphate buffer (pH 7.0) with 1% lywallzyme (w/v) and incubated at 30°C for 3 h. Cells were disrupted by sonication for 5 min on ice bath using an ultrasonic processor Scientz-IID (Ningbo Scientz Biotechnology Co., Ningbo, China). The supernatants of the crude extracts, separated from the cellular debris by centrifugation (15 min, 4°C, 13000 rpm), were used for enzymatic assays. Protein concentration was determined by the Bradford assay using bovine serum albumin as the standard. Each assay was replicated thrice. IPMS catalyzes the following reaction:

2-Ketoisovalerate + acetyl-CoA → 2-isopropylmalate + CoA

The activity of IPMS can be determined by using a continuous spectrophotometric assay measuring coenzyme A (CoA) formation with 5,5′-dithiobis-(2-nitrobenzoic acid)(DTNB) (Kohlhaw, 1988; Kohlhaw and Robert, 1988; Ulm et al., 1972).

The total volume of the reaction solution was 1 mL, containing 500 µL 50 mM Tris–HCl buffer (pH 7.5) containing 20 mM KCl, 100 µL 5,5′-dithiobis-(2-nitrobenzoic acid) (DTNB) solution (1 mM in 50 mM Tris–HCl, pH7.5), 50 µL acetyl-CoA solution (3 mM in 50 mM Tris–HCl, pH7.5), 295 µL ddH_2O and 50 µL crude extract. The reaction was started by adding 5 µL 2-ketoisovalerate solution (40 mM in 50 mM Tris–HCl, pH7.5) and terminated by adding a final concentration of 75% ethanol. The liberated CoA was measured at 412 nm with an UNICO 2802PCS UV/VIS spectrophotometer. Enzyme activities were calculated using an extinction coefficient of 13,600 $M^{-1}cm^{-1}$ for the yellow-colored 5-thio-2-nitrobenzoate dianion. The specific activity was defined as the micromoles of CoA released by per milligram of protein per minute.

Table 3. Comparison of the maximum biomass (OD_{560nm}), specific IPMS activities and L-leucine production of different strains*.

Strains	OD_{560nm}×100	L-leucine(g L^{-1})	Specific IPMS activity (μmol min^{-1} mg^{-1})
ML1-9	0.985±0.005	18.5±0.5	0.33±0.01
ML1-9/pZ8-1	0.969±0.006	17.1±0.3	0.32±0.01
ML1-9/pZ8-1*leuA*^{r}	0.976±0.004	23.6±0.7	0.63±0.02

*Values for the calculation of standard deviations were derived from three independent measurements.

The activity of IPMD was determined according to the published method (Kohlhaw and Robert, 1988; Vogt et al., 2014). It was also used A continuous spectrophotometric assay method was used and IPMD activity was determined by measuring the optical absorption of the reaction intermediate 2-isopropylmaleate at 235 nm.

The 1 mL reaction mixture, contained 400 μL potassium phosphate buffer (200 mM, pH 7.0), 40 μL 3-isopropylmalate solution (40 mM), 510 μL ddH_2O and 50 μL crude cell extract was incubated at 30°C for 10 min. The optical density of the increase of absorbance at 235 nm was measured by UNICO 2802PCS UV/VIS spectrophotometer. Enzyme activities were calculated using an extinction coefficient of 4530 $M^{-1}cm^{-1}$ for 2-isopropylmaleate. The specific activity was defined as the micromoles of 2-isopropylmalate formation by per milligram of protein per minute.

RESULTS AND DISCUSSION

Recombinant strains and plasmids

The deletions of *ilvA*, *ldh*, *alaT*, *panBC* and *ltbR* in *C. glutamicum* ML1-9 were confirmed by colony PCR using relevant primers P1 and P4. The sequence analysis results revealed that the obtained PCR product did not contain unwanted mutations.

The expression vector pZ8-1*leuA*^{r} was transformed into the ML1-9 strain and the IPMS activity of crude extracts was determined. The expression of pZ8-1*leuA*^{r} was assessed by analysis of fed-batch cultivation in a 30-L automatic fermentor. As shown in Table 3, the *C. glutamicum* ML1-9-*leuA*^{r} strain have an improved yield of L-leucine, indicating that *leuA*^{r} gene was successfully expressed by pZ8-1*leuA*^{r}, with increase of the activity of IPMS (In the ML1-9/pZ8-1*leuA*^{r} strain, there is about a two-fold higher specific IPMS activity than the ML1-9 and ML1-9-pZ8-1 levels, respectively). The phenomenon results in enhanced carbon flux for L-leucine biosynthesis. These data suggest that the feedback-resistant IPMS is crucial to the accumulation of L-leucine.

Effect of gene deletions on cell growth and L-leucine production

The ML1-9 strain that overexpressed *leuA*^{r} accumulated more L-leucine than the other ML1-9 strains. Therefore, the known feedback inhibition, especially of the *leuA*-encoded IPMS is not a major problem, probably due to the partial feedback inhibition and repression of the other enzymes like *ilvBN*-encoded AHAS.

Fed-batch fermentations of ML1-9Δ*ilvA*, ML1-9Δ*ldh*, ML1-9Δ*alaT*, ML1-9Δ*panBC*, and ML1-9Δ*ltbR* strains (without overexpression of *leuA*^{r}) were performed, and their fermentation growth curve and L-leucine production were measured (Figure 2). All modified strains produced more L-leucine than the control strain ML1-9. It is of note that although all the modified strains had quite similar growth patterns, significant differences were observed in their maximum cell densities (OD_{560nm}) and time to reach the stationary phase (Figure 2a). ML1-9ΔltbR strain that reached the maximum cell density (OD_{560nm}=115) after 18 h of fermentation had the highest cell density among these strains, including the control strain, which reached the maximum cell density after 22 h. Additionally, the highest concentration of L-leucine (20.5 g L^{-1}) was also produced by ML1-9Δ*ltbR*. It was reported that *ltbR* encoding a transcriptional regulator of IclR protein family, which was involved in transcriptional regulation of the L-leucine biosynthesis pathways of *C. glutamicum*, repressed expression of *leuCD* and *leuB* in the presence of high concentration of L-leucine in the medium (Iris et al., 2007). We therefore deleted *ltbR* to increase the IPMD and IPMDH activity significantly by increasing the expression of *leuCD* and *leuB,* which released the negative transcriptional regulation of the *leu* genes of ML1-9Δ*ltbR* (Table 5). Moreover, *ltbR* deletion strain did not need extra supplemental ingredients in the fermentation medium. In comparison to other auxotrophic strains, ML1-9ΔltbR improved the fermentation, by increasing the fermentation index and had a positive effect on the cell growth (Figure 2a).

The ML1-9Δ*ldh* strain was constructed by deletion of *ldh* which encodes the key enzyme for lactate synthesis (Garvie, 1980). Consistent with previous reports, synthesis of lactate was greatly reduced from 0.85 to 0.05% by the deletion of *ldh* (Wieschalka et al., 2012). Moreover, the deletion of *ldh* was not the limiting step in the metabolic flow, since the growth rate and the L-leucine concentration of the *ldh* deletion strains were higher than the control. This indicates that the inactivation of LDH prevented lactic acid inhibition of growth. Not only that, due to inactivation of LDH, increased precursor metabolite concentrations are available with low L-lactic acid production resulting in an increase in the yield of L-leucine (Figure 2b).

Unlike deleted *ltbR* and *ldh* gene, *ilvA*, *alaT* and *panBC*

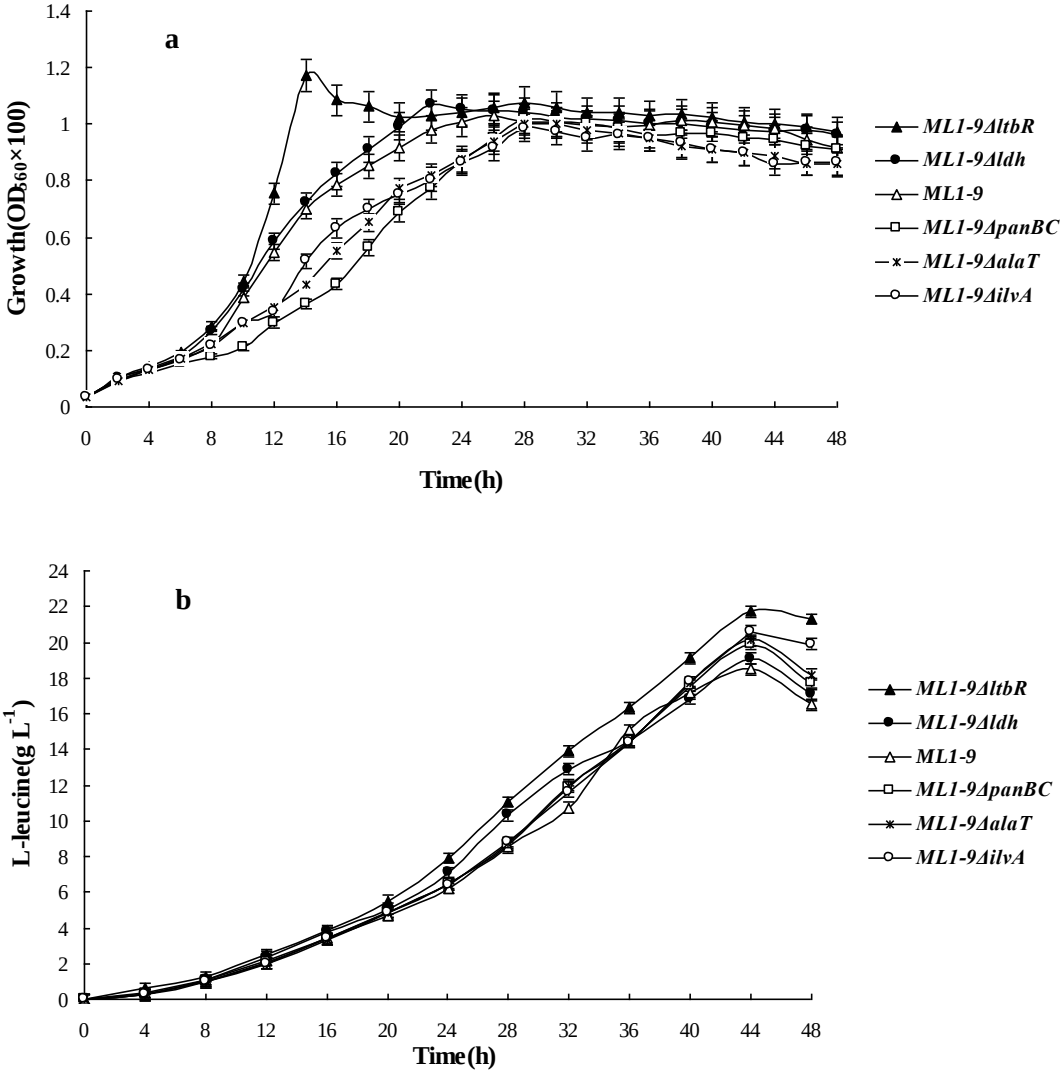

Figure 2. Fed-batch fermentations of different strains derived from the ML1-9. (a) Fermentation growth curves. (b) L-Leucine concentration in the fermentation process.

deletion strains had an impact on metabolic flux distribution and cell growth, thereby affecting the production of L-leucine. ML1-9Δ*ilvA*, an isoleucine auxotroph strain, was constructed by inactivating the threonine dehydratase (deleted *ilvA*) in order to block the biosynthesis of L-isoleucine. It is to be noted that a certain amount of L-isoleucine (0.15 g L^{-1} for this work) was supplemented into the medium in order to maintain cell growth. The result shows that the cell growth of ML1-9Δ*ilvA* was limited, prolonging the logarithmic growth phase relatively compared to the prototrophic strain, ML1-9. Moreover, the cell densities of the strain were also the lowest among all the other strains including ML1-9 (Figure 2a). It is noteworthy that despite L-isoleucine supplementation, the effects on growth were long lasting, both the cell growth rate and the highest cell density were decreased, and the adaptation period was prolonged compared with the original strain ML1-9. On the contrary, the prevention of L-isoleucine synthesis not only relieved the feedback inhibition of acetohydroxy acid synthase, but also increased the carbon metabolism, with increased precursor metabolite concentrations needed for the L-leucine biosynthesis pathway (Eggeling et al., 1997; Sahm and Eggeling, 1999). Therefore, we were able to obtain more L-leucine production through ML1-9Δ*ilvA* strain, which resulted in the second highest concentration of L-leucine compared to other strains (Figure 2b).

Similarly, AlaT (encoded by *alaT* gene) is the main enzyme for L-alanine synthesis. While AlaT converts pyruvate (amino acceptor) to L-alanine in a glutamate-dependent reaction (glutamate as amino donor), AvtA does the same in L-valine dependent manner (Jan et al., 2005). When compared to the control strain (ML1-9), the concentration of L-alanine in ML1-9Δ*alaT* strain was

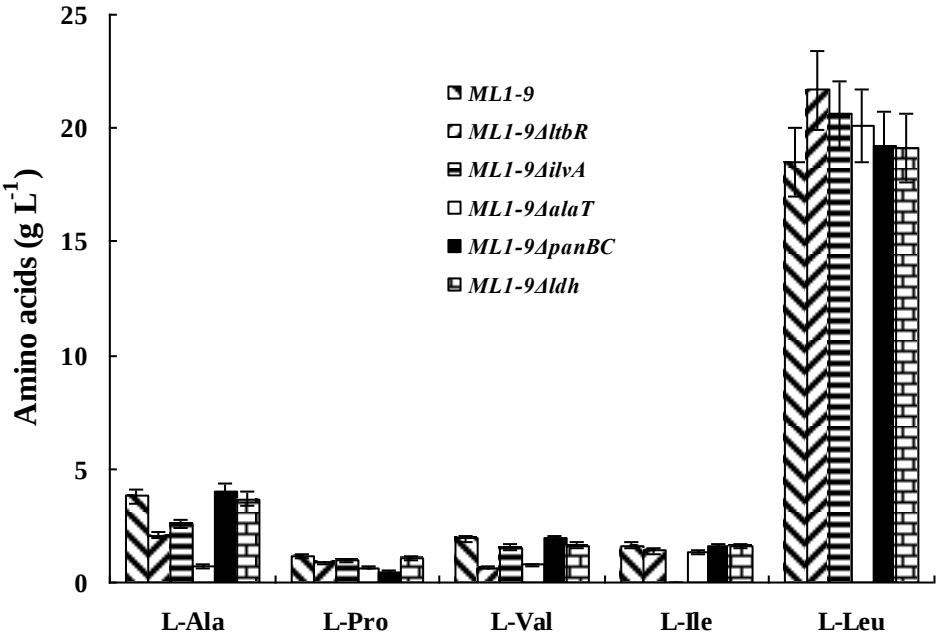

Figure 3. Comparison of L-leucine and related amino acids among the different strains.

greatly reduced because of *alaT* deletion (Figure 3). In this study, we investigated cell growth and accumulation of L- leucine by AvtA and/or AlaT inactivation. A double deletion mutant, auxotrophic for L-alanine, was generated by deletion of *avtA* and *alaT* in the same strain. Cell growth of these strains is severely limited, which could not be revived by L-alanine supplementation. These results showed that ATs (AvtA and AlaT) are not only responsible for the synthesis of L-alanine, but also play a crucial role in balancing the intracellular amino acid pools essential for normal cell growth. These results are consistent with the previous studies (Marienhagen and Eggeling, 2008). Concentration of L-alanine was reduced from 3.81 to 3.09 g L^{-1} by deletion of *avtA*, whereas L-valine concentration increased and L-leucine concentration decreased (data not shown). Unlike the strain with AvtA inactivation, deletion of *alaT* alone blocked L-alanine synthesis, impaired cell growth and extended the logarithmic growth phase (Figure 3). However, *alaT* deletion resulted in more precursor flow to L-leucine pathway, and accumulation of more L-leucine. Additionally, the L-valine concentration also decreased, which is an added advantage for L-leucine downstream processing.

The ML1-9Δ*panBC* strain was constructed by deleting *panBC*, which must be grown in a medium supplemented with 0.45 mg L^{-1} D-pantothenate or 0.5 mg L^{-1} vitamin B5. Compared to the control strain ML1-9, the adaptation period of ML1-9Δ*panBC* strain was extended, and also the growth rate became lower. It took 28 h (approximately 22 h in the control strain) for the ML1-9Δ*panBC* strain to reach the highest cell density, which was reduced compared to the control strain (Figure 2a). However, this result indicates that it can accumulate more L-leucine (Figure 2b). It has been reported that blocking D-pantothenate biosynthesis affects the TCA cycle by reducing CoA formation which ultimately affects central energy metabolism or even cellular flux properties (Lothar and Hermann, 2001; Riedel et al., 2001; Sahm and Eggeling, 1999; Shimizu et al., 1985). In addition, a reduced flux through the pyruvate dehydrogenase probably results due to the D-pantothenate limitation, leading to an increase of pyruvate availability (L-alanine synthesized directly from pyruvate). Furthermore, blocking of D-pantothenate synthesis results in increased amounts of precursors (more ketoisovalerate availability) for BCAAs synthesis pathways (including L-valine and L-leucine).Of note, more L-alanine is available than L-valine and L-leucine.

As shown in Figure 2, L-leucine showed the highest yield after 44h fermentation, However, the results presented in the 50-L fermentation did not exhibit a significant improvement in line with expectations in the production of L-leucine with single modified strains, and the increase in L-leucine yield of single modified strains were also lower than the proper integrattion strain (Table 4). Possible reasons for this failure could be the genetic background ML1-9 strain and composition of the medium that may affect the capacity of L-leucine accumulation. Another possibility could be that a single gene modification often influences the metabolic networks rather than merely affecting a single metabolic reaction, thereby limiting the target metabolic flows. A third possibility would be a general growth limitation introduced by some auxotrophs or metabolic defects.

In addition, the L-leucine accumulation, and biomass of

Table 4. Fed-batch culture parameters of L-leucine production by MDLeu-19.

Strain	Amino acid concentration (g L^{-1})				
	L-Ala	L-Pro	L-Val	L-Ile	L-Leu
MDLeu-19	0.51	0.58	0.65	0	28.5±0.5

Table 5. Enzymes activities and by-product concentrations with L-leucine production in different strains.

Strain	Specific activity(μmol min^{-1} mg^{-1} protein)			Lactic acid (g L^{-1})	D-pantothenate (g L^{-1})
	IPMS	IPMD	IPMDH		
ML1-9	0.343±0.02	0.211±0.02	0.190±0.03	10.2±0.5	0.76±0.03
ML1-9/pZ8-1	0.341±0.02	0.208±0.02	0.185±0.03	10.7±0.5	0.79±0.03
ML1-9/pZ8-1 *leuA*^{r}	0.645±0.05	0.213±0.03	0.188±0.03	10.5±0.7	0.64±0.05
ML1-9Δ*ltbR* /pZ8-1 *leuA*^{r}	0.86±0.05	0.45±0.05	0.380±0.05	9.2±0.5	0.47±0.05
ML1-9Δ*ilvA*/pZ8-1 *leuA*^{r}	0.644±0.05	0.211±0.03	0.199±0.03	10.6±0.5	0.66±0.05
ML1-9Δ*alaT*/pZ8-1 *leuA*^{r}	0.643±0.05	0.216±0.02	0.201±0.04	11.8±0.7	0.83±0.05
ML1-9Δ*panBC*/pZ8-1 *leuA*^{r}	0.645±0.05	0.209±0.02	0.191±0.03	10.9±0.6	0
ML1-9Δ*ldh*/pZ8-1 *leuA*^{r}	0.651±0.05	0.234±0.02	0.216±0.04	0	0.66±0.05
MDLeu-19/pZ8-1 *leuA*^{r}	0.91±0.05	0.53±0.03	0.421±0.06	0.16±0.03	0

strains (OD_{560nm}) decreased between 44 and 48 h, respectively. Therefore, the fermentation was terminated at 48 h. Both the L-leucine titer and production rate of the mutant strains were higher than those of the control strain (Figures 2 and 3). Based on this, we have integrated a number of favorable modifications and deleted *ltbR*, *ilvA*, *alaT*, *panBC,* and *ldh* in a ML1-9 strain in order to obtain a modified strain named MDLeu-19, based on metabolic engineering. The fermentation characteristics of this strain were investigated by the same methods.

The L-leucine concentration of MDLeu-19 (Table 4) was the highest among the strains tested in the current study, which was 54.1% higher than the control strain ML1-9 (18.5±0.5 g L^{-1}). On the the other hand, the concentrations of the other amino acids, especially L-isoleucine, L-valine, and L-alanine, were low. This was beneficial to the post-fermentation process and gives an improved glucose conversion. The results also demonstrat that some of these combinations could lead to significantly improved L-leucine production.

Activity analysis of some key enzymes in different modified strains

Our observation suggests that cloning and overexpression of *leuA*^{r} gene can significantly improve the IPMS activity by nearly two-fold (Table 3) leading to increase in the carbon flux to the L-leucine pathway. With *leuA*^{r} gene overexpressed, the maximum L-leucine productions by ML1-9Δ*ltbR*, ML1-9Δ*ilvA*, ML1-9Δ*alaT*, ML1-9Δ*panBC*, ML1-9Δ*ldh,* and MDLeu-19 strain were also increased up to 26.7±0.3, 24.7±0.5, 23.8±0.7, 22.1±0.6, 21.8±0.4 and 38.1±0.6 g L^{-1}, respectively. Moreover, the acticity of IPMS, IPMD, and IPMDH, as well as the concentrations of extracellular lactic acid and D-pantothenate were also determined (Table 5).

The above results indicate that L-leucine producing strains show elevated activities of enzymes required for L-leucine synthesis. Expression of the *leuA*^{r} gene by pZ8-1 enhanced the IPMS activity nearly two-fold in *C. glutamicum*, whereas no significant increase was observed by other metabolic modifications except deletion of *ltbR*.

L-leucine overproduction by significant increase in the enzyme activity was achieved by deletion of the leucine transcriptional repressor LtbR. Compared to the strains with overexpressed *leuA*^{r}, IPMS activity was enhanced 32.3% by deletion of *ltbR*. Besides this, the IPMD and IPMDH activity was doubled in some of the strains, which is consistent with previous studies (Iris et al., 2007; Vogt et al., 2014). Furthermore, the MDLeu-19/pZ8-1*leuA*^{r} strain has the highest L-leucine synthesis enzyme activities among these strains. The inactivation of the transcriptional regulator has directly enhanced transcription of *leuABCD* operon. However, the decisive factor is the proper integration of activities in the central metabolism and the L-leucine biosynthesis pathway. On the one hand, the use of metabolic modifications to improve precursor supply by reducing the consumption of pyruvate based on inactivation of AlaT and LDH. On the other hand, increased L-leucine synthesis enzyme activity (expression of *leuA*^{r} and deletion of the leucine transcriptional repressor LtbR) and weaken the competitive metabolism to redirect metabolic flux towards L-leucine instead L-isoleucine or D-pantothenate. Both forces provided potential for a strong increase in L-leucine production.

L-leucine originates directly from two pyruvate molecules, whereas D-pantothenate is a precursor in the biosynthesis of CoA. Deletion of *panBC* blocked D-pantothenate synthesis leading to a reduction in metabolic flux from pyruvate to acetyl-CoA. This eventually limits the cell growth, which probably requires D-pantothenate supplementation (Table 5). This also indicates that more L-leucine was accumulated just by directly increasing the availability of precursors rather than promoting the L-leucine synthesis activity e.g., deletion of *ltbR* (IPMD and IPMDH activity were not significantly increased by deletion of *panBC*).

Additionally, deletion of the *ldh*, encoding lactate dehydrogenase (LDH) not only minimized lactate production and increased the availability of precursor, but also moderately enhanced the transcription and expression of *leuB* and *leuCD* (Table 5). As expected, inactivation of LDH effectively blocked the synthesis of lactic acid and reduced the adverse effects of this organic acid on cell growth, especially in the area where there is lack of dissolved oxygen at high-density fermentation environment. Notably, an *ldh*-deficient mutant was not able to produce lactate, and synthesis of acetic acid compared to the parent strain did not increase. When acetic acid synthesis pathway was further modified by knock out the *pta* gene, the growth of the strain was severely suppressed (date not shown). This observation could perhaps be ascribed to ML1-9 strain, which has undergone multiple generations of mutation breeding. This suggests that the activity of the protein encoded by *pta* genes are not limiting L-leucine production in the ML1-9 strain background. This set of observations corroborates the view that the ability of acetic acid biosynthesis may already have been greatly reduced in ML1-9 strain. Further modifications of the acetic acid pathway may affect the TCA cycle of central metabolism. On the one hand, acetic acid may be activated by a series of enzymes to produce acetyl-CoA, further into the TCA cycle, and then promote cell pyruvate metabolism. On the other hand, acetic acid may also help to improve the critical enzyme activity of the TCA cycle, promote the efficiency of TCA cycling, increase the TCA cycle flux, and supply the carbon skeleton of a variety of compounds for cell biosynthesis (Gerstmeir et al., 2003; Sorger-Herrmann et al., 2015; Wolfe, 2005).

In conclusion, the modifications of transcriptional regulator and bypassing metabolic pathways could further improve the yield of L-leucine in such a way that the direct negative regulation of L-leucine synthesis is reduced and the metabolic flux of L-leucine biosynthesis pathway is probably redistributed.

L-leucine production and glucose conversion rate of the MDLeu-19/pZ8-1*leuA*^{r} strain

MDLeu-19/pZ8-1*leuA*^{r} strain was characterized in 50-L fed-batch cultivations in order to determine the influence of different process parameters on the productivity and to analyze the behavior of the strain under such controlled conditions. Because of a relatively higher yield and glucose conversion rate in 50-L automatic fermentor, MDLeu-19/pZ8-1*leuA*^{r} strain was carried out in 150-m^3 fermentor to explore the industrial production of L-leucine.

Cells show similar growth curves in 50-L automatic fermentor and 150-m^3 industrial fermentor. Glucose consumption and cell growth were substantially synchronous. After 8-18 h of fermentation, the cells reach the logarithmic phase with a sharp increase in glucose consumption. After 18 h the cells reached the highest cell biomass (OD_{560nm}=110.6), it entered the stationary phase. Here, the concentration of L-leucine in the fermentation broth continued to gradually increase as shown in Figure 4. After 48-h fermentation, maximum L-leucine concentration by the MDLeu-19/pZ8-1*leuA*^{r} strain was 37.5 g L^{-1}, with a glucose conversion rate of 25.8%. Both the L-leucine yield and glucose conversion rate were lower than that in 50-L automatic fermentor. First, industrial fermentor microenvironments are unfavorable and gradients are formed not found in the 50-L fermentor. Lack of oxygen in parts in these fermentors lead to unsynchronized cell growth and metabolism. There is also a possibility that the results can be interpreted as loss in plasmid stability in the industrial fermentor which might be relatively poor.

Conclusions

It has been demonstrated that modification methods to engineer the parental strain of *C. glutamicum* described here are useful for constructing novel strains that produce and export high levels of BCAAs (Blombach et al., 2008; Hasegawa et al., 2013; Wang et al., 2013; Kennerknecht et al., 2002; Radmacher et al., 2002; Satoshi et al., 2012; Vogt et al., 2014; Yin et al., 2014).

In order to achieve high L-leucine production and specific L-leucine production rate, it is necessary to reach a balance between biomass concentration, specific glucose consumption rate, and the activity of key enzymes.

The present study demonstrates the capability for greater production of L-leucine by a strain named MDLeu-19/pZ8-1*leuA*^{r}, based on the mutation breeding of L-leucine producing strain ML1-9. This was achieved by overexpression of *leuA*^{r} and reasonable modifications of L-leucine biosynthesic pathways by redistribution of various types of precursors and repression of negative regulation. Using the optimized conditions described above, the final maximum output in the 50-L automatic fermentor was 38.1 g L^{-1}. The maximal specific L-leucine production rate of 0.794 g L^{-1} h^{-1} was obtained for a 48 h fermentation with a maximum conversion efficiency of

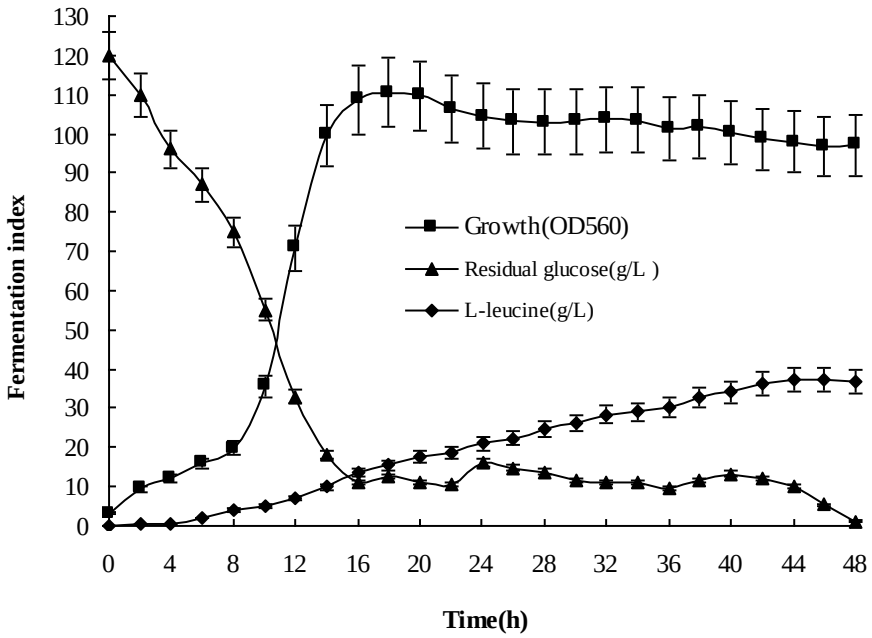

Figure 4. Strain MDLeu-19/pZ8-1*leuA*^{r} fermentation in a 150-m^3 fermentor.

0.306 g g^{-1}, with an increase compared to the original strain by 105.9 and 50.9%, respectively. Moreover, we have successfully achieved industrial–scale production of L-leucine in 150-m^3 fermentor with a yield of 37.5 g L^{-1} and a glucose conversion rate of 25.8%. Furthermore, the total content of 'contaminating' amino acids was less than 12.5% which influences the costs for downstream processing and product purification, making this strain potentially ideal for industrial application.

To the best of our knowledge, this is the first report of MDLue-19/pZ8-1*leuA*^{r} strain producing the highest yield and conversion efficiency for a bacterial L-leucine in industrial-scale production. Furthermore, in order to increase the yield of L-leucine, improve industrial fermentation efficiency and reduce cost, the use of comparative transcriptomics and proteomics analyses will allow for confirmation that the increased expression of these genes are correlated to L-leucine biosynthesis and also provide additional targets for strain improvement.

CONFLICT OF INTERESTS

The authors have not declared any conflict of interests.

REFERENCES

Ambe-Ono Y, Sato K, Totsuka K, Yoshihara Y, Nakamori S (1996). Improved L-Leucine production by an alpha-aminobutyric acid resistant mutant of *Brevibacterium lactofermentum*. Biosci. Biotechnol. Biochem. 60(8):1386-1387.

Becker J, Gießelmann G, Hoffmann SL, Wittmann C (2016). *Corynebacterium glutamicum* for Sustainable Bioproduction: From Metabolic Physiology to Systems Metabolic Engineering. Adv. Biochem. Eng. Biotechnol. epub. DOI 10.1007/10_2016_21.

Becker J, Kind S, Wittmann C (2012). Systems Metabolic Engineering of *Corynebacterium glutamicum* for Biobased Production of Chemicals, Materials and Fuels. Systems Metabolic Engineering. Springer Netherlands. pp. 151-191.

Becker J, Wittmann C (2012). Bio-based production of chemicals, materials and fuels-*Corynebacterium glutamicum* as versatile cell factory. Curr. Opin. Biotechnol. 23(4):631-640.

Becker J, Zelder O, Häfner S, Schröder H, Wittmann C (2011). From zero to hero--design-based systems metabolic engineering of *Corynebacterium glutamicum* for L-lysine production. Metab. Eng. 13(2):159-168.

Bertani G (1951). Studies on lysogenesis. I. The mode of phage liberation by lysogenic *Escherichia coli*. J. Bacteriol. 62(3):293-300.

Blombach B, Schreiner ME, Bartek T, Oldiges M, Eikmanns BJ (2008). *Corynebacterium glutamicum* tailored for high-yield L-valine production. Appl. Microbiol. Biotechnol. 79(3):471-479.

Cann AF, Liao JC (2010). Pentanol isomer synthesis in engineered microorganisms. Appl. Microbiol. Biotechnol. 85(4):893-899.

Chen Z, Bommareddy RR, Frank D, Rappert S, Zeng AP (2014). Deregulation of feedback inhibition of phosphoenolpyruvate carboxylase for improved lysine production in *Corynebacterium glutamicum*. Appl. Environ. Microbiol. 80(4):1388-1393.

Eggeling L, Bott M (2005). *Handbook of Corynebacterium glutamicum*. Taylor and Francis.

Eggeling L, Morbach S, Sahm H (1997). The fruits of molecular physiology: engineering the l-isoleucine biosynthesis pathway in *Corynebacterium glutamicum*. J. Biotechnol. 56(3):167-182.

Freund H, Dienstag J, Lehrich J, Yoshimura N, Bradford RR, Rosen H, Atamian S, Slemmer E, Holroyde J, Fischer JE (1982). Infusion of branched-chain enriched amino acid solution in patients with hepatic encephalopathy. Ann. Surg. 196(2):209-220.

Frunzke J, Engels V, Hasenbein S, Gätgens C, Bott M (2008). Co-ordinated regulation of gluconate catabolism and glucose uptake in *Corynebacterium glutamicum* by two functionally equivalent transcriptional regulators, GntR1 and GntR2. Mol. Microbiol. 67(2):305-322.

Garlick PJ (2005). The role of leucine in the regulation of protein metabolism. J. Nutr. 135(6 Suppl.):1553S-1556S.

Garvie EI (1980). Bacterial lactate dehydrogenase. Microbiol. Rev 44(1):106-139.
Gerstmeir R, Wendisch VF, Schnicke S, Ruan H, Farwick M, Reinscheid D, Eikmanns BJ (2003). Acetate metabolism and its regulation in *Corynebacterium glutamicum*. J. Biotechnol. 104(1-3):99-122.
Gluud LL, Dam G, Aagaard NK, Vilstrup H (2015). Branched Chain Amino Acids in Clinical Nutrition. Springer, New York. pp. 299-311.
Gluud LL, Gitte D, Mette B, Les I, Juan C, Giulio M, Aagaard NK, Niels R, Hendrik V (2013). Oral Branched-Chain Amino Acids Have a Beneficial Effect on Manifestations of Hepatic Encephalopathy in a Systematic Review with Meta-Analyses of Randomized Controlled Trials. J. Nutr. 143(8):1263-1268.
Hasegawa S, Suda M, Uematsu K, Natsuma Y, Hiraga K, Jojima T, Inui M, Yukawa H (2013). Engineering of *Corynebacterium glutamicum* for High Yield L-Valine Production under Oxygen Deprivation Conditions. Appl. Environ. Microbiol. 79(4):1250-1257.
Iris B, Nina J, Karina B, Hüser AT, Robert G, Eikmanns,BJ, Jörn K, Alfred P, Andreas T (2007). The IclR-type transcriptional repressor LtbR regulates the expression of leucine and tryptophan biosynthesis genes in the amino acid producer *Corynebacterium giutamicum*. J. Bacteriol. 189(7):2720-2733.
Jan M, Nicole K, Hermann S, Lothar E (2005). Functional Analysis of All Aminotransferase Proteins Inferred from the Genome Sequence of *Corynebacterium glutamicum*. J. Bacteriol. 187(22):7639-7646.
Kassing F, Kalinowski J, Arnold W, Winterfeldt A, Pühler A, Kautz PS, Thierbach G (1994). Method for the site-specific mutagenesis of DNA and development of plasmid vectors. Europe Patent, Degussa Aktiengesellschaft.
Kennerknecht N, Sahm H, Yen MR, Pátek M, Saier Jr MH Jr, Eggeling L (2002). Export of L-isoleucine from *Corynebacterium glutamicum*: a two-gene-encoded member of a new translocator family. J. Bacteriol. 184(14):3947-3956.
Kimball SR, Jefferson LS (2006). Signaling pathways and molecular mechanisms through which branched-chain amino acids mediate translational control of protein synthesis. J. Nutr. 136(1 Suppl.):227S-231S.
Kinoshita S, Udaka S, Shimono M (2004). Studies on the amino acid fermentation. Part I. Production of L-glutamic acid by various microorganisms. J. Gen. Appl. Microbiol. 50(6):331-343.
Kohlhaw GB (1988). Alpha-isopropylmalate synthase from yeast. Methods Enzymol. 166:414-423.
Kohlhaw GB (1988). Isopropylmalate dehydratase from yeast. Methods Enzymol. 166:423-429.
Layman DK (2003). The role of leucine in weight loss diets and glucose homeostasis. J. Nutr. 133(1):261S-267S.
Leuchtenberger W (2008). Biotechnology: Products of Primary Metabolism. Wiley-VCH Verlag GmbH. Pp. 465-502.
Li H, Cann AF, Liao JC (2010). Biofuels: biomolecular engineering fundamentals and advances. Annu. Rev. Chem. Biomol. Eng. 1:19-36.
Liebl W, Ehrmann M, Ludwig W, Schleifer KH (1991). Transfer of *Brevibacterium divaricatum* DSM 20297T, "*Brevibacterium flavum*" DSM 20411, "*Brevibacterium lactofermentum*" DSM 20412 and DSM 1412, and *Corynebacterium lilium* DSM 20137T to *Corynebacterium glutamicum* and Their Distinction by rRNA Gene Restriction Patterns. Int. J. Syst. Bacteriol. 41(2):255-260.
Lothar E, Hermann S (2001). The Cell Wall Barrier of *Corynebacterium glutamicum* and Amino Acid Efflux. J. Biosci. Bioeng. 92(5):201-213.
Mangal S, Meiser F, Tan G, Gagenbach T, Denman J, Rowles MR, Larson I, Morton DA (2015). Relationship between surface concentration of L-leucine and bulk powder properties in spray dried formulations. Eur. J. Pharm. Biopharm. 94:160-169.
Marienhagen J, Eggeling L (2008). Metabolic function of *Corynebacterium glutamicum* aminotransferases AlaT and AvtA and impact on L-valine production. Appl. Environ. Microbiol. 74(24):7457-7462.
Nakayama K, Kitada S, Sato Z, Kinoshita S, Nakayama K, Kitada S, Sato Z, Kinoshita S (1961). Induction of nutritional mutants of glutamic acid bacteria and their amino acid accumulation. J. Gen. Appl. Microbiol. 7(1):41-51.
Nayden K, Squire CJ, Baker EN (2004). Crystal structure of LeuA from *Mycobacterium tuberculosis*, a key enzyme in leucine biosynthesis. Proc. Natl. Acad. Sci. USA. 101(22):8295-8300.
Park JH, Lee SY (2010). Fermentative production of branched chain amino acids: a focus on metabolic engineering. Appl. Microbiol. Biotechnol. 85(3):491-506.
Pátek M, Krumbach K, Eggeling L, Sahm H (1994). Leucine synthesis in *Corynebacterium glutamicum*: enzyme activities, structure of *leuA*, and effect of *leuA* inactivation on lysine synthesis. Appl. Environ. Microbiol. 60(1):133-140.
Platell C, Kong SE, McCauley R, Hall JC (2000). Branched-chain amino acids. J. Gastroenterol. Hepatol. 15(7):706-717.
Radmacher E, Vaitsikova A, Burger U, Krumbach K, Sahm H, Eggeling L (2002). Linking central metabolism with increased pathway flux: L-valine accumulation by *Corynebacterium glutamicum*. Appl. Environ. Microbiol. 68(5):2246-2250.
Riedel C, Rittmann D, Dangel P, Möckel B, Petersen S, Sahm H, Eikmanns BJ (2001). Characterization of the phosphoenolpyruvate carboxykinase gene from *Corynebacterium glutamicum* and significance of the enzyme for growth and amino acid production. J. Mol. Microbiol. Biotechnol. 3(4):573-583.
Sahm H, Eggeling L (1999). D-Pantothenate synthesis in *Corynebacterium glutamicum* and use of *panBC* and genes encoding L-valine synthesis for D-pantothenate overproduction. Appl. Environ. Microbiol. 65(5):1973-1979.
Sambrook JF, Russell. DW. (2001). Molecular Cloning: A Laboratory Manual (3rd edition). Cold Spring Harbor Laboratory Press.
Satoshi H, Kimio U, Yumi N, Masako S, Kazumi H, Toru J, Masayuki I, Hideaki Y (2012). Improvement of the redox balance increases L-valine production by *Corynebacterium glutamicum* under oxygen deprivation conditions. Appl. Environ. Microbiol. 78(3):865-875.
Schäfer A, Tauch A, Jäger W, Kalinowski J, Thierbach G, Pühler A (1994). Small mobilizable multi-purpose cloning vectors derived from the *Escherichia coli* plasmids pK18 and pK19: selection of defined deletions in the chromosome of *Corynebacterium glutamicum*. Gene 145(1):69-73.
Scheele S, Oertel D, Bongaerts J, Evers S, Hellmuth H, Maurer KH, Bott M, Freudl R (2013). Secretory production of an FAD cofactor-containing cytosolic enzyme (sorbitol-xylitol oxidase from *Streptomyces coelicolor*) using the twin-arginine translocation (Tat) pathway of *Corynebacterium glutamicum*. Microb. Biotechnol. 6(2):202-206.
Shimizu S, Esumi A, Komaki R, Yamada H (1985). Production of Coenzyme A by a Mutant of *Brevibacterium ammoniagenes* Resistant to Oxypantetheine. Appl. Environ. Microbiol. 48(6):1118-1122.
Sorger-Herrmann U, Taniguchi H, Wendisch VF (2015). Regulation of the pstSCAB operon in *Corynebacterium glutamicum* by the regulator of acetate metabolism RamB. BMC Microbiol. 15(1):1-13.
Tsuchida T, Momose H (1986). Improvement of an l -Leucine-Producing Mutant of *Brevibacterium lactofermentum* 2256 by Genetically Desensitizing It to alpha-Acetohydroxy Acid Synthetase. Appl. Environ. Microbiol. 51(5):1024-1027.
Tsuchida T, Yoshinaga F, Kubota K, Momose H, Okumura S (1974). Production of l-Leucine by a Mutant of *Brevibacterium lactofermentum* 2256. Agric. Biol. Chem. 38(10):1907-1911.
Udaka S (1960). Screening method for microorganisms accumulating metabolites and its use in the isolation of *Micrococcus glutamicus*. J. Bacteriol. 79(5):754-755.
Ulm EH, Bhme R, Kohlhaw G (1972). Alpha-isopropylmalate synthase from yeast: purification, kinetic studies, and effect of ligands on stability. J. Bacteriol. 110(3):1118-1126.
van der Rest ME, Lange C, Molenaar D (1999). A heat shock following electroporation induces highly efficient transformation of *Corynebacterium glutamicum* with xenogeneic plasmid DNA. Appl. Microbiol. Biotechnol. 52(4):541-545.
Vogt M, Haas S, Klaffl S, Polen T, Eggeling L, van Ooyen J, Bott M (2014). Pushing product formation to its limit: Metabolic engineering of *Corynebacterium glutamicum* for l-leucine overproduction. Metab. Eng. 22:40-52.
Wang J, Wen B, Wang J, Xu Q, Zhang C, Chen N, Xie X (2013). Enhancing (L)-isoleucine production by *thrABC* overexpression combined with *alaT* deletion in *Corynebacterium glutamicum*. Appl. Biochem. Biotechnol. 171(1):20-30.
Wieschalka S, Blombach B, Eikmanns BJ (2012). Engineering

Corynebacterium glutamicum for the production of pyruvate. Appl. Microbiol. Biotechnol. 94(2):449-459.
Wolfe AJ (2005). The acetate switch. Microbiol. Mol. Biol. Rev. 69(1):12-50.
Woo HM, Park JB (2014). Recent progress in development of synthetic biology platforms and metabolic engineering of *Corynebacterium glutamicum*. J. Biotechnol. 180(15):43-51.
Yin L, Zhao J, Chen C, Hu X, Wang X (2014). Enhancing the carbon flux and NADPH supply to increase L-isoleucine production in *Corynebacterium glutamicum*. Biotechnol. Bioprocess Eng. 19(1):132-142.

academicJournals

Vol. 16(18), pp. 1061-1066, 3 May, 2017
DOI: 10.5897/AJB2017.15918
Article Number: 314492864061
ISSN 1684-5315
Copyright © 2017
Author(s) retain the copyright of this article
http://www.academicjournals.org/AJB

African Journal of Biotechnology

Full Length Research Paper

Fourier transform infrared spectroscopic analysis of maize (*Zea mays*) subjected to progressive drought reveals involvement of lipids, amides and carbohydrates

Chukwuma C. Ogbaga[1]*, Matthew A. E. Miller[2], Habib-ur-Rehman Athar[3] and Giles N. Johnson[4]

[1]Department of Biological Sciences, Nile University of Nigeria, Abuja, Nigeria.
[2]Agrimetrics, The University of Reading, United Kingdom.
[3]Institute of Pure and Applied Biology, Bahauddin Zakariya University, Multan, Pakistan.
[4]School of Earth and Environmental Sciences, The University of Manchester, United Kingdom.

Received 27 January, 2017; Accepted 18 April, 2017

Changing climate means that there will be more episodes of drought, especially in arid regions. Drought stress is an important environmental factor that reduces crop productivity. Despite the vast amount of literature on drought stress in plants, there are still many uncertainties concerning the molecular responses under water deficit. In particular, if we wish to breed plants that are able to tolerate stress, identifying novel traits that contribute to this is desirable. In this study, Fourier transform infrared (FTIR) spectroscopy was used to investigate the response of maize to progressive drought. The objective was to determine whether FTIR spectroscopy is a technique that might be used in monitoring the molecular processes involved in drought responses in plants. Maize seeds were grown for three weeks in a controlled environment before drought was imposed by withdrawing water for up to 12 days. Principal component-discriminant function analysis (PC-DFA) indicated that water deficit elicited changes in the FTIR spectra within the wavenumber ranges of 3050 to 2800, 1750 to 1250 and 1250 to 900 cm^{-1}. With water deficit, the intensities of the absorption bands were reduced. PC-DFA loadings confirmed that the signals to the changes were lipids, amides and carbohydrates, respectively. This work shows that FTIR spectroscopy can provide valuable insights into drought responses of plants and maybe useful for identifying novel drought tolerance traits.

Key words: Metabolic fingerprint, molecular changes, multivariate analysis, principal component-discriminant function analysis (PC-DFA), principal component analysis (PCA).

INTRODUCTION

Drought can occur in different degrees, which can lead to a reduction in crop production. A plant's response mechanism is highly complex and is dependent on the plant species and duration of water deficit (Anjum et al., 2016). Drought causes massive economic losses (about $20 billion loss worldwide from 1900 to 2016) and is predicted to increase in the future, due to climate change (IPCC, 2007). Hence, understanding the drought

tolerance mechanisms of plants will aid in the improvement of crops.

Maize is one of the most important crops in arid regions and a major cereal consumed worldwide (Ben-Iwo et al., 2016). The grains can be rich in protein, oil and starch (Kuhnen et al., 2010). Maize is not only important for feeding the growing human population but is also increasingly being used for biomass and biofuel purposes (Ben-Iwo et al., 2016). In order to improve its economic importance as sources of food and fuel, there is need to further understand how the crop tolerates stress, particularly drought stress, which reduces yield.

Fourier transform infrared (FTIR) spectroscopy is a method that measures the vibrations of molecular bonds and generates a spectrum that is considered the metabolic fingerprint of a sample (Amir et al., 2013; Kuhnen et al., 2010). It has been used as a tool for the analysis of plants, grain, soil, microalgae and in detecting microorganisms in food (Dean et al., 2010; Kamnev, 2008; Kuhnen et al., 2010; Lahlali et al., 2014, Winder and Goodacre, 2004). FTIR spectroscopy is a powerful and emerging tool that has the potential to be used to understand maize response to drought stress (Amir et al., 2013). To extract crucial information from a spectrum, multivariate analysis approaches such as principal component discriminant function analysis can be employed (Amir et al., 2013).

The objective of the study was to determine whether FTIR spectroscopy is a technique that might be used in monitoring the molecular processes involved in drought responses in plants. Principal component-discriminant function analysis (PC-DFA) and its loadings were employed to discriminate and detect changes in metabolites in response to drought.

MATERIALS AND METHODS

Plant growth conditions and drought treatments

Maize seeds (Cv Sundance) were supplied by Suttons Seeds (Paignton, UK). The seeds were sown in 3" small sized pots filled with John Innes No.1 soil in a growth chamber at the University of Manchester, United Kingdom with a 16 h photoperiod and a day/night regime at 23/15°C and relative humidity (RH) of 40-50%. Photosynthetic photon flux density was 130 $\mu molm^{-2}s^{-1}$ (Light meter, SKYE instruments Ltd, UK provided by warm white LED lights; colour temperature = 2800 to 3000 K). Three weeks after planting (WAP), the maize seedlings were subjected to progressive drought stress for 12 days. Plant pots were weighed every two days during the period of drought stress until the 12th day. Soil water content (SWC) was estimated relative to water saturated controls using the formula: (FW-DW)/(AvFW-DW) × 100, where FW is the fresh weight of soil, DW is the dry weight of soil after drying to constant weight at 105°C and AvFW is the average fresh weight of the soils in the pots on day 0 of the experiment (Ogbaga et al., 2014). Twelve groups were used in the experiment for 1 plant x the 12 SWC conditions.

Plant molecular analysis via Fourier transform infrared (FTIR) spectroscopy

Fully expanded leaf and shoot tissues from Days 0 to 12 and % soil water contents were excised 8 h into photoperiod with a pair of scissors, flash frozen in liquid nitrogen and lyophilized (freeze dried) with a Scan Vac Coolsafe freeze dryer (Vacuubrand, Wertheim, Germany) for 48 h as described by Ogbaga et al. (2016). FTIR spectroscopy was performed on 30 mg of dried homogenized tissues. The tissues were transferred to 2 ml micro centrifuge tubes and extracted in 600 µl of distilled water. 5 µl of homogenate was loaded onto the wells of a silicon 96 target plate (Bruker, MA, USA) and dried at 60°C. The Si plate was then placed in a Bruker Equinox-55 spectrometer and raw FT-IR data were recorded at an absorbance mode of 4000 – 600 cm^{-1} wavenumber with a resolution of ~4 cm^{-1} (Ogbaga et al., 2016).

Principal component analysis (PCA) and principal component discriminant function analysis (PC-DFA)

PCA and PC-DFA analyses were performed the same way as described previously (Ogbaga et al., 2016). Raw FTIR data were recorded at an absorbance mode of 4000 to 600 cm^{-1} wavenumber with a resolution of ~4 cm^{-1}. PC-DFA was used to analyze the data using R software (available at http://www.r-project.org/). PC-DFA scores and loading plots were visualized in Origin Pro 9 (OriginLab, Northampton, MA). PC-DFA a supervised multivariate technique was performed on the principal components (PCs) of the samples harvested on Days 0 to 12 at different soil water contents to determine the spectral regions of compounds (from PC-DFA loadings plots) that change with water deficit. PC-DFA is used to discriminate between samples based on their principal components with knowledge of which spectra were replicates. For clarity, the spectral regions of major compound classes are found at ~3050 to 2800 cm^{-1} for lipids, ~1750 to 1250 cm^{-1} for amides and ~1250 to 900 cm^{-1} for carbohydrates (Ogbaga et al., 2016).

RESULTS AND DISCUSSION

The % soil water content (SWC) fell progressively with time such that by the 10th day after drought stress was imposed, the soil was completely dry (Figure 1). The dryness was accompanied by a gradual drop in the FTIR spectra relative to the control (Figure 2). The absorption bands of the spectra dropped to approximately half of the original intensities by the 6th day when the SWC reduced to 15%. This decrease continued until the soil was completely dried (Figure 2). From the FTIR data, spectral differences were observed with water deficit. Chlorophyll fluorescence and stomatal conductance are established techniques used for non-destructive and non-invasive measurement of drought stress (Born et al., 2014). Here, the authors propose the use of FTIR spectroscopy as another method that can provide quick, high throughput

*Corresponding author. E-mail: chukwumaogbaga@gmail.com.

Author(s) agree that this article remains permanently open access under the terms of the Creative Commons Attribution License 4.0 International License

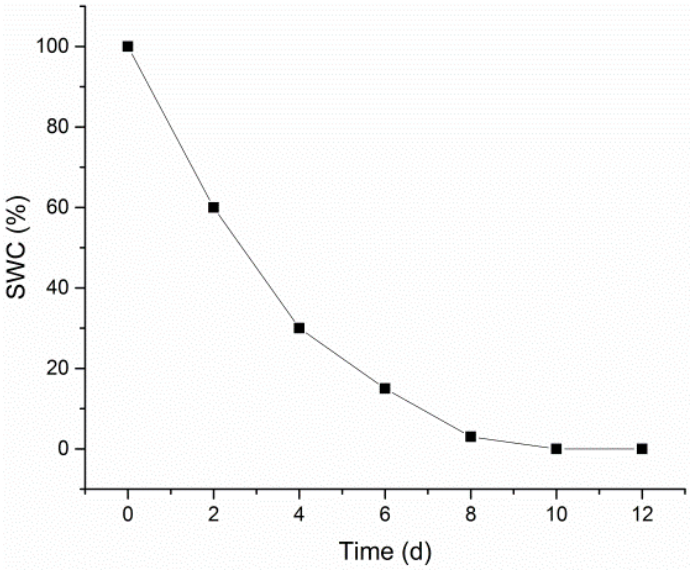

Figure 1. The change in pot water content relative to water saturation. Plants were grown for 3 weeks before drought imposed by withholding water for up to 12 days.

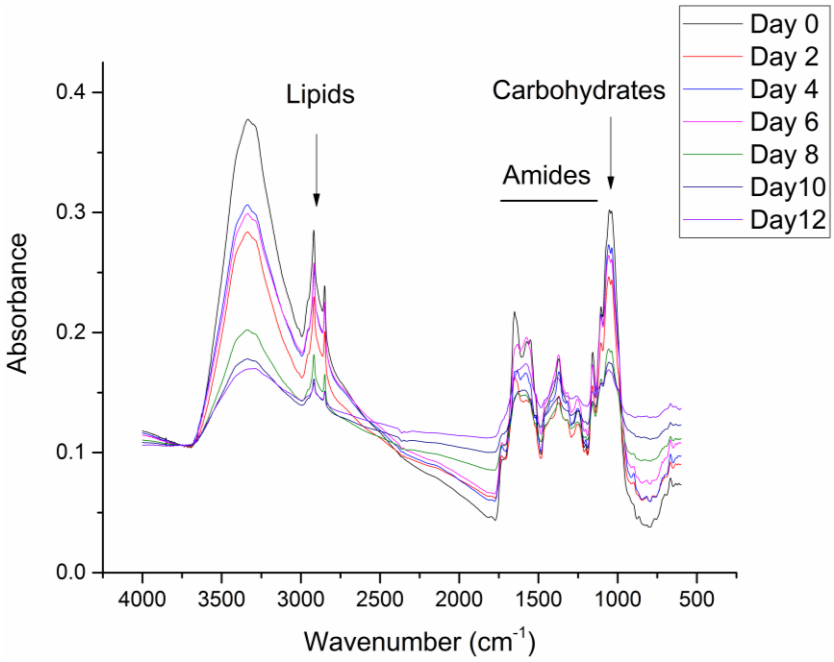

Figure 2. Average normalised FTIR spectra from days 0 to 12. FTIR spectra were normalised to wavenumber 3745 cm^{-1}.

data on drought stress.

In order to compare changes in lipids, amides and carbohydrates in the control and drought stressed plants, FTIR spectra were normalised at a wavenumber of 3745 cm^{-1}. The absorption band positions from the spectra are those corresponding to lipids, amides and carbohydrates and are similar to our earlier study which suggested that these metabolites were involved in prolonged drought in sorghum (Ogbaga et al., 2016). The intensities: 3050 to 2800, 1750 to 1250 and 1250 to 900 cm^{-1} bands corresponding to lipids, amides and carbohydrates, respectively, were higher in control plants as compared to

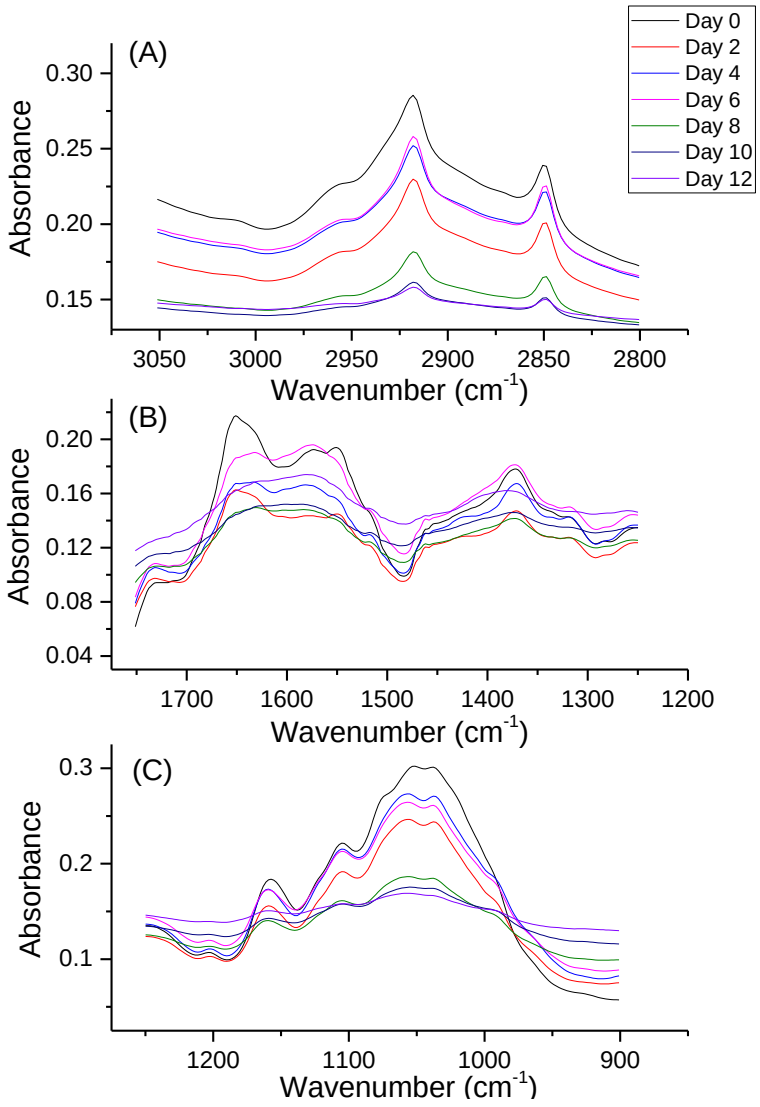

Figure 3. Average lipid (3050 to 2800 cm^{-1}) absorbance (A), average amide (1750 to 1250 cm^{-1}) absorbance (B) and average carbohydrate (1250 to 900 cm^{-1}) absorbance (C) of maize grown from days 0 to 12.

the stressed plants (Figure 3). Under drought the lowest bands were seen on the 12th day for lipid and carbohydrate regions. However, there was a differential response in the intensities observed at amide region with water deficit (Figure 3). The absorption bands from the spectra in this study suggest that the same metabolites detected in sorghum during prolonged drought are also involved in progressive drought in maize. In addition, reduction in the intensities of the bands detected with increasing drought indicated a reduction in lipid and carbohydrate content and also changes in the composition of the proteome (Lahlali et al., 2014; Athar et al., 2016). Thus, information on drought-specific responses could be extracted from the spectra.

Figure 4 shows the PC-DFA scatter plot with an initial increase in LD2 on y-axis up to the 4th day. From the 6th day, changes in the plots reduced and were explained by both LD2 and LD1 (Figure 4). The loading profiles of the changes in PC-DFA shown in Figure 4 are captured in Figure 5. The loading profiles confirmed that the signals associated with progressive drought stress in the maize plants were indeed lipids, amides and carbohydrates (Figure 5). Changes in lipid region could reflect lipid signalling in response to drought stress or the regulation of enzymes involved in lipid signalling such as phospholipase C and phospholipase D (Zhao, 2015). In terms of structure, lipids are rich in CH_2 functional group, while the amide groups are rich components of proteins mostly containing N-H structures. Carbohydrates on the other hand, are dominated by vibrations of C-O-C or C-O

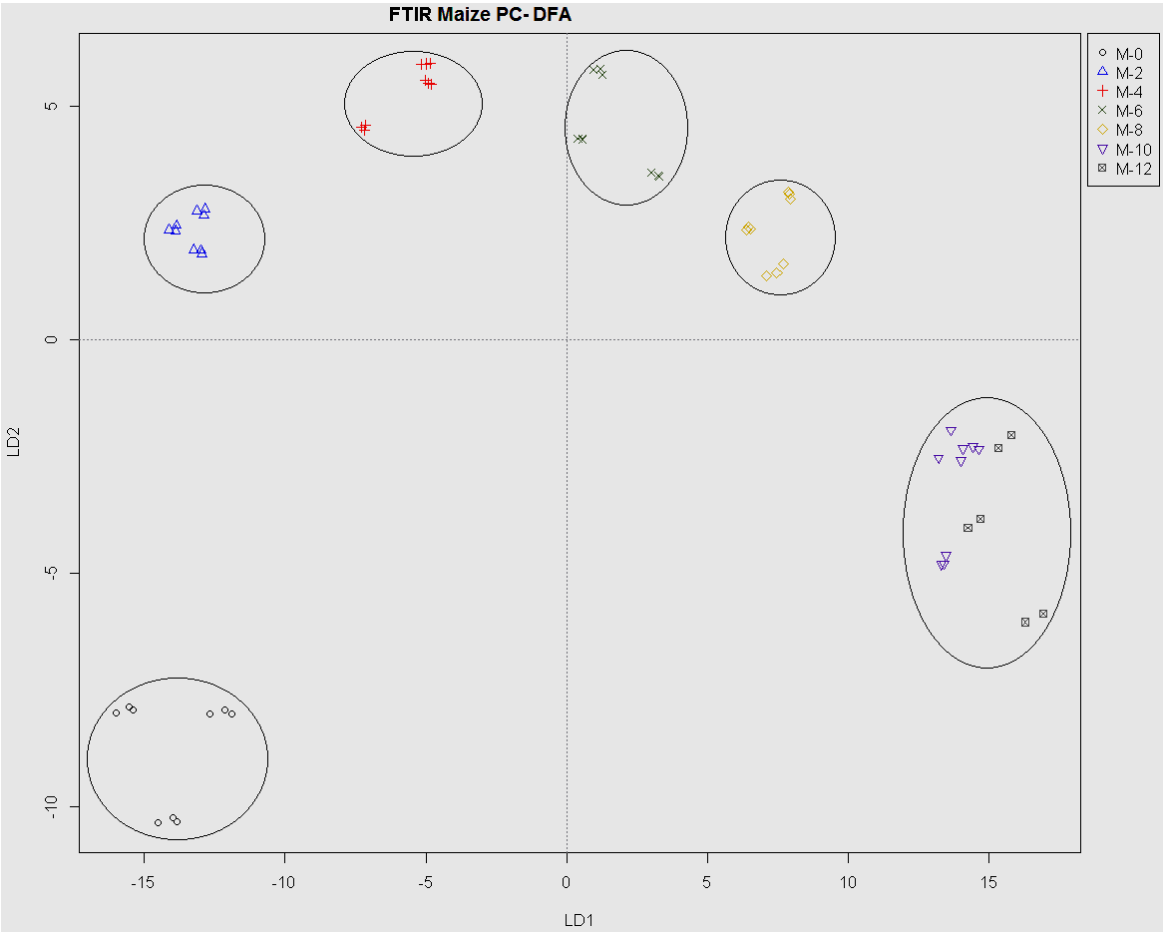

Figure 4. Principal component discriminant function analysis (PC-DFA) of maize (M) on days 0, 2, 4, 6, 8, 10 and 12. LD1- Linear discriminant 1, LD2- linear discriminant 2.

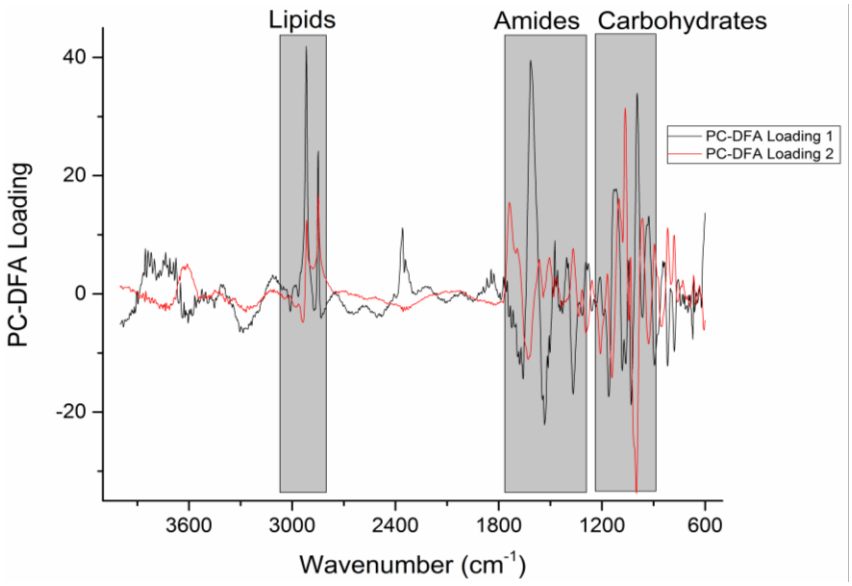

Figure 5. Principal component discriminant function (PCDF) loadings. The shaded regions from left to right represent lipids, amides and carbohydrates.

functional groups (Beekes et al., 2007).

Conclusion

The study indicated that the signals in the wavenumber ranging from 3050 to 2800, 1750 to 1250 and 1250 to 900 cm^{-1}, associated with lipids, amides and carbohydrates respectively, changed with water deficit in maize. As FTIR is a fast tool, it can be used as a probe for the estimation of drought and a rapid measure of molecular changes in drought stressed plants.

CONFLICT OF INTERESTS

The authors have not declared any conflict of interests.

ABBREVIATIONS

FTIR, Fourier transform infrared spectroscopy; **LD1,** linear discriminant 1; **LD2,** linear discriminant 2; **PCA,** principal component analysis; **PC-DFA,** principal component-discriminant function analysis; **SWC,** soil water content.

REFERENCES

Amir RM, Anjum FM, Khan MI, Khan MR, Pasha I, Nadeem M (2013). Application of Fourier transform infrared (FTIR) spectroscopy for the identification of wheat varieties. J. Food Sci. Technol. 50:1018-1023.

Anjum SA, Tanveer M, Ashraf U, Hussain S, Shahzad B, Khan I, Wang L (2016) Effect of progressive drought stress on growth, leaf gas exchange, and antioxidant production in two maize cultivars. Environ. Sci. Pollut. Res. 23:17132-17141.

Athar HR, Ambreen S, Javed M, Hina M, Rasul M, Zafar ZU, Manzoor H, Ogbaga CC, Afzal M, Al-Qurainy F, Ashraf M (2016). Influence of sub-lethal crude oil on growth,water relations and photosynthetic capacity of maize (*Zea mays* L) plants. Environ. Sci. Pollut. Res. 23(18):18320-18331.

Beekes M, Lasch P, Naumann D (2007). Analytical applications of Fourier transform-infrared (FT-IR) spectroscopy in microbiology and prion research. Vet. Microbiol. 123:305-319.

Ben-Iwo J, Manovic V, Longhurst P (2016). Biomass resources and biofuels potential for the production of transportation fuels in Nigeria. Renew. Sustain. Energy Rev. 63:172-192.

Born N, Behringer D, Liepelt S, Beyer S, Schwerdtfeger M, Ziegenhagen B, Koch M (2014). Monitoring plant drought stress response using terahertz time-domain spectroscopy. Plant Physiol. 164:1571-1577.

Dean AP, Sigee DC, Estrada B, Pittman JK (2010). Using FTIR spectroscopy for rapid determination of lipid accumulation in response to nitrogen limitation in freshwater microalgae. Bioresour. Technol. 101:4499-4507.

IPCC (2007) Climate Change 2007: The Physical Basis, Cambridge, UK.

Kamnev AA (2008). FTIR spectroscopic studies of bacterial cellular responses to environmental factors, plant-bacterial interactions and signalling. J. Spectrosc. 22(2-3):83-95.

Kuhnen S, Ogliari JB, Dias PF, Boffo EF, Correia I, Ferreira AG, Delgadillo I, Maraschin M (2010). ATR-FTIR spectroscopy and chemometric analysis applied to discrimination of landrace maize flours produced in southern Brazil. Int. J. Food Sci. Technol. 45:1673-1681.

Lahlali R, Jiang Y, Kumar S, Karunakaran C, Liu X, Borondics F, Hallin E, Bueckert R (2014). ATR – FTIR spectroscopy reveals involvement of lipids and proteins of intact pea pollen grains to heat stress tolerance. Front. Plant Sci. 5:747.

Ogbaga CC, Stepien P, Dyson BC, Rattray NJ, Ellis DI, Goodacre R, Johnson GN (2016). Biochemical analyses of sorghum varieties reveal differential responses to drought. PloS One 11:e0154423.

Ogbaga CC, Stepien P, Johnson GN (2014). Sorghum (Sorghum bicolor) varieties adopt strongly contrasting strategies in response to drought. Physiol. Plant. 152:389-401.

Winder CL, Goodacre R (2004). Comparison of diffuse-reflectance absorbance and attenuated total reflectance FT-IR for the discrimination of bacteria. Analyst 129:1118-1122.

Zhao J (2015). Phospholipase D and phosphatidic acid in plant defence response: from protein-protein and lipid-protein interactions to hormone signalling. J. Exp. Bot. 66 (7):1721-1736.

academicJournals

Vol. 16(18), pp. 1067-1077, 3 May, 2017
DOI: 10.5897/AJB2017.15971
Article Number: 0374B3664067
ISSN 1684-5315
Copyright © 2017
Author(s) retain the copyright of this article
http://www.academicjournals.org/AJB

African Journal of Biotechnology

Full Length Research Paper

The nitrogen-fixing *Bradyrhizobium elkanii* significantly stimulates root development and pullout resistance of *Acacia confusa*

Jung-Tai Lee*, Sung-Ming Tsai and Chung-Hung Lin

Department of Forestry and Natural Resources, National Chiayi University, Chiayi 60004, R.O.C. Taiwan.

Received 2 March, 2017; Accepted 18 April, 2017

Reforestation of native *Acacia confusa* Merr. on landslide areas in Taiwan is important for agroforestry and soil conservation. To ensure high survival and growth vigor, *A. confusa* seedlings must develop a strong root system. Inoculating of acacia with symbiotic nitrogen-fixing bacteria (NFB) may ameliorate the problems associated with soil nutrient deficiency on landslide sites. In this study, under plastic house condition, a NFB was isolated from the root nodules of native *A. confusa* and identified as *Bradyrhizobium elkanii*, and its effects on growth, root system morphology and pullout resistance of acacia seedlings were investigated. Our results revealed that the growth of inoculated seedlings is significantly more vigor than that of the noninoculated controls. The enhancements in height, tap root length, shoot biomass and root biomass were 40, 100, 140 and 130%, respectively. Also, inoculated seedlings had significantly longer total root length (150%), larger external root surface area (130%), larger root volume (70%), and more root tip number (60%) than the controls. Moreover, the inoculated seedlings developed significantly stronger root functional traits, that is, root density (130%), root length density (60%) and specific root length (60%), than the controls. Consistently, the root pullout resistance of inoculated seedlings was significantly higher than that of the noninoculated ones. These results demonstrate that *B. elkanii* is an effective nitrogen-fixing bacterium capable of enhancing growth, root development and pullout resistance of *A. confusa*.

Key words: Fabaceae, inoculation, nodules, pullout resistance, root morphology.

INTRODUCTION

Acacia confusa (*Acacia confusa* Merr.), belonging to the family of Fabaceae, subfamily Mimosoideae, is an endemic nitrogen-fixing hardwood tree, widespread throughout the island of Taiwan (Huang and Ohashi, 1977). *Acacia confusa* has high potential for agroforestry, lumber production and landslide prevention, and reforestation. *Acacia* species can symbiose with nitrogen-fixing microorganisms (that is, *Rhizobium* spp.,

*Corresponding author. E-mail: jtlee@mail.ncyu.edu.tw. Tel: 886-5-271-7482; 886-921-630-624.

Author(s) agree that this article remains permanently open access under the terms of the Creative Commons Attribution License 4.0 International License

Bradyrhizobium spp., *Azorhizobium* spp., and *Mesorhizobium* sp.) and form nitrogen-fixing nodules, which can fix nitrogen from air and supply nitrogen nutrient to trees for growth and development (Ferro et al., 2000; Zerhari et al., 2000; Dumroese et al., 2009; Ceccon et al., 2011; Diouf et al., 2015; Pereyra et al., 2015). Several studies have demonstrated that inoculation of seedlings (*Oryza sativa*, *Glycine max* and *Zea mays*) with rhizobial strains results in the change of root morphology, that is, increases in nodules, lateral roots, root hairs, root surface area, and total root length (Huang and Ladha, 1997; Ikeda, 1999; Souleimanov et al., 2002).

Morphological shapes of tree root systems have been categorized into three shapes, that is, taproot, heart root and plate root (Wilde, 1958). Yen (1987) classified the patterns of root growth in trees into five types, that is, H-type, R-type, VH-type, V-type and M-type. Styczen and Morgan (1995) classified root systems into three types, that is, H-type with horizontal lateral roots, VH-type with deep taproots and M-type with profusely branching roots. Trees generally develop two main classes of roots, the long taproots ensuring tree anchorage and the short lateral roots (Stokes et al., 2008). Trees with heart root and taproot systems are more resistant to uprooting than plate root systems (Dupuy et al., 2005). Wu et al. (2004) suggested that taprooted trees could be better for slope stability due to the increased slope factor of safety. The type of tree roots changes root system morphology, which in turn affects their biomechanical properties (Burylo et al., 2012). Previous studies on root distribution, root system morphology and mechanical properties of *Acacia* species were concentrated on *A. mangium*. In *A. mangium*, about 35% of its roots are distributed in the top 10 cm layer, and about 90% of its roots is in the fine root class (d < 2 mm) (Lateh et al., 2014; Avani et al., 2014). The pullout resistance of *A. mangium* is much influenced by the root than the shoot (Normaniza et al., 2011; Lateh et al., 2015). However, rhizobial symbiosis and its effect on growth, root system morphology and root biomechanics of *A. confusa* have not been investigated. The aim of the study was to (1) isolate the indigenous rhizobium strain from *A. confusa* for re-inoculating *A. confusa* seedlings, and (2) investigate the effects of the rhizobium inoculation on growth, root system morphology and pullout resistance of seedlings in order to provide strategy for landslide reforestation and soil conservation.

MATERIALS AND METHODS

Sample collection

In September 2014, an elite tree in the natural forest of *A. confusa* located at Chiayi, Taiwan (120°29'09''E, 23°28'06''N) was selected according to height, diameter at breast height (DBH), straightness, and absence of trunk defects. Root nodules were collected from roots at 5 to 20 cm depth of soil stratum, put in polyethylene bags and stored at 4°C until rhizobial strain isolation. Seeds were also collected from the same tree.

Rhizobial strain isolation and purification

Root nodules were cleaned with ultrasonic cleaner, surface sterilized twice with 75% ethanol for 5 min, rinsed by sterile water for 3 times, then sterilized 3 times with 10% sodium hypoclorite for 5 min and rinsed by sterile water for 4 times. The endophytic bacteria in nodules were isolated and purified with streak-plate method on YEMA medium (Usharani et al., 2014). The purified strain was designated as AC1.

DNA extraction, sequencing, and phylogenetic analysis

Bacterial genomic DNA extraction kit (GenElute NA2100, Sigma-Aldrich, St. Louis, MO, USA) was used for total DNA extraction, and subsequently subjected to 1.2% agarose gel electrophoresis. The spectrophotometric absorption values of the nucleic acids were used for concentration measurement. The primers used for PCR of 16S rRNA were forward primer U1 (5'-ACGCGTCGACAGAGTTTGATCCTGGCT-3'), U1R (5'-GGACTACCAGGGTATCTAAT-3') (Relman, 1993), and reverse primer 27f (5'-AGAGTTTGAC MTGGCTCAG-3'), U1492R (5'-GGT TAC CTT GTT ACG ACTT-3') (Weisburg et al., 1991). After PCR reaction, 2.5 µl amplification samples was loaded to 1.2% agarose gel for electrophoresis at 100 V, and the specific PCR products were sequenced (Tri-I Biotech, Taichung, Taiwan). The sequences were logged into NCBI to access GenBank for sequence similarity and homology study of the 16S rRNA gene sequences. The phylogenetic relationships were analyzed by Molecular Evolutionary Genetics Analysis (MEGA, Bioinformatics, Arizona State Univ., Tempe, USA). Strains with high similarity in sequence were chosen for similarity analysis.

Establishment of seedlings

After surface cleaning with tap water, seeds of *A. confusa* were sterilized with 10% sodium hypochlorite (NaOCl) solution, and pretreated with hot water (80°C) for 10 min, rinsed three times with sterilized distilled water, and then germinated in autoclaved peat moss and vermiculite mixtures (1:1, v/v) in the spring. The containers used for transplanting were wooden plant culture boxes (*l*×*w*×*h*, 30 cm × 30 cm × 60 cm) (Figure 2). Two weeks before transplanting, the containers were sterilized with 10% sodium hypochlorite solution, and sandy loam soils were sterilized with steam and then fumigated with 20 g Basamid granular soil fumigant (Engage Agro Corp., ON, Canada) for 2 days. The sterilized soil was then used to fill containers. When seedlings attained 5 cm in height, they were transplanted to the containers one plant in each container, and watered every morning. Thirty-two seedlings in containers were randomly arranged into two separate plastic houses.

Inoculation test

One week after transplanting, 16 seedlings in one plastic house were inoculated with the isolated rhizobial strain AC1 of *B. elkanii*. A 5 ml suspension of the strain (1.5×10^8 cfu/ml) was applied into four holes around the seedling. The same inoculation was repeated two weeks later in order to ensure high colonization. Another 16 noninoculated seedlings were treated with water and served as controls. The containers of inoculated and noninoculated seedlings were arranged separately in divided plastic houses. The seedlings were grown in the plastic houses at 26±4°C in the day and 18±5°C at night, with 60 to 80% relative humidity, and 1000 ± 200 µmoles photon m^{-2} s^{-1} PPFD (photosynthetic photon flux density) in the day. After 8 months of transplanting, the seedlings were sampled for

measurements of growth, root system morphology and pullout resistance.

Growth and root system morphology

Eight inoculated and eight noninoculated seedlings were randomly selected, respectively. The plant height and root collar diameter were measured with height ruler and digital caliper. The plant root systems were carefully exposed by complete excavation method (Böhm, 1979). Hand excavation with small spade was carried out to prevent root damage. The rooting depth, root numbers and length were measured. The root systems were cut off from the stems with pruning shears. For each root system, root morphological traits, that is, taproot length, total root length, external root surface root area and root tip number were measured with WinRHIZO*Pro* Image Analysis System (Regent Instruments, Quebec, Canada) (Bouma et al., 2000). WinRHIZO*Pro* is an image analysis system for automatic root measurement in morphology (that is, root length, root surface area, root tip numbers, etc.). Total root volume was measured with water displacement method (Pang et al., 2011). Roots and stems were then dried in an oven at 75°C till a constant weight. Root functional traits, that is, root density (RD), root length density (RLD), root tissue density (RTD), specific root length (SRL), and root to shoot ratio (R/S), were calculated by using the following formulas (Burylo et al., 2009, 2012; Strokes et al., 2009; Gould et al., 2016):

$$RD\ (kg\ m^{-3}) = \frac{DW_R}{V} \quad (1)$$

Where, RD is the root density, DW_R is the total root dry weight, and V is the unit volume of root-permeated soil.

$$RLD\ (km\ m^{-3}) = \frac{L_R}{V} \quad (2)$$

Where, RLD is the root length density, L_R is the total root length measured using WinRHIZO, and V is the unit volume of root-permeated soil.

$$RTD\ (g\ cm^{-3}) = \frac{DW_R}{V} \quad (3)$$

Where, RTD is the root tissue density, DW_R is the total root dry weight, and V is the total root system volume measured using WinRHIZO.

$$SRL\ (m\ g^{-1}) = \frac{L_R}{DW_R} \quad (4)$$

Where, SRL is the specific root length, L_R is the total root length measured using WinRHIZO, and DW_R is the total root dry weight.

$$R/S = \frac{DW_R}{DW_S} \quad (5)$$

Where, R/S is the root to shoot ratio, DW_R is the total root dry weight, and DW_S is the total shoot dry weight.

Pullout test

After 8 months of transplanting, the rest of the eight seedlings each of inoculated and noninoculated seedlings were used for pullout test. The soil material was classified as sandy loam (containing 67.5% sand, 9.5% clay and 23% silt; specific gravity 2.63; bulk density 1.41 g/cm^3, porosity 45%). The average soil dry weight was 12.4 kN/m^3 and the average soil moisture content was 25%. Before pullout test, plant height and root collar diameter were measured. The plant stem was cut off at 10 cm above the root collar, and the bark was girdled and removed to prevent slippage of the special pulling fixture (Figure 3). The *in situ* pullout instrument (U-Soft USPA-003, U-Soft Tech, Taiwan) was used in pullout test. The load cell (Kyowa 5T, LUK-5TBS, Kyowa, Tokyo, Japan) was connected with the loading recorder and constant pullout control unit (rate adjustable from 2 to 4 mm/min), and mounted on a portable triangular steel frame. The data of pullout resistance and displacement were acquired through a portable computer system. Then, the instrument was connected to the pulling fixture. A constant vertical pulling speed of 2 mm/min was then applied automatically until the resisting force dropped sharply.

Data analysis

Variations in growth and morphological traits data between inoculated and noninoculated seedlings were analyzed using SPSS 22.0 for Windows (SPSS, Chicago, IL., USA) with t-test and one-way analysis of variance (ANOVA) Scheffé's method. The relationships between pullout resistance and plant traits were analyzed using Microsoft Excel regression analysis (version from Office 2013).

RESULTS

Rhizobial strain isolation, sequencing and phylogenetic analysis

The rhizobial strain isolated and purified was designated as AC1. Molecular analysis revealed that the 16S rRNA gene sequence of the isolated strain AC1 has 100% similarity to that of *Bradyrhizobium elkanii* (Huang et al., 2012) and was thus classified into the same group by maximum-parsimony and neighbor joining methods (Figures 1 and 4). Thus, the local strain AC1 was identified as *B. elkanii*. Inoculation test with AC1 revealed that *B. elkanii* effectively induces nodule formation in the roots of *A. confusa* (Figure 5).

Seedling growth

Statistical analysis revealed that inoculation significantly influenced most morphological parameters (Table 1). On average, inoculated seedlings had significantly larger height (40%), tap root length (100%), root biomass (130%), and shoot biomass (140%) than the noninoculated controls, but inoculation did not significantly affect root-collar diameter of seedlings (Table 1).

Root system morphology

The inoculated *A. confusa* seedlings developed bigger and deeper root systems than the noninoculated controls (Figure 6). The pattern of root growth in the inoculated seedlings showed that the maximum root developed to a depth of 70 cm, with more than 80% of the root matrix observed in the top 30 cm, and the lateral roots grew

Score	Expect	Identities	Gaps	Strand
1240 bits(671)	0.0	671/671(100%)	0/671(0%)	Plus/Plus

```
Query  1    CATAGCAATATGTCAGCGGCAGACGGGTGAGTAACGCGTGGGAACGTACCTTTTGGTTCG  60
            ||||||||||||||||||||||||||||||||||||||||||||||||||||||||||||
Sbjct  1    CATAGCAATATGTCAGCGGCAGACGGGTGAGTAACGCGTGGGAACGTACCTTTTGGTTCG  60

Query  61   GAACAACTGAGGGAAACTTCAGCTAATACCGGATAAGCCCTTACGGGGAAAGATTTATCG  120
            ||||||||||||||||||||||||||||||||||||||||||||||||||||||||||||
Sbjct  61   GAACAACTGAGGGAAACTTCAGCTAATACCGGATAAGCCCTTACGGGGAAAGATTTATCG  120

Query  121  CCGAAAGATCGGCCCGCGTCTGATTAGCTAGTTGGTGAGGTAATGGCTCACCAAGGCGAC  180
            ||||||||||||||||||||||||||||||||||||||||||||||||||||||||||||
Sbjct  121  CCGAAAGATCGGCCCGCGTCTGATTAGCTAGTTGGTGAGGTAATGGCTCACCAAGGCGAC  180

Query  181  GATCAGTAGCTGGTCTGAGAGGATGATCAGCCACATTGGGACTGAGACACGGCCCAAACT  240
            ||||||||||||||||||||||||||||||||||||||||||||||||||||||||||||
Sbjct  181  GATCAGTAGCTGGTCTGAGAGGATGATCAGCCACATTGGGACTGAGACACGGCCCAAACT  240

Query  241  CCTACGGGAGGCAGCAGTGGGGAATATTGGACAATGGGCGCAAGCCTGATCCAGCCATGC  300
            ||||||||||||||||||||||||||||||||||||||||||||||||||||||||||||
Sbjct  241  CCTACGGGAGGCAGCAGTGGGGAATATTGGACAATGGGCGCAAGCCTGATCCAGCCATGC  300

Query  301  CGCGTGAGTGATGAAGGCCCTAGGGTTGTAAAGCTCTTTTGTGCGGGAAGATAATGACGG  360
            ||||||||||||||||||||||||||||||||||||||||||||||||||||||||||||
Sbjct  301  CGCGTGAGTGATGAAGGCCCTAGGGTTGTAAAGCTCTTTTGTGCGGGAAGATAATGACGG  360

Query  361  TACCGCAAGAATAAGCCCCGGCTAACTTCGTGCCAGCAGCCGCGGTAATACGAAGGGGGC  420
            ||||||||||||||||||||||||||||||||||||||||||||||||||||||||||||
Sbjct  361  TACCGCAAGAATAAGCCCCGGCTAACTTCGTGCCAGCAGCCGCGGTAATACGAAGGGGGC  420

Query  421  TAGCGTTGCTCGGAATCACTGGGCGTAAAGGGTGCGTAGGCGGGTCTTTAAGTCAGGGGT  480
            ||||||||||||||||||||||||||||||||||||||||||||||||||||||||||||
Sbjct  421  TAGCGTTGCTCGGAATCACTGGGCGTAAAGGGTGCGTAGGCGGGTCTTTAAGTCAGGGGT  480

Query  481  GAAATCCTGGAGCTCAACTCCAGAACTGCCTTTGATACTGAAGATCTTGAGTTCGGGAGA  540
            ||||||||||||||||||||||||||||||||||||||||||||||||||||||||||||
Sbjct  481  GAAATCCTGGAGCTCAACTCCAGAACTGCCTTTGATACTGAAGATCTTGAGTTCGGGAGA  540

Query  541  GGTGAGTGGAACTGCGAGTGTAGAGGTGAAATTCGTAGATATTCGCAAGAACACCAGTGG  600
            ||||||||||||||||||||||||||||||||||||||||||||||||||||||||||||
Sbjct  541  GGTGAGTGGAACTGCGAGTGTAGAGGTGAAATTCGTAGATATTCGCAAGAACACCAGTGG  600

Query  601  CGAAGGCGGCTCACTGGCCCGATACTGACGCTGAGGCACGAAAGCGTGGGGAGCAAACAG  660
            ||||||||||||||||||||||||||||||||||||||||||||||||||||||||||||
Sbjct  601  CGAAGGCGGCTCACTGGCCCGATACTGACGCTGAGGCACGAAAGCGTGGGGAGCAAACAG  660

Query  661  GATTAGATACC  671
            ||||||||||
Sbjct  661  GATTAGATACC  671
```

Figure 1. Partial sequence of strain AC1 16S ribosomal RNA gene (query), compared to that of *Bradyrhizobium elkanii* (subject).

horizontally and profusely (Figure 6a). In contrast, for the noninoculated seedlings, its maximum root extended only to a depth of 50 cm, with more than 90% of the root matrix confined to the top 20 cm, and its lateral roots extended sparsely (Figure 6b). The observed root system morphologies of both inoculated and noninoculated *A. confusa* seedlings were classified to the VH-type.

Analysis of morphological parameters by WinRHIZO showed that inoculation significantly affected every morphological parameter. On average, the inoculated seedlings had significantly larger total root length (150%), external root surface area (130%), root volume (70%), and root tip number (60%) than the noninoculated controls (Table 2).

Analysis of root functional traits showed that the root density (RD), root length density (RLD) and root to shoot biomass ratio (R/S) of *A. confusa* seedlings inoculated with *B. elkanii* AC1 were significantly higher than the control ones. On average, seedlings inoculated with *B. elkanii* had significantly higher RD (130%), RLD (60%) and SLR (60%) than the controls. However, inoculation did not affect RTD and R/S of seedlings (Table 3).

Pullout resistance

In total, eight replicated pullout tests were performed to investigate the pullout resistance of the inoculated and

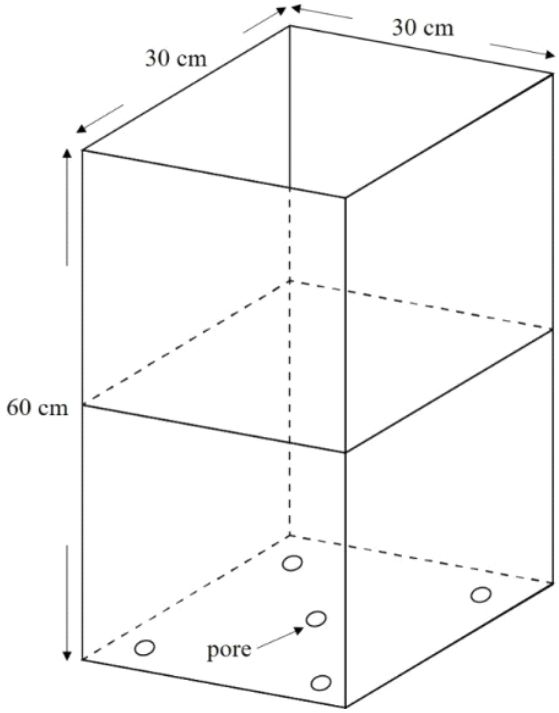

Figure 2. Plant culture box.

Figure 3. Special pulling fixture.

noninoculated *A. confusa* seedlings. The average maximum pullout resistance of the inoculated seedlings was 1.28 ± 0.11 kN, which was significantly higher than that of the noninoculated controls (0.58 ± 0.10 kN) (Table 4). The pullout resistance-displacement curves showed a steep slope up to the maximum force before the roots broke (Figure 7). Regression analysis revealed the linear positive relationship between pullout resistance and tree height (Figure 8), taproot length (Figure 9) and root biomass (Figure 10), that is, the pullout resistance increased with increasing tree height, taproot length and root biomass, with the root biomass showing the strongest relation. Meanwhile, pullout resistance also had a linear positive relationship with stem basal diameter and shoot biomass (Table 5).

DISCUSSION

In this study, the native rhizobial strain associated with *A. confusa* was isolated and identified as *B. elkanii* by 16S rRNA gene similarity analysis. Inoculation test demonstrated that *B. elkanii* effectively induces nodule formation in the roots of *A. confusa*. Many studies classified the rhizobia associated with *Acacia* spp. into three groups, that is, *Rhizobium-Sinorhizobium-Mesorhizobium* (that is, *A. Senegal*, *A. raddina* and *A. cyanophylla*, respectively) (De Lajudie et al., 1994, 1998; Khbaya et al., 1998), *Bradyrhizobium* (that is, *A. albida*, *A. mangium* and *A. auriculiformis*, respectively) (Galiana et al., 1990; Dupuy et al., 1994; Ferro et al., 2000), and two types of rhizobia (that is, *A. Seyal*) (Dreyfus and Dommergues, 1981). Diouf et al. (2015) studied the genetic and genomic diversity of *Acacia* mesorhizobia symbionts in Senegal, and discovered three new species of *Mesorhizobium*. Wang et al. (2008) indicated that rhizobia isolated from *A. mangium* in Fujian and Guangdong, China belongs to *Mesorhizobium*, whereas the strain isolated from *A. confusa* in Guangdong belonged to *Bradyrhizobium*. Huang et al. (2012) isolated a novel strain D5 from China, which is a new type of nitrogen-fixing bacterium from the nodules of *A. confusa*. In this study, the strain isolated from the local *A. confusa* was identified as *B. elkanii*, and we demonstrated in this study for the first time that it can effectively nodulate the roots of *A. confusa* seedlings.

Our functional study demonstrated that inoculation of *A. confusa* seedlings with the indigenous *B. elkanii* significantly enhanced seedling growth as compared to the non-inoculated controls. In the past, several studies have shown that inoculation of *Acacia* with *Bradyrhizobium* spp. significantly enhance growth of *Acacia* seedlings (Galiana et al., 1990, 1994; Dumroese et al., 2009; Pereyra et al., 2015). Martin-Laurent et al. (1999) showed that inoculation with the indigenous Malaysian strains *Bradyrhizobium* spp. significantly enhances seedling survival, growth and leaf chlorophyll content of *A. mangium* in the field. They also suggested

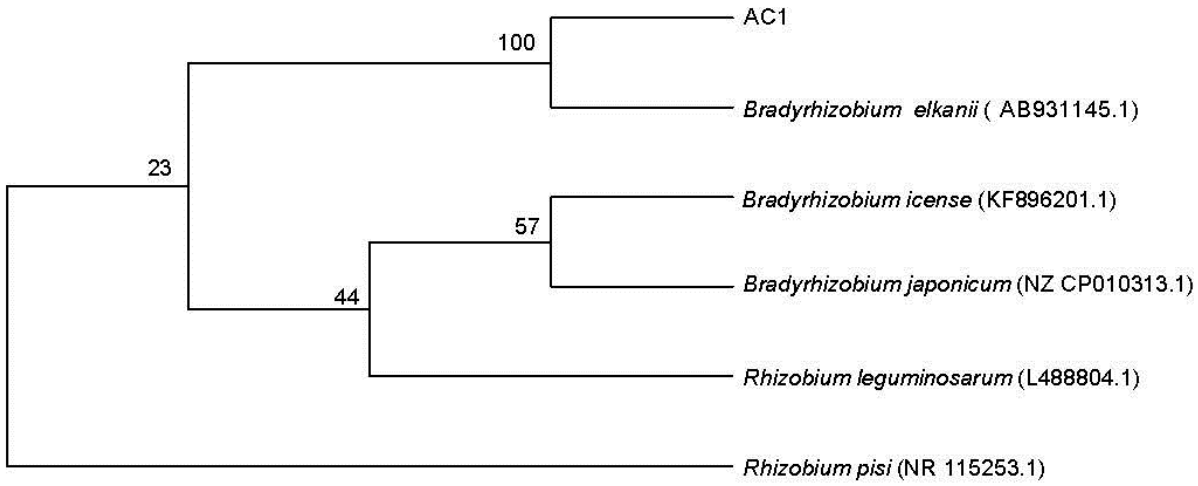

Figure 4. Phylogenetic relationship constructed by maximum-Parsimony (MP) methods based on 16S rRNA sequence of strain AC1. *Rhizobium pisi* was rooted as an out group.

Figure 5. Nodules formed on the roots of *A. confusa* inoculated with *B. elkanii* (bar = 1 cm).

Table 1. Plant morphological parameters of *A. confusa* seedlings inoculated and noninoculated with *B. elkanii* after 8 months of transplanting in the plastic house.

Treatment	Height (cm)	Root-collar diameter (mm)	Tap root length (cm)	Root biomass (g)	Shoot biomass (g)
In	251.7±5.5^{a}	17.9±0.3^{a}	89.0±13.0^{a}	64.0±16.7^{a}	152.3±18.2^{a}
C	179.0±4.0^{b}	16.2±2.4^{a}	44.3±5.1^{b}	28.0±5.5^{b}	64.3±26.1^{b}

In, inoculated; C, noninoculated control. All values are the mean ± standard error of eight replicates. Values in the same column with different superscript letters significantly differ at 5% significant level.

that indigenous *Bradyrhizobium* strains may be more efficient in competition with other strains. Several other studies also revealed the beneficial effects of *Bradyrhizobium* symbiosis on plant growth and biomass (Glick, 1995; Usharani et al., 2014). Consistent with these observations, our results also shows the positive effect of

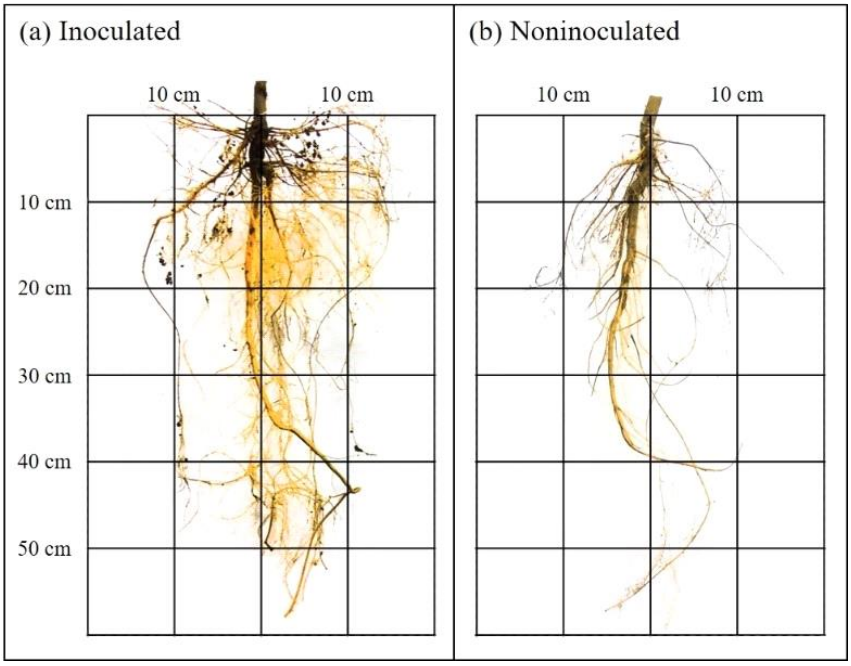

Figure 6. Root system morphologies of *A. confusa* seedlings after 8 months of transplanting in the plastic house. **(a)** Inoculated. **(b)** Noninoculated.

Table 2. Root morphological traits for *A. confusa* seedlings inoculated and noninoculated with *B. elkanii* after 8 months of transplanting in the plastic house.

Treatment	Total root length (cm)	External root surface area (cm^2)	Root volume (cm^3)	Root tip number
In	2687.5±598.2[a]	1345.0±210.2[a]	275.0±75.7[a]	5356.0±764.3 [a]
C	1066.0±196.9[b]	587.5±132.6 [b]	163.3±30.6[b]	3324.2±343.2 [b]

In, inoculated; C, non-inoculated control. All values are the mean ± standard error of eight replicates. Values in the same column with different superscript letters significantly differ at 5% significant level.

Table 3. Root functional traits of *A. confusa* seedlings inoculated and non-inoculated with *B. elkanii* after 8 months of transplanting in the plastic house.

Treatment	RD (kg m^{-3})	RLD (km m^{-3})	RTD (g cm^{-3})	SRL (m g^{-1})	R/S
In	1.19±0.31[a*]	0.29±0.11[a]	0.16±0.07[a]	0.45±0.26[a]	0.41±0.09[a]
C	0.52±0.10[b]	0.18±0.05[b]	0.26±0.21[a]	0.28±0.10[b]	0.43±0.07[a]

RD, Root density; RLD, root length density; RTD, root tissue density; SRL, specific root length; R/S, root to shoot ratio; In, inoculated; C, noninoculated control. All values are the mean ± standard error of 8 replicates. Values in the same column with different superscript letters significantly differ at 5% significant level.

Table 4. Pullout resistances of inoculated and noninoculated *A. confusa* seedlings after 8 months of transplanting in the plastic house.

Treatment	Pullout resistance (kN)
In	1.28 ± 0.11 [a]
C	0.58 ± 0.10 [b]

In, inoculated; C, noninoculated control. All values are the mean ± standard error of 8 replicates. Values in the same column with different superscript letters significantly differ at 5% significant level.

B. elkaniii on growth of *A. confusa* seedlings.

The root system morphologies of the inoculated and non-inoculated *A. confusa* seedlings in this study resembled the VH-type root system, according to previous classification (Yen, 1987; Styczen and Morgan, 1995). The inoculated seedlings developed longer taproot and more profused lateral roots than the noninoculated controls. WinRHIZO analysis revealed that inoculation with *B. elkanii* significantly influence root morphological traits of *A. confusa* seedlings. Inoculation significantly

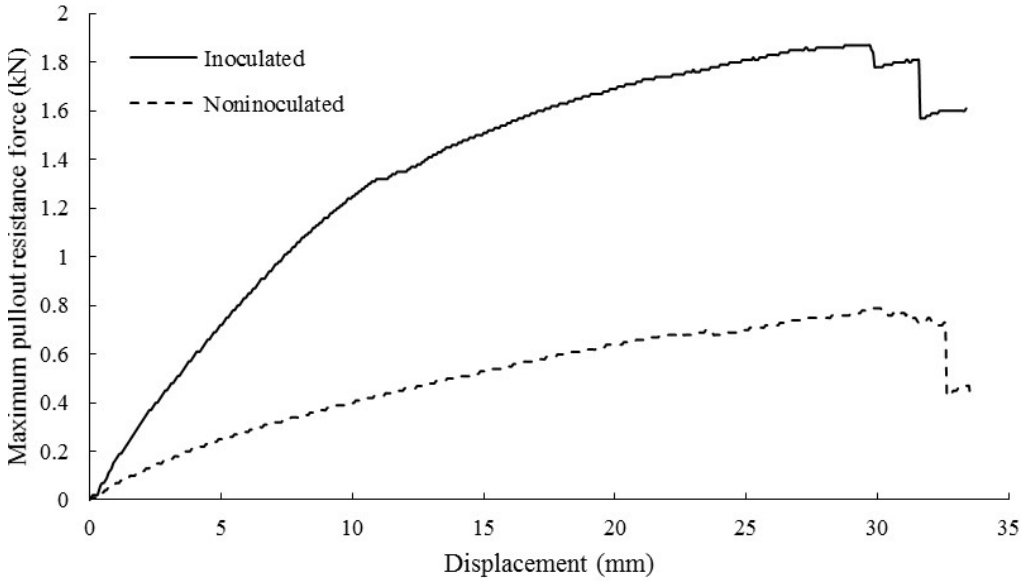

Figure 7. Pullout resistance force-displacement curves for *Acacia confusa* inoculated (**-**) and noninoculated (- -) with *B. elkanii*.

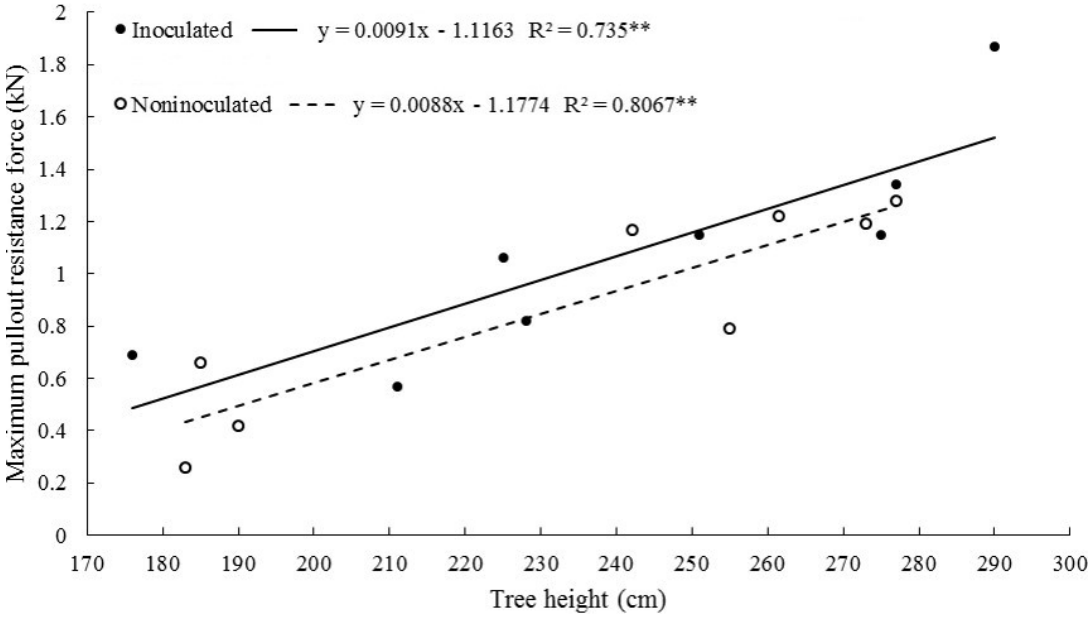

Figure 8. The relationship between the maximum pullout resistance force and tree height in the investigated *A. confusa* inoculated(●—) and noninoculated (○- -) with *Bradyrhizobium elkanii*. N = 8.

enhanced the total root length, external root surface area, root volume, and root tip number, RD, RLD and SRL, as compared to the controls; whereas inoculation had no significant effect on RTD and R/S. Stokes et al. (2009) indicated that seedlings with high RLD and SRL are desirable and useful to landslide restoration.

Our data clearly shows that inoculation with *B. elkanii* significantly increases the maximum pullout resistance of *A. confusa* as compared to the noninoculated controls, suggesting a superior root anchorage capability by the inoculated seedlings. Linear positive relationships were observed between pullout resistance and tree height, taproot length and root biomass, root collar diameter and shoot biomass. This study demonstrates that the inoculated *A. confusa* seedlings have developed longer taproot and more extensive number of lateral roots than

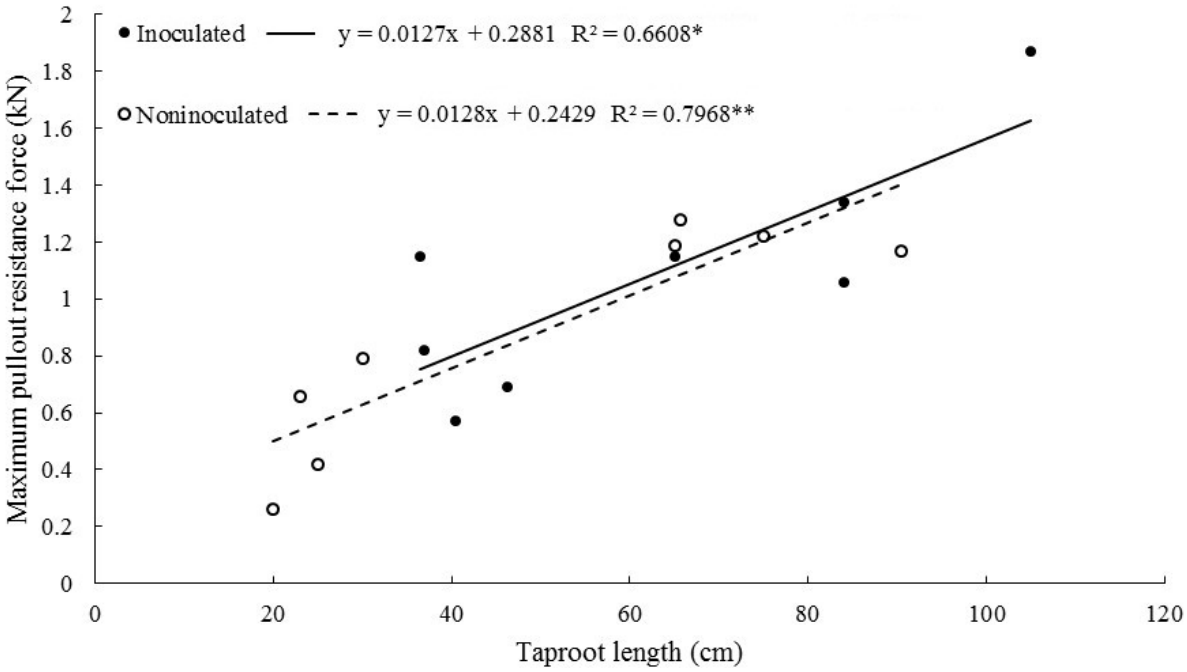

Figure 9. The relationship between the maximum pullout resistance force and taproot length in the investigated *Acacia confusa* seedlings inoculated (●—) and non-inoculated (○- -) with *B. elkanii*. N = 8.

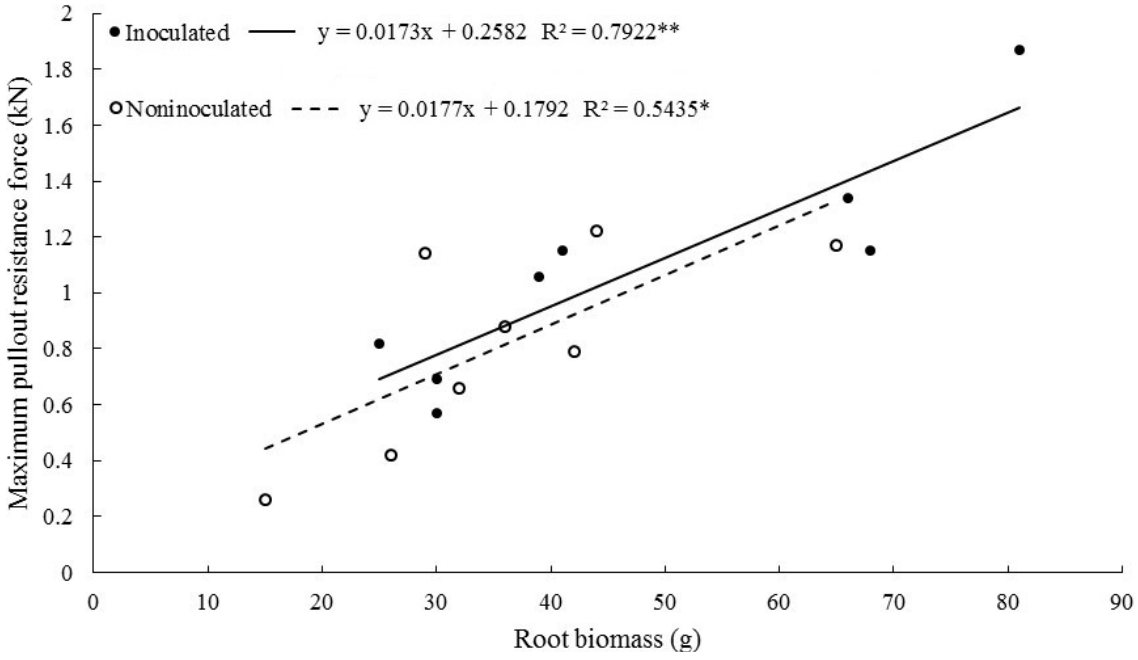

Figure 10. The relationship between the maximum pullout resistance force and root biomass in the *A. confusa* seedlings inoculated (●—) and noninoculated (○- -) with *B. elkanii*. N = 8.

the noninoculated controls. Thus, inoculation with *B. elkanii* significantly increased the numbers of lateral roots, which promote plant anchorage and pullout resistance to vertical uprooting forces. Also, inoculated *A. confusa* seedlings developed VH-type root system, which is the most resistant to uprooting (Dupuy et al., 2005;

Table 5. Relation between morphological traits and pullout resistance of *A. confusa* inoculated and noninoculated with *B. elkanii* after 8 months of transplanting in the plastic house.

Morphological traits	Treatment	Mean±SE	Regression equation	R^2	*p*
H	In	247.0±26.9[a]	y=0.009x-1.116	0.74	0.007
	C	212.5±28.8[b]	y=0.009x-1.177	0.81	0.002
D_r	In	18.53±1.48[a]	y=0.114x-1.350	0.75	0.027
	C	17.92±1.64[a]	y=0.105x-0.735	0.68	0.045
R_b	In	41.4±16.6[a]	y=0.017x+0.258	0.79	0.003
	C	33.8±7.6[a]	y=0.018x+0.179	0.54	0.037
S_b	In	128.8±36.6[a]	y=0.008x+0.255	0.74	0.006
	C	75.4±19.2[b]	y=0.008x+0.261	0.68	0.011
L_{tr}	In	79.1±22.1[a]	y=0.013x+0.288	0.66	0.014
	C	51.7±13.3[b]	y=0.013x+0.243	0.80	0.003

H, Tree height; D_r, root collar diameter; R_b, root biomass; S_b, shoot biomass; L_{tr}, taproot length; In, inoculated; C, noninoculated control; y, pullout resistance. All values are the mean ± standard error of 8 replicates. Values in the same column with different superscript letters significantly differ at 5% significant level.

Yen, 1987). Ennos et al. (1993) indicated that taproot acted like a stake guyed by lateral roots to resist vertical uprooting. Stokes et al. (2009) indicated that increased RLD augments the pullout resistance of seedlings.

Conclusions

In this study, a local rhizobial strain isolated from root nodules of *A. confusa* was identified as *B. elkanii*. Inoculation test revealed that the nitrogen-fixing *B. elkanii* can effectively nodulate the roots of *A. confusa*, and enhance the growth of its seedlings. Root excavation study showed that the root system morphologies of both inoculated and noninoculated *A. confusa* belonged to the VH-type root system, but the inoculated seedlings developed deeper taproot and more lateral roots than the non-inoculated controls. On average, inoculated seedlings had significantly larger total root length, external root surface area, root volume, and root tip number than the non-inoculated ones. Root functional traits such as RD, RLD and SRL of the inoculated seedlings were significantly higher than that of the controls. The average maximum pullout resistance of the inoculated *A. confusa* was more than twice higher than that of the non-inoculated ones. Regression analysis showed the linear positive relationship between pullout resistance and tree height, taproot length, root biomass, root collar diameter and shoot biomass. Taken together, these results clearly demonstrate that the local strain of the nitrogen fixing *B. elkanii* can significantly promote growth, root morphology and pullout resistance of *A. confusa* after eight months of transplanting. These findings are important in the application of *B. elkanii* in *A. confusa* agroforestry and plantation forestry as well as soil conservation engineering. This is the first report to show a positive effect of inoculation with *B. elkanii* on the growth, root development and root anchorage capability of *A. confusa*. Furthermore, future studies on the symbiotic compatibility and nitrogen-fixing ability between *B. elkanii* and other acacia species, that is, *A. auriculiformis*, *A. farnesiana and A. mangium* are needed for tree nursery applications. Also, researches on the influences of abiotic factors, that is, soil pH, fertility, and drought on the symbiotic association are useful in reforestation practices.

CONFLICT OF INTERESTS

The authors have not declared any conflict of interests.

ACKNOWLEDGEMENTS

The authors gratefully acknowlege the financial support from the Ministry of Science and Technology (MOST 104-2313-B415-001), Republic of China. They also wish to thank Professor Maurice S. B. Ku for reviewing the manuscript.

REFERENCES

Avani N, Lateh H, Bibalani GH (2014). Root distribution of *Acacia mangium* Willd. and *Macaranga tanarius* of rainforest. Bangladesh J. Bot. 43(2):141-145.

Böhm W (1979). Methods of Studying Root Systems. Springer-Verlag, Heidelberg.

Bouma TJ, Nielsen KL, Koutstaal K (2000). Sample preparation and scanning protocol for computerized analysis of root length and diameter. Plant Soil 218:185-196.

Burylo M, Rey F, Mathys N, Dutoit T (2012). Plant root traits affecting the resistance of soils to concentrated flow erosion. Earth Surf. Process. Landforms 37:1463-1470.

Burylo M, Rey F, Roumet C, Buisson E, Dutoit T (2009). Linking plant morphological traits to uprooting resistance in eroded marly lands (South Alps, France). Plant Soil 324:31-42.

Ceccon E, Almazo-Rogel A, Martínez-Romero E, Toledo I (2011). The effect of inoculation of an indigenous bacteria on the early growth of *Acacia farnesiana* in a degraded area. Cerne 18(1):49-57.

De Lajudie P, Willems A, Nick G, Moreira F, Molouba F, Hoste B, Torck U, Collins MD, Lindström K, Dreyfus B, Gillis M (1998). Characterization of tropical tree rhizobia and description of *Mesorhizobium plurifarium* sp. nov. Int. J. Syst. Bacteriol. 48:369-382.

De Lajudie P, Willems A, Pot B, Dewettinck D, Maestrojuan G, Neyra M, Collins M, Dreyfus BL, Kersters K, Gillis M (1994). Polyphasic taxonomy of rhizobia: emendation of the genus *Sinorhizobium* and description of *Sinorhizobium meliloti* comb. nov., *Sinorhizobium saheli* sp. nov., and *Sinorhizobium teranga* sp. nov. Int. J. Syst. Bacteriol. 44:715-733.

Diouf F, Diouf D, Klonowska A, Le Quere A, Bakhoum N, Fall D, Neyra M, Parrinello H, Diouf M, Ndoye I, Moulin L (2015). Genetic and genomic diversity studies of *Acacia* symbionts in Senegal reveal new species of *Mesorhizobium* with a putative geographical pattern. PLoS One 10(2):e0117667.

Dreyfus BL, Dommergues YR (1981). Nodulation of *Acacia* species by fast- and slow-growing tropical strains of rhizobium. Appl. Environ. Microbiol. 41:97-99.

Dumroese RK, Jacobs DF, Davis AS (2009). Inoculating *Acacia koa* with *Bradyrhizobium* and applying fertilizer in the nursery: effects on nodule formation and seedling growth. HortScience 44(2):443-446.

Dupuy L, Fourcaud T, Stokes A (2005). A numerical investigation into the influence of soil type and root architecture on tree anchorage. Plant Soil 278:119-134.

Dupuy N, Willems A, Pot B, Dewettinck D, Vandenbruane I, Maestrojuan G, Dreyfus B, Kersters K, Collins DM, Gillis M (1994). Phenotypic and genotypic characterization of bradyrhizobia nodulating the leguminous tree *Acacia albida*. Int. J. Syst. Bacteriol. 44:461-473.

Ennos A (1993). The scaling of root anchorage. J. Theor. Biol. 161:61-75.

Ferro M, Lorquin J, Ba S, Sanon K, Prome J, Boivin C (2000). *Bradyrhizobium* sp. strains that nodulate the leguminous tree *Acacia albida* produce fucosylated and partially sulfated nod factors. Appl. Environ. Microbiol. 66:5078-5082.

Galiana A, Chaumont J, Diem HG, Dommergues YR (1990). Nitrogen-fixing potential of *Acacia mangium* and *Acacia auriculiformis* seedlings inoculated with *Bradyrhizobium* and *Rhizobium* spp. Biol. Fertil. Soils 9:261-267.

Galiana A, Prin Y, Mallet B, Gnahoua GM, Poitel M, Diem HG (1994). Inoculation of *Acacia mangium* with alginate beads containing selected *Bradyrhizobium* strains under field conditions: long-term effect on plant growth and persistence of the introduced strains in soli. Appl. Environ. Microbiol. 60(11):3974-3980.

Glick BR (1995). The enhancement of plant growth by free-living bacteria. Can. J. Microbiol. 41(2):109-117.

Gould IJ, Quinton JN, Weigelt A, de Deyn GB, Bardgett RD (2016). Plant diversity and root traits benefit physical properties key to soil function in grasslands. Ecol. Lett. 19:1140-1149.

Huang B, Lv C, Zhao Y, Huang R (2012). A novel strain D5 isolated from *Acacia confusa*. PLoS One 7(11):e49236.

Huang S, Ladha JK (1997). Studies on the change of root morphology of rice inoculated with Rhizobium. J. Fujian Acad. Agric. Sci. 12(2):49-54.

Huang TC, Ohashi H (1977). Acacia. In: Flora of Taiwan, 2nd Ed., Vol. 3, Editorial Committee of Flora of Taiwan (eds). Editorial Committee of Flora of Taiwan, Taipei, Taiwan. pp. 161-163.

Ikeda J (1999). Differences in numbers of nodules and lateral roots between soybean (*Glycine max* L. Merr.) cultivars, Kitamusume and Toyosuzu. Soil Sci. Plant Nutr. 45(3):591-598.

Khbaya B, Neyra M, Normand P, Zerhari K (1998). Genetic diversity and phylogeny of rhizobia that nodulate *Acacia* spp. in Morocco assessed by analysis of rRNA genes. Appl. Environ. Microbiol. 64:4912-4917.

Lateh H, Avani N, Bibalani GH (2014). Investigation of root distribution and tensile strength of *Acacia mangium* Willd (Fabaceae) in the rainforest. Greener J. Biol. Sci. 4(2):45-52.

Lateh H, Avani N, Bibalani GH (2015) Tensile strength and root distribution of *Acacia mangium* and *Macaranga tanarius* at spatial variation (Case study: East-West highway, Malaysia). Int. J. Biosci. 6(7):18-28.

Martin-Laurent F, Fremont M, Lee SK, Tham FY, Prin Y, Tan TK, Diem HG (1999). Effect of inoculation with selected *Bradyrhizobium* spp. on the survival and growth of *Acacia mangium* saplings after 20 months in the field. J. Trop. For. Sci. 11(2):470-483.

Normaniza O, Mohamad NA, Che HA (2011). Pullout and tensile strength properties of two selected tropical trees. Sains Malays. 40(6):577-585.

Pang W, Crow WT, Luc JE, McSorley, Giblin-Davis RM (2011). Comparison of water displacement and WinRHIZO software for plant root parameter assessment. Plant Dis. 95:1308-1310.

Pereyra G, Hartmann H, Michalzik B, Ziegler W, Trumbore S (2015). Influence of rhizobia inoculation on biomass gain and tissue nitrogen content of *Leucaena leucocephala* seedlings under drought. Forests 6:3686-3703.

Relman D (1993). Universal bacterial 16S rRNA amplification and sequencing. In: Persing DH, Smith TF, Tenover FC, White TJ (eds) Diagnostic Molecular Biology, Principles and Applications. Mayo Foundation Rochester, MN, USA. pp. 489-495.

Souleimanov A, Prithiviraj B, Smith DL (2002). The major nod factor of *Bradyrhizobium japonicum* promotes early growth of soybean and corn. J. Exp. Bot. 53(376):1929-1934.

Stokes A, Atger C, Bengough AG, Fourcaud T, Sidle RC (2009). Desirable plant root traits for protecting natural and engineered slopes against landslides. Plant Soil 324:1-30.

Stokes A, Norris JE, van Beek LPH, Bogaard T, Cammeraat E, Mickovski S B, Jenner A, Di Iorio A, Fourcaud T (2008). How vegetation reinforce soil on slope. In: Norris JE, Stokes A, Mickovski SB, Cammeraat E, van Beek R, Nicoll BC, Achim A (eds) Slope Stability and Erosion Control: Ecological Solution. Springer, Dordrecht, Netherlands. pp. 65-118.

Styczen ME, Morgan RPC (1995). Engineering properties of vegetation. In: Morgan RPC, Rickson RJ (eds) Slope Stabilization and Erosion Control: a Bioengineering Approach. McGraw Hill, New York, USA. pp. 5-58.

Usharani G, Jayanthi M, Kanchana D, Saranraj P (2014). Effects of *Bradyrhizobium* isolates for the maximization of growth and yield of black gram (*Vigna mungo* L.). Int. J. Adv. Multidiscip. Res. 1(4):33-39.

Wang FQ, Zhang YF, Liu J, Liu EM (2008). Comparison of phylogeny analysis methods for rhizobia isolated from *Albizia* spp., *Acacia* spp. and *Leucaena leucocephala*. Acta Microbiol. Sin. 48(1):1-7.

Weisburg WG, Bains SM, Pelletier DA, Lane DJ (1991). 16S ribosomal DNA amplification for phylogenetic study. J. Bacteriol. 173:697-703.

Wilde SA (1958). Forest Soils: Their Protection and Relation to Silviculture. Ronald Press, New York, USA. 537p.

Wu TH, Watson AJ, El-Khouly MA (2004) Soil-root interaction and slope stability. In: Barker DH, Watson AJ, Sombatpanit B, Northcut B, Magliano AR (eds) Ground and Water Bioengineering for Erosion Control and Slope Stabilization. Science Publishers Inc. USA. Pp 183-192.

Yen CP (1987). Tree root patterns and erosion control. In: Jantawat S (ed) Proceedings of the International Workshop on Soil Erosion and Its Countermeasures. Soil Conservation Society of Thailand, Bangkok, Thailand. pp. 92-111.

Zerhari K, Aurag J, Khbaya B, Kharchaf D, Fliali-Maltouf (2000) Phenotypic characteristics of rhizobia isolates nodulating *Acacia* species in the arid and Saharan regions of Morocco. Lett. Appl. Microbiol. 30:351-357.

academicJournals

Vol. 16(18), pp. 1078-1084, 3 May, 2017
DOI: 10.5897/AJB2017.15907
Article Number: B9AC9F464069
ISSN 1684-5315
Copyright © 2017
Author(s) retain the copyright of this article
http://www.academicjournals.org/AJB

African Journal of Biotechnology

Full Length Research Paper

Screening of exopolysaccharide-producing coccal lactic acid bacteria isolated from camel milk and red meat of Algeria

Imène Kersani*, Halima Zadi-Karam and Nour-Eddine Karam

Laboratory of Biology of Microorganisms and Biotechnology, University of Oran1 Ahmed Ben Bella, Oran, Algeria.

Received 21 January, 2017; Accepted 29 March, 2017

The analysis of coccal lactic acid bacteria (CLAB) strains for their competence in polysaccharide production has been given proper attention as texturing and thickening agents. The characterization of these strains has been performed from two natural environments (camel milk and red meat). All the isolates were evaluated for exopolysaccharides (EPS) production on certain solid medium and ruthenium red milk agar plate. Based on their EPS-producing colony phenotype, five strains were chosen giving an important white-color and mucoid aspect on sucrose-based media which being the best for detecting the EPS. Quantitative estimation of EPS indicated that amount of this polymer rendered more than 400 mg/L and the apparent viscosity ranged from 2.1 to 2.9 milli Pascals per second (mPa.s). Therefore, there was not found a close relationship between the amount of EPS and the apparent viscosity. Three strains were selected for their significant production of EPS. For protein assay, a low content of protein was obtained on crude polymer revealing the quality of EPS extracts.

Key words: Coccal lactic acid bacteria (CLAB), exopolysaccharides (EPS), sucrose-based medium, apparent viscosity, amount of EPS.

INTRODUCTION

Lactic acid bacteria (LAB) are generally recognized as safe organisms that have been used since ancient times in fermentations food. Besides, these bacteria are also being exploited for the production of various food-grade biomolecules such as vitamins, conjugated linoleic acid, lactic acid and bacteriocins (Leroy and De Vuyst, 2004). Certain LAB are able to produce exopolysaccharides (EPS) either attached to the cell wall (capsular EPS) or released to the extracellular environment (EPS) (Torino et al., 2015). Term of EPS as proposed by Sutherland (1972) provides a general name for all these forms of bacterial polysaccharides found outside the cell wall. EPS from LAB can be subdivided into two groups: the homopolysaccharides (HoPS) composed of one type of monosaccharide, and the heteropolysaccharides (HePS) composed of a repeating unit that contains two or more different monosaccharides, substituted monosaccharides and other organic and inorganic molecules (De Vuyst et

*Corresponding author. E-mail: kersani_imene@yahoo.fr. Tel: +213 550213535.

Author(s) agree that this article remains permanently open access under the terms of the Creative Commons Attribution License 4.0 International License

al., 2001; Laws and Marshall, 2001; Monsan et al., 2001).

EPS produced by LAB has been clearly demonstrated for both thermophilic (for example *Streptococcus thermophilus*) and mesophilic (for example *Lactococcus lactis*) strains (De Vuyst and Degeest, 1999). This interest is due to their useful role in improvement of physical, rheological and sensory properties of fermented milks (Behare et al., 2009a, b, 2010). Moreover, consumer concern for healthy, natural, and low calorie foods has generated more demand in the market for fat-free or reduced-fat products (Khurana and Kanawjia, 2007). The alternative approach to such commercial additives is the use of EPS-producing LAB that act as natural biothickeners (Ruas-Madiedo and de los Reyes-Gavilan, 2005). In addition, the EPS produced by microorganisms vary in their composition and properties such as anti-bacterial, anti-cancer, anti-tumoral, anti-ulcer, anti-immune stimulation along with cholesterol-lowering ability (Nagaoka et al., 1994; Pigeon et al., 2002; Yoo et al., 2004; Kumar et al., 2007; Raveendran et al., 2013; Li et al., 2014; Raposo et al., 2014). An additional physiological benefit of EPS is that, it will remain for longer time in the gastro-intestinal tract, thus enhancing the colonization of probiotic bacteria (German et al., 1999). The EPS of LAB are in a great variety, which depends on the type of LAB strains, culture conditions, and medium composition (Guzel-Seydim et al., 2005; Ismail and Nampoothiri, 2010), age of the cell, pH and temperature (De Vuyst et al., 2003; Ruas-Madiedo and de los Reyes-Gavilan, 2005).

The objectives of this study consist to isolate and screen EPS producing strains of Coccal LAB (CLAB) obtained from camel's milk and fresh red meat of Algeria, in order to evaluate their capacity to produce these exopolymers and select the most performing strains.

MATERIALS AND METHODS

Sampling and isolation of CLAB strains

CLAB were isolated from camel's milk and red fresh meat of Algeria by serial dilution plating on M17 medium (Terzaghi and Sandine, 1975) and incubated anaerobically for 24 h at 30°C. All strains were subcultured in M17 broth medium (1%) and stored at -20°C in 70% skim milk (enriched with 0.05% yeast extract and 0.05% glucose) containing 30% glycerol (Samelis et al., 1994). The strains were phenotypically identified by adapting of conventional bacteriological characterization techniques.

Detection of EPS

Qualitative analysis

Visual appearance: The simplest way to detect EPS-producing strain is to examine a colony on agar plates. The screening test was carried according to Dave and Shah (1996) and Dupont (1998) with few modifications. The selection process of EPS-producing bacterial strains was fundamentally based on the development of mucoid aspect of strain colonies, according to Ricciardi et al. (1997); Welman et al. (2003) and Ruas-Madiedo and de los Reyes-Gavilan (2005), by studying the production of EPS on several solid media. Use of suitable screening medium increases the probability of EPS-producing phenotypes (Ruas-Madiedo and de los Reyes-Gavilan, 2005; Behar et al., 2009b,c).

For this purpose, we have used M17-agar medium with 50 g of sucrose per liter (M17 hypersaccharosed or M17HS) instead of lactose, M17 (5 g of lactose per liter: LM17) and MSE medium (Mayeux et al., 1962). The strains of CLAB were incubated at 30°C for 24 to 48 h and macroscopic appearance in each medium was compared.

The mucoid colonies have a glistening and slimy appearance on agar plates (Vescovo et al., 1989; Dierksen et al., 1997). It was determined by visual appearance and ropiness was determined by touching them with a sterile inoculation loop (Ricciardi et al., 1997; Welman et al., 2003; Ruas-Madiedo and de los Reyes-Gavilan, 2005). The colonies which have mucoid and ropy phenotype were picked up and purified by following the streaking method, then preserved at 4°C on M17 agar and selected for the next step. The symbols for mucoid polysaccharide production as observed visually were given as less mucoid (+), medium mucoid (++), highly mucoid (+++) or non-mucoid (-).

Ruthenium red staining: Ruthenium red staining method could be used for the detection of EPS producing LAB strains (Dabour and LaPointe, 2005). Pink and white colonial variants of the strain were isolated from the plate surface of a solid semi-synthetic medium containing skim milk, sucrose, yeast extract, and ruthenium red (Gancel et al., 1988). After 48 h of incubation at 30°C, ruthenium red stains the bacterial cell wall, producing pink colonies for non-ropy strains and white colonies for ropy strains.

Quantitative analysis

Apparent viscosity: Production of EPS by LAB leads to a change in texture of the medium, due to change of its viscosity. Viscosity was measured in basal minimal medium hypersaccharosed (BMMHS) (Morishita et al., 1981), at 25°C using a Thermo Scientific Haake^{TM}, and falling ball viscometer with a coaxial cylinder at a steady shear rate of 173/s along with a MK50 rotor assembly. Viscosity is expressed as the dynamic viscosity using the internationally standardized absolute unit of milli Pascals per second (mPa.s). Optical density (OD_{600nm}) of the culture was also assessed to estimate the growth of cell in order to relate to the viscosity.

Quantification of EPS

EPS were isolated from the various culture strains using the ethanol precipitation as described by Cerning et al. (1994).

Extraction and purification of polysaccharide

For each isolate, the EPS was recovered and purified from the BMMHS. Fresh cultures were prepared in M17HS broth, incubated at 30°C for 18 h. These subcultures were propagated in 50 ml BMMHS medium. After incubation, the cultures were heated at 100°C for 15 min, and the cells were removed by centrifugation (9950 *g* for 30 min at 4°C).

A cold ethanol (95%) was gradually added to the supernatant in the amount from one to two and three supernatant volumes and the mixture was centrifuged (9950 *g* for 30 min at 4°C). The supernatant was discarded and the pellet was dissolved in deionized water, dialyzed against sterile water for 24h at 4°C and lyophilized. The crude EPS was purified by 10% trichloroacetic acid

Table 1. Mucoidy character of EPS in different agar media with CLAB strains.

Strain	LM17	M17HS	MSE
L4	-	+++	++
L5	-	+++	++
L6	-	+++	++
V1	-	++	+
V2	-	++	+
V3	-	+++	++
V4	-	++	+
V5	-	+++	++
Other CLAB strains	-	-	-

(TCA) and washed three times, then centrifuged, dialyzed for 5 days at 4°C, lyophilized and dissolved in sterile distilled water.

After the isolation steps, a lyophilized powder is obtained, its weight being the simplest indication of the EPS yield (De Vuyst et al., 1998; van Geel-Schutten et al., 1999; Frengova et al., 2000; Degeest et al., 2001a).

Quantification of total proteins and polysaccharides in EPS was achieved, using assays, such as the Bradford (Bradford, 1976) and the Dubois (Dubois et al., 1956) methods. These experiments were performed in duplicate and repeated three times.

Sugar determination

A spectrophotometric procedure for the determination of sugar and related compounds is the phenol sulfuric acid method described by Dubois et al. (1956) using glucose as the standard (Torino et al., 2001). The quantities of EPS were expressed as the equivalent milligrams of glucose per liter using standard curve of glucose.

Protein determination

The protein content in each dialyzed supernatant fluid was quantified as described by Bradford (1976) using bovine serum albumin (BSA) as a standard. The weight of protein was plotted against the corresponding absorbance with a UV-Vis Optizen POP spectrophotometer (A_{595nm}) resulting in a standard curve used to determine the protein in unknown samples. This weight was expressed in micrograms of protein.

RESULTS AND DISCUSSION

Screening of EPS-producing CLAB strains

In this study, 43 strains of CLAB were used to search their ability to produce EPS and it was found that eight isolates were able to produce EPS, based on the colony morphology. Three strains isolated from camel milk (L4, L5 and L6), five strains isolated from red meat (V1, V2, V3, V4 and V5). They were screened for mucoidy appearance on agar plates. All selected strains formed big slimy and mucoidy colonies on M17HS compared to MSE (Table 1). Thus, ropiness character was detected for some strains when extended with an inoculation loop. However, no mucoidness phenotype was detected on LM17 agar.

The studies noted by Ruas-Madiedo and de los Reyes-Gavilan (2005) indicated that the carbon source added to the screening media plays an important role in the detection of the EPS phenotype in LAB. In fact, incorporation of a carbon source such as sucrose in a M17 agar medium increases the number of EPS-producing and stimulated their formation, but not the growth, suggesting that most of the sugar is employed for EPS biosynthesis and little as an energy source for growth. The opposite was observed with lactose for that mucoidness phenotype could not be detected on LM17.

Consequently, M17HS was the best medium for detecting the mucoid character. These results are in accordance with those obtained by Grosu-Tudor and Zamfir (2011) who screened 31 strains of LAB developing mucoid colonies on MRS with sucrose and less or no mucoid on media with glucose or lactose as a carbon source. On the contrary, Degeest and De Vuyst (2000) and Degeest et al. (2001b) reported that HePS production is enhanced as compared to growth in media with glucose or lactose as the sole carbohydrate sources. Also, Gancel and Novel (1994) reported that the EPS production in a defined medium by *Streptococcus thermophilus* S22 was found to be higher with glucose and fructose and lower with lactose and sucrose, although the latter supported better growth.

Detection of EPS production using ruthenium red

Ruthenium red is a carbohydrate-binding dye used to stain biofilms formed by EPS-producing bacteria (Prouty et al., 2002; Borucki et al., 2003). The EPS production was determined by evaluating the color of the colonies grown in ruthenium red milk (RRM) containing sucrose by spot-seeded.

Our strains readily produced mucoid material (Muc^+) when grown on RRM medium which is used in this investigation as the method of choice because it is ideal both for growth and high EPS production (no interfering polysaccharides). As already observed by Zhang et al.

Figure 1. White colonies formed on RRM agar.

Table 2. Growth and apparent viscosity of mucoid strains.

Strain	OD=600 nm	Apparent viscosity (mPa.s)
L4	0.694	2.9
L5	0.564	2.8
L6	0.851	2.7
V3	0.664	2.1
V5	0.21	2.2

(2001), *S. thermophilus* ST1 produced a maximal amount of EPS, when this strain was grown in skim milk supplemented with sucrose.

All selected mucoid strains showed white colonies with different capacities of production. This indicates that EPS was synthesized and secreted. Figure 1 shows EPS production in RRM agar plate with white colonies of strain L4.

The production of EPS prevents the staining, and hence ropy colonies appear white on the same plates (Stingele et al., 1996). In fact, Mora et al. (2002) found that half of the analyzed strains of *S. thermophilus* were able to grow as white or pink colonies in ruthenium red skim milk indicating their ability to produce EPS.

Five isolates (L4, L5, L6, V3 and V5) were retained and chosen in the second step of screening of EPS production by CLAB, based on their high ability to produce EPS in RRM. Therefore, this result confirmed the biothickening character of our strains.

Viscosity measurement and EPS yield

The visual inspection of bacterial colonies on agar plates is most probably the easiest method, but it is insensitive and indicative. This method is unable to detect LAB strains that produce low amounts of EPS, unless they are very ropy (van den Berg et al., 1993; Smitinont et al., 1999). In this case, quantitative detections (including viscosity) were necessary for screening of EPS produced by our isolates.

Most investigators focused their attention on viscosity measurements, since those were used traditionally as an indication for EPS production in liquid media (Cerning et al., 1986, 1988). BMMHS were chosen for this investigation, in order to facilitate EPS analysis. It contains a carbon source, amino acids, vitamins, and mineral salts.

The measurements of the growth and viscosities are shown in Table 2 which revealed that viscosities are extremely variable and are dependent on the strain tested. For the ropy strains, the apparent viscosity was elevated ranging from 2.1 to 2.9 mPa.s. Whereas the bacterial growth was significantly less than OD_{600nm}=1.0. This data confirmed our previous study of mucoid phenotype that medium supplemented with sucrose induced EPS production. However, it is difficult to make a precise correlation between the ropy/mucoid phenotype and production of exopolysaccharides (Van der Meulen et al., 2007).

Many authors studied the effect of medium composition, temperature, pH and fermentation time on

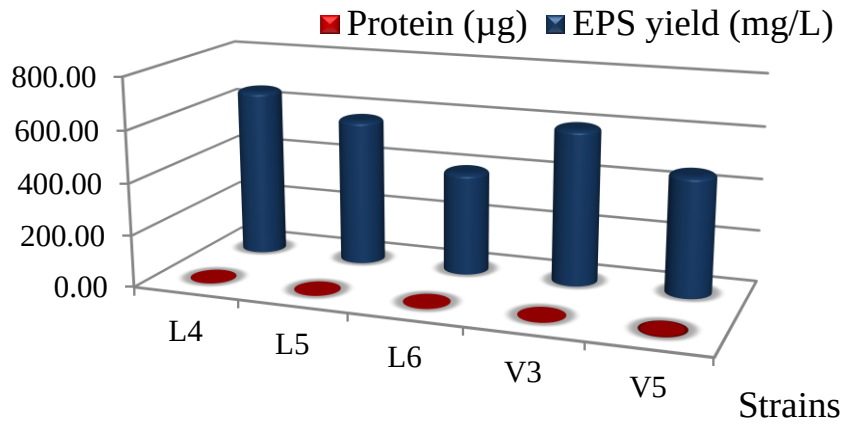

Figure 2. EPS yields and proteins content in fraction of polysaccharide.

the bacterial growth and exopolysaccharide yields (Cerning, 1990; Degeest and De Vuyst, 1999; Degeest et al., 2001a, 2002; Zisu and Shah, 2003; Vaningelgem et al., 2004). Suitable conditions for growth could be not favorable for EPS production and viscosity. For instance, L4 had a high value of viscosity (2.9 mPa.s) while cell growth reached an OD_{600nm} of over 0.69 after 72 h of incubation. These results are clearly explained by the mechanism proposed by Sutherland (1972), who postulated that there is a competition between EPS and cell-wall polymer biosynthesis. If the cells are growing slowly, wall polymer synthesis will also be slow, thereby making more isoprenoid phosphate available for exopolymer synthesis. The total yield of EPS produced by CLAB strains was monitored quantitatively by using the phenol-sulfuric acid method. Figure 2 shows the amounts of sugar and protein in EPS fraction. There was a great variation in content of EPS (mg/L) which ranged from 400.33 to 658.06 mg/L. The amounts of EPS produced by the dairy strains vary considerably (Ludbrook et al., 1997; Badel et al., 2011). In general, EPS yield among majority of *S. thermophilus* strains varies from 20 to 600 mg/L in milk-based medium under optimal conditions (De Vuyst et al., 2003; Vaningelgem et al., 2004).

Natural biothickeners with their structural diversity and functional versatility have gained commercial importance in the field of glycotechnology (Lule et al., 2016). In effect, Han et al. (2016) suggested that strains producing higher EPS might contribute to the higher viscosity of fermented milk. High-yielding of EPS was obtained by L4 (658.06 mg/L) with the highest apparent viscosity (2.9 mPa.s; Table 2). However, our results revealed no straightforward relationship between EPS concentration of most strains and the positive effect of these polymers on the rheological properties. These results are in concordance with previous studies (Cerning et al., 1986; van Marle and Zoon, 1995; Petry et al., 2003; Iwański et al., 2012).

L5 and L6 strains gave almost same viscosity (≥ 2.7 mPa.s) but the amounts of EPS were variable, 572.03 and 400.33 mg/L respectively. It appeared that EPS production depend to their structure, composition, chain stiffness, branches and side groups in the polysaccharide chain (Ruas-Madiedo et al., 2002), the average molecular mass distribution (van den Berg et al., 1995), organism used for production (Cerning, 1995) and conditions of experimentation (Badel et al., 2011). Hence, three strains (L4, L5 and V3) of CLAB were screened for their great potential of EPS production in liquid medium.

The protein content in the EPS sample was determined to give an estimate of purity. The protein was accounted for lower than 1.21 µg for samples from all studied strains (Figure 2). Our results indicate that the purification of polysaccharide with TCA was successfully performed and removed most of the initial protein content. Although according to Kimmel et al. (1998) it seems likely that the protein was carried over from medium ingredients during recovery and is not tightly bound to EPS. Consequently, the protein was not considered to interfere in the phenol-sulphuric acid method (Gentès et al., 2011).

Conclusion

This study was undertaken to screen CLAB isolated from camel milk and red meat of Algeria for their ability to produce EPS in several mediums was carried out. Eight strains conferred a highly mucoid colony on M17HS and thirty-five were not able to produce these biopolymers. Ruthenium red staining reveals the same findings. No clear-cut relationship between the slimy phenotype, the medium viscosity occurs and amount of EPS produced by a ropy strain when different strains were compared. Three strains yielded an important amount of polysaccharide. For protein contents of crude EPS, a small weight of protein contaminating these polymers was noted.

CONFLICT OF INTERESTS

The authors have not declared any conflict of interests.

ABBREVIATIONS

CLAB, Coccal lactic acid bacteria; **EPS,** exopolysaccharides; **HePS,** heteropolysaccharides; **HoPS,** homopolysaccharides; **LAB,** lactic acid bacteria; **M17HS,** M17 hypersaccharosed; **LM17**, M17 lactose; **RRM,** ruthenium red milk; **TCA,** trichloroacetic acid.

REFERENCES

Badel S, Bernardi T, Michaud P (2011). New perspectives for Lactobacilli exopolysaccharides. Biotechnol. Adv. 29:54-66.

Behare PV, Singh R, Kumar M, Prajapati JB, Singh RP (2009a). Exopolysaccharides of lactic acid bacteria. J. Food. Sci. Technol. 46:1-11.

Behare PV, Singh R, Nagpal R, Kumar M, Tomar SK, Prajapati JB (2009c). Comparative effect of exopolysaccharides produced *in situ* or added as bioingredients on dahi properties. Milchwissenschaft. 64:396-400.

Behare PV, Singh R, Singh RP (2009b). Exopolysaccharide-producing mestophilic lactic cultures for preparation of fat-free dahi-An Indian fermented milk. J. Dairy. Res. 76:90-97.

Behare PV, Singh R, Tomar SK, Nagpal R, Kumar M, Mohania D (2010). Effect of exopolysaccharide-producing strains of *Streptococcus thermophilus* on technological attributes of fat-free lassi. J. Dairy Sci. 93:2874-2879.

Borucki MK, Peppin JD, White D, Loge F, Call DR (2003). Variation in biofilm formation among strains of *Listeria monocytogenes*. Appl. Environ. Microbiol. 69:7336-7342.

Bradford MM (1976). A rapid and sensitive method for the quantitation of microgram quantities of protein utilizing the principle of protein dye binding. Anal. Biochem. 72:248-254.

Cerning J (1990). Exocellular polysaccharide produced by lactic acid bacteria. FEMS. Microbiol. Rev. 87:113-130.

Cerning J (1995). Production of exopolysaccharides by lactic acid bacteria and dairy propionibacteria. Dairy Sci. Technol. 75:463-472.

Cerning J, Bouillanne C, Desmazeaud MJ, Landon M (1986). Isolation and characterization of exocellular polysaccharide produced by *Lactobacillus bulgaricus*. Biotechnol. Lett. 8:625-628.

Cerning J, Bouillanne C, Desmazeaud MJ, Landon M (1988). Exocellular polysaccharide production by *Streptococcus thermophilus*. Biotechnol. Lett. 10:255-260.

Cerning J, Renard CMGC, Thibault JF, Bouillanne C, Landon M, Desmazeaud M, Topisirovic L (1994). Carbon source requirements for exopolysaccharide production by *Lactobacillus casei* CG11 and partial structure analysis of the polymer. Appl. Environ. Microbiol. 60:3914-3919.

Dabour N, LaPointe G (2005). Identification and molecular characterization of the chromosomal exopolysaccharide biosynthesis gene cluster from *Lactococcus lactis* subsp. *cremoris* SMQ-461. Appl. Environ. Microbiol. 71(11):7414-7425.

Dave RI, Shah NP (1996). Evaluation of media for selective enumeration of *Streptococcus thermophilus*, *Lactobacillus delbrueckii* ssp. *bulgaricus*, *Lactobacillus acidophilus* and Bifidobacteria. J. Dairy Sci. 79:1529-1536.

De Vuyst L, De Vin F, Vaningelgem F, Degeest B (2001). Recent developments in the biosynthesis and applications of heteropolysaccharides from lactic acid bacteria. Int. Dairy J. 11:687-707.

De Vuyst L, Degeest B (1999). Heteropolysaccharides from lactic acid bacteria. FEMS. Microbiol.Rev.23:157-177.

De Vuyst L, Vanderverken F, Van de Van S, Degeest B (1998). Production by and isolation of exopolysaccharides from *Streptococcus thermophilus* grown in a milk medium and evidence for their growth-associated biosynthesis. J. Appl. Microbiol. 84:1059-1068.

De Vuyst L, Zamfir M, Mozzi F, Adriany T, Marshall V, Degeest B, Vaningelgem F (2003). Exopolysaccharide-producing *Streptococcus thermophilus* strains as functional starter cultures in the production of fermented milks. Int. Dairy. J.13:707-717.

Degeest B, De Vuyst L (1999). Indication that the nitrogen source influences both amount and size of exopolysaccharides produced by *Streptococcus thermophilus* LY03 and modelling of the bacterial growth and exopolysaccharide production in a complex medium. Appl. Environ. Microbiol. 65:2863-28707.

Degeest B, De Vuyst L (2000). Correlation of activities of the enzymes α-phosphoglucomutase, UDP-galactose 4-epimerase, and UDP-glucose pyrophosphorylase with exopolysaccharide biosynthesis by *Streptococcus thermophilus* LY03. Appl. Environ. Microbiol. 66:3519-3527.

Degeest B, Janssens B, De Vuyst L (2001a). Exopolysaccharide (EPS) biosynthesis by *Lactobacillus sakei* 0-1: production kinetics, enzyme activities and EPS yields. J. Appl. Microbiol. 67:470-477.

Degeest B, Mozzi F, De Vuyst L (2002). Effect of medium composition and temperature and pH changes on exopolysaccharide yields and stability during *Streptococcus thermophilus* LY03 fermentations. Int. J. Food. Microbiol. 79:161-174.

Degeest B, Vaningelgem F, Laws AP, De Vuyst L (2001b). UDP-N-acetylglucosamine 4-epimerase activity indicates the presence of N-acetylgalactosamine in exopolysaccharides of *Streptococcus thermophilus* strains. Appl. Environ. Microbiol. 67:3976-3984.

Dierksen KP, Sandine WE, Tremp JE (1997). Expression of ropy and mucoid phenotypes in *Lactococcus lactis*. J. Dairy Sci. 80:1528-1536.

Dubois M, Gilles KA, Hamilton JK, Rebers PA, Smith F (1956). Colorimetric method for determination of sugars and related substances. Anal. Chem. 28:350-356.

Dupont I (1998). Identification moléculaire de souches de lactobacilles productrices d'exopolysaccharides et comparaison de la production d'exopolysaccharides par trois de ces souches (deux *Lactobacillus rhamnosus* et un *Lactobacillus casei*). Thèse de doctorat, Université Laval.

Frengova GI, Simova ED, Beshkova DM, Simov ZI (2000). Production and monomer composition of exopolysaccharides by yogurt starter cultures. Can. J. Microbiol. 46:1123-1127.

Gancel F, Novel G (1994). Exopolysaccharide production by *Streptococcus salivarius* ssp. *thermophilus* cultures 1: Conditions of production. J. Dairy Sci.77:685-688.

Gancel F, Novel G, Ramos P, Carcano D, Loones A, Ramos P(1988). Selection procedure for bacterial exopolysaccharide-producing clones. (In French) Fr. Pat. 88, 08009.

Gentès MC, St-Gelais D, Turgeon S (2011). Gel formation and rheological properties of fermented milk with *in situ* exopolysaccharide production by lactic acid bacteria. Dairy Sci. Technol. 91(5):645-661.

German B, Schiffrin E, Reniero R, Mollet B, Pfeifer A, Neeser JR (1999). The development of functional foods: Lessons from the gut. Trends Biotechnol. 7:492-499.

Grosu-Tudor S, Zamfir M (2011). Isolation and characterization of lactic acid bacteria from Romanian fermented vegetable. Rom. Biotechnol. Lett. 16(6):148-154.

Guzel-Seydim ZB, Sezgin E, Seydin AC (2005). Influences of exopolysaccharide producing cultures on the quality of plain set type yogurt. Food Control 16:205-209.

Han X, Yang Z, Jing X, Yu P, Zhang Y, Yi H, Zhang L (2016). Improvement of the texture of yogurt by use of exopolysaccharide producing lactic acid Bacteria. Biomed. Res. Int. 7945675:2314-6133.

Ismail B, Nampoothiri KM (2010). Production, purification and structural characterization of an exopolysaccharide produced by a probiotic *Lactobacillus plantarum* MTCC 9510. Arch. Microbiol.192:1049-1057.

Iwański RZ, Wianecki M, Dmytrów I, Krzysztof K (2012). Effect of fermentation reactions on rheological properties of foods: Fermentation, effects on food properties. Boca Raton, Florida, USA: CRC Press, Taylor and Francis Group. pp. 90-109.

Khurana H, Kanawjia SK (2007). Recent trends in development of

fermented milks. Curr. Nutr. Food Sci. 3:91-108.
Kimmel SA, Roberts RF, Ziegler GR (1998).Optimization of exopolysaccharide production by *Lactobacillus delbrueckii* subsp. *bulgaricus* RR grown in a semidefined medium. Appl. Environ. Microbiol. 64:659-664.
Kumar AS, Mody K, Jha B (2007). Bacterial exopolysaccharides: A perception. J. Basic Microbiol. 47:103-117.
Laws AP, Marshall VM (2001). The relevance of exopolysaccharides to the rheological properties in milk fermented with ropy strains of lactic acid bacteria. Int. Dairy J. 11:709-721.
Leroy F, De Vuyst L (2004). Lactic acid bacteria as functional starter cultures for the food fermentation industry. Trends Food. Sci. Technol. 15:67-78.
Li S, Huang R, Shah NP, Tao X, Xiong Y, Wei H (2014). Antioxidant and antibacterial activities of exopolysaccharides from *Bifidobacterium bifidum* WBIN03 and *Lactobacillus plantarum* R315. J. Dairy Sci. 97(12):7334-7343.
Ludbrook KA, Russell CM, Greig RI (1997). Exopolysaccharide production from lactic acid bacteria isolated from fermented foods. J. Food Sci. 62:597-600.
Lule VK, Singh R, Pophaly SD, Tomar SK (20 16). Production and structural characterisation of dextran from an indigenous strain of *Leuconostoc mesenteroides* BA08 in Whey. Int. J. Dairy Technol. 69:520-531.
Mayeux JV, Sandine WE, Elliker PR (1962).A selective medium for detecting *Leuconostoc* in mixed-strain starter cultures. J. Dairy Sci. 45:655-656.
Monsan P, Bozonnet S, Albenne C, Joucla G, Willemot RM, Remaud-Siméon M (2001). Homopolysaccharides from lactic acid bacteria. Int. Dairy J. 11:675-685.
Mora D, Fortina MG, Parini C, Ricci G, Gatti M, Giraffa G, Manachini PL (2002). Genetic diversity and technological properties of *Streptococcus thermophilus* strains isolated from dairy products. J. Appl. Microbiol. 93:278-287.
Morishita T, Deguchi Y, Yajima M, Sakurai T, Yura T (1981). Multiple nutritional requirements of lactobacilli: Genetic lesions affecting amino acid biosynthesis pathways. J. Bacteriol. 48(1):64-71.
Nagaoka M, Hashimoto S, Watanabe T, Yokokura T, Mori Y(1994). Anti-ulcer effects of lactic acid bacteria and their cell-wall polysaccharides. Biol. Pharm. Bull. 17:1012-1017.
Petry S, Furlana S, Waghornec E, Saulnierd L, Cerning J, Maguin E (2003). Comparison of the thickening properties of four *Lactobacillus delbrueckii* subsp. *bulgaricus* strains and physicochemical characterization of their exopolysaccharides. FEMS Microbiol. Lett. 221:285-291.
Pigeon RM, Cuesta EP, Gilliland SE (2002). Binding of free bile acids by cells of yogurt starter culture bacteria. J. Dairy Sci. 85:2705-2710.
Prouty AM, Schwesinger WH, Gunn J S (2002). Biofilm formation and interaction with the surfaces of gallstones by *Salmonella* spp. Infect. Immun. 70:2640-2649.
Raposo DJ, Filomena M, Morais AMMB, Morais RMSC (2014). Influence of sulphate on the composition and antibacterial and antiviral properties of the exopolysaccharide from *Porphyridium cruentum*. Life Sci. 101:56-63.
Raveendran S, Poulose AC, Yoshida Y, Maekawa T, Kumar DS (2013). Bacterial exopolysaccharide based nanoparticles for sustained drug delivery, cancer chemotherapy and bioimaging. Carbohydr. Polym. 91:22-32.
Ricciardi A, Parente E, Clementi F (1997). Exopolysaccharide production in a whey based medium by *Streptococcus thermophilus* and *Lactobacillus delbrueckii* subsp. *bulgaricus* in pure culture and in association. An. Microbiol. Enzym. 47:213-222.
Ruas-Madiedo P, de los Reyes-Gavilan CG (2005). Invited Review: Methods for the screening, isolation, and characterization of exopolysaccharides produced by lactic acid bacteria. J. Dairy Sci. 88(3):843-856.
Ruas-Madiedo P, Tuinier R, Kanning M, Zoon P (2002). Role of exopolysaccharides produced by *Lactococcus lactis* subsp. *cremoris* on the viscosity of fermented milks. Int. Dairy J. 12:689-695.
Samelis J, Maurogenakis F, Metaxopoulos J (1994). Characterization of lactic acid bacteria isolated from naturally fermented Greek dry salami. Int. J. Food Microbiol. 23:179-196.
Smitinont T, Tansakul C, Tanasupawat S, Keeratipibul S, Navarini L, Bosco M, Cescutti P (1999). Exopolysaccharide producing lactic acid bacteria strains from traditional Thai fermented foods: Isolation, identification and exopolysaccharides characterization. Int. J. Food Microbiol. 51:105-111.
Stingele F, Neeser JR ,Mollet B (1996). Identification and characterization of the *eps* (Exopolysaccharide) gene cluster from *Streptococcus thermophilus* Sfi6. J. Bacteriol. 178:1680-1690.
Sutherland IW (1972). Bacterial exopolysaccharides. Adv. Microbiol. Physiol. 8:143-212.
Terzaghi BE, Sandine WE (1975). Improved medium for lactic steptococci and their bacteriophages. Appl. Environ. Microbiol. 29:807-813.
Torino MI, Font de Valdez G, Mozzi F (2015). Biopolymers from lactic acid bacteria: Novel applications in foods and beverages. Front. Microbiol. 6:834.
Torino MI, Taranto MP, Sesma F, Font de Valdez G (2001). Heterofermentative pattern and exopolysaccharide production by *Lactobacillus helveticus* 15807 in response to environmental pH. J. Appl. Microbiol. 91:846-852.
van den Berg DJC, Robijn GW, Janssen AC, Giuseppin MLF, Vreeker R, Kamering JD, Vliegenthart JFG, Ledeboer AM, Verrips CT (1995). Production of a novel extracellular polysaccharide by *Lactobacillus sake* 0-1 and characterization of the polysaccharide. Appl. Environ. Microbiol. 61:2840-2844.
van den Berg DJC, Smits A, Pot B, Ledeboer AM, Kersters K, Verbakel JMA, Verrips CT (1993). Isolation, screening and identification of lactic acid bacteria from traditional food fermentation processes and culture collections. Food Biotechnol. 7:189-205.
Van der Meulen R, Grosu-Tudor SS, Mozzi F, Vaningelgem F, Zamfir M, De Valdez GF, De Vuyst L (2007). Screening of lactic acid bacteria isolates from dairy and cereal products for exopolysaccharide production and genes involved. Int. J. Food Microbiol. 118:250-258.
Van Geel-Schutten GH, Faber EJ, Smit E, Bonting K, Smith MR, Ten Brink B, Kamerling JP, Vliegenthart JFG, Dijkhuizen L (1999). Biochemical and structural characterization of the glucan and fructan exopolysaccharides synthesized by *Lactobacillus reuteri* wild-type strain and by mutant strains. Appl. Environ. Microbiol. 65:3008-3014.
Van Marle ME, Zoon P (1995). Permeability and rheological properties of microbially and chemically acidified skim-milk gels. Neth. Milk Dairy J. 49:47-65.
Vaningelgem F, Zamfir M, Mozzi F, Adriany T, Vancanneyt M, Swings J, De Vuyst L (2004). Biodiversity of exopolysaccharides produced by *Streptococcus thermophilus* strains is reflected in their production and their molecular and functional characteristics. Appl. Environ. Microbiol. 70:900-912.
Vescovo M, Scolari GL, Bottazzi V (1989). Plasmid-encoded ropiness production in *Lactobacillus casei* spp. *casei*. Biotechnol. Lett. 10:709-712.
Welman AD, Maddox IS, Archer RH (2003). Screening and selection of exopolysaccharides-producting strains of *Lactobacillus delbrueckii* subsp. *bulgaricus*. J. Appl. Microbiol. 95:1200-1206.
Yoo SH, Yoon EJ, Cha E, Lee HG (2004). Antitumor activity of levan polysaccharides from selected microorganisms. Int. J. Biol. Macromol. 34:37-41.
Zhang T, Zhang C, Li S, Zhang Y, Yang Z (2001). Growth and exopolysaccharide production by *Streptococcus thermophilus* ST1 in skim milk. Braz. J. Microbiol. 42(4):1470-1478.
Zisu B, Shah NP (2003). Effects of pH, temperature, supplementation with whey protein concentrate, and adjunct cultures on the production of exopolysaccharides by *Streptococcus thermophilus* 1275. J. Dairy Sci. 86:3405-3415.

academicJournals

Vol. 16(18), pp. 1085-1091, 3 May, 2017
DOI: 10.5897/AJB2016.15841
Article Number: A4BB53964073
ISSN 1684-5315
Copyright © 2017
Author(s) retain the copyright of this article
http://www.academicjournals.org/AJB

African Journal of Biotechnology

Full Length Research Paper

Proximate composition, microbiological safety and heavy metal contaminations of garri sold in Benue, North-Central Nigeria

Innocent Okonkwo Ogbonna*, Blessing Ifeoma Agbowu and Felix Agbo

Microbiology Unit, Department of Biological Sciences, University of Agriculture, Makurdi, Nigeria.

Received 17 December, 2016; Accepted 28 February, 2017

This study investigated the proximate composition, microbial safety and heavy metal contaminations of garri: a cassava ready-to-eat food product. Garri is prepared from *Manihot esculenta* Crantz tubers by peeling, washing and grating of the tubers and fermentation. Production, storage and selling locations could be necessary predictors of the quality and safety of garri. A total of two hundred and sixteen (n=216) samples of garri were purchased at two-weeks intervals starting from September 2014; from two major garri markets in Benue State, North-central Nigeria. The heavy metals assessed were Cu, Pb, Cd, Ni, Cr and Hg using atomic absorption spectrophotometer (AAS). The moisture, ash contents and titratable acidity were studied alongside some bacterial pathogens that appear frequently in food-borne diseases outbreaks. The moisture, ash contents and titratable acidity were within the permissible limits. The bacteria isolated included *Escherichia coli*, *Staphylococcus aureus*, *Salmonella* and *Shigella* spp. whereas the fungi isolated included *Mucor*, *Aspergillus* and *Fusarium*. The mean total coliform count (TCC), yeast and mould count (YMC) and total viable count (TVC) ranged from minimum values of not detectable (ND) to 1.75, 2.11 and 2.60 log CFU/g, respectively. While cadmium and chromium were not detected in any of the garri samples, lead, nickel, and copper were the most abundant. The values obtained from microbiological assessments indicate potential food safety problems. Heavy metal and the measured physicochemical attributes and the ash content were within the permissible limits.

Key words: Food safety, garri, microorganisms, toxic heavy metals.

INTRODUCTION

Garri is prepared from *Manihot esculenta* Crantz tubers by peeling, washing and grating of the tubers and fermentation. This is followed by pressing, fragmentation, granulation, drying, sifting and suitable heat treatment (frying) (CODEX STAN 151 - 1989). Sometimes, red palm oil is added to improve the quality. Samuel and Ugwuanyi (2014) described garri as a cream coloured, white or yellow starchy food from cassava root. It is a flour of variable granule size. Virtually, all indigenous people eat garri. Millions of people in tropical countries

*Corresponding author. E-mail: innocentia09@yahoo.com. Tel: +2348055706372.

Author(s) agree that this article remains permanently open access under the terms of the Creative Commons Attribution License 4.0 International License

worldwide consume it (Edem et al., 2001; Kostinek et al., 2005; Ogiebor et al., 2007; Samuel and Ugwuanyi, 2014). Urban dwellers consume more garri than their rural counterparts (Jekayinfa and Olajide, 2007) probably because of its ease of preparation, storage efficiency or since it could be put into many uses.

Garri consumption cuts across all socio-economic classes. This product is consumed without cooking, soaked in water with sugar or common salt, smoked fish, roasted groundnuts, cooked beans porridge, palm kernel and groundnut cake (kwuli-kwuli). Sometimes, beverages and milk are value additions to the garri for the improvement of flavour, aroma and the nutrient contents during consumption. Sometimes, garri is cooked and eaten as 'foo foo'. Foo foo is a mixture of hot water and garri granules which has been turned into a stiff paste or gelatinized paste (Asegbeloyin and Onyimonyi, 2007) which is eaten with soup or stew.

Consumption of improperly handled, garri could lead to ill health. Some unhygienic practices are associated with the processing of cassava to garri and post-processing operations of garri. Post-processing handling operations include spreading on the floor and mats after frying, display in open containers like basins in the markets during sales. Producers and sellers of garri use none sterilized packaging materials to transport garri from the villages where they were processed to the towns or market. This could be a viable means of carrying infectious agents in the product (Ogiehor and Ikenebomeh, 2005; Ogugbue and Obi, 2011; Ogugbue et al., 2011; Aguoru et al., 2014).

Microorganisms especially moulds have been associated with processed ready-to-eat gari (Aguoru et al., 2014). Processed garri which had been stored for some time before consumption have various fungal species including *Aspergillus*, *Cladosporium, Fusarium*, *Mucor*, *Penicillium* and *Rhizopus* (Ekundayo, 1984; Ogugbue et al., 2011; Aguoru et al., 2014). Some of these organisms are not friendly to human as they produce potent toxins (mycotoxin) leading to some detrimental health effects. Some mycotoxins cause neurological impairment while some have cytocidal effects. When pathogens are in ready-to-eat foods, humans get them through consumption.

The presence of some heavy metals in the body at certain levels has inimical effects and therefore, calls for concern if allowed to accumulate. Thus, in food, heavy metal contents have strict limits. Some of the most toxic heavy metals are arsenic, cadmium, lead, chromium and nickel. Cadmium, chromium and nickel are carcinogenic. Arsenic and cadmium are teratogenic. Lead causes neurological impairment and central nervous system (CNS) damage by its ability to mimic and inhibit the actions of calcium in its neurotransmission function (Markus and McBratney, 2001; Nadal et al., 2004). Some heavy metals such as cobalt, copper, iron, manganese and zinc are essential micro-elements for living things; however, they are toxic at high concentrations (Nadal et al., 2004; Ani, 2006; Ochieng et al., 2007).

This work investigated proximate compositions, microbial quality and heavy metal contents of garri with a view of establishing its safety for human consumption.

MATERIALS AND METHODS

Samples of garri were bought at two weeks intervals starting from September 2014; from two major garri markets in Benue State, North-central Nigeria (Edumoga Olangbechur along Enugu-Makurdi expressway and Adoka). A total of two hundred and sixteen (n=216) samples representing triplicates of thirty-six yellow and thirty-six white garri were purchased. In every sampling time, six samples each of white and yellow gari were purchased randomly. Thereafter, the purchased garri samples were carried in sterile polyethylene bags to the Research Laboratory, Department of Microbiology of the University where they were analysed. Peeled cassava root tubers used in the preparation of garri were also purchased for analysis. Benue State of Nigeria lies within the area bounded by latitude 6°30' and 8°15'N and longitudes 6°30' and 9°40'E.

Microbiological analyses

Media used for the isolation and identification of the microorganisms were as reported below. Media were sterilized according to the manufacturers' recommendations. Ten grams (10 g) of garri was weighed into a conical flask (250 ml), 90 ml of sterile saline was added, and homogenized by vortex mixing for 5 min. The solubilized garri was, thereafter, diluted further to 10^{-6} and 0.1 ml aliquot of the dilutions spread-plated on agar plates. Colonies that resulted from each plate was counted using Latch colony counter (Latch New Delhi, India) and counts were expressed as log CFU/g. For total viable count (TVC), sterile nutrient agar (Biotechnology Lab. Ipswich, UK) was inoculated and incubated at 37°C for 24 h. Potato dextrose agar -PDA- (Laboratory M Limited, Bury Lancashire BL9 6As, UK) plates were used for yeasts and mould counts. A PDA medium containing chloramphenicol was sterilized by autoclaving at 121°C for 15 min and inoculated as above. Incubation was done at 28°C for 5 days. *E. coli* was isolated and enumerated on Eosin Methylene Blue Agar -EMBA- (Himedia Lab Pot Limited, India) incubated at 37°C overnight, and indole test was conducted on colonies that showed green metallic sheen for test of *E. coli. S. aureus* was isolated on Bair-Parker medium (Laboratory M Limited, Bury Lancashire BL9 6As, UK) as recommended by Macfaddin (1977). *Salmonella* and *Shigella* spp. were isolated and enumerated on deoxycholate citrate agar (DCA) (Park Scientific Ltd, Moultan, Northampton) with tetrathionate and selenite cystine pre-enrichment broths (Macfaddin, 1977).

Bacterial isolates identification using biochemical reaction

Indole test, methyl red test, Voges-Proskauer and citrate utilization (IMVIC) were some of the biochemical tests used in the identification of all the bacterial isolates from the garri. The procedure for the tests was as indicated in Cheesbrough (2006). Additionally, other tests used to identify the isolates included triple sugar iron (TSI) (for *Salmonella* and *Shigella* spp. differentiation), urease test, oxidase, coagulase and catalase (for *S. aureus* differentiation) (Cheesbrough, 2006). Indole test was conducted on colonies that showed green metallic sheen on EMBA. A positive

indole test confirmed *E. coli*.

Identification of the fungal isolates

The procedure of Alexopoulus et al. (1996) was used for the identification of the fungal isolates using morphological and colonial characteristics. All the moulds in the plates were purified by successive sub culturing on sterile PDA medium containing chloramphenicol and were subsequently identified. All morphologically contrasting colonies were checked for purity microscopically and pure cultures were sub-cultured on PDA slants. Mixed colonies were separated by streaking on agar plates before final transfer to agar slants. Storage was at 4°C in the refrigerator pending when these cultures were subjected to final tests for further identification of the organisms. Colonial or morphological appearance of the isolates from the respective cultures were made and recorded taking note of the size, colour and edge of each colony, and the nature of surface.

Elemental analysis

For all the elements analysed, garri sample was oven-dried at 100°C for 3 h. Thereafter, the sample was ground into a fine powder and 0.5 g was weighed into a 100 ml volumetric flask. Thirty millilitres (30 ml) of mixed concentrated acid (650 ml nitric acid + 80 ml perchloric acid + 20 ml H_2SO_4) was added and the mixture was heated at 150°C until dense fumes of nitric acid escaped. Thereafter, it was cooled and brought to a volume of 50 ml using sterile distilled water in a 50 ml volumetric flask. The resulting solution was analysed with an Atomic Absorption Spectrophotometer (AAS, Model Pa990). The spectrophotometer was standardized using the standard solutions of the elements analysed and distilled water was acidified and aspirated to zero using an air-acetylene flame for Cu, Pb, Cd, Ni, Cr and nitrous oxide-acetylene flame for Hg. The absorption radiations of Cu, Pb, Cd, Ni, Cr and Hg produced from the samples at various wavelengths was measured using AAS.

Moisture content

Moisture content was determined by weighing 10 g of garri or cassava tuber (W1), and drying to constant weight in an oven. This was subsequently reweighed (W2). The moisture content calculated in percent was given by the equation previously reported by Manyi et al. (2015).

$$Moisture\ Content\ (MC)(\%) = \frac{Loss\ in\ Weight\ (W2)}{Original\ Weight\ (W1)} \times 100$$

Ash content

Ash content was determined by AOAC (1990) method.

Total acidity

Total acidity was determined by AOAC method (1975) 14.064 – 14.065.

Statistical analysis

Data were analysed using SPSS version 16.0 and results were presented as descriptive statistics.

RESULTS AND DISCUSSION

The moisture contents of the present study ranged from 9.8 ± 1.02 to 14.8 ± 0.29% (Table 1a and b). Similarly, the moisture contents obtained for peeled cassava tubers used in making garri ranged from 64.5 ± 1.40 to 68.2 ± 1.60% (Table 1a and b). There was no statistically significant difference ($p>0.05$) in the moisture contents of garri exposed for sale and that direct from frying. Similarly, the values of the moisture contents recorded for the different cassava tubers are statistically related. The moisture contents of the tubers were significantly higher ($p<0.05$) than that of processed garri. Excessive moisture contents attract high bacterial growth because of increased water activity. However, most of the moisture contents obtained in the present study were within that recommended by Codex Alimentarius Commission for garri. The mean values of the moisture contents in this study support the previous reports of some authors (Adebola et al., 2014; Aguoru et al., 2014; Samuel and Ugwuanyi, 2014). Similarly, the moisture contents of the cassava tubers of the present study supported that reported by Kanim et al. (2009).

The ash content (%) ranges of 1.5 ± 0.06 to 2.4 ± 0.08 and 0.50 ± 0.02 to 0.80 ± 0.02 for garri and peeled cassava tubers respectively were obtained in this study (Table 1). Following the Codex Alimentarius Commission for garri, the ash contents obtained were within the permissible limit (CODEX STAN 151 - 1989). The present ash content values were lower than that previously recorded (Kanim et al., 2009). Even though the ash contents varied from one garri sample to another, the values are statistically homogenous. The ash contents of all the garri samples analysed were consistently higher than the ash contents of the cassava tubers.

Total titratable acidity (%) determined as lactic acid obtained in this study ranged from 0.4 ± 0.07 to 0.8 ± 0.05 (Table 1a and b). The recommended value of total acidity (%) is between 0.6 and maximum of 1.0 (CODEX STAN 151 - 1989). Low acidity presupposes longer fermentation and better quality of garri. Acidity in gari was more than that obtained from the cassava tubers. The results of this study show that there was no statistically significant difference ($p>0.05$) in the titratable acidity. The titratable acidity values reported by Ogiehor and Ikenebomeh (2004, 2005) (0.01 ± 0.00 to 0.4 ± 0.00) were significantly lower than 0.4 ± 0.07 to 0.7 ± 0.05 of the present study. The significance of the determination of some of these physicochemical attributes of food lies in their possibility of inducing microbial spoilage or colonization. For instance, high moisture contents favour bacterial colonization of food, whereas high acidity favours mould growth either of which could predispose the food to microbial invasion.

The highest number of *E. coli* isolated from garri in this study is 1.80 log CFU/g. Many of the samples had no detectable *E. coli* (Table 2a and b). The presence of an *E. coli* is an indicator of poor hygiene and faecal pollution

Table 1. Moisture content, ash content and total acidity of garri samples (a) and cassava root tuber (b).

S/N	Sample analysed	Moisture content (%)	Ash content (%)	Total acidity (%) (lactic acid)
a				
1	Edu-M1W	13.5 ± 0.16	1.5 ± 0.18	0.6 ± 0.08
2	Edu-M2W	12.2 ± 0.33	1.8 ± 0.13	0.4 ± 0.07
3	Edu-M1Y	12.8 ± 0.54	2.2 ± 0.14	0.5 ± 0.07
4	Edu-M2Y	13.1 ± 0.93	1.5 ± 0.06	0.7 ± 0.05
5	Ado-M1W	12.4 ± 1.00	2.0 ± 0.23	0.5 ± 0.07
6	Ado-M2W	14.8 ± 0.29	1.6 ± 0.04	0.6 ± 0.00
7	Ado-M1Y	10.8 ± 0.38	2.0 ± 0.12	0.7 ± 0.03
8	Ado-M2Y	12.0 ± 0.17	1.7 ± 0.09	0.6 ± 0.06
9	Edu-M1W GDF	11.2 ± 0.44	2.4 ± 0.08	0.7 ± 0.05
10	Edu-M2W GDF	9.8 ± 1.02	1.8 ± 0.17	0.6 ± 0.03
11	Edu-M1Y GDF	10.4 ± 0.50	1.9 ± 0.05	0.6 ± 0.07
12	Edu-M2Y GDF	11.6 ± 0.32	2.1 ± 0.03	0.8 ± 0.05
13	Ado-M1W GDF	11.8 ± 0.21	2.3 ± 0.04	0.7 ± 0.00
14	Ado-M2W GDF	12.8 ± 0.33	2.0 ± 0.07	0.6 ± 0.04
15	Ado-M1Y GDF	12.0 ± 0.60	2.2 ± 0.0 4	0.6 ± 0.08
16	Ado-M2Y GDF	10.5 ± 0.32	2.1 ± 0.07	0.5 ± 0.00
b				
17	Edu-M1	65.5 ± 1.26*	0.50 ± 0.09*	0.4 ± 0.02
18	Edu-M2	68.2 ± 1.60*	0.80 ± 0.0 2*	0.3 ± 0.02
19	Ado-M1	64.5 ± 1.40*	0.60 ± 0.03*	0.5 ± 0.00
20	Ado-M2	66.10 ± 0.47*	0.50 ± 0.02*	0.4 ± 0.06

Figures indicated with the asterisks means that there is statistically significant difference ($p<0.05$) between them and the non-asterisked column. Results are mean of six samples. Edu-M1 = Edumoga Market 1, Edu-M2 = Edumoga Market 2; Ado-M1 = Adoka Market 1, Ado-M2 = Adoka Market 1; GDF = garri direct from frying; W = white garri; Y = yellow garri.

Table 2. Mean values of microorganisms isolated from the garri samples (a) and peeled cassava root tubers (b) (expressed as log CFU/g of garri).

Sample analysed	*E. coli*	*S. aureus*	*Salmonella* sp	*Shigella* sp	TCC	YMC	TVC
a							
Edu-M1W	1.00 ± 0.02	0.90 ± 0.01	0.30 ± 0.06	1.20 ± 0.03	1.00 ± 0.00	1.85 ± 1.01	2.00 ± 1.04
Edu-M2W	1.08 ± 0.09	1.15 ± 0.05	ND	ND	1.25 ± 0.03	1.79 ± 1.02.	2.15 ± 0.36
Edu-M1Y	ND	1.30 ± 0.40	ND	ND	1.38 ± 0.67	2.11 ± 0.8	2.18 ± 0.96
Edu-M2Y	ND	1.36 ± 0.06	1.00 ± 0.10	0.60 ± 0.00	1.46 ± 0.7	2.06 ± 1.00	2.20 ± 0.90
Ado-M1W	ND	1.00 ± 0.01	ND	ND	0.30 ± 0.01	1.92 ± 1.01	2.57 ± 1.16
Ado-M2W	1.04 ± 0.40	1.08 ± 0.86	0.30 ± 0.03	ND	1.75 ± 0.36	1.66 ± 0.64	2.60 ± 0.42
Ado-M1Y	ND	0.31 ± 0.00	ND	ND	1.04 ± 0.72	1.97 ± 0.60	2.23 ± 0.43
Ado-M2Y	0.90 ± 0.26	0.47 ± 0.30	ND	ND	1.36 ± 0.33	2.09 ± 0.72	2.56 ± 1.01
Edu-M1W GDF	ND	ND	ND	ND	ND	ND	ND
Edu-M2W GDF	0.70 ± 0.02	ND	ND	ND	1.38 ± 1.01	1.69 ± 1.06	1.78 ± 0.90
Edu-M1Y GDF	ND	ND	ND	ND	0.70 ± 0.60	0.30 ± 0.00	1.23 ± 1.06
Edu-M2Y GDF	ND	ND	ND	ND	ND	ND	1.65 ± 0.60
Ado-M1WGDF	ND	ND	ND	ND	1.18 ± 0.50	ND	1.47 ± 0.66
Ado-M2WGDF	ND	ND	ND	ND	1.56 ± 0.40	0.60 ± 0.05	1.83 ± 0.82
Ado-M1Y GDF	0.90 ± 0.00	ND	ND	ND	1.08 ± 0.22	ND	2.07 ± 0.18
Ado-M2Y GDF	ND	ND	ND	ND	ND	ND	ND

Table 2. Contd.

b							
Edu-M1	2.13 ± 1.01	1.98 ± 0.66	1.70 ± 0.80	2.33 ± 1.16	3.33 ± 1.07	3.10 ± 0.86	3.86 ± 0.40
Edu-M2	2.47 ± 0.10	2.38 ± 0.50	1.88 ± 0.45	ND	2.98 ± 1.23	3.56 ± 1.41	3.78 ± 1.61
Ado-M1	2.75 ± 0.22	1.36 ± 0.54	ND	2.88 ± 0.77	3.51 ± 1.04	2.82 ± 1.00	4.03 ± 0.86
Ado-M2	2.60 ± 0.60	2.51 ± 1.10	2.03 ± 0.77	2.75 ± 1.06	2.81 ± 1.04	1.64 ± 0.90	3.97 ± 1.16

TCC, Total coliform counts; YMC, yeast and mould counts; TVC, total viable counts. Edu-M1= Edumoga Market 1, Edu-M2 = Edumoga Market 2; Ado-M1 = Adoka Market 1, Ado-M2 = Adoka Market 1, ND = not detected in 1 g of gari or peeled cassava tuber, GDF = garri direct from frying; W = white garri; Y = yellow garri.

of a material. The low level of the organism is a pointer to its good quality and hygiene standard across the processing and distribution line. However, the recommended level of *E. coli* in a ready-to-eat food of this nature is <3 CFU/g for the food to be satisfactory (Millard and Rockliff, 2005).

In the present study, maximum *Staphylococcus aureus* isolated from garri of 1.85 log CFU/g and mean 1.36 (Table 2a and b) were significant enough to cause a health concern. *S. aureus* is a normal flora of human skin and nose horizontally transferred to the garri by processors and vendors. *S. aureus* is an important and major food-borne pathogen worldwide producing enterotoxins not digested by a protease, can withstand high heat treatments and a major contaminant of foodstuffs (Wu et al., 2016). Besides, toxigenic *S. aureus* contamination in ready-to-eat foods is the leading cause of food-borne illness in some countries of the world (Oh et al., 2007).

The levels of *Salmonella* and *Shigella* spp. isolated from garri in the present study were relatively low as compared to *E. coli* and *S. aureus*. Both *Salmonella* sp. and *Shigella* were not isolated in many of the samples (Table 2a and b). They were however isolated from peeled cassava root tubers used in garri production. Food safety guideline considers most ready-to-eat foods satisfactory if *Salmonella* and *Shigella* spp. are not detectable in 25 g of the food.

The mean total coliform count (TCC), mean yeast and mould count (YMC) and mean total viable count (TVC) indicate the mean levels of coliform, fungi and bacteria respectively in the product. These means as presented in Table 2a and b, ranging from minimum values of not detectable (in 1 g of garri or peeled cassava tuber) to 1.75, 2.11 and 2.60 log, CFU/g, respectively for processed ready-to-eat garri. The mean values of these organisms for cassava root tubers were 2.81 to 3.51, 1.64 to 3.56 and 3.78 to 4.03 log CFU/g, respectively. These values indicate that the food products are potentially problematic considering the recommended food safety limits. The use of TVC, TCC, and YMC as indices of measurement of food quality is a useful quantitative assay of microbial load and contamination.

The fungi isolated in this study included *Mucor*, *Aspergillus* and *Fusarium* spp. (results not shown). While *Mucor*, *Aspergillus* and *Fusarium* spp. can cause spoilage of the food and great economic loss, some *Aspergillus* spp. can produce mycotoxins. Mycotoxins are threats to global food security as well as to human health. Fungal species including *Aspergillus*, *Cladosporium, Fusarium*, *Mucor*, *Penicillium* and *Rhizopus* (Ekundayo, 1984; Ogugbue et al., 2011; Aguoru et al., 2014) had been isolated previously from garri. *Cladosporium, Penicillium* and *Rhizopus* were however not isolated in this study.

The presence of some selected heavy metals were investigated in this study and the presence of cadmium and chromium was not detect in any of the garri samples while lead, nickel and copper were the most abundant (Table 3). The highest values of lead, nickel and copper in the garri samples were 1.300 ± 0.0004, 0.448 ± 0.0021 and 0.274 ± 0.0002 mg/kg, respectively. These values were within the Codex Alimentarius Commission (2011) tolerable limits of some heavy metals (Table 4) in some food items. Mercury was detected in three gari samples with the highest value of 0.082 ± 0.0001 mg/kg. The mean values of lead, cadmium and chromium obtained from garri direct from frying in the present study, are similar to that reported by Dibofori-Orji and Edori (2015). The range of the permissible quantity of these metals in food items is as presented in Table 4.

Even though, heavy metals are naturally occurring in soils, heavy vehicular traffic accounts for a significant source of heavy metals in most of the roadside soils (Zakir et al., 2014; Dibofori-Orji and Edori, 2015). Similarly, Dibofori-Orji and Edori (2015) reported that lead and some heavy metals are emitted through the exhaust of motor vehicles. These metals are retained from the refining process of the crude oil (Dibofori-Orji and Edori, 2015). The argument is that since heavy vehicular traffic can deposit a significant amount of heavy metals on the roadside soils, ready-to-eat garri displayed uncovered and exposed for sale along busy roads could also have significant deposits. Other factors leading to heavy metals contamination could arise from the implements used in the processing of garri. Similarly, the increased use of fertilizers and other agrochemicals like insecticides and pesticides to increase crop production could also

Table 3. Heavy metal concentration in garri and cassava root tubers (mg/kg).

Sample analysed	Cu	Pb	Cd	Ni	Cr	Hg
Edu-M1W	0.274 ± 0.0002	1.057 ± 0.0007	ND	0.448 ± 0.0021	ND	ND
Edu-M2	0.225 ± 0.0005	0.772 ± 0.0006	ND	0.379 ± 0.0001	ND	ND
Edu-M1Y	0.219 ± 0.0032	1.223 ± 0.0007	ND	0.378 ± 0.0009	ND	0.002 ± 0.0001
Edu-M2Y	0.252 ± 0.0021	1.300 ± 0.0004	ND	0.404 ± 0.0005	ND	0.082 ± 0.0001
Ado-M1W	0.228 ± 0.0022	0.921 ± 0.0014	ND	0.382 ± 0.0005	ND	ND
Ado-M2W	0.207 ± 0.0003	0.889 ± 0.0014	ND	0.243 ± 0.0076	ND	ND
Ado-M1Y	0.335 ± 0.0002	0.214 ± 0.0008	ND	0.127 ± 0.0055	ND	ND
Ado-M2Y	0.054 ± 0.0001	0.192 ± 0.0010	ND	0.221 ± 0.0001	ND	0.004 ± 0.0001
Edu-M1W GDF	0.031 ± 0.0001	0.004 ± 0.0001	ND	ND	ND	ND
Edu-M2W GDF	0.012 ± 0.0003	ND	ND	ND	ND	ND
Edu-M1Y GDF	0.032 ± 0.0001	0.028 ± 0.0001	ND	0.153 ± 0.0032	ND	ND
Edu-M2Y GDF	ND	0.013 ± 0.0001	ND	0.042 ± 0.0001	ND	ND
Ado-M1W GDF	ND	0.007 ± 0.0001	ND	0.115 ± 0.0001	ND	ND
Ado-M2W GDF	0.093 ± 0.0001	ND	ND	ND	ND	ND
Ado-M1Y GDF	ND	ND	ND	ND	ND	ND
Ado-M2Y GDF	ND	ND	ND	ND	ND	ND
Edu-M1 Cassava root tubers	0.454 ± 0.0004	1.322 ± 0.0071	1.03 ± 0.0063	0.248 ± 0.0009	0.13 ± 0.0003	ND
Edu-M2 Cassava root tubers	1.200 ± 0.0009	2.781 ± 0.0027	0.42 ± 0.0008	0.544 ± 0.0009	ND	0.012 ± 0.0001
Ado-M1 Cassava root tubers	0.028 ± 0.0001	1.244 ± 0.0009	0. 27 ± 0.0003	0.192 ± 0.0005	ND	0.081 ± 0.0001
Ado-M2 Cassava root tubers	0.990 ± 0.0001	0.490 ±	0.55 ± 0.0002	0.562 ± 0.0008	0.012 ± 0.0001	ND

Edu-M1 = Edumoga Market 1, Edu-M2 = Edumoga Market 2; Ado-M1 = Adoka Market 1, Ado-M2 = Adoka Market 1, ND = not detected in 1 g of garri or peeled cassava tuber, GDF = garri direct from frying; W = white garri; Y = yellow garri.

Table 4. Tolerable limits of some heavy metals (mg/kg).

Heavy metal	Tolerable limits	Reference	Daily allowance	Reference
Pb	0.1 – 1.5	Codex Alimentarius Commission (2011)	0.30 mg/day	Dibofori-Orji and Edori (2015)
Cd	0.05 – 1.0	Codex Alimentarius Commission (2011)	1.59 µg/day	Dibofori-Orji and Edori (2015)
Cr	-	-	1.50 µg/day	Dibofori-Orji and Edori (2015)
Cu	0.1 – 1.0	Codex Alimentarius Commission (2011)	-	-
Ni	-	-	-	-
Hg	0.001 – 1.0	Codex Alimentarius Commission (2011).	-	-

release some heavy metals to the atmosphere and increase the health risks (Khan et al., 2009). In the same way, Khan et al. (2009) reported that industrial effluents and other anthropogenic activities contribute heavy metals to the environments.

Perhaps, one assumes that once the recommended levels of these metals are exceeded, they automatically cause a health hazard to man. However, health risk index (HRI) or the hazard quotient (HQ) needs to be quantified as the tolerable limit and the exposure quantity should be ascertained (Khan et al., 2009). Information on the quantity of the heavy metals transferred to a consumer is necessary. As garri is a ready-to-eat food product, the quantity of the heavy metal transferred to a consumer is directly proportional to both the quantity of garri consumed and that of the heavy metals therein. The present study is a quantitative approach and did not assess health risk due to the consumption of the product. However, using the health risk index formula adapted from Khan et al. (2009):

$$\text{Health Risk Index (HRI)} = \frac{\text{Daily intake of metals}}{\text{Reference oral dose}}$$

one extrapolates the risk assessment.

The safe limits by Codex Alimentarius Commission (2011) for Pb, Cd and Cu are 124 µg, 60 µg, and 3 mg, respectively. Sales of garri in properly packaged bags or plastic containers and preferably not along roadsides is recommended.

Conclusions

The measured physicochemical attributes, the ash

content and the concentrations of the heavy metals of garri were within the permissible limits. The values of the microorganisms indicate potential food safety problems which could be reduced by increased hygiene and food safety consciousness.

CONFLICT OF INTERESTS

The authors have not declared any conflict of interests.

REFERENCES

Adebola MO, Dadi-Mamud, NJ, Nusa Halima MK (2014). The effects of packaging materials of shelf-life stability of garri bought from markets in Lapai Niger State Nigeria. J. Appl. Environ. Microbiol. 2:12-15.

Aguoru CU, Onda MA, Omoni VT, Ogbonna IO (2014). Characterization of moulds associated with processed garri stroed for 40 days at ambient temperature in Makurdi, Nigeria. Afr. J. Biotechnol. 13:673-677.

Alexopoulus CJ, Mims CW, Blackwell M (1996). Introductory Mycology, (4th Edition). New York. John Wiley. pp. 1-50.

Ani JY. (2006). Assessment of conparative toxicities of lead and copper using plant assay. Chemosphere 62:1359-1365.

AOAC (1975). Association of Official Analytical Chemists. Official methods of analysis, 12th edition. Washington DC, USA.

AOAC (1990). Association of Official Analytical Chemists. Official methods of analysis, 15th edition. Washington DC, USA.

Asegbeloyin JN, Onyimonyi AE (2007). The effect of different processing methods on the residual cyanide of 'gari'. Pak. J. Nutr. 62:163-166.

Cheesbrough M (2004). District Laboratory Practice in Tropical Countries. Part 2. Cambridge University Press, Great Britain. pp. 62-70.

Codex Alimentarius Commission (2011). Joint FAO/WHO Food Standards Programme, Codex Committee on Contaminants in Foods. Fifth Session, the Hague, the Netherlands, 21 – 25 March 2011.

Codex STAN 151 (1989). (Rev. 1 -1995). Codex standard for gari. pp. 1-6.

Dibofori-Orji AN, Edori OS (2015). Analysis of some heavy metals (Pb, Cd, Cr, Fe, Zn) in processed cassava flour (garri) sold along the road side of a busy highway. Arch. Appl. Sci. Res. 7:15-19.

Edem DO, Ayatse JOI, Itam EH (2001). Effect of soy protein supplementation on the nutritive value of garri farina from *Manihot esculenta*. Food Chem. 75:57-62.

Ekundayo CA (1984). Microbial spoilage of packaged garri in storage. Microbiol. Lett. 23:271-278.

Jekayinfa SO, Olajide JO (2007). Analysis of energy usage in the production of three cassava-based foods in Nigeria. J. Food Eng. 82:217-226.

Kanim OR, Fasasi OS, Oyeyinka SA (2009). Gari yield and composition of cassava roots stored using traditional methods. Pak. J. Nutr. 8:1830-1833.

Khan S, Farooq R, Shahbaz S (2009). Health risk assessment of heavy metals for population via consumption of vegetables. World Appl. Sci. J. 6:1602-1606.

Kostinek M, Specht I, Edward VA, Schillinger U, Hertel C, Holzapfel WH, Franz CM (2005). Diversity and technological properties of predominant lactic acid bacteria from fermented cassava used for the preparation of gari, a traditional African food. Syst. Appl. Microbiol. 28:527-540.

Macfaddin JF (1977). Biochemical tests for Identification of Medical Bacteria. Williams and Wilkins, New York.

Markus J, McBratney AB (2001). A review of the contamination of soil with lead ii, spatial distribution and risk assessment of soil lead. Environ. Int. 27:399-411.

Manyi MM, Idu OF, Ogbonna IO (2015). Microbiological and parasitic quality of suya (roasted beef) sold in Makurdi, Benue State, Nigeria. Afr. J. Microbiol. Res. 8:3235-3242.

Millard G, Rockliff S (2005). Microbiological quality of ready-to-eat foods. Act Health Protection Service. July 2004 – June 2005.

Nadal M, Schuhanachar M, Domingo JL (2004). Metal pollution of Soils and Vegetation in Area with Petrochemical industry. Sci. Total Environ. 321:59-69.

Ochieng EZ, Lalah JO, Wandiga SO (2007). Analysis of Heavy Metals in Water and Surface Sediments in five rift Valley Lakers in Kenya reassessment of recent increase in Anthropogenic Activities. Bull. Environ. Contam. Toxicol. 79:570-576.

Ogiehor IS, Ikenebomeh MJ (2004). Quality characteristics of market garri destined for consumption in ten selected Nigerian states: Baseline for industrialization. Adv. Nat. Appl. Sci. Res. 2:17-25.

Ogiehor IS, Ikenebomeh MJ (2005). Extension of shelf life of garri by hygienic handling and sodium benzonate treatment. Afr. J. Biotechnol. 4:744-748.

Ogugbue CJ, Mbakwem-Aniebo C, Akubuenyi F (2011). Assessment of microbial ari contamination of post processed garri on sale in markets. Afr. J. Food Sci. 5:503-512.

Ogugbue CJ, Obi G (2011). Bioburden of garri stored at different packaging materials under tropical market conditions. Middle East J. Sci. Res. 7:741-745.

Oh SK, Lee N, Cho YS, Shin DB, Choi SY, Koo M (2007). Occurrence of toxigenic *Staphylococcus aureus* in ready-to-eat food in Korea. J Food Prot. 70:1153-1158.

Samuel T, Ugwuanyi JO (2014). Moisture sorption behaviour and mould ecology of trade garri sold in southern eastern Nigeria. Int. J. Food Sci. Volume 2014 (2014), Article ID 218959, 10 pages.

Wu S, Duan N, Gu H, Hao L, Ye H, Gong W, Wang Z (2016). A Review of the Methods for Detection of Staphylococcus aureus Enterotoxins. Toxins 8(7):176.

Zakir HM, Sultana N, Akter M (2014). Heavy metal contamination in roadside soils and grasses, a case study from Dhaka city, Bangladesh. J. Chem. Biol. Phys. Sci. 4:1661-1673.

academicJournals

Vol. 16(18), pp. 1092-1097, 3 May, 2017
DOI: 10.5897/AJB2016.15512
Article Number: 1030A0364075
ISSN 1684-5315
Copyright © 2017
Author(s) retain the copyright of this article
http://www.academicjournals.org/AJB

African Journal of Biotechnology

Full Length Research Paper

Efficacy evaluation of spinosad bioinsecticide capsules suspension for the control of *Helicoverpa armigera*

Francinea Souza, Leila T. Maranho and Ligia A. C. Cardoso*

Industrial Biotechnology Program, Universidade Positivo, Prof. Pedro Viriato Parigot de Souza Street, 5300, Campo Comprido, Curitiba, Paraná, Brazil.

Received 3 June, 2016; Accepted 12 April, 2017

Helicoverpa armigera **caterpillar causes serious economic crop losses in Brazil, mainly in the corn, cotton and soybean farming. The aim of this study was to compare the efficiency of bioinsecticide Spinosad in the form of suspension capsules and emulsifiable concentrate in the dosage of 48 g i.a. ha^{-1} for control of *H. armigera*. The experiment was conducted in three different groups treated separately with emulsifiable concentrate (EC) with 48% of spinosad; suspension capsules (SC) with 48% of spinosad; and control group treatment with deionized water. Caterpillars were used in the early stage (1 and 2 days old larvae), and maintained under laboratory conditions (24 ± 1°C, 65 ± 5% RH and a 12:12 h light: dark photoperiod). The mortality was recorded and the affected behavior of treated larvae was checked every 30 min for a period of 8 h. The results show the efficacy of spinosad for control of *H. armigera* in the emulsifiable concentrate group treatment at 92.6 and 88.9%, and in the suspension capsule group treatment at 88.9 and 87.0%, respectively, in the first and second bioassay. It was concluded that the spinosad 48 g i.a. ha^{-1} is efficient in the control of *H. armigera* in micro encapsulated formulations, promoting less environmental damage by reducing the level of pesticides in the environment by the smaller concentration of the active ingredient through capsule suspension formulation and revealed economic viability and promotion of extended release of active ingredients.**

Key words: Industrial biotechnology, biological control, biopesticide, caterpillar control, microcapsules, emulsifiable concentrate.

INTRODUCTION

Helicoverpa armigera (Hubner) (Lepidoptera: Noctuidae) belongs to the subfamily, Heliothinae. It has broad occurrence throughout the world, being found in various countries from Asia-China and India, Africa-Benin, Cameroon and Nigeria, Europe and Oceania-Australia (Brévault et al., 2009; Perini et al., 2016). Female *H. armigera* generally lays around 1,000 to 1,500 eggs and the hatching takes place between five and seven days after the laying (Czepak et al., 2013). *H. armigera* larvae eats leaves, stems, buds, fruits and pods, it causes damage in the vegetative and reproductive plant stages and serious economic crop damage in Brazil, mainly in the corn, cotton and soybean that are important crops for Brazilian agriculture (Pomari-Fernandes et al., 2015).

*Corresponding author. E-mail: ligiacardoso@up.edu.br.

Author(s) agree that this article remains permanently open access under the terms of the Creative Commons Attribution License 4.0 International License

Bueno and Sosa (2014) has reported that in Brazil, the damage caused by *H. armigera* in 2012/2013, reached approximately $0.8 billion.

Population growth of the *Helicoverpa* as well as losses of the production systems were caused by following a cumulative process of inadequate cultivation practices and successive planting of host vegetable species (corn, soybean, etc.) in very extensive management contiguous areas with non-judiciars use of high toxicity pathology category agrochemicals has contributed to resistance development in *H. armigera*, which resultand in heavy crop losses each year (Vijayabharathi et al., 2014; Specht et al., 2013; Suzana et al., 2015).

The success of the control in pest management depends on the choice, stability and acceptance of after years of use, in which chemical control was used the most (Samri et al., 2015). It was considered that abusive use and lack of technical criteria can result in problems, jeopardizing sustainability by the development of plague resistance to defensive products (Obopile, 2006).

Due to their effectiveness and availability, the products mostly used in farming for biological control of plagues in crops are strains of pathogenic bacteria like *Bacillus thuringiensis*, whose pathogenicity has already been well established against demonstrated insect pest of lepidopteron, coleopteran, dipteran, arthropod and nematode orders (Faten et al., 2011). Among other biopesticides which have been exploited in predators crop management is spinosad, an aerobic fermentation of *Saccharopolyspora spinosa* products spinosyns, which is found to show a broad spectrum activity as an insecticide for the control of insects of the lepidopteran and dipteran species (Amiri-Besheli, 2009).

Pesticides are conventionally applied to crops by periodic broadcasting or spraying. Very high and possibly toxic concentrations are applied initially, and decrease rapidly in the field to concentrations that fall below the minimum effective level, for example, the emulsifiable formular. As a result, repeated level applications are needed to maintain pest control. Knowles (2008) mentioned that the insecticide formulations used are normally in the form of emulsifiable concentrate, in which the active ingredient is solubilized in hydrocarbons and other synthetic solvents, and associated with surfactants and emulsifiers to stabilize the emulsion on the aspersion tanks.

According to Liu et al. (2016), the encapsulated or release-control formulations present better benefits when compared with emulsifiable concentrates, due to reduced levels of hydrocarbons on this formule, longer action time of the active ingredient, reduction of the evaporation rate of the insecticides. All these specifications are important for the reduction of the level of pesticides in the environment by the smaller concentration of the active ingredient and, consequently, less damage to the plants, non-target insects and humans, lower photodegradation, hydrolysis, bacterial decomposition and leaching.

The aim of this study was to evaluate the efficiency of the insecticide, spinosad in the form of suspension capsules in comparison with the bioinsecticide, in the form of emulsifiable concentrate, in the concentration of 48% active ingredients in the dosage of 48 g i.a. ha^{-1} for control of *H. armigera*.

MATERIALS AND METHODS

The current research was conducted in the bioterium of Universidade Positivo, Curitiba, PR, Brazil. Caterpillar eggs of *H. armigera* were used; acquired from the Company Promip Manejo Integrado de Pragas. After the eggs have hatched, the larvae were placed in plastic cups (diameter of 15 cm, and depth of 0.94 cm). The plastics cups were kept in glass terrariums with an approximate area of 10 x 10 x 20 cm and adapted to the environment for 12 h. The glass terrariums were maintained in acclimatized room, with a temperature of 24 ± 1°C and relative humidity of 70 ± 10% and a 12L:12D photoperiod, absence of ventilation and artificial feeding. These conditions were maintained during all the periods of the experiment.

In this study, the concentration of spinosad for the control of *Helicoverpa* sp. in soybean crop was used; Tracer®, that is, a commercial product used in Brazil for the control of *Helicoverpa* sp. (Perini et al., 2016). It is used in the concentration of 48 g active ingredient per hectare (equivalent to 100 $mL.ha^{-1}$).

In the form of emulsifiable concentrate, the bioinsecticide was formulated through a mixture of active ingredients, emulsifiers and solvents (Knowles, 2008); in the form of suspension capsules, it was made through the interfacial polymerization method by coacervation in liquid phase (Benita et al., 1984); and deionized water was used for aspersion in the negative control group.

Three experimental groups were formed, each group comprised three replications, each treatment contained 18 larvae of first instar stage (1 day). The groups were treated with spinosad in the form of emulsifiable concentrate (EC) with 48% of spinosad, 46% of C9 solvent (AB9) and 6% of calcium dodecylbenzene sulfonate; spinosad in the form of suspension capsules (SC) with 48% of spinosad, 41.8% of deionized water, 7% of amine, 3% of ethoxylated fatty alcohol and 0.2% of xanthan gum; and control group (CG) was treated with deionized water. For the aspersion of the insecticides formulations (SC, EC and water), a glass sprinklers was used.

The formulations were observed in a digital microscope with an increase of 1600 times. A micrometric slide for biological microscope of 0.10 mm scaled in 0.01 mm was used in order to confirm the formation of mycelium in the bioinsecticide formulation of the emulsifiable concentrate, as well as the formation of microcapsules in the formulation of suspension capsules. Spherical capsules that are characteristic in encapsulation and micelle formation in the emulsifiable concentrate are shown in Figure 1.

Data on mortality and mobility were collected by means of observations carried out every 30 min for a period of 8 h, aiming to measure control results within a time interval similar to the interval that can be observed in the field, using natural luminosity; initially through the performance of a first bioassay and then by a second bioassay (24 h later). The number of dead larvae was noted down and the mobility of the larvae was observed from the record of photographs. Efficacy in each treatment was calculated according to Abbott (1925):

$$E\ (\%) = \left(1 - \frac{n1}{n2} * 100\right) \quad (1)$$

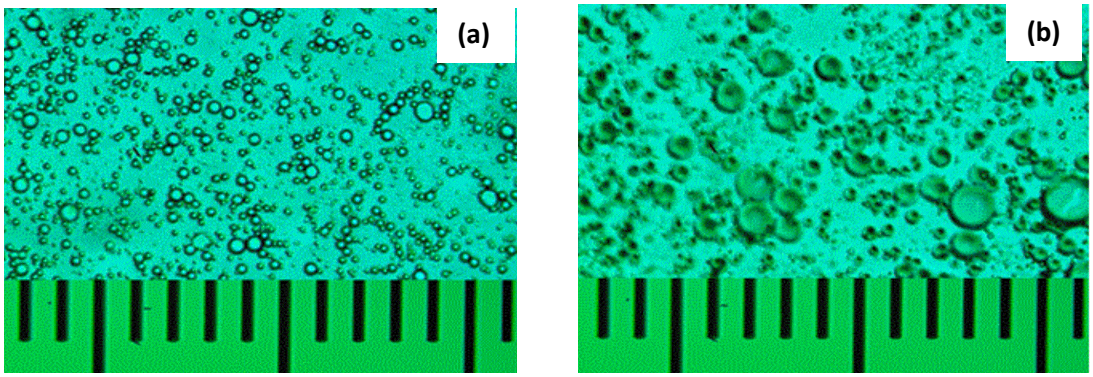

Figure 1. Photomicrography of the spinosad bioinsecticide formulation in digital microscopy with an increase of 1600 times, scale 14 µm (a) microencapsulated formulation and (b) emulsifiable concentrated formulation.

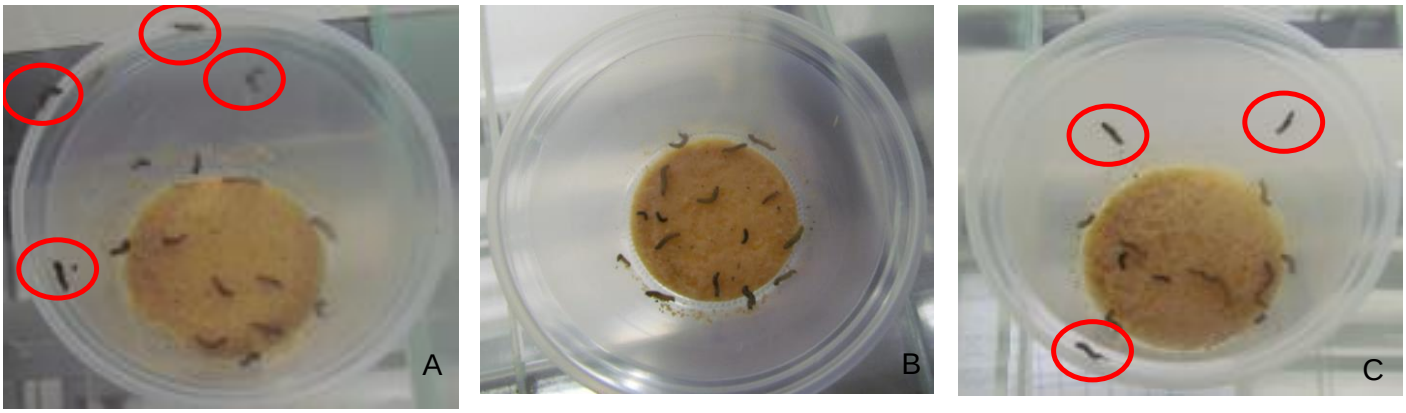

Figure 2. Activity of *H. armigera* in the presence of the bioinsecticide spinosad. A) control group, B) group treated with spinosad in the form of emulsifiable concentrate (EC) and C) group treated with spinosad in the form of suspension capsules (SC). The circled areas show the caterpillars on the walls of the plastic containers indicating their constant mobility during the study.

Where, E (%) is the efficacy of the treatment, n1 is the average number of living moths after treatment (EC and SC) and n2 is the number of living moths in control (CG).

The statistical analysis was carried out by the piece of software ACTION, as supplement to Excel software. The treatments were submitted to distribution and normality analyses by the Anderson-Darling statistical method. As the distribution presented linearity, T-student test was also applied. The groups treated with spinosad in the form of EC, SC and CG were compared and considered as statistically different when they presented value of $p \leq 0.05$.

RESULTS AND DISCUSSION

To prevent problems with the pulverization of the formulated substances (density must be lower than 1.0 g mL^{-1}), the bioinsecticides were subjected to density analysis, with a result of 0.93 g mL^{-1} at 25°C for the product in the form of emulsifiable concentrate and 1.03 g L^{-1} at 25°C for the microencapsulated product.

The increase of the mortality of caterpillars can be observed in Figure 2, which refers to the control group (A), the group treated with spinosad in the form of emulsifiable concentrate (B), and the group treated with spinosad in the form of encapsulated suspension (C).

In relation to mortality, after the data analyses of the groups, EC and SC presented a significant difference in relation to the control group, where no death of caterpillars was observed. The treatments made in groups EC and SC, when compared, also showed significant differences between them in the bioassay. Significant differences were observed between the efficiency indexes in the mortality of the *H. armigera* moths in the early stage when treated with spinosad in the form of emulsifiable concentrate and suspension capsules.

After 8 h from applying the bioinsecticide, the efficiency in mortality of the *H. armigera* caterpillars was obtained as follows: in the form of EC, it was 92.6 and 88.9%, respectively, for the first and second bioassays; and for the moths treated with the bioinsecticide in the form of SC, it was 88.9 and 87.0%, respectively, for the first and

Table 1. Average mortality of *H. armigera* after eight hours of applying bioinsecticide spinosad in the form of emulsifiable concentrate (EC) and suspension capsules (SC).

Time (min)	Bioassay 01			Bioassay 02		
	CG	EC	SC	CG	EC	SC
0	0.0±0.0	0.0±0.0	0.0±0.0	0.0±0.0	0.0±0.0	0.0±0.0
30	0.0±0.0	0.0±0.0	0.0±0.0	0.0±0.0	0.0±0.0	0.0±0.0
60	0.0±0.0^{bc}	2.0±0.6^{ac}	0.0±0.0b	0.0±0.0	0.0±0.0	0.0±0.0
90	0.0±0.0^{bc}	5.0±0.6^{ac}	0.0±0.0^{ab}	0.0±0.0^{bc}	0.0±0.0^{ac}	0.0±0.0^{ab}
120	0.0±0.0^{bc}	7.0±1.1^{ac}	5.0±0.6^{ab}	0.0±0.0^{bc}	9.0±0.6^{ac}	8.0±0.0^{ab}
150	0.0±0.0^{bc}	8.0±0.6^{ac}	5.0±0.0^{ab}	0.0±0.0^{bc}	12.0±1.7^{ac}	9.0±1.7^{ab}
180	0.0±0.0^{bc}	11.0±1.7^{ac}	8.0±1.1^{ab}	0.0±0.0^{bc}	14.0±1.5^{ac}	10.0±2.1^{ab}
210	0.0±0.0^{bc}	11.0±0.6^{ac}	8.0±0.6^{ab}	0.0±0.0^{bc}	14.0±1.5^{ac}	10.0±2.1^{ab}
240	0.0±0.0^{bc}	11.0±0.6^{ac}	10.0±0.6^{ab}	0.0±0.0^{bc}	14.0±1.5^{ac}	11.0±1.5^{ab}
270	0.0±0.0^{bc}	13.0±0.6^{ac}	10.0±0.0^{ab}	0.0±0.0^{bc}	14.0±1.1^{ac}	11.0±1.7^{ab}
300	0.0±0.0^{bc}	14.0±0.6^{ac}	11.0±0.0^{ab}	0.0±0.0^{bc}	15.0±1.0^{ac}	14.0±0.6^{ab}
330	0.0±0.0^{bc}	14.0±0.0^{ac}	12.0±0.0^{ab}	0.0±0.0^{bc}	15.0±1.0^{ac}	14.0±0.6^{ab}
360	0.0±0.0^{bc}	14.0±0.6^{ac}	12.0±0.0^{ab}	0.0±0.0^{bc}	15.0±1.0^{ac}	15.0±0.6^{ab}
390	0.0±0.0^{bc}	16.0±0.6^{ac}	12.0±0.0^{ab}	0.0±0.0^{bc}	16.0±1.1^{ac}	15.0±1.0^{ab}
420	0.0±0.0^{bc}	16.0±0.0^{ac}	12.0±0.0^{ab}	0.0±0.0^{bc}	16.0±1.1^{ac}	15.0±1.0^{ab}
450	0.0±0.0^{bc}	16.0±0.6^{ac}	14.0±0.6^{ab}	0.0±0.0^{bc}	16.0±1.5^{ac}	15.0±1.5^{ab}
480	0.0±0.0^{bc}	17.0±0.6^{ac}	16.0±1.0^{ab}	0.0±0.0^{bc}	17.0±0.6^{ac}	16.0±1.1^{ab}

*a, b and c express the significant difference ($p<0.05$) through the T-student test among the control group (CG), EC and SC.

second bioassays.

According to Tsunoda and Nishimoto (1986), the value of efficiency must be above 80% so that a chemical formulation can be considered efficient. In this manner, the satisfactory efficiencies in the group EC were obtained from the intervals of 150 and 210 min, respectively, after applying the bioinsecticide for bioassays 01 and 02 with the values of the average and standard deviations of 14.0 ± 1.1 and 16.0 ± 0.6. For the group SC, satisfactory efficiencies were obtained after applying the bioinsecticide at intervals of 210 and 420 min after the treatment with results of the averages and standard deviations, respectively, 15.0 ± 1.0 and 16.0 ± 1.0 (Table 1); this suggests that efficiency in the treatment above 80% took place faster in the control of moths treated with the bioinsecticide in the form of emulsifiable concentrate.

The efficiency index of the SC formulation, when compared with the groups treated with EC, showed a greater toxicity effect found in the components of the EC formulation, that is, lipophilic action of the organic solvents on the moths larvae as greater amount of the active ingredient available in the syrup in the form of encapsulation as most part of the active ingredients at the time of application found within the capsules.

Wang et al. (2012) reported that, traditionally, evaluation of the effects of the spinosad against the target-pest is based on the average lethal dose (DL_{50}) or on the average lethal concentration (CL_{50}) of the active ingredients and, in addition to direct mortality, the survived larval after treatment of insecticide can be found to malfunction, resulting in retarded development, fertility and fecundity. These consequences can lead to negative impacts and must be taken into account in the management of integrated handling of the pest. The greater time of bioavailability of the active ingredient in the form of suspension capsules for the length of the time of permanence in the environment can also favor and establish the lethal concentration as necessary for the desired control. Harter et al. (2015) found efficiency of above 80% in up to 7 days after applying spinosad (Tracer®) 0.096 g i.a. ha^{-1} in the control of *Anastrepha fraterculus*.

Wang et al. (2012) demonstrated the high toxicity of the spinosad in the control of *S. exigua* in the second instar stage and Wang et al. (2009) reported on the high toxicity of the spinosad for lepidopteron, in corroboration with Sayyed et al. (2012), who showed that the toxicity of the spinosad chlorfenapyr is significantly greater for *S. exigua* than compounds of the groups of pyrethroids and organophosphates.

Tello et al. (2013) presented a significant result of mortality for adults *E. paulistus* in the concentration of 0.48 mg of i.a. L^{-1} of spinosad after 12 and 24 h. Spinosad also has the capacity of reduction in weight gain of the moth neonates, possibly associated with the toxicity of the bioinsecticide.

Moths have defense mechanisms such as a short development period, polyphagia, mimicry, thanatopsis and also genetic and biochemical adaptations that favor

the maintenance of the species (Mello and Silva-Filho, 2002). In relation to mobility, a low mobility rate of moths was ascertained in the group treated with bioinsecticide spinosad in the form of EC, when compared with the control group and the group treated with the bioinsecticide spinosad in the form of SC; this is shown in Figure 2A and C through the demarcation of the moths on the walls of the containers. Mobility of the moths was ascertained in 100% of the observation period. Figure 2B shows that, with low mobility, the moths held themselves at the base of the container during the entire period of the bioassay.

The reduction of mobility observed in the moths of group EC (Figure 2B) can be associated either with the stress caused by primary dermal irritability of a few formulation components, mainly solvents and a few tensioactives, or with the presence of a greater amount of insecticide in its free form in this kind of formulation (Benita et al., 1984). In the present study, the behavior of thanatopsis was observed, so, the insect was considered dead when it did not move for a period of three minutes of observation after being stimulated. According to Couturier et al. (1996), thanatopsis is the behavioral reaction in the insects that simulate death when threatened. This is a defense strategy presented by insects, and it simulates death by remaining immobile or static, or with the intention of avoiding an attack, predation and death itself.

Thanatopsis can reduce the efficiency of the insecticide, which would have its action lowered by the consumption of leaves and fruits; the feeding of the moths can be retaken after the concentration of the insecticide is reduced through evaporation and/or leaching.

The absence of thanatopsis in the moths treated with the bioinsecticide in the form of suspension capsules can allow for continuity in the ingestion of treated plants, thus favoring the action by ingestion of the bioinsecticide and extending its efficiency, since capsules are more resistant to the evaporation and leaching processes.

Conclusion

The bioinsecticide, spinosad in the form of concentrate emulsion, showed better efficacy with 80% higher efficiency in a shorter time interval after application of the biopesticide for the control of caterpillars, *H. armigera* when compared with capsules suspension. Microencapsulated formulations of bioinsecticides are a feasible and innovative alternative to control caterpillars, but in this study, the formulation used for capsules suspension did not induce the caterpillars to apparent death (thanatopsis) from environmental and toxicological point of view; the use of spinosad bioinsecticide in encapsulated form showed increased protection when compared with formulations using aliphatic hydrocarbons.

CONFLICT OF INTERESTS

The authors have not declared any conflict of interests.

REFERENCES

Abbott WS (1925). A method of computing the effectiveness of an insecticide. J. Econ. Entomol. 18:265-267.

Amiri-Besheli B (2009). Toxicity evaluation of Tracer, Palizin, Sirinol, Runner and Tondexir with and without mineral oils on Phylocnistis citrella Stainton. Afr. J. Biotechnol. 8:3382-3386.

Benita S, Poly PA, Puisieux F, Delattre J (1984). Radiopaque liposomes: Effect of formulation conditions on encapsulation efficiency. J. Pharm. Sci. 73(12):1751-1755.

Brévault T, Prudent P, Vaissayre M, Carrière Y (2009). Susceptibility of *Helicoverpa armigera* (Lepidoptera: Noctuidae) to Cry1Ac and Cry2Ab2 Insecticidal Proteins in Four Countries of the West African Cotton Belt. J. Econ. Entmol. 102(6):2301-2309.

Bueno AF, Sosa-Goméz DR (2014). The old world bollworm in the Neotropical region: the experience of Brazilian growers with *Helicoverpa armigera*. Outlooks on Pest Management 25(4):261-264.

Couturier G, Tanchiva E, Gonzales J, Cardenas R, Inga H (1996). Preliminary observations on the insect pests of araza, a new fruit crop in Amazonia. Fruits 51:229-239.

Czepak C, Albernaz KC, Vivan LM, Guimarães HO, Carvalhais T (2013). First reported occurrence of Helicoverpa armigera (Hübner) (Lepidoptera: Noctuidae) in Brazil. Pesq. Agropec. Trop. 43:110-113.

Faten FA, Najlaa YA, Nawal SA (2011). Impact of Bacillus thuringiensis β– exotoxin to some biochemical aspects of Musca domestica (Diptera: Muscidae). J. Bacteriol. Res. 3:92-100.

Harter Wr, Botton M, Nava DE, Grutzmacher AD, Da Silva Gonçalves R, Junior RM, Bernardi D, Zanardi OZ (2015). Toxicities and residual effects of toxic baits containing spinosad or malathion to control the adult *Anastrepha fraterculus* (Diptera: tephritidae). Fla. Entomol. 98(1):202-208.

Knowles A (2008). Recent developments of safer formulations of agrochemicals. Environmentalist 28(1):35-44.

Liu B, Wang Y, Yang F, Wang X, Shen H, Cui H, Wu D (2016). Construction of a controlled-release delivery system for pesticides using biodegradable PLA-based microcapsules. Colloids Surf B Biointerfaces 144:38-45.

Mello MO, Silva-Filho MC (2002). Plant-insect interactions: an evolutionary arms race between two distinct defense mechanisms. Braz. J. Plant Physiol. 14(2):71-81.

Obopile M (2006). Economic threshold and injury levels for control of cowpea aphid, *Aphis craccivora* Linnaeus (Homoptera: Aphididae) on cowpea. Afr. Plant Prot. 12:111-115.

Perini CE, Arnemann JA, Melo AA, Pes MP, Valmorbida I, Beche M, Guedes JV (2016). How to control *Helicoverpa armigera* on soybean in Brazil? What we have learned since its detection. Afr. J. Agric. Res. 11:1426-1432.

Pomari-Fernandes A, de Freitas Bueno A, Sosa-Gómez DR (2015). *Helicoverpa armigera*: current status and future perspectives in Brazil. Curr. Agric. Sci. Technol. 21:1-7.

Samri SE, Baz M, Jamjari A, Aboussaid H, El Messoussi S, El Meziane A, Barakate M (2015). Preliminary assessment of insecticidal activity of Moroccan actinobacteria isolates against mediterranean fruit fly (*Ceratitis capitata*). Afr. J. Biotechnol. 14:859-866.

Sayyed AH, Naveed M, Rafique M, Arif MJ (2012). Detection of insecticides resistance in Spodoptera exigua (Lipidoptera: Noctuidae) depends upon insect collection methods. Pak. Entomol. 34:7-15.

Specht A, Sosa-Gómez DR, de Paula-Moraes SV, Yano SA (2013). Identificação morfológica e molecular de Helicoverpa armigera (Lepidoptera: Noctuidae) e ampliação de seu registro de ocorrência no Brasil. Pesq. Agropec. Bras. 48:689-692.

Suzana CS, Damiani R, Fortuna LS, Salvadori JR (2015). Desempenho de larvas de Helicoverpa armigera (Hübner) (Lepidoptera: Noctuidae) em diferentes fontes alimentares. Pesq. Agropec. Trop. 45:480-485.

Tello V, Díaz L, Sánchez M (2013). Side effects on the natural pesticide Spinosad (GF 120 Formulation) on Eretmocerus paulistus

(Hymenoptera: Aphenilidae), a parasitoid of the whitefly Aleurhotrixus floccosus (Hemiptera: Aleyrodidae), under laboratory conditions. Cienc. Inv. Agr. 40:407-417.
Tsunoda K, Nishimoto K (1986). Evaluation of wood preservatives for surface treatments. Int. Biodeterior. 22:27-30.
Vijayabharathi R, Kumari BR, Gopalakrishnan S (2014). Microbial agents against *Helicoverpa armigera*: Where are we and where do we need to go? Afr. J. Biotechnol. 13:1835-1844.
Wang D, Gong P, Li M, Qiu X, Wang K (2009). Sublethal effects of spinosad on survival, growth and reproduction of Helicoverpa armigera (Lepidoptera: Noctuidae). Pest Manage. Sci. 65:223-227.
Wang D, Wang YM, Liu HY, Xin Z, Xue M (2012). Resistance and resistance management. Lethal and sublethal effects of spinosad on Spodoptera exígua (Lepidoptera: Noctuidae). J. Econ. Entomol. 106(4):1825-1831.

African Journal of Biotechnology

Related Journals Published by Academic Journals

- *Biotechnology and Molecular Biology Reviews*
- *African Journal of Microbiology Research*
- *African Journal of Biochemistry Research*
- *African Journal of Environmental Science and Technology*
- *African Journal of Food Science*
- *African Journal of Plant Science*
- *Journal of Bioinformatics and Sequence Analysis*
- *International Journal of Biodiversity and Conservation*

academicJournals